Development of a laser induced fluorescence technique for the analysis of organic air pollutants

by

Patricia B.C. Forbes

Submitted in partial fulfillment of the requirements for the degree

PhD (Chemistry)

in the Faculty of Natural & Agricultural Science

University of Pretoria

February 2010

I declare that the thesis that I hereby submit for the degree PhD Chemistry at the University of Pretoria is my own work and has not previously been submitted by me for degree purposes at any other university or institution.

_____ _____

Date

Abstract

Polycyclic aromatic hydrocarbons (PAHs) are ubiquitous environmental pollutants which are of concern due to their potential human toxicity. They are formed during numerous combustion processes, including biomass burning and diesel vehicular emissions, which are of relevance in developing countries.

A novel analytical screening method for atmospheric polycyclic aromatic hydrocarbons (PAHs) was developed in this study based on laser induced fluorescence (LIF) of samples on quartz multi-channel polydimethylsiloxane (PDMS) traps. A tunable dye laser with a frequency doubling crystal provided the excitation radiation, and a double monochromator with a photomultiplier tube detected emitted fluorescence. The method allowed for the rapid (<5 min), cost effective analysis of samples. Those yielding interesting results could be further analysed by direct thermal desorption-gas chromatography-mass spectrometry (TD-GC-MS, with limits of detection of ~0.3 $ng.m^{-3}$), as photodegradation was minimal (<10 % over 5 min irradiation). Without any signal optimization, a LIF detection limit of ~1 $\mu g.m^{-3}$ was established for naphthalene using a diffusion tube (diffusion rate of 2 $ng.s^{-1}$) and 292 nm excitation. Gas standards which facilitated the uniform distribution of analyte across each of the 22 PDMS tubes were provided by easily constructed diffusion tubes for naphthalene and by a gas chromatographic fraction collection method for the less volatile target PAHs.

The methods developed were successfully tested in a number of applications which are of relevance to southern Africa, as emissions from sugar cane burning, household fires, diesel vehicles and industries were monitored. The LIF method allowed for the differentiation between impacted and non-impacted industrial sites, and the importance of naphthalene as an indicator for atmospheric PAHs was verified in that this PAH was the most abundant in the various applications which were investigated. The multi-channel silicone rubber traps were also evaluated theoretically and practically in the denuder configuration, in order to monitor PAHs in both the gas and particle phases, which is important in terms of human health effects.

The novel LIF method developed in this study has the potential to serve as a screening tool to avoid the comprehensive and costly analysis of samples which do not contain appreciable levels of PAHs. The experimental procedure is simple and rapid, with acceptably low limits of detection, even with the initial, unoptimized optical arrangement and without extensive time-averaging. LIF also provides selectivity without the need for sample clean-up and separation processes.

The LIF method could be further optimized by improving the laser energy stability, as well as by the investigation of possible time resolution techniques. As equipment cost considerations were important, it is possible that the LIF screening method could find application in a centralized environmental laboratory for the southern African region. This would facilitate the widespread monitoring of atmospheric PAHs in a cost effective manner.

Acknowledgements

The CSIR, National Laser Centre (NLC), National Research Foundation (NRF, Thuthuka programme) and DAAD are gratefully acknowledged for funding provided for this research.

Henk van Wyk from the NLC is thanked whole-heartedly for his invaluable technical input with respect to the LIF setup.

Thanks are extended to my family and the numerous friends and colleagues who assisted me along this life journey, and who motivated me to see it to completion. I would like to make special mention of Dr Erla Harden and Yvette Naudé for their guidance and support, and Andreas Trüe for assisting with the TD-GC-MS analyses.

My supervisor, Professor Egmont Rohwer, was "a rock in the pounding ocean of life" during this time. His patience, guidance and expert mentorship is greatly appreciated.

I would also like to thank my greatest supporter (and harshest critic): my husband Andrew, as well as my daughter Juliet, for their love and for always being there for me.

Table of contents

Abbreviations

ACGIH	American Conference of Governmental Industrial Hygienists
APINA	Air Pollution Information Network for Africa
AQA	Air Quality Act
ATSDR	Agency for Toxic Substances and Disease Registry
BBO	Beta Barium Borate
BVOC	Biogenic Volatile Organic Compound
CI	Chemical Ionization
CIS	Cooled Injection System
DCM	Dichloromethane
EI	Electron Ionization
EIA	Environmental Impact Assessment
EPA	Environmental Protection Agency
FAGE	Fluorescent Assay by Gas Expansion
FlA	Fluoranthene
FID	Flame Ionization Detector
GAW	Global Atmospheric Watch
GC	Gas Chromatography
HPLC	High Performance Liquid Chromatography
IDLH	Immediately Dangerous to Life and Health
INEC	Infrastructure and Economic Cooperation
LIF	Laser Induced Fluorescence
LOD	Limit of Detection
LOQ	Limit of Quantitation
MS	Mass Spectrometry
MSD	Mass Selective Detector
Naph	Naphthalene
NIOSH	National Institute for Occupational Safety and Health
NIST	National Institute of Standards and Technology
OECD	Organization for Economic Cooperation and Development
OPPO	Optically Pumped Parametric Oscillator
OSHA	Occupational Safety and Health Administration
PAH	Polycyclic aromatic hydrocarbon
PCB	Polychlorinated biphenyls
PCN	Polychlorinated aromatic hydrocarbons
PDMS	Polydimethylsiloxane
PhA	Phenanthrene
PM_{10}	Particulate Matter of size ≤ 10 micron
$PM_{2.5}$	Particulate Matter of size ≤ 2.5 micron
PMT	Photomultiplier Tube

Py	Pyrene
POP	Persistent Organic Pollutant
PTFE	Polytetrafluoroethylene
PUF	Polyurethane Foam
RAPIDC	Regional Air Pollution in Developing Countries
RMS	Root Mean Square
SAFARI-92	Southern Africa Fire-Atmosphere Research Initiative of 1992
SAFARI 2000	Southern African Regional Science Initiative of 2000
SEANAC	Southern and Eastern Africa Network of Analytical Chemists
SEP	Sample Enrichment Probe
SIC	Single Ion Current
SIDA	Swedish International Development Cooperation Agency
SPME	Solid Phase Microextraction
STP	Standard Temperature and Pressure
SVOC	Semi-volatile Organic Compound
TD	Thermal Desorption
TDS	Thermal Desorption System
TIC	Total Ion Current
TSP	Total Suspended Particulates
UK	United Kingdom
USA	United States of America
UV	Ultraviolet
VOC	Volatile Organic Compound
WMO	World Meteorological Organization

List of tables

List of figures

Chapter 1

Introduction

1.1 AIR POLLUTION IN DEVELOPING COUNTRIES

The air quality of developing countries is of concern due to industrial development, economic growth and large-scale migration of rural residents to urban areas. Consequences of this include a decline in food security, an increase in respiratory related illnesses, and a degradation of both the quality of life and the environment (Mmolawa, 2006). Comprehensive and reliable air monitoring data is key to the improvement of air quality, as without this information it is impossible to identify and apportion emission sources (Hight and Ferrier, 2006).

Whilst it is acknowledged that significant progress has been made in organic air pollutant monitoring in many developing countries in Asia and South America, here we focus on southern Africa. The geographic delineation for the region was used, i.e. the portion of Africa south of the Cunene and Zambezi rivers. This incorporates the countries of Botswana, Lesotho, Namibia, Mozambique, South Africa, Swaziland and Zimbabwe, as shown in Figure 1.1.

Figure 1.1: Southern African countries.

In addition to industrial emissions, major sources of air pollutants in developing countries include dependence on fossil fuels, and increasing traffic densities in urban areas, mainly involving an aged vehicle fleet without catalytic converters. Poor indoor air quality is also often of concern, due to the use of open fires for cooking and heating purposes. Besides the relatively commonly monitored inorganic pollutants which are released from these combustion processes, for example, nitrogen oxides, sulphur dioxide and carbon dioxide; organic pollutants may also be released in the gaseous form or associated with particles. Hydrocarbons and polycyclic aromatic hydrocarbons (PAHs) are examples of such pollutants, as are polychlorinated dibenzodioxins and furans which may be generated when chlorinated material is combusted. Although the organic pollutants would generally be present at lower concentrations than the inorganic species, they are nevertheless of environmental significance due to their potential impacts (including health effects) at low levels.

1.2 HINDRANCES TO AIR POLLUTANT MONITORING IN DEVELOPING COUNTRIES AND MEANS BY WHICH THESE ARE BEING ADDRESSED

Organic air pollutant monitoring has been minimal in many developing countries to date, particularly those on the African continent. This is due to a number of reasons, some of which are the result of socio-political priorities. In addition, a lack of resources is often the most prominent hindrance, where funding, skilled human capital, and suitable equipment may be unavailable.

Various initiatives have been established in order to address these issues. For example, the Air Pollution Information Network for Africa (APINA) is a sub-Saharan regional network of scientists, policy-makers and non-governmental organizations, and its member countries include Botswana, Mozambique, South Africa and Zimbabwe. APINA aims to address air pollution problems, as part of the RAPIDC (Regional Air Pollution in Developing Countries) programme. RAPIDC is funded by the Department of Infrastructure and Economic Cooperation (INEC) of SIDA, the Swedish International Development Cooperation Agency and includes initiatives in both Asia and Africa (APINA, 2008).

The Southern and Eastern Africa Network of Analytical Chemists (SEANAC) was established to assist with capacity building and collaboration in the region, specifically in the areas of health, food security and environmental monitoring. One of the problems cited as being faced by African analytical chemists is that many of them received training abroad in techniques which are much more appropriate to the developed world (SEANAC, 2008).

The Organisation for Economic Cooperation and Development (OECD) has investigated the impact of monitoring equipment on air quality management in developing countries (Hight and Ferrier, 2006). Capacity building is achieved through case studies, where participant countries are assisted with monitoring equipment and training. The case studies conducted to date do not include southern African countries, and have focused on inorganic pollutants, with the exception of one study involving fuel testing in India, where PAHs were monitored.

1.3 OVERVIEW OF ORGANIC AIR POLLUTANT MONITORING IN SOUTHERN AFRICA

It is relevant to consider southern Africa as a region in terms of air quality, as the climate and air circulation of the region south of northern Angola is dominated by a gyre centred on Botswana. The air rotates anti-clockwise, completing one revolution approximately every week and the gyre thus formed remains in place for several weeks, particularly in winter, which leads to a build up of various trapped atmospheric pollutants, resulting in deterioration in visibility and air quality over parts of the subcontinent (Scholes and Biggs, 2004).

Monitoring activities are largely driven by legislation, thus an overview of the existing air quality legislation pertaining to the region is included in this section. It is generally accepted that environmental legislation in many African countries is outdated, or is poorly enforced due to a lack of capacity or poor institutional organisation. In some cases, more modern legislation still allows industries which were in existence before promulgation to continue operating outdated equipment, even if this leads to excessive pollution.

Some monitoring is undertaken by local government municipalities, industries, and research institutions in the different countries of interest, but in most cases such monitoring is currently restricted to inorganic air pollutants. Published organic air pollutant monitoring activities, conducted prior to 2007, are summarised in the following sections. It is acknowledged that additional monitoring may have taken place such as for the purpose of Environmental Impact Assessments (EIAs), where the reports are not readily accessible.

1.3.1 Botswana

Routine air quality monitoring began in Botswana in the mid 1970s, upon the promulgation of the Atmospheric Pollution Prevention Act in 1971. Continuous monitoring of hydrocarbons has been conducted in Botswana at one site since 1999 (Scholes, 2001), but most of the monitoring sites focus on inorganics (SO_2, NO_x, O_3, CO and particulate matter) and associated meteorological data. Ambient air quality objectives for Botswana do not include organic air pollutants. A National Environmental Laboratory was established in 2002, however, which has the capabilities to analyse organic pollutants (Mmolawa, 2006).

1.3.2 Lesotho

The Environment Act 2001 provides for the management of the environment and all natural resources of Lesotho. The Act makes provision for the establishment of environmental quality standards and environmental monitoring, but it is unclear as to whether such provisions have been enacted (Department of Tourism, Environment and Culture, 2001).

1.3.3 Mozambique

Mozambique has an Environmental Law of 1997, but few air pollutant monitoring studies have been conducted in this country (Mmolawa, 2006).

1.3.4 Namibia

The Namibian Directorate of Environmental Affairs has noted that air pollution is a less serious problem than in many other countries, although the need to update the environmental legislation to enable effective law enforcement is acknowledged (Namibia Directorate of Environmental Affairs, 2008). No systematic air quality monitoring had occurred in Namibia, as of 2001 (Scholes, 2001).

1.3.5 South Africa

A new era in air quality management in South Africa began with the promulgation of the National Environmental Management: Air Quality Act (Act No. 39 of 2004) (AQA), which replaced the Air Pollution Prevention Act (Act No. 45 of 1965). This has resulted in a shift from an emission control focus to an airshed approach, which culminated in the establishment of national standards for permissible ambient concentrations of air pollutants (Department of Environmental Affairs and Tourism, 2006).

This has implications in terms of air quality monitoring, as methods are required which are suitable for monitoring pollutants at ambient concentrations, which are generally lower than emission levels. Alternative methods, which allow for pre-concentration of analytes of interest and which have lower detection limits, are therefore of importance. Sampling methods employed in ambient and emission air monitoring are also different. Development of the capacity and capabilities to perform ambient air monitoring (as well as in air quality

management) is therefore receiving attention in South Africa, particularly at local government level.

At present, benzene is the only organic air pollutant for which ambient standards have been set (an annual average of 5 $\mu g.m^{-3}$), although the AQA makes provision for the Minister of Environmental Affairs and Tourism to make notice of additional air pollutants, as necessary.

In terms of monitoring, local municipalities in South Africa currently monitor Volatile Organic Compounds (VOCs) (specifically benzene, toluene, ethylbenzene and xylenes) at nine sites across three provinces. Methane is also monitored at four stations in two provinces, one of which is the World Meteorological Organisation (WMO) Global Atmospheric Watch (GAW) site at Cape Point (Department of Environmental Affairs and Tourism, 2007). Non-methane hydrocarbons are also monitored monthly at the GAW site, by means of grab sampling into canisters which are analysed in Europe. These samples have yielded interesting results in the context of biomass burning episodes, for example (Brunke et al., 2001).

VOCs have been studied in various contexts, including that of emissions from spontaneous combustion of coal (Pone et al., 2007) and the Cape Town brown haze, which forms in winter months under inversion conditions (Burger et al., 2004).

In addition to monitoring campaigns, fundamental research has been conducted in South Africa in terms of novel means of sampling and analysing organic air pollutants. Burger et al. (2006) have developed a high capacity, polydimethylsiloxane (PDMS) rubber sample enrichment probe (SEP), which can be thermally desorbed for GC analysis. A novel thermal modular array for comprehensive two-dimensional gas chromatography has also been produced by these researchers (Burger et al., 2003).

Ortner and Rohwer (1996) developed thick film multi-channel silicone rubber traps, as shown in Figure 1.2, which have been applied in semi-volatile organic air pollutant sampling. These traps serve as pre-concentrators and can be thermally desorbed for gas chromatographic (GC) analysis, thereby negating the need for solvent extraction and concentration, and there is also a low pressure drop across the traps, due to their open geometry. It has been found that the blank runs of PDMS traps, where pre-concentration occurs by sorption of the analytes into

the silicone, are significantly better than those of most adsorbents, such as Tenax TA, and do not deteriorate with continued use (Balthussen et al., 1998). PDMS is also more inert than most adsorbents, and the PDMS degradation products can be easily identified by mass spectrometry. The multi-channel silicone rubber traps of Ortner et al. (1996) are inexpensive to manufacture and can be re-used, therefore they were employed in our study for sampling and pre-concentration of trace organic air pollutants.

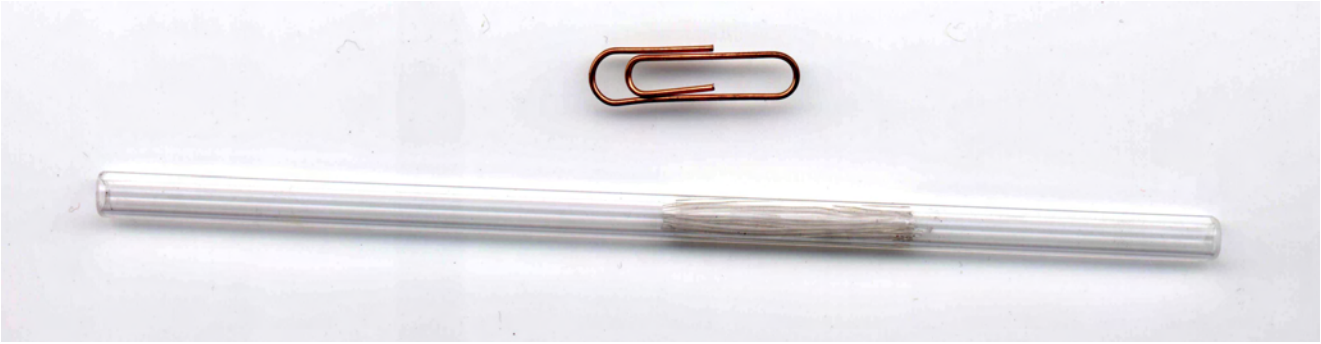

Figure 1.2: A silicone rubber trap containing multiple PDMS channels.

1.3.6 Swaziland

Air Pollution Control Regulations have been drafted for Swaziland, which include air quality objectives for a number of inorganic air pollutants only (Department of Tourism, Environment and Communications, 1999).

1.3.7 Zimbabwe

Zimbabwe has an Atmospheric Pollution Control Act (No. 33 of 1971 as amended by Act No. 22 of 2002) and Atmospheric Pollution Prevention Regulations of 1975. The Environmental Management Act was enacted in December 2002, which will repeal the existing air legislation in due course, and will provide for the establishment of Air Quality Standards (Mmolawa, 2006).

Some random air monitoring studies have been conducted in Zimbabwe, and the Air Pollution Control Unit of the City of Harare Health Department has carried out routine air pollution monitoring of SO_2, NO_2 and soot at eight sites over the past 20-30 years. Other

parameters which have been monitored include methane and VOCs, in addition to inorganic analytes (Pb, NH_3, HCl and particulate matter) (Mmolawa, 2006).

1.3.8 Other African studies

Few published organic air pollutant monitoring campaigns have been conducted in other African countries, such as the monitoring of PAHs from charcoal burning in Kenya (using liquid chromatography with fluorescence detection) (Gachanja and Worsfold, 1993). The majority of these studies were carried out in collaboration with developed countries, which assisted primarily with analyses. Studies of organic pollutants, particularly pesticides, in other environmental media (Torto et al., 2007), also indicate that there is some existing capacity that could provide a basis for air monitoring. An example is the determination of PAHs in surface runoff and sediments in Nigeria (Ogunfowokan et al., 2003). A study of relevance to Africa was the ship-board monitoring of atmospheric PAHs and polychlorinated aromatic hydrocarbons (PCNs) along a north-south Atlantic transect between the Netherlands and South Africa. The highest levels of these pollutants were found near to the land masses (Europe, West Africa and South Africa) (Jaward et al., 2004a).

1.3.9 Involvement of southern Africa in international conventions

In terms of organic pollutant monitoring, the Stockholm Convention on Persistent Organic Pollutants (POPs) is of relevance. The majority of southern African countries have become signatories to this convention, and as such have a responsibility to manage and monitor POPs (Bouwman, 2004). Existing monitoring progammes, activities and datasets have recently been compiled (United Nations Programme, 2007), and are summarised in Table 1.1. Although concentrations of POPs were determined in ambient air in Durban, South Africa (Batterman et al., 2006), all analyses were performed in the United States of America (USA). It is evident that capabilities in the region require further development.

Table 1.1: Existing national monitoring programmes, activities and datasets for southern African countries (United Nations Programme, 2007).

Country	Monitoring activities
Botswana	No data
Lesotho	No data
Mozambique	No data
Namibia	Limited data
South Africa	No existing national POPs information gathering activities. Academic research studies have been conducted and published to assess POPs in various media (Note: air was not included).
Swaziland	No data
Zimbabwe	Limited data

1.3.10 Southern African air monitoring campaigns

The Southern Africa Fire-Atmosphere Research Initiative of 1992 (SAFARI-92) and the Southern African Regional Science Initiative of 2000 (SAFARI 2000) provided scientists in the region with the opportunity to participate in large research projects with international experts. SAFARI-92 investigated the role of savanna fires in atmospheric chemistry, climate and ecology, where organic monitoring included CH_4 and non-methane hydrocarbons (Lindesay et al., 1996). More than 150 scientists from 14 countries were involved, including the southern African countries of Botswana, Namibia, South Africa, Swaziland and Zimbabwe. SAFARI 2000 addressed a broad range of phenomena related to land-atmosphere interactions and biogeochemical functioning of the southern African system. Here biogenic volatile organic compounds (BVOCs), VOCs, oxygenated VOCs, and semi-volatile organic compounds (SVOCs) were also monitored (Swap et al., 2003).

1.4 USE OF ALTERNATIVE MONITORING METHODS

In light of the hindrances experienced in developing countries, as discussed under section 1.2, alternative monitoring methods to the standard comprehensive methods may be more appropriate. Such methods should be cost effective and simple, in order to allow for

more widespread monitoring in the region. A few options in this regard, with respect to organic air pollutants are briefly discussed in this section.

1.4.1 Passive sampling

Passive air samplers provide a useful means of monitoring in developing countries due to their simplicity, cost effectiveness and non-reliance on provision of a power source. Passive sampling may provide pre-concentration of analytes, thereby increasing analytical sensitivity, and may reduce or eliminate solvent consumption for sample preparation purposes. Sampling is based on diffusion or permeation of the analyte into the sampler, as reviewed by Seethapathy (Seethapathy et al., 2008). Passive samplers have found widespread application in airborne POPs monitoring, for example (Shoeib and Harner, 2002; Jaward et al., 2004b).

Besides the use of evacuated canisters for passive organic air pollutant sampling, passive samplers of interest include solid phase microextraction (SPME), polyurethane foam (PUF) based samplers, and samplers containing adsorbents such as graphitised charcoal or Tenax.

Studies have been conducted in South Africa to assess the chronic health impacts of exposure to VOCs (as well as naphthalene), by means of passive sampling, using 3M badges (John, 1998) and IVL passive samplers (Wichmann, 1999). There is significant scope to implement passive sampling more widely in the field of organic air pollutant monitoring in southern Africa, and to utilise this technique for a wider range of organic analytes. It should be noted, however, that passive samplers may not provide the time resolution required in some monitoring campaigns, due to the relatively long sampling intervals usually employed (one to several weeks).

1.4.2 Indicator compounds

The monitoring of by-products (indicator compounds) of reaction pathways which generate the analyte of interest has been successfully utilised for various classes of chemicals. A relevant example is the monitoring of chlorobenzenes and chlorophenols as indicators for dioxins and furans, where correlation coefficients are used to relate the indicator compound

concentrations to that of the target analyte (Kaune et al., 1998). Precursor compounds may be similarly utilised where intermediates in the synthesis of the target analyte are monitored.

The choice of indicator compound is based on the existence of a correlation with the target compound(s), ease of sampling, as well as other characteristics which simplify analysis, such as a higher concentration and existence of fewer congeners compared to the target analyte(s). The monitoring of indicator or precursor compounds for organic air pollutant monitoring therefore has significant potential for application in developing countries, where resources and capacity are limited.

1.4.3 Screening methods

Screening methods find application in large sampling campaigns, in that numerous samples can be taken and analysed in order to determine whether more comprehensive analysis (by standard accepted methods) is required, such as of those samples which screen positive. A screening method should ideally be fast, simple and of low cost, yet meet the sensitivity and selectivity requirements of the application. It is therefore evident that the advantages of screening methods would be particularly beneficial in a developing country context.

1.5 PURPOSE OF THIS STUDY

This study was initiated in order to develop methods for organic air pollutant monitoring, which are more applicable to developing countries and which have benefits over comprehensive, detailed methods in this context, thereby allowing for significantly more sampling campaigns to be conducted, particularly in southern Africa. The techniques are required to be rapid, and have acceptably low limits of detection for the envisaged applications thereof. In addition, sufficient selectivity is needed and sample clean-up and separation processes prior to analysis should be minimal. Interface with more comprehensive techniques for further comprehensive, quantitative analysis post screening should ideally also be possible. Although equipment cost considerations are important, it is possible that some techniques may be more suitable for application in a centralized environmental laboratory for the southern African region.

1.6 STRUCTURE OF THE THESIS

Following the background to organic air pollutant monitoring and the objectives of this study, as provided in this chapter, the generation of trace organic gas standards for such monitoring is detailed in Chapter 2. The development of a novel, laser induced fluorescence screening method for PAH monitoring with PDMS based sampling is presented in Chapter 3, whilst the use of the multi-channel silicone rubber traps in a novel denuder configuration is described in Chapter 4. Chapter 5 covers the applications of these methods, whilst overall conclusions are drawn in Chapter 6.

1.7 REFERENCES

Air Pollution Information Network for Africa (APINA), **2008**, accessed online at www.sei.se/rapidc/apina.htm

Balthussen, E., David, F., Sandra, P., Janssen, H.-G. and Cramers, C.A., *Journal of High Resolution Chromatography*, **1998**, *21*, 332-340.

Batterman, S., Chernyak, S., Gounden, Y. and Matooane, M., *Organohalogen Compounds*, **2006**, *68*, 1111-1114.

Bouwman, H., *South African Journal of Science*, **2004**, *100*, 323-328.

Brunke, E.-G., Labuschagne, C. and Scheel, H.E., *Atmospheric Environment*, **2001**, *35*, 777-786.

Burger, B.V., Marx, B., le Roux, M. and Burger, W.J.G., *Journal of Chromatography A*, **2006**, *1121*, 259-267.

Burger, J.W., Pienaar, J.J., Fourie, L. and Jordaan, J.H.L., *Air Pollution 2004*, **2004**, WIT Press, UK, 631-640.

Burger, B.V., Snyman, T., Burger, W.J.G. and van Rooyen, W.F., *Journal of Separation Science*, **2003**, *26* (1-2), 123-128.

Department of Environmental Affairs and Tourism, South Africa, 9 June **2006**, National Environmental Management: Air Quality Act No. 39 of 2004, Government Notice No. 528, Government Gazette No. 28899.

Department of Environmental Affairs and Tourism, South Africa, May **2007**, *Technical Compilation to inform the Initial State of Air Report*, National Air Quality Management Programme.

Department of Tourism, Environment and Communications, Swaziland, **1999**, Air Pollution Control Regulations, accessed online at www.ecs.co.sz

Department of Tourism, Environment and Culture, Republic of Lesotho, **2001**, Environment Act, accessed online at www.faolex.fao.org/faolex

Gachanja, A.N. and Worsfold, P.J., *Science of the Total Environment*, **1993**, *138*, 77-89.

Hight, J., and Ferrier G., **2006**, *The impact of monitoring equipment on air quality management capacity in developing countries*, Organisation for Economic Cooperation and Development, Joint Working Party on Trade and Environment, Report COM/ENV/TD(2006)7/FINAL, France.

Jaward, F.M., Barber, J.L., Booij, K. and Jones, K.C., *Environmental Pollution*, **2004a**, *132*, 173-181.

Jaward, F.M., Farrar, N.J., Harner, T., Sweetman, A.J. and Jones, K.C., *Environmental Science and Technology*, **2004b**, *38*, 34-41.

John, J., January **1998**, *Research to quantify atmospheric volatile organic compounds in the major metropolitan areas of South Africa*, CSIR internal report ENV-P-C-98016, South Africa.

Kaune, A., Lenoir, D., Schramm, K.-W., Zimmermann, R., Kettrup, A., Jaeger, K., Rückel, H.G. and Frank, F., *Environmental Engineering Science*, **1998**, *15* (1), 85-95.

Lindesay, J.A., Andreae M.O., Goldammer, J.G., Harris, G., Annegarn, H.J., Garstang, M., Scholes, R.J. and van Wilgen, B.W., *Journal of Geophysical Research*, **1996**, *101* (D19), 23521-23530.

Mmolawa, M.D., **2006**, Scoping report on existing monitoring activities in the 7 APINA member countries, Issued as part of Phase III Activity 2.3 of the RAPIDC Programme 2005-07, Botswana.

Namibia Directorate of Environmental Affairs, **2008**, accessed online at www.met.gov.na/dea

Ogunfowokan, A.O., Asubiojo, O.I. and Fatoki, O.S., *Water, Air, and Soil Pollution*, **2003**, *147*, 245-261.

Ortner, E.K. and Rohwer, E.R., *Journal of High Resolution Chromatography*, **1996**, *19*, 339-344.

Pone, J.D.N., Hein, K.A.A., Stracher, G.B., Annegarn, H.J., Finkleman, R.B., Blake, D.R., McCormack, J.K. and Schroeder, P., *International Journal of Coal Geology*, **2007**, *72*, 124-140.

Scholes, R.J. and Biggs, R. (eds), **2004**, *Ecosystem services in Southern Africa: A regional assessment*, CSIR, ISBN 0-7988-5527-4, 55, South Africa.

Scholes, R., February **2001**, *Regional Implementation Plan for Southern Africa*, *Global Terrestrial Observing System GTOS-21*, CSIR internal report ENV-P-R 2001-002, South Africa.

Seethapathy, S., Górecki, T. and Li, X., *Journal of Chromatography A*, **2008**, *1184*, 234-253.

Shoeib, M. and Harner, T., *Environmental Science and Technology*, **2002**, *36*, 4142-4151.

Southern and Eastern Africa Network of Analytical Chemists (SEANAC), **2008**, accessed online at www.seanac.org

Swap, R.J., Annegarn, H.J., Suttles, T., King, M.D., Platnick, S., Privette, J.L. and Scholes, R.J., *Journal of Geophysical Research*, **2003**, *108* (D13), SAF 1-1 – 1-15.

Torto, N., Mmualefe, L.C., Mwatseteza, J.F., Nkoane, B., Chimuka, L., Nindi, M.M. and Ogunfowokan, A.O., *Journal of Chromatography A*, **2007**, *1153*, 1-13.

United Nations Environmental Programme, **2007**, Stockholm Convention on Persistent Organic Pollutants (POPs), *Compilation of existing national monitoring programmes, activities and datasets*, Document UNEP/POPS/GMP/TWG-2/6, Geneva.

Wichmann, J., October **1999**, *Human health risk assessment case study – value addition of passive sampler generated data*, CSIR internal report ENV-P-I-99008, South Africa.

Chapter 2

The generation of trace gas standards

2.1 INTRODUCTION

In trace gas analysis, it is important that reliable gas standards can be produced at the appropriate concentrations. For initial analytical method development, liquid injections of standards onto the sampling traps may suffice. During method optimization for application purposes, however, gas phase standards may be more appropriate.

A number of means of generating gas standards have been developed, as reviewed by Barratt (1981), Namieśnik (1984) and Naganowska-Nowak et al. (2005), which may be broadly classified into static and dynamic methods. Static techniques involve the introduction of a specific amount of analyte into a known volume of diluent gas in a closed container, such as a gas cylinder, whilst with dynamic methods, the analyte enters the diluent gas stream on a continuous basis (Naganowska-Nowak et al., 2005).

Static systems are used primarily for small volumes of mixtures and fairly high concentrations, but losses of components of the mixture to the wall of the container may occur, and these systems are usually not very portable. They have been used primarily in the calibration of GC detectors. Dynamic systems can produce larger volumes, with surface losses being lower than in static systems due to the existence of equilibrium conditions after saturation of contact surfaces, and are thus more suitable for polar and reactive species (Barratt, 1981).

In deciding on an appropriate means of generating a gas standard, the particular application needs to be considered, such as the vapour pressure of the analyte concerned, the need for portability, and so on.

In order to generate gas standards of organic air pollutants at trace levels in our study, a number of techniques were utilized, as detailed in this Chapter, where sampling was performed onto the multi-channel silicone rubber traps referred to in Chapter 1.

2.2 PERMEATION TUBES

2.2.1 Theory

The principle of permeation was first used in 1966 to prepare primary standards for trace gas analysis (Barratt, 1981). Since then, permeation tubes have found application in air pollution, occupational hygiene and instrumental analysis, as evidenced by their current commercial availability.

Permeation methods are based on the dissolution of the compound of interest into and permeation through a sealed polymeric tube or membrane, at a constant and reproducible rate. Polyethylene, polytetrafluoroethylene (PTFE or Teflon) and silicone rubber have been used as tube or membrane material (Namieśnik, 1984), although Teflon is commonly used due to its durability, low reactivity, and commercial availability in a range of diameters and wall thicknesses (Mitchell, 2000; O'Keeffe and Ortman, 1966). The configurations of permeation tubes commonly used are sealed Teflon tubes, Teflon tubes with sample storage reservoirs (sometimes called permeation vials), and membrane devices for highly volatile compounds, which have a wafer structure, with a small area for permeation. Permeation tubes can be prepared for gases, liquids or solids. The latter two cases consist of two-phase systems, where the liquid or solid and its vapour (at a fixed vapour pressure) are present.

Fick's law of diffusion governs the permeation process, due to the difference in partial pressure of the compound of interest between the inner and outer walls of the tube. After construction of a permeation device, a period of equilibration is required before steady-state

conditions are reached, when the permeation rate is constant as long as a two phase system is present. After a period of time, the compound of interest will become depleted, and the permeation rate will consequently decrease to zero. The lifetime of a particular permeation device depends on the permeation rate and the mass of compound of interest placed inside the tube.

The permeation rate is given by the equation (Namieśnik, 1984):

$$R = DS(p_1 - p_2)\frac{A}{L}, \qquad \text{Equation 2.1}$$

where R is the permeation rate of the gas through the plastic membrane; D is the diffusion coefficient; S is the solubility constant; p_1 and p_2 are the partial pressures on the two sides of the membrane; A is the surface area of the membrane; and L is its thickness.

The permeation rate (and the vapour pressure) is temperature dependant, as shown in equation 2.2 (Namieśnik, 1984), thus accurate temperature control is vital in their application.

$$\log\frac{R_2}{R_1} = 2950\left(\frac{1}{T_1} - \frac{1}{T_2}\right), \qquad \text{Equation 2.2}$$

where R_1 and R_2 are the permeation rates at temperature T_1 and T_2, respectively. The equation was empirically derived for various permeation materials, and it allows for the permeation rate to be predicted at temperatures different from the calibration temperature. It is also evident that the permeation rate would change by ~10 % for each 1^{o}C change in temperature.

Under standard temperature and pressure conditions (STP), the concentration of the compound of interest (C) in a gas stream flowing over the permeation tube can be calculated from (Namieśnik, 1984):

$$C = \frac{22.45R}{MQ}, \qquad \text{Equation 2.3}$$

where R is the permeation rate; M is the molar mass of the compound of interest; and Q is the flow rate of the diluting gas.

A number of means of calibrating permeation tubes have been reported (Namieśnik, 1984), however, the gravimetric method of determining permeation rates from mass loss over an extended time period is most commonly used. Theoretical calculation of permeation rates is hindered by a lack of data regarding diffusion coefficients and solubility constants in the polymer materials of interest. Errors in determining small mass losses gravimetrically, however, may arise from static electricity effects, dust in the weighing room, and air currents.

Advantages of permeation tubes as sources of trace gas standards include their versatility, portability and ease of use. They do, however, require long initial equilibration times, and they are a continuous source of the component (i.e. it is not possible to "switch them off"). In addition, they are not suitable for compounds which have very low vapour pressures and low diffusion rates.

Various permeation systems have been developed (Scaringelli et al., 1970; Barrat, 1981), which include temperature controlled systems (provided by a water bath, for example). Such permeation systems are, however, bulky and fragile for field use, and are therefore more suitable for laboratory environments. A permeation-based dynamic gas generator system was developed for naphthalene (Temime et al., 2002), which allowed for the generation of a range of PAH concentrations. The permeation cell consisted of a glass tube containing crystals of the PAH of interest, which was sealed with a PTFE membrane, and was housed in a temperature controlled water bath. The flow rate of the carrier (diluent) gas was between 20 and 40 $m\ell.min^{-1}$, and gravimetric calibration was employed (1 mg mass loss was recorded after a 2 day period, which equates to 6 $ng.s^{-1}$).

In our study, individual permeation tubes were prepared for a number of chorophenols, chlorobenzenes and naphthalene, as discussed in the following sections. Mixed gas standards were also generated from these permeation tubes by placing the selected permeation tubes together in a holder, through which clean diluent air was passed.

2.2.2 Experimental method

2.2.2.1 Permeation tube preparation

Permeation tubes were manufactured using shrink fit PTFE Teflon tubing (Supelco, Sigma Aldrich, 1.4 mm o.d., which shrinks to 0.81 mm, ~40 mm long) into which the standard of interest was placed using a 5 µℓ microcap (chlorobenzenes and chlorophenols: Riedel-de-Haën, analytical grade, Pestanal®; naphthalene: Fluka, GC grade). The open ends of the Teflon tubing were heat sealed onto short (~40 mm long, 10 mm o.d.) solid glass capillaries, which served as stoppers (Figure 2.1). Duplicate permeation tubes were prepared for 1,2-dichlorobenzene; 1,2,4-trichlorobenzene; 2,3,4,6-tetrachlorophenol; and naphthalene, in order to determine the repeatability of this method, and to ensure that the heat seals were effective closures for the permeation tubes (loss of analyte through a leak at the seal would result in differences in permeation rates between the duplicate permeation tubes). In the case of 1,2,4-trichlorobenzene, short and long permeation tubes of the same compound were prepared (43 mm and 61 mm long, respectively).

The permeation tubes were stored in a temperature controlled room (20 ± 2 ^{o}C), and were calibrated gravimetrically using a semi-micro balance (Mettler, readability of 0.01 mg) over a period of > 5000 hours.

2.2.2.2 Permeation tube usage

When using the permeation tubes as gas standards, the tubes of interest were placed in a cylindrical glass holder (body: 165 mm long with 25 mm o.d.; end connections: 40 mm long with 9 mm i.d., Figure 2.2) and allowed to equilibrate without air flow. Clean air (laboratory air which had passed through an activated charcoal bed) was drawn through the holder followed by the silicone rubber trap(s) at a defined flow rate (~500 mℓ.min^{-1}). In this manner, a known concentration of each analyte was loaded onto the sample trap.

Figure 2.1: Examples of chlorobenzene permeation tubes.

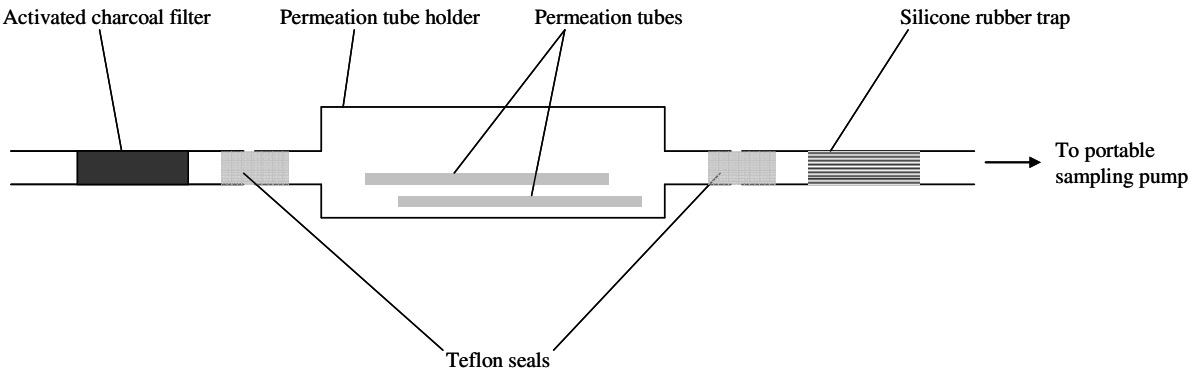

Figure 2.2: Usage of permeation tubes.

2.2.3 Results and discussion

The permeation rates, as determined gravimetrically for each permeation tube, are given in Table 2.1.

Table 2.1: Permeation rate of analytes through Teflon permeation tubes.

Compound	Molar mass ($g.mol^{-1}$)	Purity (%)	Vapour pressure (Pa)	Average permeation rate ($ng.min^{-1}$)	r^2
Chlorobenzenes					
Chlorobenzene[a]	112.6	99.9	1.57×10^3 (at 25 °C)	41.7	0.986
1,2-dichlorobenzene (A)[a]	147.0	99.9	160 (at 20 °C)	9.62	0.997
1,2-dichlorobenzene (B)[a]	147.0	99.9	160 (at 20 °C)	7.07	0.996
1,3-dichlorobenzene[b]	147.0	99.3	200 (at 20 °C)	18.3	0.992
1,2,4-trichlorobenzene (A; short)[b]	181.5	99.4	130 (at 20 °C)	6.92	0.984
1,2,4-trichlorobenzene (B; long)[b]	181.5	99.4	130 (at 20 °C)	18.3	0.981
1,2,3,4-tetrachlorobenzene	216.0	99.1	Not available	NSC	NA
1,2,4,5-tetrachlorobenzene	216.0	99.3	Not available	NSC	NA
Chlorophenols					
3-chlorophenol[b]	128.6	99.5	100 (at 44 °C)	NSC	NA
4-chlorophenol[b]	128.6	99.8	15 (at 20 °C)	NSC	NA
2,4-dichlorophenol[c]	163.0	99.4	16.0	2.33	0.982
2,4,5-trichlorophenol[c]	197.5	99.6	2.9	NSC	NA
2,3,6-trichlorophenol	197.5	98.9	Not available	NSC	NA
2,3,4,6-tetrachlorophenol (A)	232.0	99.9	Not available	NSC	NA
2,3,4,6-tetrachlorophenol (B)	232.0	99.9	Not available	NSC	NA
Pentachlorophenol[c]	266.3	99.0	0.019	NSC	NA
PAHs					
Naphthalene (A)[c]	128.2	99.8	10.4	NSC	NA
Naphthalene (B)[c]	128.2	99.8	10.4	NSC	NA

NOTES: NSC refers to "no significant change" and NA is not applicable.
[a] refers to vapour pressure data obtained from the material safety data sheets as provided by Sigma Aldrich.
[b] refers to vapour pressure data obtained from ChemDat ® (Merck, 1999).
[c] refers to vapour pressure data obtained from the Danish Environmental Protection Agency (2006) for Standard Temperature and Pressure.

The permeation rate graphs for all the compounds which showed a significant mass loss are also presented in Figures 2.3 to 2.6 (i.e. chlorobenzene; 1,2-dichlorobenzene; 1,3-dichlorobenzene; 1,2,4-trichlorobenzene and 2,4-dichlorophenol). Permeation rates were considered to be insignificant for the purpose of gas standard generation when permeation rates were < 1 ng.min^{-1}.

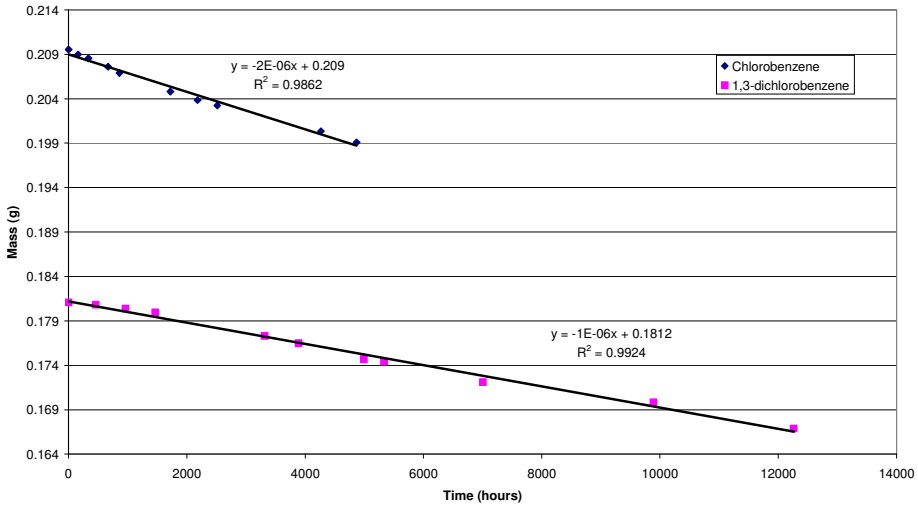

Figure 2.3: Mass loss from the chlorobenzene and 1,3-dichlorobenzene permeation tubes.

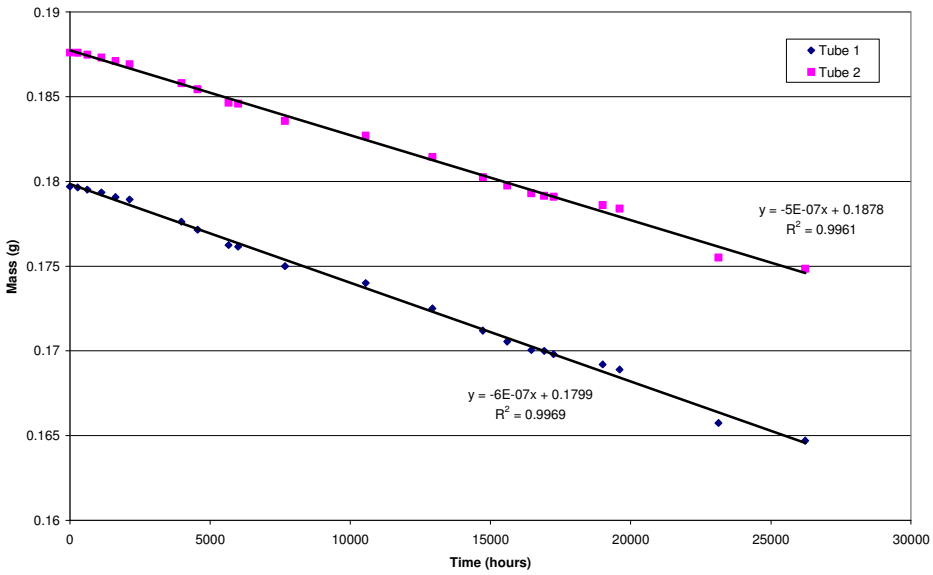

Figure 2.4: Mass loss from the two 1,2-dichlorobenzene permeation tubes over ~26 000 hours.

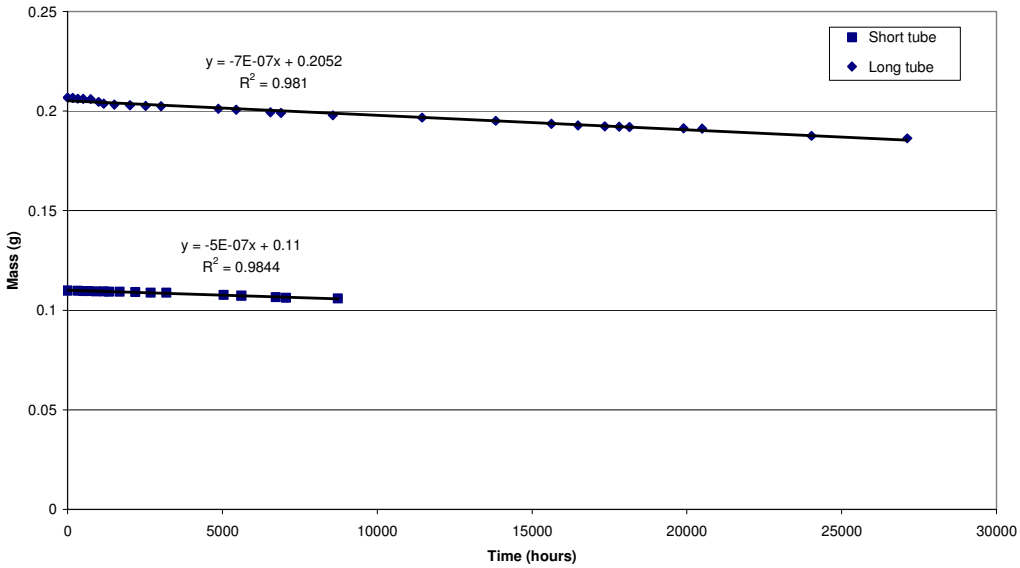

Figure 2.5: Mass loss from the short and long 1,2,4-trichlorobenzene permeation tubes.

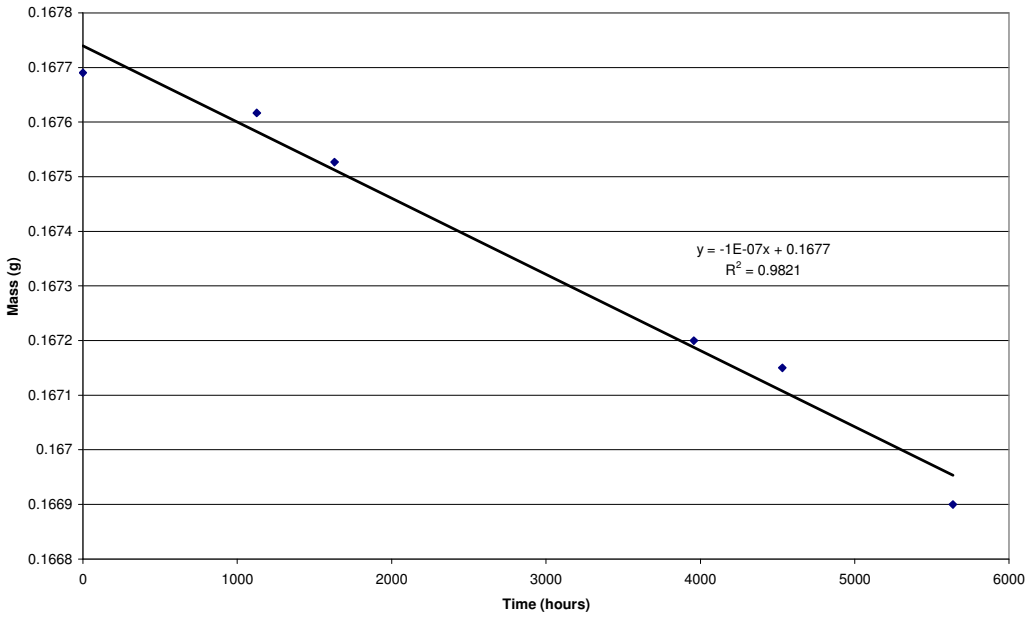

Figure 2.6: Mass loss from the 2,4-dichlorophenol permeation tube over ~5500 hours.

The mass loss of the permeation tubes for which permeation rates could be calculated was found to be relatively constant, as can be seen from the r^2 values in Table 2.1, which were all > 0.98. The permeation rates ranged from 2.3 to 42 $ng.min^{-1}$.

Due to the very slow rate of permeation of naphthalene, one of the permeation tubes (A) was sandpapered to reduce the wall thickness, i.e. *L* in equation 2.1, which should have increased the permeation rate. However no significant change in the permeation rate occurred, as no significant change in the mass of the permeation tube could be detected.

The duplicate permeation tubes for 1,2-dichlorobenzene were of a similar order of magnitude and differed by 27 %. The permeation rate has a standard deviation of 20 %, however, based on the smallest mass loss of 0.05 mg recorded between readings for 1,2-dichlorobenzene, and a mass accuracy of 0.01 mg. The repeatability between the two 1,2-dichlorobenzene permeation tubes is therefore considered to be acceptable. There was no significant mass loss for the other two duplicate permeation tubes (naphthalene and 2,3,4,6-tetrachlorophenol). No losses from the heat seals were therefore evident.

For the two 1,2,4-trichlorobenzene permeation tubes of different lengths, the increased area of the Teflon tube in the case of the long permeation tube, increased the permeation rate almost three fold. This is expected from equation 2.1, as the area of the long tube was 1.4 times that of the short tube, and the walls of the long tube were thinner at one end due to stretching of the Teflon tubing during the heating stage of the permeation tube manufacture, which would have also increased the permeation rate.

2.2.4 Conclusion

Permeation tubes were not suitable for gas standard generation for naphthalene, the tetrachlorobenzenes, and most of the chlorophenols, as the rates of mass loss (permeation rates) were insignificant in these cases. It appears that the vapour pressure of the compound of interest needs to be greater than that of the trichlorobenzenes for permeation tubes to be a viable option for gas standard generation (approximately > 100 Pa at 20 ^{o}C).

The duplicate permeation tubes for 1,2-dichlorobenzene were of a similar order of magnitude and differed by 27 %, whilst the standard deviation of the permeation rate for these tubes was ~20 %, based on the smallest mass loss between readings and the mass accuracy of the balance.

Reducing the diffusion length by sandpapering the wall of the naphthalene permeation tube did not significantly change the permeation rate, whilst increasing the permeation area by increasing the length of the permeation membrane (Teflon tubing) did result in a significant increase in permeation rate of 1,2,4-trichlorobenzene.

It can be concluded that permeation tubes are a cost effective means of generating portable gas standards of the more volatile trace organic air pollutants.

2.3 DIFFUSION TUBES

2.3.1 Theory

Diffusion tubes provide a simple and useful means of preparing a mixture of low concentrations of a vapour in a gas, which is based on the diffusion of the vapour from a tube of accurately known dimensions. The technique was originally used to determine diffusion data, but was then used to generate known concentrations of vapours in 1956 (Barratt, 1981). Diffusion tubes are often used for vapour generation from volatile organic liquids, however, they may also be applied to organic solids of sufficiently high vapour pressure.

Diffusion is the process which transports material from one part of a system to another as a result of random molecular motions and concentration gradients, in the absence of mixing (Cho et al., 1992).

Diffusion tubes consist of a reservoir of the pure compound of interest, which evaporates (or sublimates) under constant temperature conditions. The vapour thus generated diffuses along a capillary tube of known dimensions into a flowing gas stream. The rate of diffusion can be determined gravimetrically, and is used in conjunction with the flow rate of the diluent gas in order to calculate the vapour concentration in the resultant gas mixture.

The diffusion rate can also be calculated from theoretical considerations:

$$S = \frac{DMPA}{RTL} \ln \frac{P}{P - p}, \qquad \text{Equation 2.4}$$

where S is the diffusion rate in $g.s^{-1}$; D is the diffusion coefficient ($cm^2.s^{-1}$); M is the molar mass of the compound ($g.mol^{-1}$); P is the pressure in the diffusion cell at the open end of the capillary (atm); A is the cross-sectional area of the diffusion tube (cm^2); R is the molar gas constant ($m\ell.atm.mol^{-1}.K^{-1}$); T is the absolute temperature (K); L is the diffusion path length (cm), and p is the partial pressure of the diffusing vapour at temperature T (atm).

The diffusion rate will only become constant once steady-state conditions have been reached.

This can be estimated from the function (Altshuller and Cohen, 1960):

$$t > \frac{L^2}{2D}, \qquad \text{Equation 2.5}$$

where t is the total time for steady-state conditions to be reached, in seconds.

The diffusion rate can be changed by altering the length or bore of the capillary after sufficient time has been allowed for re-equilibration after such changes have been made. Alternatively, the flow rate of the diluent gas can be varied in order to adjust the volumetric concentration of the vapour of interest, although it is important that this flow rate does not result in turbulent flow regimes at the diffusion tube outlet, which would impact on the diffusion rate. The diffusion rate is also temperature dependant, thus temperature control is very important.

Various diffusion vessel geometries have been successfully utilized in different applications (Barratt, 1981; Namieśnik, 1984). The diffusion tube design used in this research for PAH standards is discussed under section 2.3.2. The use of these tubes was attempted for the PAHs, due to their lower vapour pressures, which prevented the use of permeation tubes for these compounds.

2.3.2 Experimental method

2.3.2.1 Diffusion tube preparation

The diffusion tube assembly consisted of a glass vessel (45 mm long, 8 mm i.d.), which was attached to a glass capillary (35 mm long, 6 mm i.d.) by means of a ground glass joint (Figure 2.7). The PAH standard of interest (naphthalene: Fluka, 99.8 % purity, GC grade; phenanthrene and pyrene: Supelco, 99.9 % and 96.6 % purity, respectively) was placed inside the vessel, and the capillary was then positioned and the joint tightly closed. The diffusion tube was allowed to equilibrate under temperature controlled conditions, and was then weighed at various time intervals to 0.01 mg (Mettler analytical balance).

Figure 2.7: Naphthalene diffusion tube.

2.3.2.2 Diffusion tube usage

The diffusion tube was placed in a glass diffusion chamber, which comprised two portions joined by a tightly sealed ground glass joint, as shown in Figure 2.8. This allowed for easy insertion and removal of the diffusion tube. The diffusion chamber consisted of both an inlet and outlet port for the diluent gas flow. Sufficient re-equilibration time was allowed after insertion of the diffusion tube into the diffusion chamber prior to usage of the device. A

battery operated portable sampling pump was used to draw air at ~ 500 mℓ.min^{-1} into the sample holder and then onto the silicone rubber trap, in order to load the trap with naphthalene, as shown in Figure 2.9.

The GC-MS laboratory room air was also sampled onto a trap for 5 and 60 min, respectively, at 477 mℓ.min^{-1} prior to TD-GC-MS analysis, in order to verify that all the naphthalene present on loaded traps originated from the diffusion tube. Laser laboratory room air was similarly sampled onto a clean trap for 85 min, after a laser induced fluorescence (LIF) scan had been recorded of the blank trap, as detailed in Chapter 3. After sampling, a LIF scan was recorded again. The trap was then end-capped, wrapped in aluminium foil and refrigerated prior to TD-GC-MS analysis.

The loaded silicone rubber traps were thermally desorbed using a thermal desorber system (TDS) (Gerstel TDS 3) and the desorbed analytes were cryogenically focused via a cooled injection system (CIS). The traps were desorbed from 0 °C (0.2 min) to 270 °C (2 min) at 120 °C.min^{-1} in the solvent vent mode (100 mℓ.min^{-1} until 0.2 min). Cryo-focusing of the PAHs was achieved using liquid nitrogen at -40 °C (0.5 min) followed by rapid heating at 12 °C. s^{-1} to 300 °C (1 min). The GC-MS system was an Agilent GC 7890A coupled to a Hewlett Packard 5975 inert XL electron ionisation/chemical ionisation (EI/CI) mass selective detector (MSD). The GC inlet was in the split mode (10:1) with helium (Ultra High Purity, Afrox) as the inlet gas. The flow rate through the column was 1.3 mℓ.min^{-1} at 40 °C. An Agilent HP5 (30 m x 250 µm x 0.25 µm) GC column was used and the column head pressure was 68.8 kPa using helium as the carrier gas. The GC oven was temperature programmed from 40 °C (1.5 min) at 20 °C.min^{-1} to 150 °C (0 min) and at 30 °C.min^{-1} to 300 °C (1 min). The GC-MS transfer line was at 300 °C, the mass scan range was 80-250 atomic mass units (amu), the solvent delay 6.8 min, and the electron multiplier voltage ~1070 V. Calibrations were performed with 1 µℓ naphthalene standard injections onto blank silicone rubber traps (100, 200 and 300 ng for the analysis of the GC-MS laboratory room air, and 50, 250, 500, 1000 and 2000 ng for the analysis of the laser laboratory air samples).

The limit of detection (LOD) of this TD-GC-MS method (CIS split of 10:1) was determined by the analysis of silicone rubber traps onto which 1 µℓ of PAH standards in toluene had been injected (0; 0.2; 1; 2; 4; 8; 20; 40 and 80 ng, respectively).

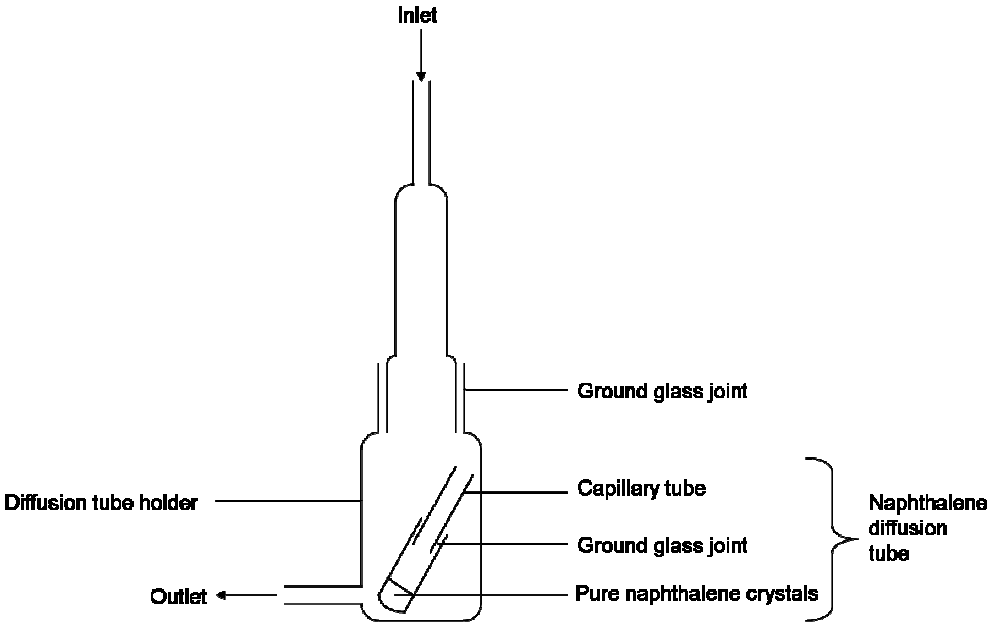

Figure 2.8: Naphthalene diffusion tube inside the diffusion tube holder.

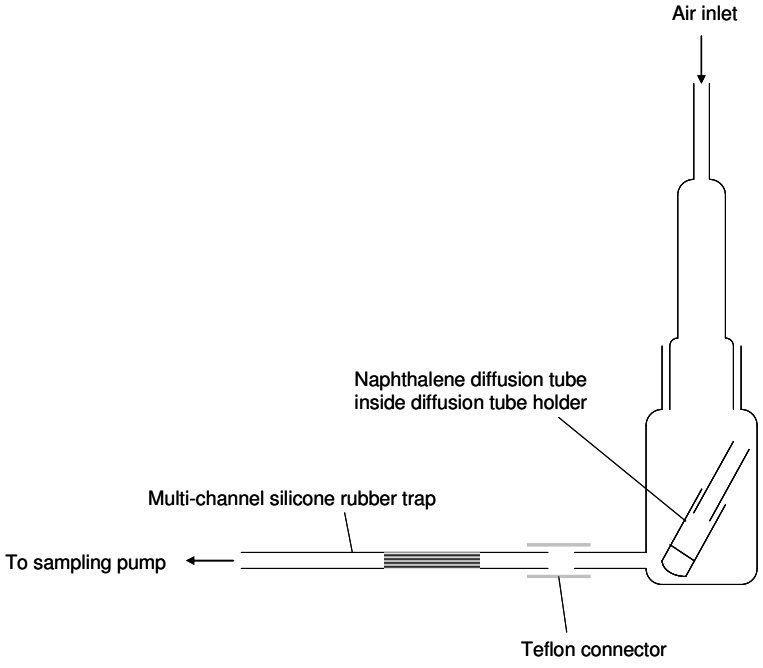

Figure 2.9: Use of the naphthalene diffusion tube to load a silicone rubber trap with gaseous phase standard.

2.3.2.3 Alternative diffusion tube orientation

The direction of air flow through the diffusion tube chamber was reversed, as shown in Figure 2.10, in order to determine whether the flow regime was inducing turbulent conditions, which would impact on the rate of diffusion. A trap was repeatedly loaded for a period of 5 min. TD-GC-MS analyses were performed using the method detailed under section 2.3.2.2, with 50, 100, 200 and 500 ng naphthalene standards and a sample CIS split of 100:1.

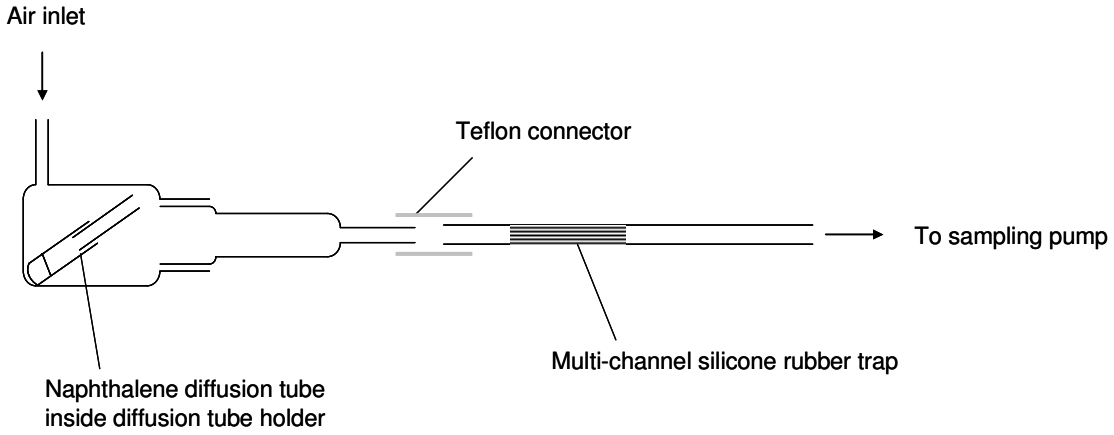

Figure 2.10: Alternative diffusion tube configuration.

2.3.2.4 Evaluation of the effect of air flow on the rate of diffusion

The mass loss of the diffusion tube was determined over a period of 1096 min, whilst placed in the diffusion tube holder and connected to the sampling pump, operating at the usual sampling flow rate of 489 mℓ.min^{-1}, in order to determine whether there were any effects of air flow on the rate of diffusion.

2.3.3 Results and discussion

2.3.3.1 Theoretical calculations

From equation 2.4, diffusion rates were calculated for the diffusion tubes at 20 ^{o}C (due to availability of vapour pressure and diffusion rates at this temperature), and P = 0.859 atm (average atmospheric pressure in Pretoria, South Africa, as obtained from the National Metrology Institute of South Africa, 2007), with R = 82.06 mℓ.atm.mol^{-1}.K^{-1}, as presented in Table 2.2. An average value for the diffusion path length was used for fluoranthene for comparative purposes.

Table 2.2: Theoretical diffusion rates, for L = 35 mm.

Compound	D (cm^2.s^{-1})$^{\#}$	M (g.mol^{-1})	p (atm)$^{\#}$	S (ng.s^{-1})
Naph	0.069	128.2	1.03 x 10^{-4}	3.1
PhA	0.058	178.2	1.58 x 10^{-7}	5.5 x 10^{-3}
FlA	0.055	202.3	1.28 x 10^{-8}	4.8 x 10^{-4}
Py	0.055	202.3	6.02 x 10^{-9}	2.2 x 10^{-4}

$^{\#}$ Obtained from the Danish Environmental Protection Agency (2006).

From these calculations, it is evident that the theoretical diffusion rate for naphthalene was in the low ng.s^{-1} range, whilst that for the other, less volatile PAHs were much lower at pg.s^{-1} levels.

The time required for steady-state conditions to be reached for each of the diffusion tube configurations was calculated from equation 2.5, and are shown in Table 2.3. Steady-state conditions would thus have been reached within 1 – 2 min.

Table 2.3: Time required for steady-state conditions to be reached for the PAH diffusion tubes.

Compound	t (s)
Naph	89
PhA	106
FlA	111
Py	111

2.3.3.2 Experimental results and discussion

The results obtained for the naphthalene diffusion tube over an extended period of ~250 days are presented in Figure 2.11. The linear trendline obtained from this data had an r^2 value of 0.95, which is a reasonable fit. The experimental diffusion rate can be obtained from the slope of this trendline, which was 7.0 x 10^{-6} g.hr^{-1}, or 1.9 ng.s^{-1}. This is in good agreement with the theoretical diffusion rate of 3.1 ng.s^{-1} (refer to Table 2.2), even though there was a high mass ratio of the tube to its contents, and the diffusion path length was relatively short.

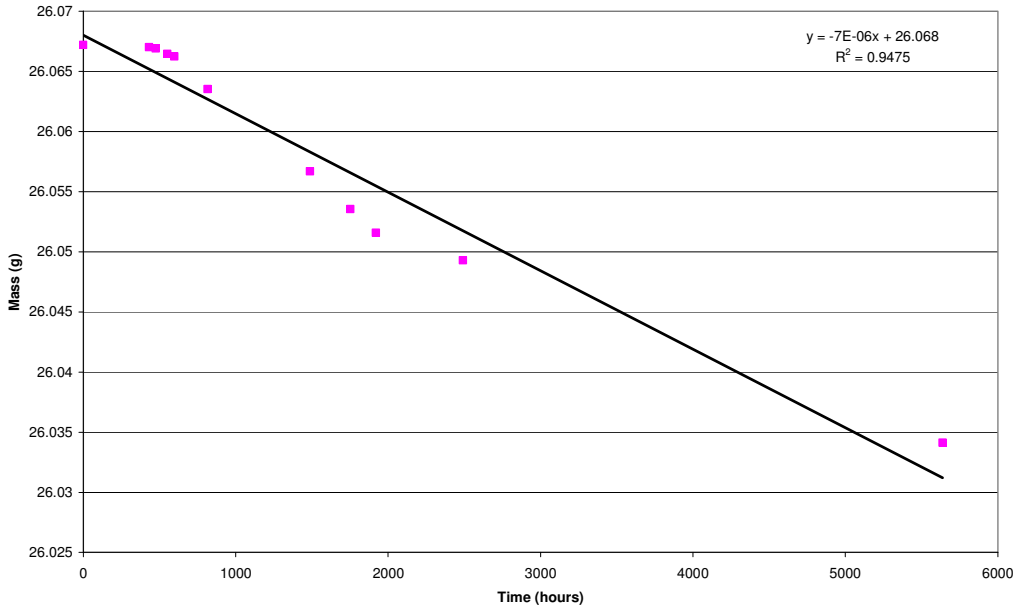

Figure 2.11: Experimental diffusion rate obtained for the naphthalene diffusion tube.

The LOD of the TD-GC-MS method was found to be <0.5 ng for each PAH, where the LOD was based on three times the standard deviation of the blank divided by the slope of the calibration graph for each PAH.

The GC-MS laboratory air loading experiments yielded concentrations of < 1 ng naphthalene after 5 min loading, and ~ 1 ng for a 60 min loading time (using a calibration curve of $y = 3.17 \times 10^3 x$ with $r^2 = 0.98$). There was no difference evident in the LIF spectra of the blank trap and the trap after sampling of the laser laboratory air for 85 min, and subsequent TD-GC-MS analysis of the trap revealed a concentration of 10 ng naphthalene (using a calibration curve of $y = 3.81 \times 10^3 x$ with $r^2 = 0.996$). It was therefore deemed unnecessary to pre-clean laboratory air prior to its passage through the diffusion tube. This had the advantage of not increasing the back pressure through the system.

The gravimetric results for the other two diffusion tubes (phenanthrene and pyrene) showed very low mass changes over an extended period, which made them unsuitable for use as trace gas standards in our study. The diffusion tube containing pyrene, for example, showed a 60 µg loss over a period of approximately 6.5 months; whilst the diffusion tube containing phenanthrene decreased by 120 µg over 5 months (relating to an experimental diffusion rate of 7×10^{-3} ng.s^{-1}). These low diffusion rates are in agreement with the diffusion rates determined theoretically, as shown in Table 2.2, as the diffusion rates were in the pg.s^{-1} range. Although a diffusion tube was not prepared for fluoranthene, the theoretical diffusion rate indicates that the diffusion rate would also be very low for this compound.

The chromatographic peak area for naphthalene doubled when the alternative diffusion tube configuration was employed (calibration curve of $y = 1.38 \times 10^4 x$ with $r^2 = 0.98$), which would indicate that the flow regime of the original configuration was more stable, and was therefore used for trap loading purposes. We ascribe the measured differences to the small length to diameter ratio of the diffusion tube, where even slight turbulence at the tube outlet can alter the diffusion rate of the analyte. This clearly means that wider and shorter tubes should not be used to increase the diffusion rate of the less volatile standards.

A diffusion rate of 2.1 $ng.s^{-1}$ was found under air flow conditions, which is in good agreement with that obtained when there was no air flow, thus it was determined that the air flow was not disturbing the diffusion process.

2.3.4 Conclusion

The theoretical and experimental diffusion rates for the naphthalene diffusion tube showed good agreement, which indicates that the tube can be used as a trace gas standard for naphthalene. Although the capillary was relatively short (the area to length ratio was ~1 mm), constant diffusion rates were obtained.

Diffusion tubes proved to be unsuitable for gas standard generation of the less volatile PAHs (phenanthrene, pyrene, and fluoranthene), due to the very low diffusion rates obtained, which were below that required, and were also too low for accurate gravimetric determinations. This was verified by the theoretical calculations, which gave values in the $pg.s^{-1}$ range for the configurations employed.

The diffusion tube holder geometry allowed for easy gas phase loading of sampling traps, whilst maintaining a constant rate of diffusion for naphthalene at the sampling flow rate of interest (~500 $m\ell.min^{-1}$).

2.4 PDMS TRAP LOADING VIA GAS CHROMATOGRAPHIC FRACTION COLLECTION

2.4.1 Background

In order to load the less volatile PAHs onto traps in the gas phase, an alternative method to permeation and diffusion tubes was needed. Although injection of a liquid standard onto a trap, followed by passing a fixed volume of nitrogen gas through the trap has been reported (Wauters et al., 2008), this method is not ideal for multi-channel silicone rubber traps in the laser induced fluorescence application developed in this study, as it is difficult to equally distribute a small volume of liquid over the 22 inlets of the silicone tubes. It was therefore decided to attempt to load these compounds onto traps by injecting known concentrations of

the individual liquid standard onto a GC column inside a GC oven with collection of the analyte vapour on a trap placed on the flame ionization detector (FID) tip. This method is essentially a chromatographic fraction collection technique, where knowledge of the retention time of the analyte under the GC conditions employed allowed for the collection of the analyte only, and not the solvent or other impurities. A similar method has been used to collect individual components of beer (Lim Ah Tock, 2008) and milk (Naudé et al., 2009) aroma, in this case for organoleptic evaluation of such fractions. The practicality of this collection method is based on the negligible pressure drop of the open tubular structure of the trap, which does not influence the flow rate through the GC column. It was necessary to optimize the experimental setup in order to minimize analyte loss and to maximize trapping efficiencies.

2.4.2 Experimental method

Liquid standards of the PAHs (naphthalene: Fluka, 99.8 % purity, GC grade; phenanthrene, pyrene, fluorene and anthracene: Supelco, 99.9 %, 96.6 %, 98.6 % and 99.0 % purity respectively, GC grade) were prepared in toluene (Riedel de Haen, GC grade, 99.7 % purity), and were manually injected onto an EQUITY^{TM}-5 fused silica capillary column (Supelco, 30 m x 0.25 mm x 0.25 µm) of an Agilent 7890A GC equipped with an FID, which was maintained at 250 ^{o}C. In order to minimize losses at the FID outlet, the top assembly of the detector, as well as the collector/insulator were removed and the multi-channel silicone rubber trap was connected directly to the flame tip by means of a small piece of Teflon tubing and was manually pressed into position at the appropriate time during collection runs. The FID is shown in Figure 2.12 and the experimental setup is presented in Figure 2.13.

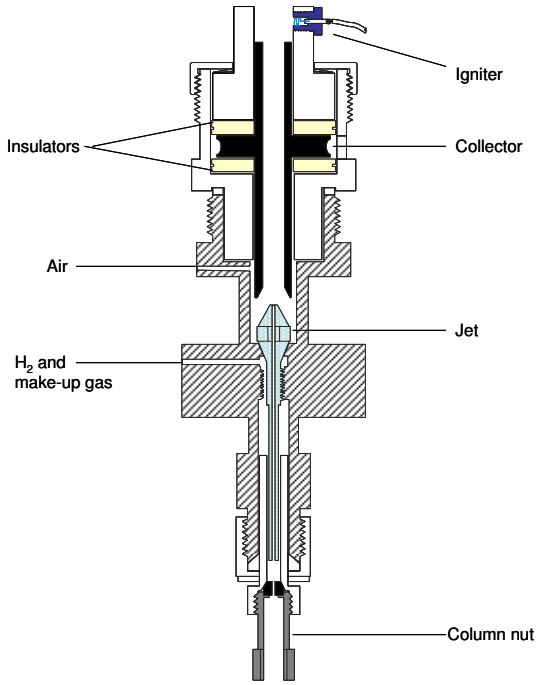

Figure 2.12: Cross section of the Agilent FID (Agilent Technologies, 2008).

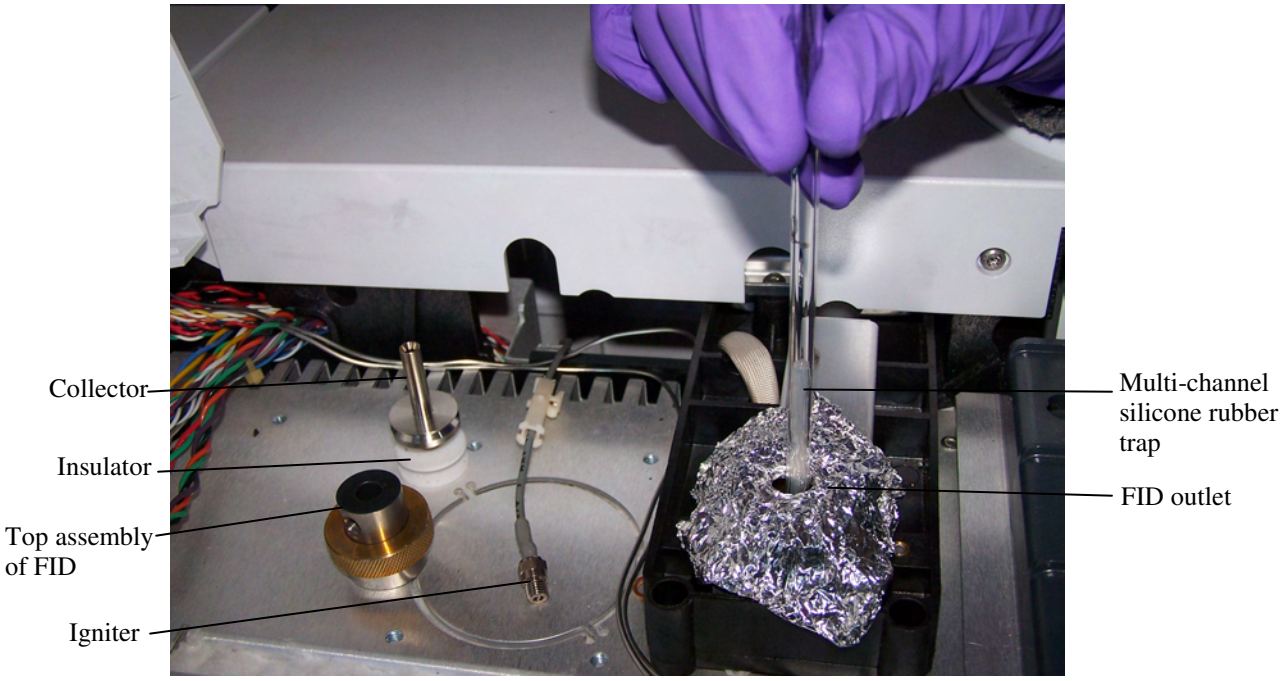

Figure 2.13: Experimental setup for the loading of PAHs onto multi-channel silicone rubber traps from the FID outlet. FID components which were removed from the detector are also shown on the left hand side of the figure.

The efficiency of loading was determined by comparison of TD-GC-MS peak areas obtained for GC loaded traps to that obtained for the direct injection of 1 μℓ of the mixed PAH standard (equivalent to 20 ng of each PAH) initially onto an empty glass tube and later onto a sample trap, as specified for each experiment. A similar TD-GC-MS method to that detailed in section 2.3.2.2 was used with a CIS split of 10:1, except for the analyses of traps relating to sections 2.4.2.1, 2.4.2.2 and 2.4.2.3, where the solvent vent mode was employed (100 mℓ.min^{-1} until 0.1 min). The desorption hold time at 270 ^{o}C was 10 min; the CIS final temperature hold time at 300 ^{o}C was 10 min and the initial GC hold time at 40 ^{o}C was 2 min for all samples.

2.4.2.1 Optimization of the FID make-up flow rate

20 ng of a mixed PAH standard (containing fluorene, anthracene, naphthalene, phenanthrene and pyrene) was injected as 1 μℓ using different FID make-up flow rates: 5; 10; 20; 50 and 100 mℓ.min^{-1}. Initially, after a hold time of 10 min at 40 ^{o}C, the GC oven was ramped to 150 ^{o}C at 20 ^{o}C.min^{-1} and then to 300 ^{o}C at 30 ^{o}C.min^{-1}. PAHs were collected onto a trap between 14 and 21 min and were analysed by TD-GC-MS using an empty glass tube for standard injection comparisons.

In later experiments, the hold time at 40 ^{o}C was decreased to 1.5 min, and the PAHs were collected from the FID outlet from 6 to 14.5 min after injection.

2.4.2.2 Repeatability

a) Initial experiments

Four traps were loaded using the method described under section 2.4.2.1 (10 min GC hold time at 40 ^{o}C). They were then end-capped and refrigerated overnight prior to TD-GC-MS analysis (using standard injections onto empty glass tubes for comparison purposes).

This experiment was then repeated (n = 4) with a slightly shorter PAH collection time from 15 to 21 min.

b) Optimised conditions

The loading method was optimized by shortening the inner Teflon spacer between the FID tip and the trap from 14 mm to 4 mm in order to prevent losses by bringing the trap into closer contact with the flame tip thereby minimizing cooling and contact with the Teflon. The system was checked for leaks by measuring the flow rate of the gas exiting the trap to that of the detector make-up and column flow rate (using a Porter Instrument Company B495 flow meter).

The repeatability experiment was then re-done using a mixed PAH standard (1 μℓ of 20 mg.ℓ^{-1}), with the shorter initial GC hold time and collection at the FID outlet from 6 to 14.5 min after injection (n = 7). Collection efficiencies were determined upon comparison with standards injected directly onto silicone rubber traps.

2.4.2.3 Breakthrough experiments

During the repeatability experiments described under section 2.4.2.2, one trap was loaded whilst a second trap was positioned in series (connected to the primary trap by means of a short piece of Teflon tubing). The secondary trap was then analysed by TD-GC-MS, using injections of standards onto empty glass tubes for comparison.

This experiment was also repeated after optimization of the collection time and the FID connection.

2.4.2.4 Cooling of traps during loading

In order to determine whether losses during loading could be decreased by cooling of the trap, nitrogen vapour from a small liquid nitrogen dewar was directed onto the portion of the trap where the silicone rubber tubes are located (refer to Figure 2.14). Loading was performed with and without cooling 0; 2; 4 and 6 min after injection of 1 μℓ of 50 μg.mℓ^{-1} naphthalene standard (i.e. the most volatile PAH was tested), with n = 2 for each time delay, and the peak areas were compared to direct loading onto a silicone rubber trap. The different time delays post loading were used in order to verify that no naphthalene was lost during the early stages of the process.

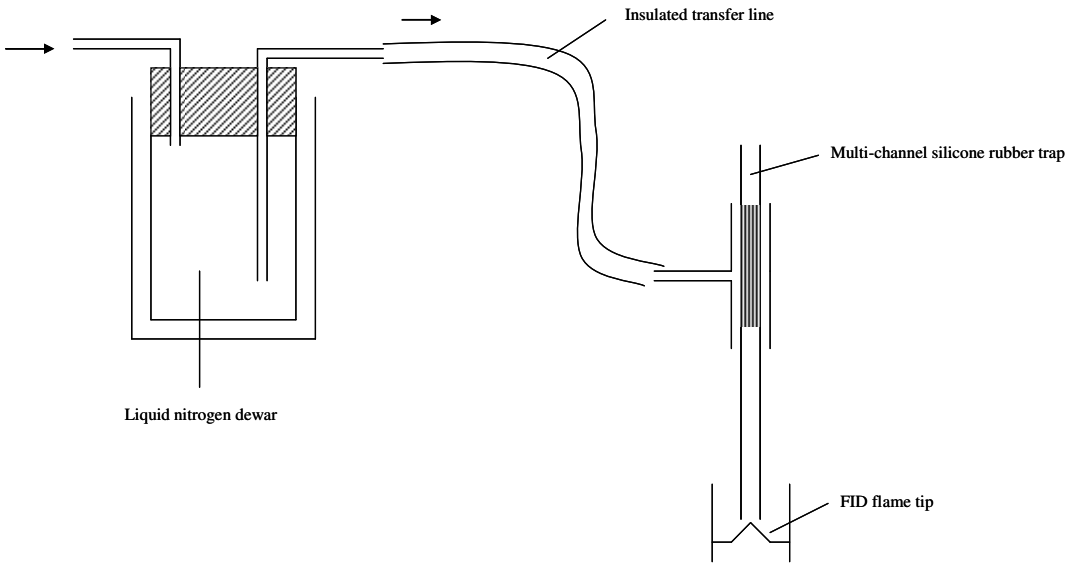

Figure 2.14: Liquid nitrogen cooling during gas chromatographic loading.

2.4.2.5 Stability of loaded traps

In order to determine whether traps could be loaded with phenanthrene and pyrene the day before they were required as standards for analytical method development, five traps were loaded from the FID outlet with phenanthrene and pyrene, respectively (1 μℓ of 100 μg.mℓ$^{-1}$) according to the procedure described under section 2.4.2.1, with the shorter initial GC hold time at 40 ^{o}C and with a three min hold time at 300 ^{o}C. The PAHs were collected onto the traps from 8 to 13 min, after which they were analysed by TD-GC-MS. The results were compared to the analysis of five direct injections of a standard solution (1 μℓ of 100 μg.mℓ$^{-1}$) onto a silicone rubber trap. Three traps were then loaded again with phenanthrene and pyrene, respectively. These traps were end-capped and stored in the refrigerator overnight. They were analysed the next day by TD-GC-MS, and the results were compared to that of direct injection onto a trap.

2.4.3 Results and discussion

When the system was checked for leaks, by measuring the flow rate of the gas exiting the trap to that of the detector make-up and column flow rate, no losses were evident.

2.4.3.1 Optimization of the FID make-up flow rate

The results of these experiments are presented in Figure 2.15. It was decided to proceed with make-up flow rates of 50 mℓ.min^{-1}, as this appeared to give the best recoveries in most cases, particularly for phenanthrene and pyrene, for which gas standard loading was most needed.

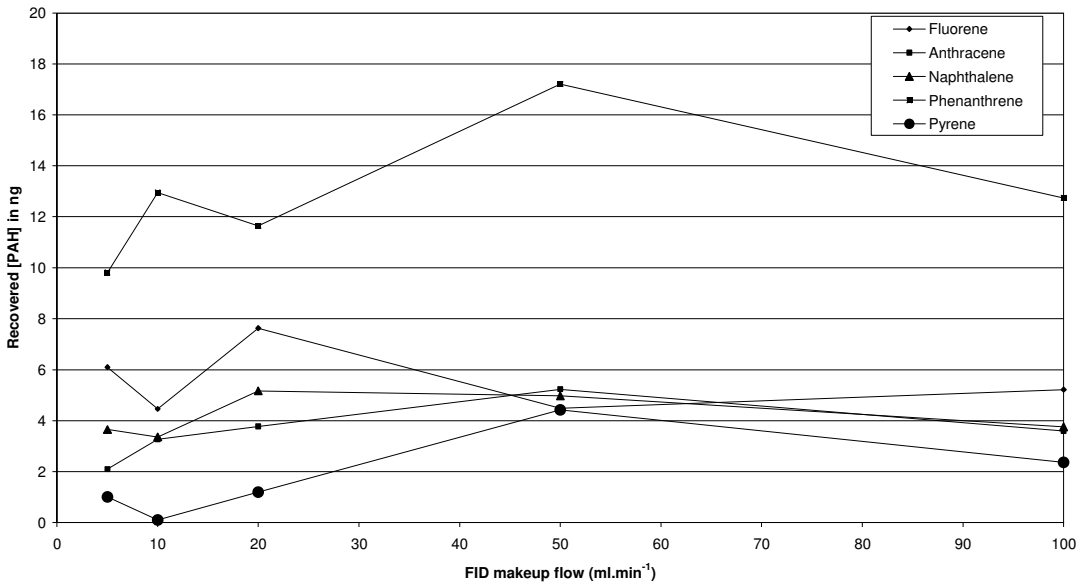

Figure 2.15: Recovery of 20 ng of individual PAHs from multi-channel silicone rubber traps after gas chromatographic loading of a mixed standard using different FID make-up flow rates.

2.4.3.2 Repeatability

a) Initial experiments

The results of the two sets of repeatability experiments are presented in Table 2.4. The delayed collection time improved the repeatability for most of the PAHs, except phenanthrene and pyrene, but decreased the collection efficiency in most cases. It was evident that the collection efficiencies and repeatability required further optimization.

Table 2.4: Percentage recoveries for PAHs from GC loading of a 20 ng mixed standard, using different traps and different collection times.

PAH	Trap A	Trap B	Trap C	Trap D	Average % trapped	% RSD
14-21 min collection, n = 4						
Fluorene	44	35	54	33	41	23
Anthracene	12	18	33	22	21	41
Naphthalene	21	28	39	52	35	38
Phenanthrene	64	68	80	50	66	19
Pyrene	27	48	79	53	52	41
15-21 min collection, n = 4						
Fluorene	26	23	33	25	27	17
Anthracene	27	19	33	26	26	22
Naphthalene	34	19	31	27	28	24
Phenanthrene	74	42	53	72	60	26
Pyrene	40	18	56	40	39	40

b) Optimized conditions

The results of the later set of experiments under optimized conditions (as detailed in section 2.4.2.2 (b)) are presented in Table 2.5.

Table 2.5: Percentage recoveries for PAHs from GC loading of a 20 ng mixed standard using optimized collection conditions.

PAH	Average % trapped	% RSD
6-14.5 min collection, n = 7		
Fluorene	61	12
Anthracene	71	27
Naphthalene	57	14
Phenanthrene	52	18
Pyrene	61	16

It is evident that the recoveries had improved compared to the initial experiments, with the exception of phenanthrene, and that the repeatability had improved.

2.4.3.3 Breakthrough experiments

The peak areas obtained for the secondary trap for each PAH are given in Table 2.6, from which it is evident that breakthrough from the primary trap was minimal (< 1 %).

Table 2.6: Breakthrough of PAHs from the primary trap upon GC loading of a 20 ng mixed standard with a make-up flow rate of 50 mℓ.min^{-1}.

PAH	Primary trap peak area	Secondary trap peak area	% breakthrough
Fluorene	94691	73	0.08
Anthracene	72711	462	0.64
Naphthalene	60610	405	0.67
Phenanthrene	255669	1421	0.56
Pyrene	21751	151	0.69

No significant breakthrough was also found when the experiment was repeated under optimized conditions, as the peak areas found on the secondary trap for each PAH were all less than 0.75 % of the primary trap.

2.4.3.4 Cooling of traps during loading

The results of the experiments conducted with and without cooling are presented in Table 2.7. It is evident that cooling did not improve recoveries, but actually had a negative impact. Cooling was therefore deemed unnecessary and was not used in the final method. The collection efficiency was poorer for earlier (and therefore longer) collection times, which was most likely due to the breakthrough volume of naphthalene on the trap being exceeded under these conditions, leading to loss of the analyte. Collection was therefore only conducted from 6 min after injection in the final loading method.

Table 2.7: Effect of trap cooling on analyte recoveries and repeatability during GC loading (n = 2 for each time interval).

Delay between injection & loading (min)	**0**	**2**	**4**	**6**	**Direct injection onto trap**
With cooling					
% recovery	30	47	43	51	100
% RSD	50	9	16	14	8
Without cooling					
% recovery	35	66	76	75	100
% RSD	40	24	1	1	9

2.4.3.5 Stability of loaded traps

The results of these experiments are summarized in Table 2.8. The recovery of GC loaded traps was ~50 % for both phenanthrene and pyrene when compared to direct injection, and the recovery did not decrease significantly when the loaded traps were stored overnight. The repeatability was generally good, with % RSDs of less than 15 %, with the exception of the stored phenanthrene traps, which had a % RSD of 29 %. This may have been improved by increasing the number of stored traps analysed.

Table 2.8: Effect of storage of GC loaded traps on analyte recoveries.

PAH	Direct loading n = 5	GC loading, immediate analysis n = 5	GC loading, stored overnight n = 3
Phenanthrene			
Average peak area	173 635	94 865	87 824
% RSD	6	10	29
% recovery	100	55	51
Pyrene			
Average peak area	172 019	85 360	92 944
% RSD	11	12	5
% recovery	100	50	54

2.4.4 Conclusion

It was found that there were no detectable gas leaks from the experimental setup described, and that an FID make-up gas flow of 50 mℓ.min^{-1} was best for loading purposes. Repeatability experiments revealed that % RSDs of < 20 % were possible with a short Teflon connection between the FID outlet and the silicone rubber trap. Analyte was collected over a period of ~8 min and recoveries were 57; 52; and 61 % for naphthalene, phenanthrene, and pyrene, respectively, based on loading of 20 ng of each PAH via a 1 µℓ injection of a mixed standard. As the repeatability was fairly good, correction for losses can be made by injection of a larger amount of analyte. It is possible that losses occur via the mandatory septum purge flow on the split/splitless injector. It was verified that complete analyte desorption occurred during TD-GC-MS analysis, as no significant concentrations of the PAHs of interest were detected upon a second desorption analysis, therefore losses due to incomplete desorption are not likely.

Experiments on the effect of the presence of solvent in traps analysed by TD-GC-MS indicated an increase in peak area with increase in solvent volume up to 20 µℓ and even resulted in peak splitting in some cases. Solvent injection volumes onto traps or empty tubes, as appropriate, were therefore maintained at 1 µℓ for calibration and comparison purposes, although it is possible that this effect contributed to the perceived losses.

No significant breakthrough occurred for any of the PAHs investigated under the loading conditions employed, as evidenced from the analysis of a secondary backup trap. Cooling of the trap during loading did not improve recoveries and storage overnight did not significantly decrease the recoveries obtained.

It was later found that slight carryover between loading runs was occurred in some cases (refer to Chapter 3, section 3.2.3), therefore it is advisable to bake out the system between loading events.

The loading of PAHs, specifically phenanthrene and pyrene, via GC injection of liquid standards and collection of the vapours on the GC outlet was therefore shown to be a viable means of loading less volatile analytes onto the silicone rubber traps in the vapour phase. This method allowed for the comparison of LIF and GC-MS analyses of the less volatile PAHs, as described in Chapter 3, and is cost effective for laboratories equipped to analyse the analytes of interest, where standards and GC equipment is available. It offers the additional advantage of loading analytes after capillary chromatographic purification in cases where high purity standards are not readily available and may find application in other spectroscopic studies.

2.5 OVERALL CONCLUSION

In trace gas analysis, it is important that reliable gas standards can be produced at concentrations which are appropriate both in terms of the relevant applications as well as the method detection limits. In addition, portability and cost are also important factors. Various means of generating gas standards have therefore been developed.

In our study, the permeation tubes we prepared were found to be a cost effective means of providing portable gas standards for the more volatile trace organic air pollutants, such as chlorobenzene and the dichlorobenzenes, with permeation rates in the range of a few to ~40 ng.min^{-1}. Constant permeation rates were obtained within a month from manufacture, and duplicate tubes had permeation rates of a similar order of magnitude. Storage of the permeation tubes adjacent to activated charcoal or inside a fumehood is necessary, as permeation is a constant process.

Of the PAHs which were investigated, only the naphthalene diffusion tube had a sufficiently high rate of diffusion to be of experimental use in our studies (~2 $ng.s^{-1}$). Good correlation was found in this case between the theoretical and experimental diffusion rates, which was not altered by the flow of gas through the diffusion tube holder. Steady-state conditions were calculated to be attained in under 5 min. Diffusion tubes are therefore a useful, cost-effective and portable means of generating gas phase standards for the somewhat more volatile trace organic air pollutants, but are not suitable for the heavier semi-volatile compounds. Storage considerations are also relevant here, as diffusion is a constant process, as for permeation.

Vapour loading of liquid injected analytes at the FID outlet of a GC via the fraction collection technique developed here proved useful for the PAHs which were less volatile than naphthalene, specifically phenanthrene and pyrene. Repeatability experiments revealed that % RSDs of < 20 % were possible and recoveries were of the order of 50-60 %, based on the loading of 20 ng of each PAH via a 1 $\mu\ell$ injection of a mixed standard. Possible reasons for the low recoveries include losses at the manual injection inlet during trap loading, or errors in comparing peak areas of FID loaded traps with peak areas obtained with liquid standards for recovery calculations. No significant breakthrough occurred from the multi-channel silicone rubber traps during loading for any of the PAHs investigated under the conditions employed. Although this method is not portable, it is cost effective for laboratories equipped to analyse the analytes of interest, where standards and GC equipment is available. It offers the additional advantage of loading analytes after capillary chromatographic purification in cases where high purity standards are not readily available.

It has been shown that the methods and devices investigated have different applications, based on the volatility of the analyte of interest. It is possible to generate gas standards using devices which are not costly and do not require sophisticated apparatus in manufacture or use, therefore they have potential application in developing countries for trace organic air pollutant method research and development, as well as implementation.

2.6 REFERENCES

Agilent Technologies, *Gas Chromatograph Detectors*, **2008**.

Altshuller, A.P. and Cohen, I.R., *Analytical Chemistry*, **1960**, *32* (7), 802-810.

Barratt, R.S., *Analyst*, **1981**, *106* (1265), 817-849.

Cho, K., Irvine, T.F. and Karni, J., *International Journal of Heat and Mass Transfer*, **1992**, *35* (4), 957-966.

Danish Environmental Protection Agency, **2006**, Guidelines on remediation of contaminated sites, Appendix 5.5 Physical and chemical data, accessed on 17 February 2006 at http://www.mst.dk/udgiv/publications

Lim Ah Tock, M.J., April **2008**, Aroma analysis of alcoholic beverages using multi-channel silicone rubber traps, MTech Thesis, Tshwane University of Technology.

Merck, **1999**, ChemDat ®, The Merck Chemical Database, 99'2, available on CD.

Mitchell, G.D., *Separation and Purification Methods*, **2000**, *29* (1), 119-128.

Naganowska-Nowak, A., Konieczka, P., Przyjazny, A. and Namieśnik, J., *Critical Reviews in Analytical Chemistry*, **2005**, *35*, 31-55.

Namieśnik, J., *Journal of Chromatography A*, **1984**, *300*, 79-108.

National Metrology Institute of South Africa, personal communication with Angelique Botha, **2007**.

Naudé, Y., van Aardt, M. and Rohwer, E.R., *Journal of Chromatography A*, **2009**, *1216* (14), 2798-2804.

O'Keeffe, A.E. and Ortman, G.C., *Analytical Chemistry*, **1966**, *38* (6), 760-763.

Scaringelli, F.P., O'Keeffe, A.E., Rosenberg, E. and Bell, J.P., *Analytical Chemistry*, **1970**, *42* (8), 871-876.

Temime, B., Francois, S., Monod, A. and Wortham, H., *Environmental Pollution*, **2002**, *120*, 609-616.

Wauters, E., Van Caeter, P., Desmet, G., David, F., Devos, C. and Sandra, P., *Journal of Chromatography A*, **2008**, *1190*, 286-293.

Chapter 3

Laser induced fluorescence of atmospheric polycyclic aromatic hydrocarbons

3.1 INTRODUCTION

Polycyclic aromatic hydrocarbons (PAHs) are emitted from a number of anthropogenic sources, including combustion processes. They are of environmental concern due to their potential toxicity, particularly carcinogenicity. PAH monitoring campaigns have thus been conducted globally, focusing on such sources as vehicles (Marr et al., 1999 and 2004; Tang et al., 2001; Koziel et al., 2001; and Odziemkowski et al., 2001), biomass burning (Yang et al., 2006; Hays et al., 2003; Fang et al., 1999; and dos Santos et al. 2002) and incineration (Chiang et al., 1992).

PAHs consist of aggregates of condensed aromatic rings (as shown in Figure 3.1), which may be formed from low molar mass hydrocarbons via pyrosynthesis at temperatures above 500 ^{o}C, under oxygen deficient conditions. Free radicals are formed upon cleavage of the carbon-carbon and carbon-hydrogen bonds of these hydrocarbon precursors. The radicals then undergo dehydrogenation and combine to form aromatic ring structures. PAHs may also be formed from free radicals produced during pyrolysis of higher alkanes (Manahan, 2000).

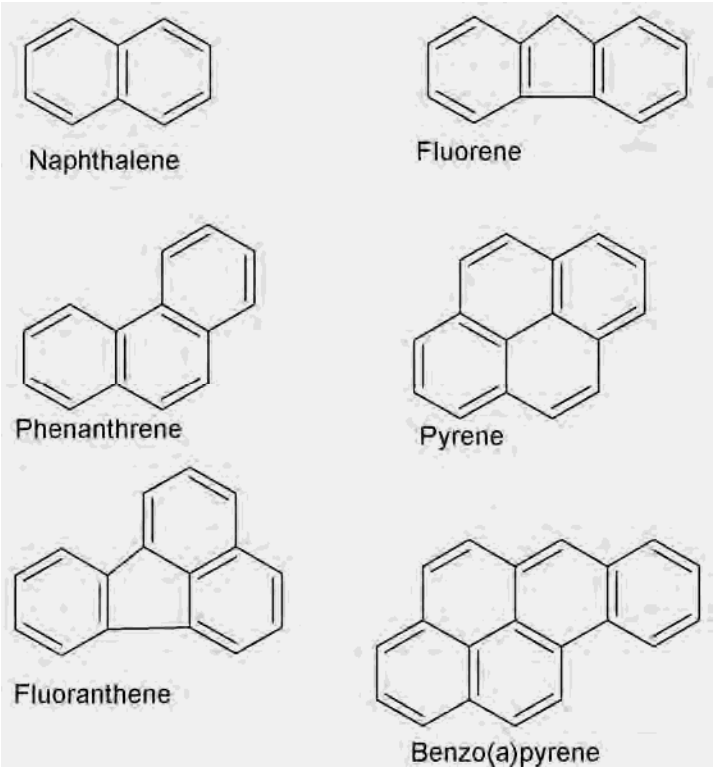

Figure 3.1: Structure of selected PAHs.

The larger ring structures (> 5 rings) are usually predominantly particle bound under ambient conditions, whilst the smaller species (2- and 3-ring PAHs) are usually in the gas phase, with 4- membered rings being found in both phases (Ohura et al., 2004a and Ono-Ogasawara and Smith, 2004). In terms of health effects, it is important that both of phases be monitored (Chang et al., 2006 and Westerholm et al., 1991).

3.1.1 Problem statement and aim

Current analytical methods for atmospheric PAH determinations are time consuming and usually require the use of solvent extraction of samples. This may limit the widespread sampling and analysis of PAH samples for spatial and temporal trend determinations.

A technique was therefore to be developed and investigated, which would allow for the rapid screening of samples for the presence of PAHs, prior to comprehensive, quantitative analysis, if required.

This method would be based on the sampling of air onto a multi-channel silicone rubber trap, in which the polydimethylsiloxane (PDMS) serves as a solvent for the analyte species. The inert nature of the silicone minimizes the possibility of artifact formation and the low pressure drop across the trap allows for a large volume of air to be drawn through the traps by means of a small, battery operated portable pump. Two traps can also be coupled in series, in order to verify the absence of breakthrough of analytes from the first trap.

Laser-induced fluorescence (LIF) was to be employed to selectively excite the PAH(s) of interest on the trap, and the resulting fluorescence would be determined at the wavelength characteristic for the target PAH. The technique would be basically non-destructive, thus enabling the subsequent GC-MS analysis of samples of interest, for example those containing the target analytes at levels exceeding a specified threshold concentration. It would also lend itself to real-time monitoring and the provision of chemical "finger-prints" via the fluorescence spectra (Gridin et al., 2000).

This chapter provides a background to PAHs in the environment and the use of fluorescence based methods for monitoring these compounds. The development and optimization of our laser induced fluorescence screening method is then described, including the results of repeatability, sensitivity, breakthrough volume and photodegradation studies.

3.1.2 PAHs in the environment

PAHs are classified as persistent organic pollutants, and may be subject to long range atmospheric transport. Although man has a long history of burning materials, such as coal, oil, petrol and wood, which inevitably has resulted in substantial releases of PAHs worldwide, they were first subjected to international emission controls under the United Nations Economic Commission for Europe protocol in 1998 (Prevedouros et al., 2004).

PAHs are derived from a number of different sources, and it has been found that the specific PAHs present in an atmospheric sample can be used as source fingerprints, as indicated in Table 3.1.

Table 3.1: Main PAHs emitted from various sources, which can be used for source fingerprinting (Harrison et al., 1996).

Source	**PAH markers**
Coal combustion	Anthracene; phenanthrene; fluoranthene; pyrene; benz(*a*)anthracene; chrysene
Coke production	Anthracene; phenanthrene; benz(*a*)pyrene; benzo(*ghi*)perylene
Incineration	Phenanthrene; fluoranthene; pyrene
Wood combustion	Anthracene; phenanthrene; fluoranthene; pyrene
Oil burning	Fluoranthene; pyrene
Petrol fueled automobiles	Fluoranthene; pyrene; benzo(*ghi*)perylene; coronene
Diesel fueled automobiles	Similar to petrol fueled automobiles

Emission inventories for the United Kingdom (UK) estimated that domestic burning contributes ~80 % of the total PAH emissions annually, and four PAHs, namely phenanthrene, fluoranthene, fluorene and pyrene, contributed ~75 % to this total (Lohmann et al., 2000). Another UK source inventory and budget estimated that over 100 tons of PAHs are emitted into the UK atmosphere per annum from primary combustion sources, with over 95 % derived from domestic coal burning, unregulated fires and vehicle emissions (Wild and Jones, 1995).

In a European study spanning 22 countries, which was based on passive polyurethane foam (PUF) sampling of PAHs, fluorene, phenanthrene, fluoranthene, pyrene, chrysene and 1-methylphenanthrene were detected in all samples (Jaward et al., 2004). Three- and four-ring PAHs, specifically phenanthrene, fluorene, fluoranthene and pyrene, also comprised ~90 % of the total PAHs detected in a similar passive sampler campaign in Kuwait, with phenanthrene contributing ~35 % (Gevao et al., 2006).

These trends are to be expected when considering the information presented in Table 3.1, as it is evident that phenanthrene, fluoranthene and pyrene are emitted from most of the sources, thus they were chosen as the PAHs of interest in this study, as further elaborated under section 3.1.6.

As previously mentioned, PAHs are of environmental concern due to their potential toxicity. Exposure to naphthalene, for example, which can be smelled at a concentration of 84 ppb in air (Agency for Toxic Substances and Disease Registry (ATSDR), 2005), may lead to hemolytic anemia, as a result of damage and destruction of red blood cells. Naphthalene is also a possible human carcinogen (EPA Group C rating) (ATSDR, 2005).

As naphthalene was covered in most detail in our study, due to the analytical challenges it presented, the sources of this compound are of relevance. The main source of naphthalene is from the burning of wood and fossil fuels, followed by the use of moth repellents. Studies have been conducted to determine naphthalene (and *p*-dichlorobenzene and camphor) concentration profiles in a wardrobe containing moth repellents, using passive sampling onto PDMS stir bars for 120 hours, although equilibrium is reached after approximately 2 hours (De Coensel et al., 2008), where the results indicate momentary concentrations to which the stir bars are exposed. Solvent extraction of exposed clothing indicated that the clothing could also serve as a secondary source of airborne naphthalene, as a result of re-volatilisation.

Gasoline and diesel engine exhausts, with concomitant vaporization from fuels, was found to contribute almost half of the total daily naphthalene burden in human exposure studies conducted in Southern California (Lu et al., 2005), where naphthalene average hourly exposure levels were estimated at between 270 and 430 $ng.m^{-3}$ for summer and winter, respectively.

Cigarette smoking also releases small amounts of naphthalene into the air, at a rate of between 40 and 110 µg per cigarette. 10 % of naphthalene entering the environment is from coal production and distillation, and less than 1 % is from losses during naphthalene production from coal tar or petroleum (ATSDR, 2005). Naphthalene is an intermediate in the production of phthalic anhydride, which is used in the production of phthalate plasticizers, pharmaceuticals, insect repellents and other materials. Naphthalene has also been used as an intermediate in the production of other chemicals for use in leather tanning, as surfactants, and so on. Due to these sources, as well as the use of naphthalene in many consumer products, including multipurpose solvents, lubricants, charcoal lighters, degreasers and hair spray,

naphthalene indoor air concentrations of 1000 to 2200 ng.m^{-3} have been reported in various studies (Lu et al., 2005).

A range of concentrations of PAHs in air have been reported, and are summarized in Table 3.2. A strong seasonality in measured ambient concentrations is evident in many studies, which is attributed to increased emissions from combustion sources for heating during the winter, as well as enhanced degradation of PAHs by sunlight during summer. It should be noted that other meteorological conditions besides solar radiation, such as wind speed and temperature also have significant impacts on the atmospheric concentrations of PAHs (Chang et al., 2006). A negative correlation was found between wind speed and concentrations of phenanthrene and anthracene, for example (Prevedouros et al., 2004).

Table 3.2: Summary of selected reported atmospheric PAH concentrations. Note: PM_{10} refers to particulate matter of size ≤ 10 micron.

[a] Gundel et al., 1995; [b] Šišović et al., 2008; [c] Chang et al., 2006; [d] Odabasi et al., 1999; [e] Jaward et al., 2004; [f] Ohura et al., 2004a; [g] Park et al., 2002.

PAH	Average indoor air ($ng.m^{-3}$) [a]	Suburban PM_{10} PAH in summer ($ng.m^{-3}$) [b]	Suburban PM_{10} PAH in winter ($ng.m^{-3}$) [b]	Thailand traffic (gas + particle) ($ng.m^{-3}$) [c]	China traffic (particle) ($ng.m^{-3}$) [c]	Korea urban (gas + particle) ($ng.m^{-3}$) [c]	Japan traffic (particle) ($ng.m^{-3}$) [c]	Taiwan urban (gas) ($ng.m^{-3}$) [c]	Taiwan urban (particle) ($ng.m^{-3}$) [c]	Thailand traffic (gas + particle) ($ng.m^{-3}$) [c]	Average Chicago ambient air ($ng.m^{-3}$) [d]	European ambient air ($ng.m^{-3}$) [e]	Japan indoor air (summer) ($ng.m^{-3}$) [f]	Japan indoor air (winter) ($ng.m^{-3}$) [f]	Seoul ambient total ($ng.m^{-3}$) [g]
Naphthalene	338					11.2		283	10.2	9570			1130	955	11.23
Phenanthrene	23					16.5	4.2				200.3	0.24-26	28.4	8.82	16.46
Fluoranthene	6.5	0.13	4.22					53.7	5.2	154	44.1	0.012-13.2	2.57	1.11	8.10
Pyrene	3.0	0.12	4.17		0.30	12.6	42	53.3	1.2	134	24.6	0.012-7.3	1.81	0.832	12.56
Acenaphthene and acenaphthylene	8.3				0.01	3.35; 7.39		118	8.3	200	76.9		8.93	5.18	3.35; 7.39
Fluorene	8.2			0.02	0.03	6.46	25				74.8	0.1-7.3	11.2	4.17	6.46
Anthracene	0.4			0.21	0.29	2.07		105	4.1	103	14.1	<0.004 -1.2	0.739	0.185	2.70
Benz(*a*)anthracene	0.4			1.06	0.36	2.62	11	19.2	1.1	31.5	2.1	0.004-0.6	0.118	0.162	2.62
Chrysene	1.4			1.12	0.55	3.62					3.6	0.006-1.3	0.284	0.331	3.62
Benzo(*b*)fluoranthene				0.94	0.53		3.0	6.7	2.4	154	2.3		0.497	0.528	
Benzo(*a*)pyrene				1.7	0.67	2.55	11	1.8	0.9	121	1.6	<0.004 -0.25	0.240	0.343	2.55

In a Japanese study, the gaseous PAH concentrations in both indoor and outdoor air were higher in summer than in winter, whilst the opposite trend was true for particle-bound PAHs (Ohura et al., 2004a), as would be expected. The gaseous indoor PAH concentrations were mostly derived from insect repellents and heating sources, whilst that of indoor particulate PAH was a result of cigarette smoking and was also related to the age and type of wood from which the house was constructed and outdoor PAH concentrations.

Urban centres in the United Kingdom have been found to have PAH concentrations of 1-2 orders of magnitude higher than that found in rural Europe, and up to 3 orders of magnitude higher than Arctic Canada (Prevedouros et al., 2004). In a medium traffic area in Rome, a slightly decreasing trend in annual PAH mean values was noted from 1994-1998 (Menichini et al., 1999).

Semi-rural ambient concentrations of gaseous naphthalene of 13.1 - 45.2 $ng.m^{-3}$ and urban levels of 70.2 - 167.4 $ng.m^{-3}$ have been reported in France (Temime-Roussel et al., 2004), whilst in urban Greece, the most abundant PAHs (gas + particles) were phenanthrene (20.0 $ng.m^{-3}$), pyrene (6.6 $ng.m^{-3}$) and fluoranthene (6.5 $ng.m^{-3}$) (Tsapakis and Stephanou, 2005).

The overall environmental fate of PAHs in the context of different environmental compartments (air, water, soil, etc), is summarized in Figure 3.2, from which it can be seen that there are various means by which PAHs may be removed from the atmosphere including degradation, deposition and precipitation. The effect of precipitation on less volatile PAHs is greater than that on the more volatile PAHs (such as naphthalene and phenanthrene), as the less volatile PAHs tend to be associated with particles which can be washed out during precipitation (Subramanyam et al., 1994). Soil has been identified as the major repository in the UK for PAHs (Wild and Jones, 1995).

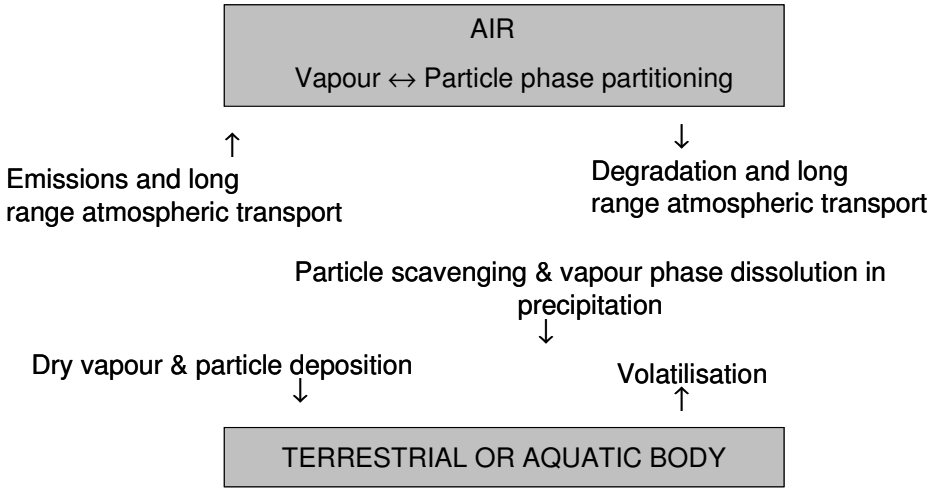

Figure 3.2: Environmental fate of PAHs (adapted from Prevedouros et al., 2004).

Gas phase PAHs present in the atmosphere may undergo various reactions with reactive species, such as the hydroxyl radical. PAHs, especially the larger ring structures, are sensitive to electrophilic substitution and to oxidation (Nikolaou et al., 1984). Reported atmospheric lifetimes of selected gas phase PAHs are summarized in Table 3.3.

Table 3.3: Atmospheric lifetimes of gas-phase PAHs, based on reaction with reactive species (USA EPA, 2002).

PAH	**OH•** at 1.6 x 10^6 molecules.cm^{-3} (12 h average)	**O_3** at 7 x 10^{11} molecules.cm^{-3} (24 h average)	**NO_3** 5 x 10^8 molecules.cm^{-3} (12 h average)
Naph	6.8 h	> 80 days	1.5 years
PhA	11.2 h	41 days	4.6 h
FlA	~2.9 h	-	~1 year
Py	~2.9 h	-	~120 days

It is evident that the hydroxyl radical is the most important species in removing these gas phase PAHs from the atmosphere, and would result in their removal in under a day. Particulate phase PAHs have been found to undergo long range transport from Asia to North America and atmospheric lifetimes of particulate phase PAHs are reported to be in the order of a week (Primbs et al., 2008).

Photodegradation of PAHs in the environment is also an important atmospheric removal process, and will be discussed under section 3.2.4.

Microbial degradation is of relevance to PAHs which have been deposited onto soil, although due to the high hydrophobicity of PAHs, they are not readily available for microbial degradation, as bacteria degrade compounds dissolved in water (Johnsen et al., 2005). This is of particular concern for high molecular weight PAHs, due to their lower water solubilities. The dense cloud of π-electrons above and below the PAH ring structures also makes them resistant to nucleophilic attack, however degradation pathways have been proposed (Zhang et al., 2006).

3.1.3 Fluorescence characteristics of PAHs

The spectroscopic features of PAHs include large absorption cross-sections and high fluorescence quantum yields (Song et al., 2003), thus fluorescence has been used as a means of detection of these compounds in applications such as HPLC for many years (for example, NIOSH methods 5506 and 5800, 1998). Enhanced sensitivity of HPLC-based PAH methods over GC-MS based methods have also been reported (Ohura et al., 2004a). Fluorescence excitation and emission wavelengths pertaining to the PAHs of interest in this study are given in Table 3.4, which are based on room temperature fluorescence of PAHs on extraction membranes.

Table 3.4: Reported fluorescence excitation and emission wavelengths for selected PAHs, with preferred wavelengths given in bold (Whitcomb et al., 2002).

PAH	Excitation wavelength (nm)	Emission wavelength (nm)
Naph	281; **292**	323; **337**
PhA	258; 279; 286; **298**	**388**; 407
FlA	292; **365**	465
Py	278; 326; **341**	386; **395**; 474

Fluorescence detection was also one of the methods used, in addition to ultraviolet (UV) and visible analysis, to determine PAHs in column chromatography derived benzene extracts of urban air particulates by Sawicki et al. in 1960, as well as for the analysis of PAHs in thin layer chromatography extracts of traffic related aerosol samples (Handa et al., 1980). The detection limits relating to HPLC fluorescence detection for the PAHs of interest in this study are included in Table 3.5, and are based on a signal to noise ratio of 2:1. Other studies have reported limits of quantitation for PAHs of < 0.1 ng.m^{-3} (Šišović et al., 2008).

Table 3.5: HPLC fluorescence detection limits of selected PAHs, based on a signal to noise ratio of 2:1 (Harrison et al., 1996).

PAH	Detection limit (ng)
Naph	0.43
PhA	0.49
FlA	0.85
Py	0.48

The aromatic rings of PAHs serve as *chromophores*, as the delocalized π-electron systems exhibit characteristic UV-visible absorption spectra. The most probable electron transitions are π → π*, which thus have the most intense absorption bands in the absorption spectra of these compounds (except for naphthalene, where such transitions are forbidden) (Schwarzenbach et al., 2003).

A *bathochromic shift* occurs as the number of aromatic rings increases, in that the absorption maximum of the lowest energy π → π* transition generally shifts to lower energies

(Schwarzenbach et al., 2003). This allows for different size classes of PAHs to be selectively detected based on their fluorescence: excitation with wavelengths < 300 nm results in fluorescence of PAHs containing 2-3 aromatic rings at 300-450 nm; whilst PAHs containing > 4 aromatic rings will tend to fluoresce at 300-700 nm, with the fluorescence maximum generally in the visible region of the spectrum (Vander Wal et al., 1997).

It should be noted, however, that not only the number of aromatic rings, but also the way in which they are fused together, influences the absorption spectrum of PAHs, as does the physical state of the PAH and the presence of solvent.

The fluorescence quantum yield is defined as the ratio of the number of photons emitted to the number of photons absorbed. Molecules with higher quantum yields may therefore be determined at lower concentrations compared to those with lower quantum yields, and the sensitivity of the method will be enhanced. Quantum yields and fluorescence lifetimes of the PAHs of interest in this study are given in Table 3.6. It is evident that naphthalene does not have as high a fluorescence quantum yield as pyrene, for example, thus it is expected that the detection limit obtained for naphthalene will not be as low as for pyrene. The fluorescence lifetimes reported are in the order of ns, with pyrene having the longest fluorescent lifetime of 450 ns.

Table 3.6: Fluorescence lifetimes and quantum yields for PAHs of interest (as reported in Kumke et al., 1995).

PAH	**Florescence lifetime (τ_F) (ns)**	**Quantum yield (Φ_F)**
Naph	96	0.23
PhA	57.5	0.13
FlA	53	0.30
Py	450	0.65

The fluorescence is affected by the presence of solvents, which may lead to redshifting, such as that found in the fluorescence spectrum of pyrene dissolved in cyclohexane as compared to that in the vapour phase, which was ascribed to solvent stabilization effects (Chi et al., 2001).

Fluorescence bandwidths in vapour phase samples tend to broaden with increase in sample temperature, due to thermal vibrational sequence congestion effects, although the fluorescence intensity of pyrene increased with increase in temperature, as a consequence of an increase in the absorption cross-section at the excitation wavelength of 337 nm at elevated temperatures (Chi et al., 2001).

3.1.4 Literature review of the use of laser induced fluorescence in the monitoring of PAHs

Quantitative analysis of vapour phase PAHs at elevated temperatures (> 150 ^{o}C) by LIF, utilizing an excitation wavelength of 337.1 nm, has been reported (Chi et al., 2001 and Allain et al., 2003). Pyrene in cigarette smoke has been determined by LIF based on fiber optics with time resolution to enhance sensitivity (Song et al., 2003), and similar systems have been developed for PAH determinations on aerosols (Panne et al., 2000) and in water (Kotzick and Niessner, 1996). Again excitation at 337 nm was utilized, due to the ease of obtaining this wavelength by means of a nitrogen laser, and the system was time-resolved. A disadvantage of fibre optic based systems is the distortion of the fluorescence spectra in the (usually long) fibres that are employed (Kotzick and Niessner, 1996). A similar fibre optic based system, which utilized a frequency doubled excimer pumped dye laser, was developed for the detection of particle-bound PAHs, which allowed for excitation wavelength tunability (Niessner et al., 1991).

Mixtures of PAHs are difficult to separate into component concentrations when analyzing at a single wavelength, thus deconvolution algorithms have been employed in this regard, although only mixtures of ≤ 3 components could be effectively treated in this manner (Kotzick and Niessner, 1996; Knorr and Harris, 1981). The technique reported here employs a number of (shorter) wavelengths, allowing for improved selectivity and the detection of two- and three-membered ring structures.

The on-line monitoring of airborne PAHs by LIF and multi-photon ionization is described by Gridin et al., 2000. Here the sample gas was bubbled through a quartz measurement chamber containing hexane and the emitted fluorescence was collected by means of an optical fiber. Detection limits of 1 mg.m^{-3} were obtained for pyrene and naphthalene.

Two-photon excitation fluorescence microscopy, where each photon contributes a portion of the energy necessary to excite the molecule, has been used to visualize the fate and behaviour of PAHs (anthracene, phenanthrene and fluoranthene) within living vegetation (Wild et al., 2005 and Wild et al., 2007). Such studies are important in the context of understanding the environmental fate of picogram amounts of PAHs, which may be taken up by vegetation from the air and soil, and may then undergo processes such as transportation and storage within the plant. This is a significant advancement on previous methods for this application, which are largely destructive or damaging to the plant. A pulsed solid state laser, which scanned over the sample, was used for excitation purposes. Fluorescence microscopy has also been employed for the qualitative analysis of PAH contaminated soils (Roper et al., 2006).

In addition, LIF coupled with fiber optics has been employed in the determination of PAHs in soils and sediments (Grundl et al., 2003). Solid-phase extraction onto octadecyl membranes has been used to monitor PAHs in aqueous solutions with LIF detection of the analytes pre-concentrated on these membranes (Whitcomb et al., 2002). Detection limits at the parts per trillion level were achieved.

Naphthalene has been detected in air using the Fluorescent Assay by Gas Expansion (FAGE) technique, where the gas phase analyte (without pre-concentration) is excited by laser pulses at 308 nm passing through a detection chamber (Martinez et al., 2004). Quenching of naphthalene fluorescence by N_2 and O_2 in the air sample was reported.

The graphite furnace has been used as a vapourisation source for laser induced fluorescence of PAHs from engine exhaust and cigarette smoke (Kirsh and Winefordner, 1987).

Commercial PDMS solid-phase microextraction (SPME) fibers have been employed in the sampling of airborne particulate matter, such as that arising from diesel vehicular exhausts, followed by GC-MS analysis (Koziel et al., 2001). SPME fibers have also been used in aqueous PAH determinations, coupled with fluorescence microscopy (Mayer et al., 2000), as well as single-particle analysis by Raman spectroscopy (Odziemkowski et al., 2001). SPME utilizing a 50 μm coating of PDMS on a glass fiber rod coupled with LIF detection has

recently been tested for PAH determinations in sediment pore water (Hawthorne et al., 2008). The larger volume of PDMS present in the sampling traps used in our study, however, allows for larger sampling volumes and therefore potential improvements to the detection limits of the method.

3.1.5 The role of screening methods in PAH analysis

Internationally accepted analytical methods for environmental monitoring are based on comprehensive techniques in order to ensure accuracy and precision of the results obtained. These methods for PAHs are based on sampling ~300 m^3 of air onto an adsorbent (typically XAD-2 resin) or a PUF cartridge and a filter, followed by solvent extraction and pre-concentration (often also incorporating sample cleanup using liquid chromatography) (Liu et al., 2007). The liquid extract is then analysed by GC-MS (USA EPA based methods), or by HPLC with UV or fluorescence detection (Japanese Ministry of the Environment based methods) (Ono-Ogasawara and Smith, 2004). There are also additional steps in the procedure, which involve the use of (isotopically-labelled) standards to check for both extraction and analytical recoveries. Extensive cleanup of the sorbent may be required prior to use due to the presence of contaminants, where naphthalene for example, has been detected at ~5 $ng.m^{-3}$ in XAD-2 resin blanks (Ohura et al., 2004a). Methods have been adapted to shorten sample preparation time such as by the use of accelerated solvent extraction (Ravindra et al., 2008), ultrasonic extraction, and supercritical fluid extraction of PAHs from sample matrices, as alternatives to traditional Soxhlet extraction.

Comprehensive methods are time consuming and costly to perform, thus screening methods which can be used to isolate samples of interest for detailed analysis using internationally accepted best practice, may find application in studies to understand the temporal and spatial variations in the concentration of PAHs, where many samples would need to be analysed. There is also a greater need for cost saving screening methods in developing countries, where access to funds and instrumentation may be limited.

In terms of screening studies for PAHs, Shekiro et al. (1988) developed a method for this purpose based on electrothermal vaporization - multiple-wavelength spectrometry, using an electrothermal atomizer usually used for atomic absorption spectroscopy and a photodiode

array detector. The vapour phase absorption of the sample was thus recorded over the 200-350 nm region. A liquid sample was injected into the device, which was then heated to remove the solvent prior to measurements being taken. This method therefore requires solvent extraction of samples prior to analysis, and the more volatile PAHs (particularly naphthalene) may be lost during the drying step. Spectral overlap is also a problem with this method, although determination limits of 0.05 μg were reported.

Other reported methods for PAH screening include those based on photoelectric aerosol sensors (Tang et al., 2001) and UV-induced photoemission (Hart et al., 1993), however these devices do not provide speciation information and do not detect vapour phase PAHs, which is of particular importance for the lower molar mass, more volatile PAHs.

Passive samplers have been developed in order to save costs and to allow for sampling in remote areas away from a power supply. These samplers include SPME devices made from PDMS (Liu et al., 2007) and the use of PUF disks, which sample PAHs at ~3-4 m^3 of air per day (Jaward et al., 2004). In the latter study, samplers were exposed for a six week period in 22 European countries, which allowed for an understanding of the long range transport of these chemicals.

A recent review article on analytical methods for PAHs in airborne particulates (Liu et al., 2007) noted the following areas as being important for further method development:

- Avoidance of volatilization and loss of PAHs during sampling
- Prevention of the reaction of PAHs and other compounds and redistribution of PAHs between different particle sizes
- Development of a noiseless and lower-volume sampler
- Removal of the need for sample pretreatment in a cost effective manner.

The method developed in this study sought to address a number of these needs.

3.1.6 Choice of PAHs to be studied

The choice of PAHs on which to focus this work was based on the concentrations at which they are emitted from sources, as well as their ubiquity in the environment (refer to

section 3.1.2), and the environmental concerns associated with them. It was important that the chosen analytes would be present at concentrations which could be measurable by the proposed LIF screening method, and they could thus be used as indicators for those PAHs usually present at far lower concentrations which are also of environmental concern. Good correlations have been found, for example, between phenanthrene concentrations (which averaged at 200 $ng.m^{-3}$) and the concentrations of PAHs with molecular masses between 154 and 202 (average concentrations ranged from 6 to 77 $ng.m^{-3}$) (Odabasi et al., 1999).

Although the lighter PAHs have lower carcinogenic properties than benzo(*a*)pyrene, for example, which has a toxic equivalency factor of 1 as compared to that of 0.001 for naphthalene, fluoranthene, phenanthrene and pyrene (Nisbet and LaGoy, 1992), they are the most abundant PAHs in the urban atmosphere and they may react with other pollutants to form more toxic derivatives (Odabasi et al., 1999). It has been found in some studies that the carcinogenicity of indoor air is dominated by naphthalene, and that this PAH was the most abundant in all samples (summer and winter), reaching 1100 $ng.m^{-3}$ in summer (Ohura et al., 2004a). Ohura also suggested the use of naphthalene as a surrogate compound for PAH mixtures in indoor air, and others have also reported the importance of naphthalene as a marker for PAH contamination (Wauters et al., 2008). The use of fluoranthene as an indicator compound for more toxic PAHs has similarly been recommended (Boström et al., 2002).

It has been noted in previous studies that there is a serious lack of data on low molecular weight PAHs and vapour phase emissions from some combustion sources, which may lead to significant underestimations of inputs of PAHs into the environment (Wild et al., 1995).

Naphthalene (Naph), phenanthrene (PhA), fluoranthene (FlA) and pyrene (Py) were therefore identified from the USA EPA list of 16 priority PAHs as suitable test analytes. An additional consideration for focusing primarily on naphthalene, was due to the analytical challenges it presents as the most volatile PAH.

3.1.7 Multi-channel silicone rubber traps

Due to the generally low environmental levels of organic air pollutants, pre-concentration of the analytes prior to analysis is necessary. This can be achieved during

sampling by means of traps which extract the analytes of interest from the sample air stream by adsorption or sorption processes (Baltussen et al., 1998). Common adsorptive traps are based on Tenax TA (a polymer of 2,6-diphenyl-*p*-phenylene oxide), XAD-2 and polyurethane foam (PUF), for example, whilst polydimethylsiloxane (PDMS) has been used in various configurations in sorptive samplers, including the use of mixed bed traps containing PDMS foam, PDMS particles and Tenax TA for the sampling of PAHs in air (Wauters et al., 2008). Adsorptive traps have the disadvantages of artifact formation, high background concentrations (therefore cleaning prior to usage is necessary) and irreversible analyte loading, although they generally have high capacities. Sorptive samplers are based on the reversible transfer of the analyte into the sorptive medium (PDMS), therefore breakthrough volumes are an important consideration in the utilization of these traps (Baltussen et al., 1997). Silicone degradation products are usually evident in the chromatograms obtained upon sample analysis, and can be easily identified by mass spectrometry.

Multi-channel silicone rubber traps, as first described by Ortner (1994), were utilized in this study, which comprised 22 parallel PDMS tubes of 0.3 mm i.d. housed in a quartz tube (refer to section 3.2.1.2b). Quartz was used due to its well known transparency in the UV-visible region. PDMS was found to absorb at wavelengths below 300 nm, which may impact on the excitation process but should not affect the sensitivity of the method as fluorescence emission wavelengths longer than this can be selected for the PAHs of interest.

The operation of the trap can be viewed as a gas chromatography column, where the gas phase organic analyte partitions between the stationary phase (PDMS) and the air flowing through the trap. The breakthrough volume (V_b) of the trap may be defined as the sample volume at a particular flow rate, at which 10 % of the total concentration of analyte which is entering the trap is exiting the trap at the outlet. The breakthrough volume will be smaller for higher sampling flow rates, due to the smaller number of theoretical plates (N) generated under these conditions, whilst V_b will be larger at low flow rates (refer to equation 3.1). The retention volume (V_R) is, however, independent of the flow rate.

$$V_b = V_R\left(1-\frac{2}{\sqrt{N}}\right) \qquad \text{Equation 3.1}$$

The more volatile analytes, such as naphthalene, will also have lower V_b than the less volatile compounds, such as pyrene. The determination of breakthrough volumes is discussed under section 3.2.3.

3.2 DEVELOPMENT OF THE LIF METHOD

3.2.1 Initial method development

3.2.1.1 Background

The first series of experiments which were conducted to provide an indication of the viability of the use of LIF to monitor PAHs sampled onto quartz multi-channel silicone rubber traps, were based on liquid injections of PAH standards onto these traps. Initially benzo(*a*)pyrene was used, but due to the toxicity of this compound, and for reasons discussed in section 3.1.6, naphthalene was subsequently used for method development. This section describes the initial experiments conducted and the results obtained, as well as the laser system used. In later experiments, gas phase standards were provided by diffusion tubes and gas chromatographic fraction collection, as described in Chapter 2.

3.2.1.2 Experimental method

a) Liquid standards

Benzo(*a*)pyrene (ChemService, > 95 % purity) and naphthalene (Fluka, 99.8 % purity, GC grade) PAH standards were prepared in AR grade toluene (99 % purity, Merck). These standards were loaded onto the silicone rubber traps by liquid injection; or by evaporation from a bulk liquid holding vessel of the liquid naphthalene standard (for qualitative experiments), where a portable GilAir pump was used to draw the analyte-loaded air through the trap at a pre-determined flow rate (measured by means of a bubble flowmeter).

b) Multi-channel silicone rubber traps

Multi-channel silicone rubber traps were prepared in 178 mm long quartz tubes of 4 mm i.d. and 6 mm o.d., according to the method described by Ortner (1996). This involved

folding a length of PDMS tubing the required number of times and then threading it through the quartz tube using a hairpin shaped wire. The looped ends of the tubing were then cut through using a scalpel. In these experiments, each trap contained twenty two 55 mm polydimethylsiloxane channels (0.64 mm o.d., 0.3 mm i.d., Sil-Tec, Technical Products, USA) (and one trap contained sixteen 90 mm long PDMS tubes denoted as a "long trap"). Some of the traps were prepared by the author and the remainder were prepared by a supervised laboratory technician at the University of Pretoria. The traps were conditioned before use by heating in a GC oven at 300 ^{o}C for ~24 hrs with a hydrogen carrier gas flow of ~60 mℓ.min^{-1}. After use, the traps were re-conditioned at 250 ^{o}C under nitrogen gas flow for 2 hours in a Gerstel Tube Conditioner (TC1).

c) Laser setup

An excimer laser (Lambda Physik EMG201) was used to optically pump a dye laser (LC6200 dye for benzo(*a*)pyrene and Rhodamine 6G dye for naphthalene, both dyes were supplied by Lambda Physik). Rhodamine 6G is *o*-(6-ethylamino-3-ethylimino-2,7-dimethyl-3H-xanthen-9-yl) benzoic acid ethylester, as shown in Figure 3.3.

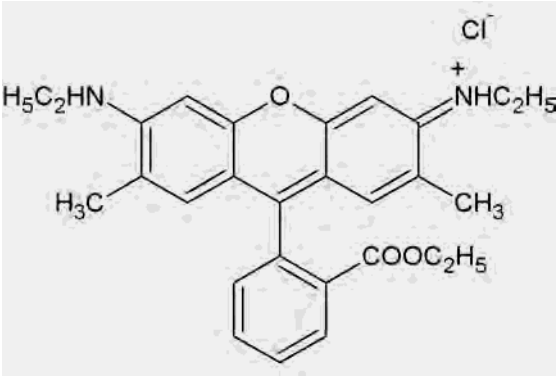

Figure 3.3: Chemical structure of Rhodamine 6G.

An intra-cavity grating allowed for wavelength tuneability over the gain bandwidth of the dye, and ensured a narrow bandwidth output (0.1 cm^{-1} at 495 nm). In the case of naphthalene, the 584 nm output beam was frequency doubled through second harmonic generation in a non-linear crystal (beta barium borate (BBO)), resulting in the desired 292 nm excitation laser wavelength (302 nm was obtained for benzo(*a*)pyrene). The unconverted

pump wavelength was filtered out using a prism arrangement. The 292 nm laser beam had a pulse energy of roughly 500 μJ in a 30 ns pulse. This laser beam was directed onto the silicone rubber trap without any focusing elements resulting in a roughly 5 mm diameter spot at the trap. The resulting fluorescence was optically collected with a plano-convex lens (f = 75 mm), and resolved with a scanning double monochromator (Kratos, Schoeffel Instruments) equipped with a photomultiplier tube (PMT). Results were recorded on a PC linked to an oscilloscope (Tektronix TDS 360).

The initial experimental setup is shown graphically in Figure 3.4. The layout of the system was later optimized and the final configuration is shown in Figure 3.5. It should be noted that for later experiments, the pinhole diaphragm was removed, and both a folding prism and an enhanced UV coated aluminium mirror were placed between the Pelin Broker crystal and the silicone rubber trap. These adjustments were needed due to other experiments being conducted in the laser laboratory, which were in the original path of the laser beam.

Similar experiments were attempted for naphthalene using the frequency doubled output from an Optically Pumped Parametric Oscillator (OPPO) laser (Lambda Physik Scanmate), which was pumped with a 10 Hz Continuum laser. Less than 100 μJ of energy reached the sample, which proved to be insufficient and therefore experiments were resumed using the dye laser system.

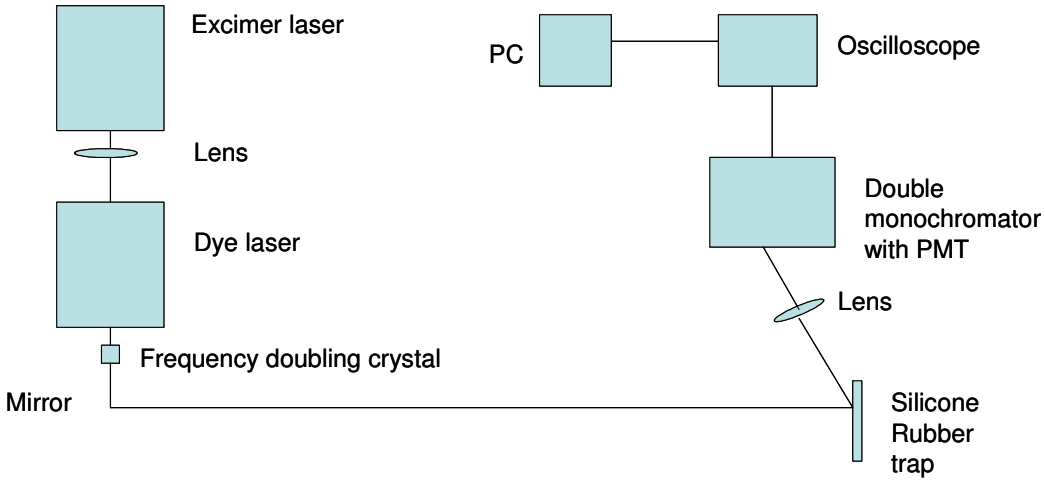

Figure 3.4: Initial experimental setup for the dye laser system.

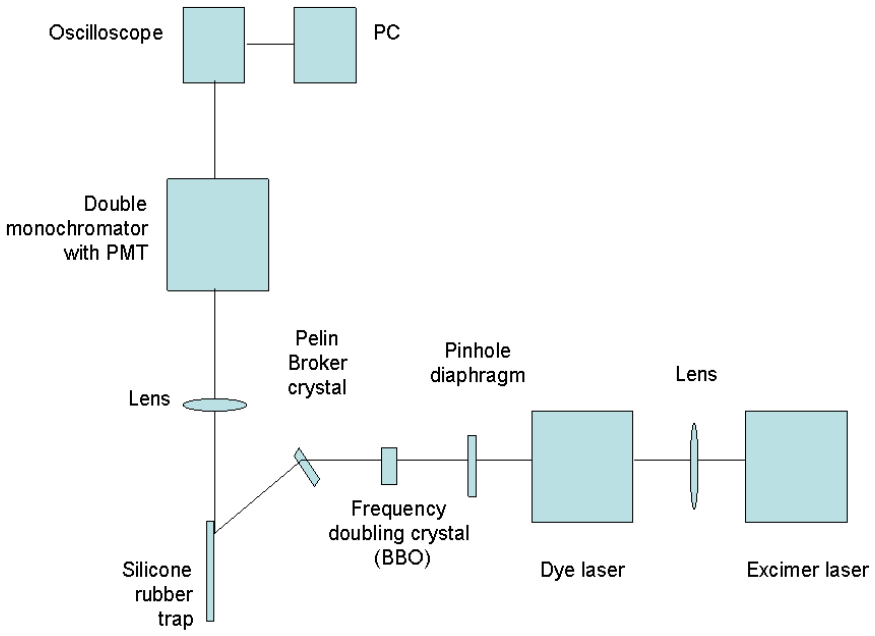

Figure 3.5: Final experimental setup for the dye laser system.

3.2.1.3 Results and discussion

The spectra obtained by liquid injection of standards onto the trap provided a first approximation of the detection limits of the method. These were in the order of 30 ng for both benzo(*a*)pyrene and naphthalene (for a signal-to-noise ratio of 3:1), as shown in Figures 3.6 and 3.7.

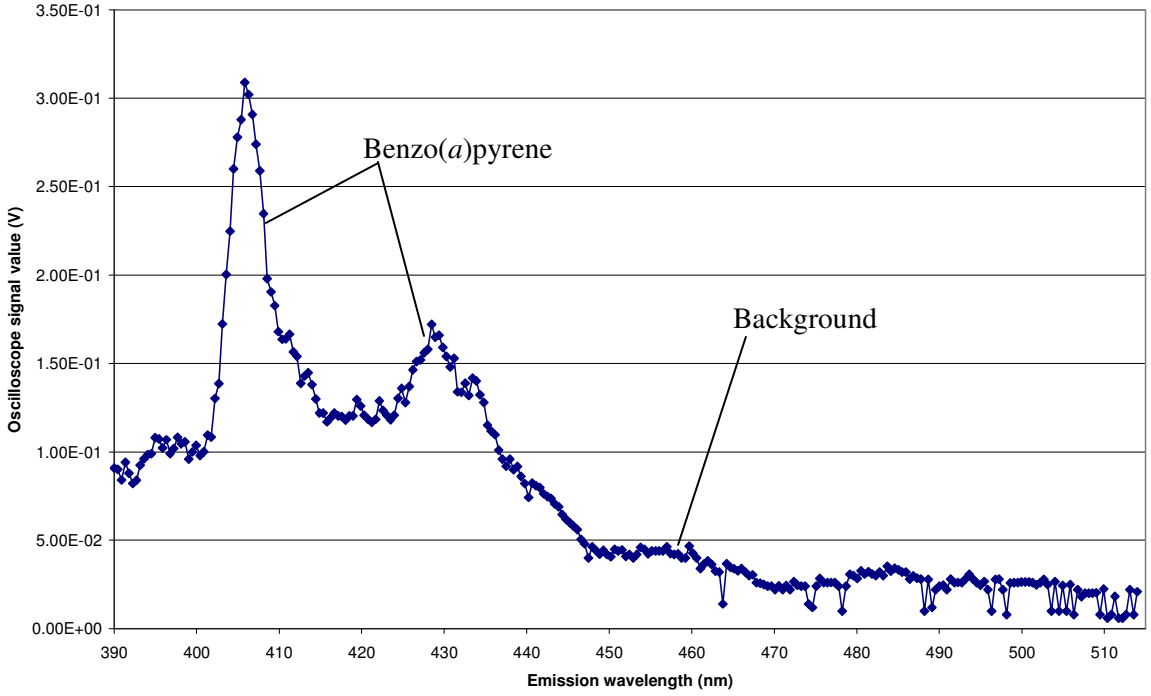

Figure 3.6: Fluorescence spectrum obtained for 27 ng of benzo(*a*)pyrene on a quartz multi-channel silicone rubber trap, with 302 nm excitation.

The well-documented fluorescence maximum of benzo(*a*)pyrene at 406 nm is clearly evident from Figure 3.6, which was obtained upon the injection of 1 μℓ of a liquid standard onto a silicone rubber trap.

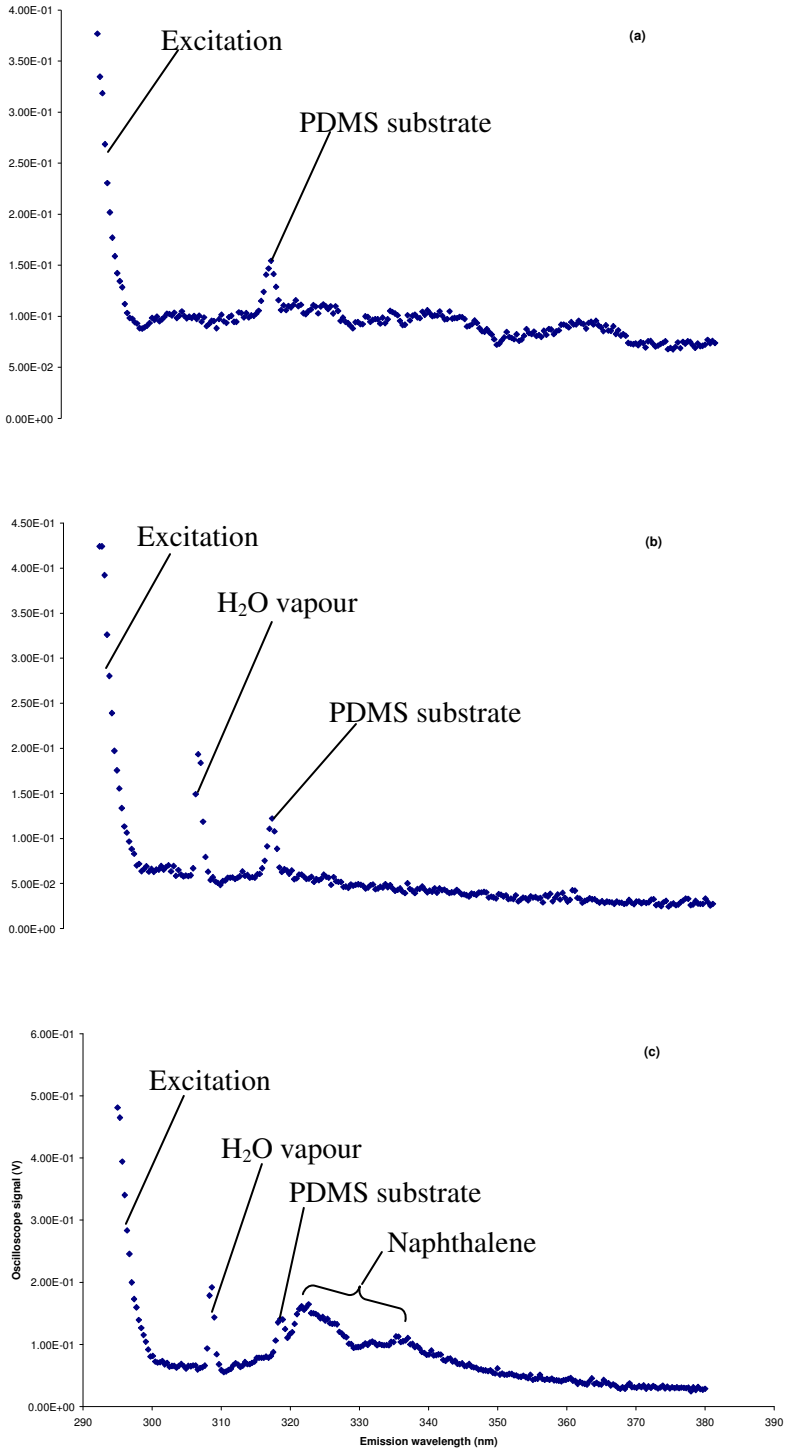

Figure 3.7: Fluorescence spectrum of (a) a blank quartz silicone rubber trap; (b) a quartz silicone rubber trap with laboratory air flowing through it at 580 mℓ.min^{-1}; and (c) a quartz silicone rubber trap containing 30 ng of naphthalene (added as a liquid standard). All spectra were obtained with the dye laser system operating at an excitation wavelength of 292 nm.

Similarly, 30 ng of naphthalene (injected onto a trap as 1 μℓ of liquid standard in toluene) was detected by means of excitation at 292 nm, with a characteristic emission around 323 nm evident (Figure 3.7). The signal-to-noise ratio was not as good as in the case of benzo(*a*)pyrene, possibly due to the smaller absorption cross-section of PAHs containing fewer aromatic rings. Volatilisation of naphthalene from the trap during analysis is also possible due to its lower vapour pressure, leading to sample loss.

The spectra of the blank trap and that of laboratory air flowing though the trap are included in Figure 3.7. It is evident from these that the peak at 319 nm most likely arose from the PDMS substrate, whilst that at 309 nm was due to humidity in the ambient laboratory air.

Experiments conducted with the introduction of naphthalene onto the trap in the gas phase via volatilization of liquid standard placed in a glass vessel upstream of the sample trap, whilst drawing air through the system at approximately 100 mℓ.min^{-1}, indicated that the solvent was not impacting significantly on the results.

3.2.1.4 Conclusion

These initial experiments indicated that this LIF method had potential for use as a screening tool for atmospheric PAH monitoring, and an approximate limit of detection of 30 ng was obtained for benzo(*a*)pyrene and naphthalene in this unoptimised system. It was also shown that the solvent did not have a significant impact on the fluorescence results when liquid PAH injections were performed. Due to the intended use of the method for atmospheric monitoring, however, a more accurate and quantitative means of achieving gas phase introduction of the PAHs was needed, and therefore naphthalene diffusion tubes were used in future experiments, as described in Chapter 2.

3.2.2 Repeatability of the method

3.2.2.1 Background

The repeatability of an analytical method is important to ensure that samples containing the same concentration of an analyte yield the same response from the detector, and that the

extent of any variation is quantified. In the case of the LIF method developed in this study, it was also important to determine the variation in detector signals obtained for different blank traps, as this has an impact on the detection limit of the method, which is covered in section 3.2.3. The effect of slight variations in loaded trap positioning in the LIF system was also explored.

3.2.2.2 Experimental method

a) *Diffusion tube loading repeatability: GC-MS experiment*

In order to determine the contribution of variations in diffusion tube loading of naphthalene to the amount detected by LIF in repeat experiments, TD-GC-MS analyses were first conducted on repeatedly loaded traps.

The silicone rubber traps were thermally desorbed using a thermal desorber system (TDS) (Gerstel TDS 3) and the desorbed naphthalene was cryogenically focused via a cooled injection system (CIS). The traps were desorbed from 0 °C (0.2 min) to 270 °C (2 min) at 120 °C.min^{-1} in the solvent vent mode (100 mℓ.min^{-1} until 0.1 min). Cryo-focusing of the PAHs was achieved using liquid nitrogen at -40 °C followed by rapid heating at 12 °C. s^{-1} to 300 °C (1 min). The GC-MS system was an Agilent GC 7890A coupled to a Hewlett Packard 5975 inert XL EI/CI mass selective detector (MSD). The GC inlet was in the split mode with helium (Ultra High Purity, Afrox) as the inlet gas. An Agilent HP5 (30 m x 250 µm x 0.25 µm) GC column was used and the column head pressure was 68.8 kPa using helium as the carrier gas. The total flow rate of the gas was 40.3 mℓ.min^{-1} for a split ratio of 30:1, where the split flow was 39 mℓ.min^{-1}, thus the flow rate through the column was 1.3 mℓ.min^{-1} at 40 °C. The GC oven was temperature programmed from 40 °C (1.5 min) at 20 °C.min^{-1} to 150 °C (0 min) and at 50 °C.min^{-1} to 300 °C (0 min). The GC-MS transfer line was at 300 °C, the mass scan range was 80-250 atomic mass units (amu), the solvent delay 6.8 minutes, and the electron multiplier voltage ~1070 V.

It should be noted that for the later analyses of traps containing other PAHs (such as pyrene and phenanthrene), this TD-GC-MS method was adjusted slightly in that the desorption was from 0 °C (0.2 min) to 270 °C (1.5 min) at 120 °C.min^{-1} in the solvent vent mode (100 mℓ.min^{-1} until 0.2 min). Cryo-focusing of the PAHs was achieved using liquid nitrogen

at -40 °C followed by rapid heating at 12 °C.s $^{-1}$ to 300 °C (10 min). The GC oven was temperature programmed from 40 °C (10.5 min) at 20 °C.min $^{-1}$ to 150 °C (0 min) and at 30 °C.min^{-1} to 300 °C (1 min).

After a blank TD-GC-MS analysis had been performed on a conditioned multi-channel silicone rubber trap, it was loaded with naphthalene from a diffusion tube (as discussed in Chapter 2) for a period of 5 minutes, at a flow rate of 493 mℓ.min^{-1}. The trap was then analysed by TD-GC-MS using a CIS split ratio of 30:1 with the TDS in solvent vent mode. The gas phase loading of naphthalene was repeated three times; and the experiment was then repeated three times with another trap.

After the first TD-GC-MS analysis of the gas phase loaded trap, it was analysed again which proved that no naphthalene remained on the trap after analysis (it was equivalent to a blank), thus a second desorption analysis was deemed unnecessary and was not repeated.

The GC-MS laboratory room air was also sampled onto a trap for 5 and 60 minutes, respectively, at 477 mℓ.min^{-1}, and laser laboratory room air was similarly sampled onto a clean trap for 85 min in order to verify that all the naphthalene present on loaded traps originated from the diffusion tube, as described in section 2.3 of Chapter 2.

b) *LIF experiments*

i) Variations in detector response to blank trap signals

Fluorescence spectra of seven blank multi-channel silicone rubber traps were recorded from 290 to 470 nm, with 292 nm excitation, and the energy of the incident beam at the trap location was measured by means of a Gentec energy meter. These experiments were conducted over two days, with one trap being analysed on both days for comparative purposes.

ii) Variations in detector response to similarly loaded traps

A conditioned multi-channel silicone rubber trap was loaded with naphthalene from a diffusion tube, by the method previously described, for a period of 5 minutes, at a flow rate of 484 mℓ.min^{-1}. The diffusion tube was disconnected from the trap, which was then positioned in the LIF excitation beam. The resulting fluorescence at 323 nm was recorded for 60 s. The

energy of the incident radiation was then measured at the trap location using a Gentec energy meter. This experiment was repeated with two other conditioned traps.

iii) Variations in detector response due to slight variations in positioning a loaded trap

A multi-channel silicone rubber trap, which had previously been loaded with naphthalene from a diffusion tube for 900 s prior to a photodegradation experiment (refer to section 3.2.4), was loaded again for 30 seconds, at a flow rate of 514 mℓ.min^{-1}. The diffusion tube was disconnected from the trap which was then positioned in the LIF excitation beam after the energy had been measured at the trap location using a Gentec energy meter. The oscilloscope signal was recorded at 323 nm for 60 s, and the trap was then removed from the laser beam (which continued to fire) for a period of approximately 60 s. The trap was then re-positioned in the laser beam and measurements were resumed for approximately 60 s. This process of measurement and re-positioning was repeated a number of times. The experiment was repeated using a different trap and with re-loading from the naphthalene diffusion tube during out-of-beam periods, in order to compensate for any volatilization or photodegradation losses.

3.2.2.3 Results and discussion

a) *Diffusion tube loading repeatability: GC-MS experiment*

The results of these experiments are presented in Table 3.7, from which the variability in diffusion tube loading of ~ 14 % was determined. This was deemed acceptable for the purposes of this study. As mentioned in section 2.3 of Chapter 2, the GC –MS laboratory air loading experiments yielded concentrations of < 1 ng naphthalene for 5 minute loading, and ~ 1 ng for 60 minute loading periods, whilst 10 ng of naphthalene was detected in the laser laboratory air sample. It was therefore deemed unnecessary to pre-clean laboratory air prior to its passage through the diffusion tube.

Table 3.7: TD-GC-MS results of repeated 5 minute diffusion tube loading of naphthalene onto two different traps.

Run #	Trap 1 (P1) Naphthalene peak area	Trap 2 (P4) Naphthalene peak area
1	1 689 582	1 519 977
2	1 584 184	1 773 389
3	1 317 746	1 345 629
Average	1 530 504	1 546 332
Standard deviation	191 642	215 094
% RSD	13	14

b) *LIF experiments*

i) Variations in detector response signals to blank traps

The fluorescence spectra of the blank traps are presented in Figure 3.8, and the repeat measurements of trap P11 are shown more clearly in Figure 3.9. The emission signal obtained at 323 nm for each trap is given in Table 3.8, as this is of interest with respect to naphthalene analyses (each oscilloscope reading is an average response over eight laser pulses).

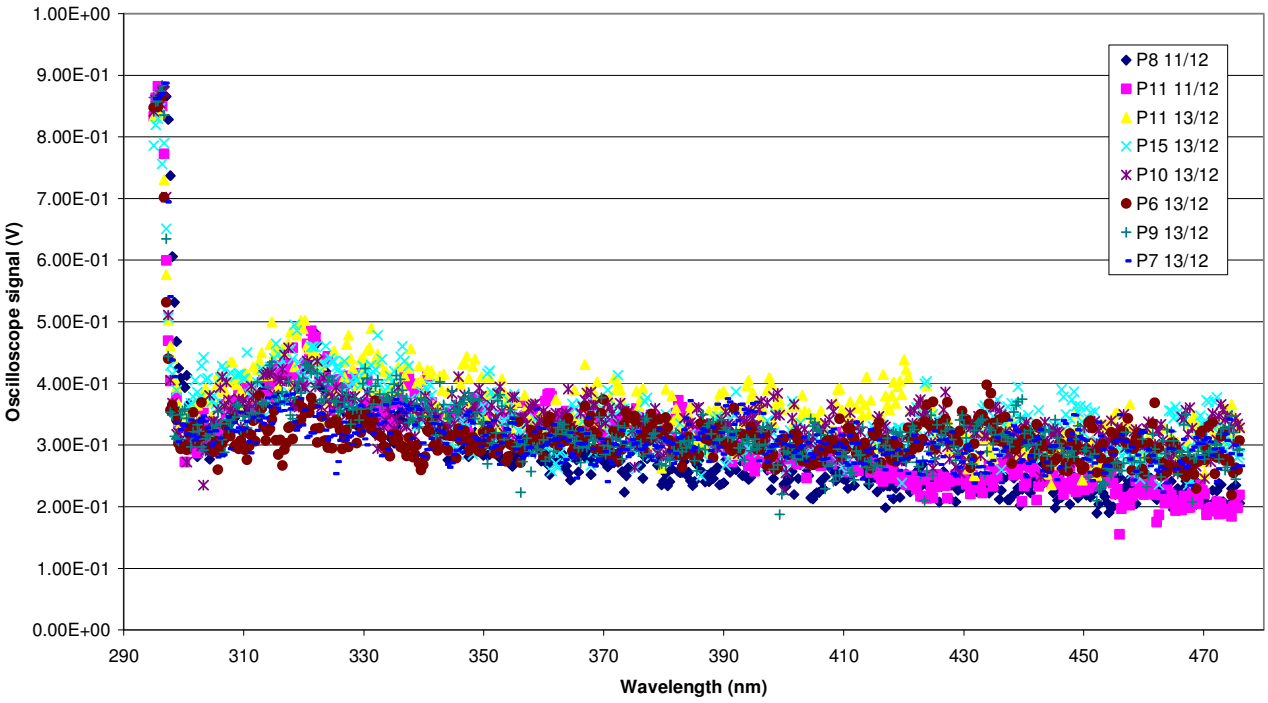

Figure 3.8: Blank trap fluorescence spectra for various traps with 292 nm excitation.

From the results in Table 3.8, it is evident that the variation in detector response was less than that of the incident laser energy (9.3 % RSD as compared to 14.7 %), which would indicate that the incident energy would dominate the variation in blank fluorescence signals more than the variations in fluorescence signals between traps.

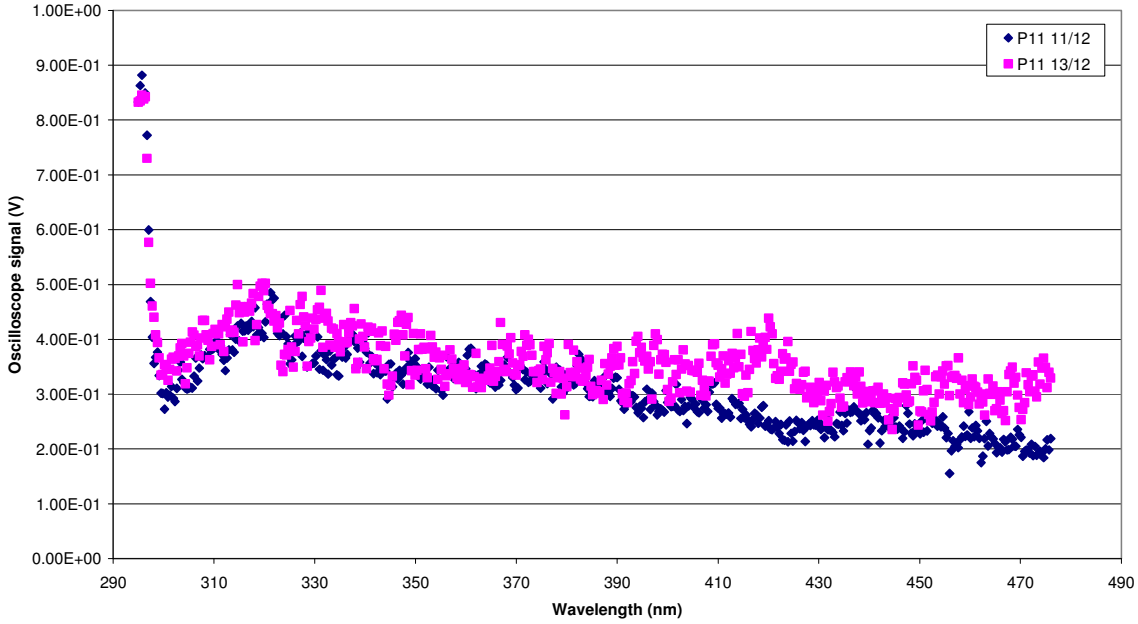

Figure 3.9: Comparison of the fluorescence spectra of blank trap P11, recorded on different days, with different laser incident energies.

Table 3.8: Variations in detector response at 323 nm for blank traps, with incident laser energies.

Trap	Oscilloscope signal at 323 nm (V)	Incident laser energy (µJ)
P8	0.395	576
P11	0.407	576
P11	0.430	657
P15	0.433	851
P10	0.361	678
P6	0.346	624
P9	0.373	622
P7	0.342	554
Average	**0.386**	**642**
Standard deviation	**0.036**	**94.4**
% RSD	**9.3**	**14.7**

ii) Variations in detector response to similarly loaded traps

It was evident that the incident laser energy decreased during the experiment, which impacted on the oscilloscope signal for the three sets of results, as shown in Figure 3.10 and Table 3.9, although the % RSD in the oscilloscope results was less than that of the incident energy. The second trap was loaded for 15 s longer than the other two traps, hence slightly more naphthalene was loaded in this case at a diffusion rate of 1.88 ng.s^{-1}, as indicated in Table 3.9. The top 5 mm portion of each trap, which was analysed in these LIF experiments, would most likely have been loaded to equilibrium conditions, as determined in later experiments.

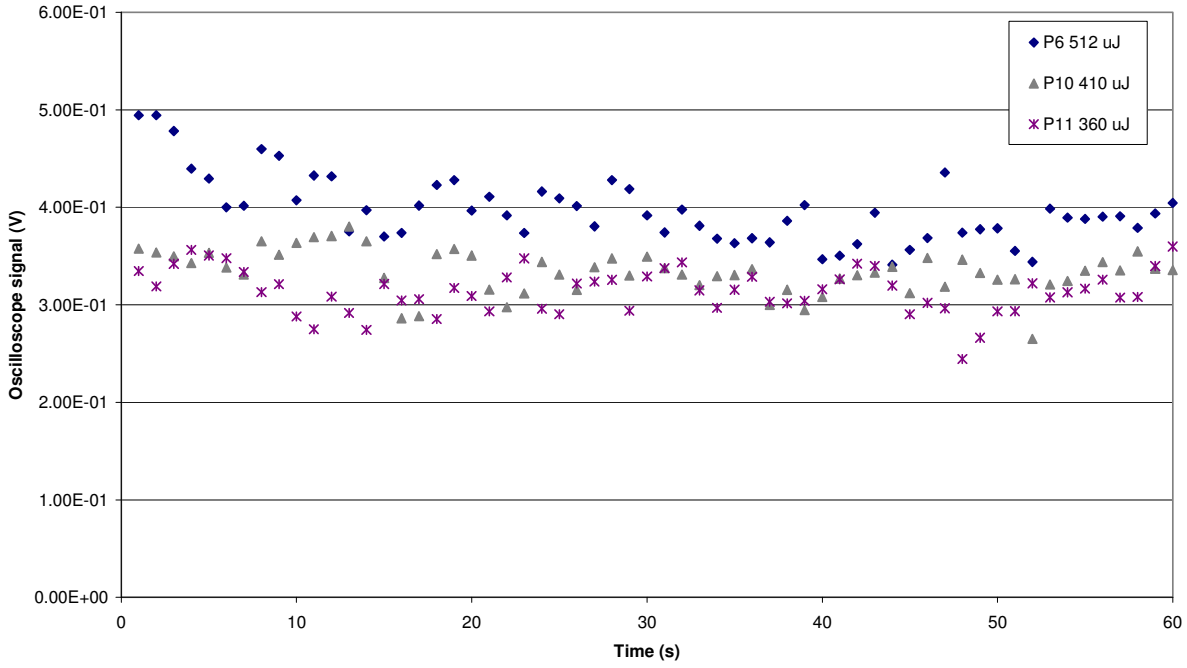

Figure 3.10: Naphthalene fluorescence signal at 323 nm after diffusion tube loading onto three different traps in the same manner.

Table 3.9: Average oscilloscope signals over 60 s for naphthalene loaded onto different multi-channel silicone rubber traps.

Sample number	Incident energy (µJ)	Naphthalene loading (ng)	Average oscilloscope signal (V)
1	512	564	0.397
2	410	592	0.334
3	360	564	0.314
Overall average	**427**	**573**	**0.348**
Overall standard deviation	**77.5**	**16.2**	**0.043**
Overall % RSD	**18.1**	**2.8**	**12.4**

It would appear that variations between different traps as well as variations in loading are small in comparison to the variations in oscilloscope response brought about by changes in the laser incident energy. Incident energy considerations were therefore investigated in more detail under section 3.2.5.

iii) Variations in detector response due to slight variations in positioning a loaded trap

The results of these experiments are presented in Figures 3.11 and 3.12. In the first experiment, where no re-loading was performed during the experiment, the in-beam detector signal varied less (4.5 % RSD) than in the second experiment (13.5 % RSD), although the energy varied less in the second experiment (2.9 % RSD as compared to 14.8 % RSD in the first experiment).

The increase in oscilloscope signal over time in the second experiment (even with a decrease in incident energy) could have been as a consequence of the trap not having reached equilibrium loading conditions at the start of the experiment, thus additional (and not just replacement) naphthalene was loaded during the re-loading periods, which resulted in an elevated detector response.

The slight decrease in oscilloscope signal towards the end of the first experiment would most likely have arisen from volatilization and photodegradation losses of naphthalene

from the trap. The decrease in incident energy would also have contributed to the lower oscilloscope signal.

Slight variations in the positioning of the trap therefore did not appear to result in significant variations in the oscilloscope signal when the analyte was evenly distributed over the silicone surfaces.

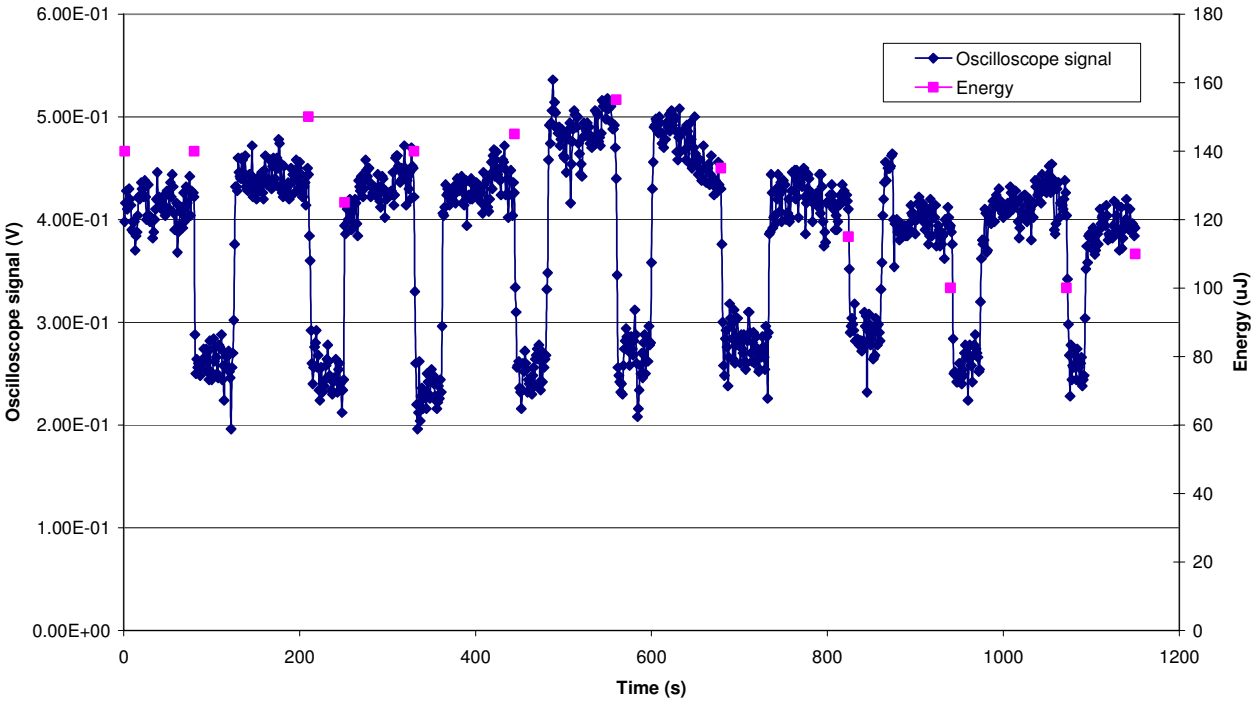

Figure 3.11: Naphthalene repeatability experiment to determine the effect of slight variations in trap positioning, showing consecutive in- and out-of-beam periods. Oscilloscope signal measured at 323 nm. No re-loading of the trap during out-of-beam periods was performed.

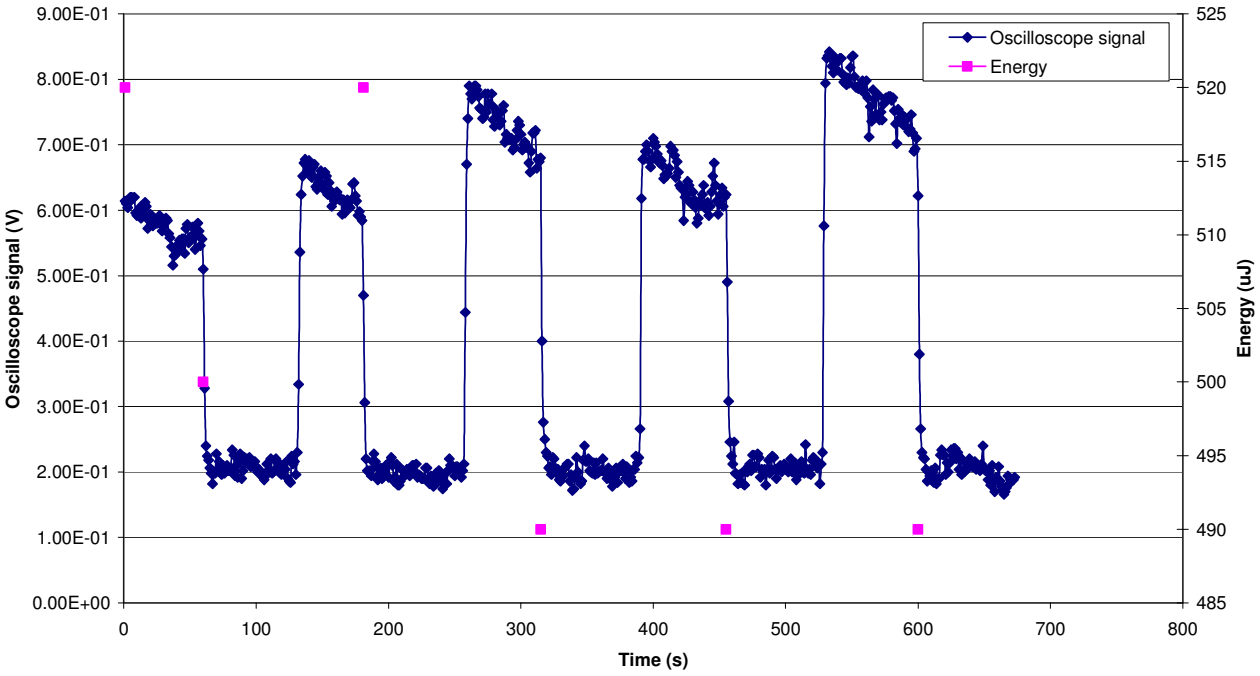

Figure 3.12: Second naphthalene repeatability experiment to determine the effect of slight variations in trap positioning, showing consecutive in- and out-of-beam periods. The trap was re-loaded with naphthalene from the diffusion tube during out-of-beam periods. Oscilloscope signal measured at 323 nm.

3.2.2.4 Conclusion

From these experiments it would appear that the incident laser energy had the most impact on the detector response, and that variations in blank trap fluorescence, detector response to similarly loaded traps (and differences in this loading), as well as slight variations in trap positioning, were of minor importance in this experimental setup. The effect of variations in incident laser energy was therefore investigated in more detail, as discussed under section 3.2.5. Even with fluctuations in incident energy, the % RSD of the oscilloscope response did not exceed 15 % in these experiments, which was deemed acceptable for a screening method.

3.2.3 Sensitivity of the method

3.2.3.1 Background

In order for a monitoring method to find practical application, it is important that it is sufficiently sensitive to enable detection of the relevant analyte(s) at application specific levels. The levels at which environmental effects occur, primarily human health effects, are also important considerations, as the limit of detection (or quantitation) of a monitoring method should be below any legislated limits of these pollutants. Depending on the application, occupational exposure limits, industrial emission limits, or maximum permissible ambient air concentrations may have relevance.

In terms of occupational exposure, the United States National Institute for Occupational Safety and Health (NIOSH) has set a recommended occupational exposure limit, based on a time-weighted average for a 10-hour workday within a 40-hour workweek, of 0.1 $mg.m^{-3}$ for PAHs arising from coal tar products. The American Conference of Governmental Industrial Hygienists (ACGIH) recommends an occupational exposure limit of 0.2 $mg.m^{-3}$ for coal tar products (based on an 8-hour day and 40-hour workweek) and the Occupational Safety and Health Administration (OSHA) has legally enforced this limit over an 8-hour exposure period (ATSDR, 1995).

Concentrations of PAHs in ambient air are presented in Table 3.2, however, concentrations in air near sources of PAHs are expected to be higher than general ambient levels.

The OSHA, ACGIH and NIOSH occupational exposure limit for naphthalene is 10 ppm (50 $mg.m^{-3}$) over an 8-hour workday, and 15 ppm (75 $mg.m^{-3}$) for short term exposures (ATSDR, 2005). In addition, NIOSH have an Immediately Dangerous to Life and Health (IDLH) limit for naphthalene of 250 ppm (1250 $mg.m^{-3}$).

Phenanthrene and pyrene both have OSHA exposure limits of 0.2 $mg.m^{-3}$ (NIOSH, Method 5506, 1998). In our study we investigated whether these PAHs could also be detected using the 292 nm excitation wavelength, which is optimal for naphthalene, in order to simplify the proposed method without losing a significant amount of selectivity.

The low breakthrough volume of the more volatile PAHs, particularly naphthalene, with the multi-channel silicone rubber traps hinders significant pre-concentration of these analytes, which thus necessitates low analytical detection limits, or else precludes the monitoring of low concentrations of these analytes. Fortunately the more volatile species are usually emitted from sources at higher concentrations than the less volatile PAHs, as previously discussed. The breakthrough volume for naphthalene was determined in this study by means of both a GC-MS and a LIF-based method, in order to assess V_B for the traps used in this study, which were of a different configuration to those used for previous V_B determinations, where a value of ~500 cm^3 was found (Ortner, 1994).

The minimum detectable concentrations of the atmospheric analytes of interest are also limited by the instrument or method detection limit (LIF), the variability in blank values, and by the sample volume (Rosenberg et al., 1988).

The LIF method presented here is for use as a screening tool for PAHs near possible source emissions, thus comparisons of limits of detection to concentrations in impacted environments is appropriate. Comparisons are therefore made to occupational exposure limits rather than ambient background levels, for which there are no South African limit values.

In terms of the limits of detection (LOD) and limits of quantitation (LOQ) of PAH methods, the NIOSH method 5506 provides a useful comparison. This method is used to analyse atmospheric PAH samples which have been adsorbed onto XAD-2, and is based on the detection of the PAHs by HPLC either with fluorescence (fluoranthene and pyrene with 340 nm excitation and 425 nm emission) or UV detection (naphthalene and phenanthrene at 254 nm). LODs and LOQs of method 5506 for the PAHs of interest in our study are presented in Table 3.10.

Table 3.10: NIOSH method 5506, LOD and LOQ values for PAHs (NIOSH, 1998).

PAH	LOD (µg per sample)	LOQ (µg per sample)
Naph	0.20 – 0.80	0.39 – 2.6
PhA	0.0070 – 0.060	0.023 – 0.19
FlA	0.0020 – 0.090	0.0066 – 0.30
Py	0.0010 – 0.30	0.0036 – 0.99

3.2.3.2 Experimental method

a) Analytical detection limits

i) Background signal

This parameter has been covered under section 3.2.2, although these experiments also have relevance to the determination of the analytical detection limits of our method.

ii) LIF derived limit of detection

A silicone rubber trap was positioned in the laser system, as described under section 3.2.1, and it was then loaded with naphthalene from a diffusion tube (as discussed in Chapter 2) at a flow rate of 486 mℓ.min^{-1}, until equilibrium had been reached (at 50 seconds) at the sample spot (the entrance end of the silicone tubes). Irradiation was at 292 nm, and the fluorescence was recorded at 323 nm via the PC linked to the oscilloscope.

b) Breakthrough volume

i) LIF experiments

Two multi-channel silicone rubber traps were placed in series (primary and secondary or backup trap). A portable Gilair pump was used to draw air at 387 mℓ.min^{-1} through the naphthalene diffusion tube and then through the two traps. The excitation beam (at 292 nm) was focused on the inlet side of the secondary trap (5 mm spot size), and fluorescence emission from the secondary trap was collected by the monochromator at 323 nm for detection purposes. The experimental setup is shown in Figure 3.13. After 900 s, the pump was

switched off, and an emission spectrum was obtained of the secondary trap. The trap side of the experimental setup was then dismantled and an emission spectrum was obtained of the primary trap. Both traps were then capped and refrigerated prior to analysis by TD-GC-MS (standards: 30, 50, 100 and 200 ng).

This experiment was repeated using a diffusion tube loading flow rate of 480 mℓ.min^{-1}, and loading was conducted for 1 hour (incident laser energy = 180 μJ). LIF scans were then recorded for both traps, and the profile of naphthalene loading through the primary trap was investigated by recording LIF scans along the length of the trap. 50, 100, 200 and 500 ng TD-GC-MS standards were used.

In a third experiment, diffusion tube loading was conducted for 2 hours at a flow rate of 495 mℓ.min^{-1}. 50, 250, 500 and 2000 ng TD-GC-MS standards were used.

The impact of flow rate on the breakthrough volume profile was then investigated by conducting similar experiments at flow rates of 1276 mℓ.min^{-1} and 200 mℓ.min^{-1}.

ii) TD-GC-MS experiments

In order to determine the breakthrough volume of naphthalene on the traps by TD-GC-MS a series of experiments was conducted. A trap was loaded with naphthalene from a diffusion tube (as discussed in Chapter 2) for a period of 5 minutes, at a flow rate of ~475 mℓ.min^{-1}. The trap was then analysed by TD-GC-MS using a suitable CIS split ratio (refer to Table 3.11) with the TDS in solvent vent mode. The instrument was calibrated by injection of liquid standards in toluene onto traps (100, 200 and 300 ng of naphthalene ranging from 1 to 6 μℓ), followed by TD-GC-MS analysis. The experiment was repeated with another trap, as well as for increased loading times up to 60 minutes, at 10 minute intervals.

Figure 3.13: Experimental setup for the LIF breakthrough experiments. The naphthalene diffusion tube is mounted on two multi-channel silicone rubber traps in series, which are connected to a portable sampling pump. The monochromator is shown in the background.

This experiment was again repeated in order to determine naphthalene TD-GC-MS peak areas for lower sampling volumes ranging from 500 to 4933 mℓ with a sampling flow rate of 370 mℓ.min^{-1} (the CIS split ratio used ranged from 100:1 to 400:1).

In another series of experiments, a trap was loaded with naphthalene from a diffusion tube for 5 min at increasing flow rates from 492 to 775 mℓ.min^{-1}. Experiments were also repeated using another trap for comparison.

c) Excitation of other PAHs of interest utilizing 292 nm excitation

i) Pyrene

Three multi-channel silicone rubber traps were loaded with pyrene by means of the gas chromatographic fraction collection method described in Chapter 2. Correction was made to the concentration of PAH injected into the GC system, based on the average recoveries obtained with the optimized method so that the final amount of pyrene on each trap was ~100, 150 and 200 ng, respectively. After loading, the traps were end-capped, wrapped in aluminium foil and refrigerated prior to use.

LIF analysis of each loaded trap was performed in the same manner as for naphthalene, with 292 nm incident radiation focused as a spot on the top of the trap. The fluorescence spectrum was recorded from 295 – 465 nm. The traps were then end-capped, wrapped in aluminium foil and refrigerated prior to TD-GC-MS analysis, using the method described under section 3.2.2.2, with injection of 1 μℓ of 100 and 200 ng standards onto multi-channel silicone rubber traps for calibration purposes.

ii) Phenanthrene

Three multi-channel silicone rubber traps containing ~100, 150 and 200 ng phenanthrene respectively, were prepared and analysed in the same manner as for pyrene. In this case, the fluorescence scan was recorded from 295 – 480 nm.

3.2.3.3 Results and discussion

a) Analytical detection limits

i) Background signal

The analytical detection limit has been defined as 3x the standard deviation of repeated 100 μℓ, 1 μg.mℓ$^{-1}$ standard injections (which equates to 100 ng loading) by Rosenberg et al. (1988), whilst blank tube values were defined as the mean value of 10 determinations. For this LIF method, the average blank trap detector response at 323 nm with 292 nm excitation irradiation was found to be 0.386V (n = 8) (refer to Table 3.8).

ii) LIF derived limit of detection

Figure 3.14 shows the 323 nm fluorescence emission which was recorded over a period of time as naphthalene was drawn into the short trap from the diffusion tube (diffusion rate ~2 ng.s^{-1}). A mass detection limit of ~20 ng can be calculated using a signal:noise ratio of 3:1, and equilibrium conditions were obtained for the analysed sample spot within ~16 s (each data point is an average over 8 laser pulses).

The noise (0.001 V) was calculated from the root mean square (RMS) value of the data points post equilibrium, as there were statistically insufficient data points in the region prior to the signal increase, and it was found that the RMS values were in fact the same for both regions. The voltage at equilibrium averaged 0.873 V, thus the signal:noise ratio was 873:1 for a diffusion rate of ~2 ng.s^{-1} and operation at ~500 mℓ.min^{-1}. For a signal:noise ratio of 3:1, a diffusion rate of ~7 pg.s^{-1} at this flow rate could therefore be used, which equates to a limit of detection of ~1 µg.m^{-3}, which is suitable for impacted environments, including workplace exposure.

b) Breakthrough volume

i) LIF experiments

No increase in emission signal at 323 nm was observed on the secondary trap throughout the 900 s loading period, as shown in Figure 3.15, thus the quantity of naphthalene present in the irradiated portion of the trap was below the LOD of the method, which was confirmed by the emission spectrum for this trap which did not differ from that of the blank trap at the wavelength of interest (Figure 3.16). A significant emission was found on the primary trap, however, indicating extensive loading of naphthalene.

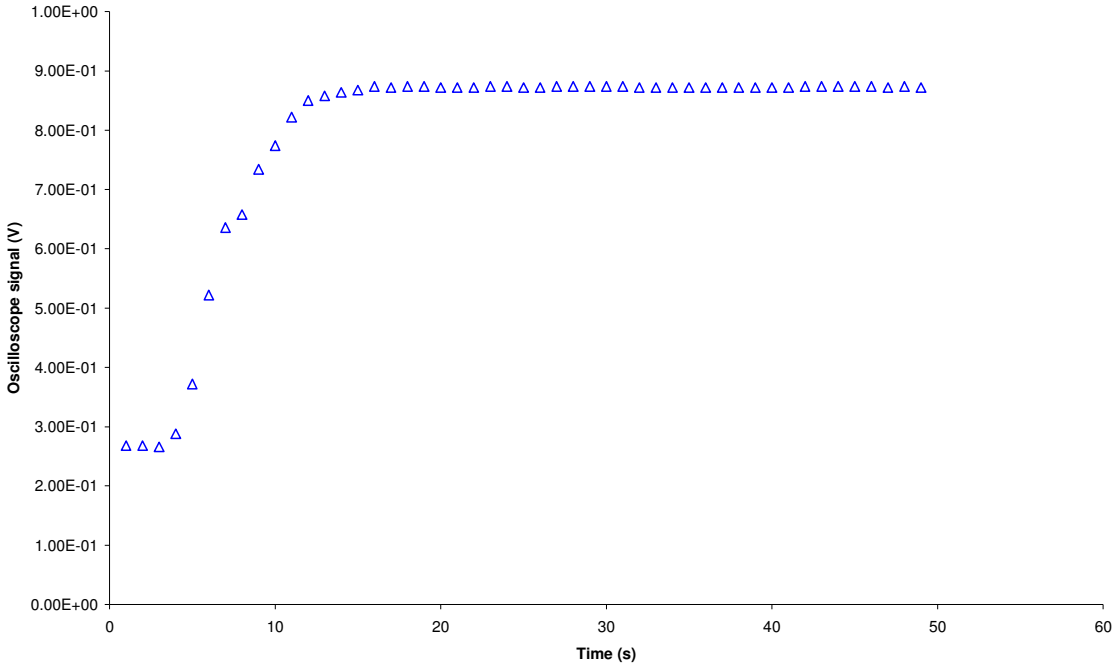

Figure 3.14: Fluorescence signal at 323 nm (naphthalene emission) obtained with 292 nm excitation as a function of time at a sample spot at the entrance of the trap. Loading of naphthalene vapour was from a diffusion tube onto a short trap.

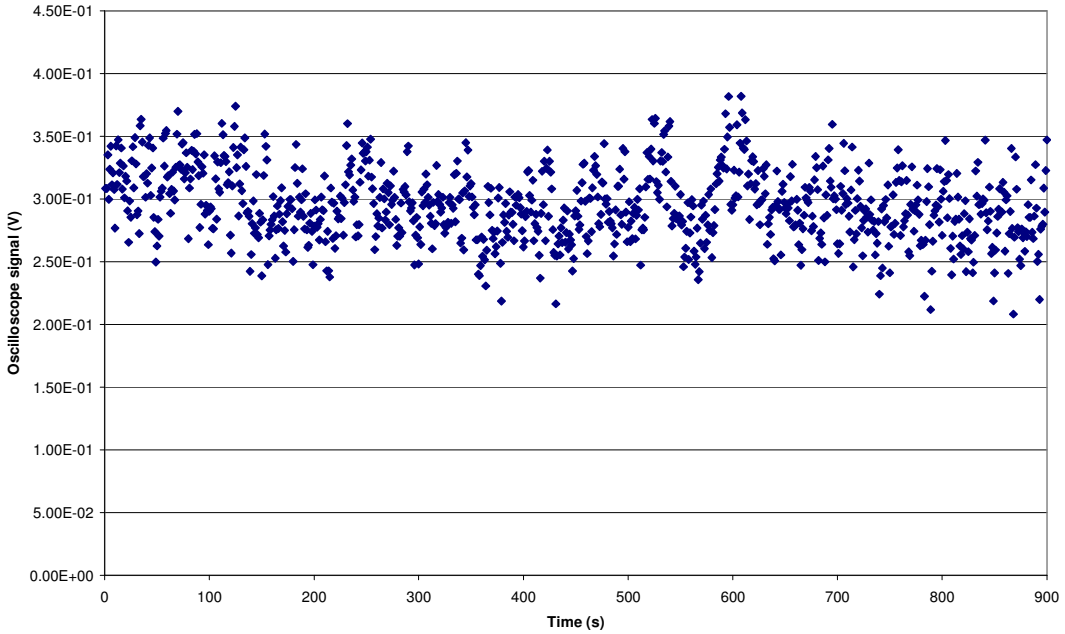

Figure 3.15: Secondary trap fluorescence at 323 nm during the loading phase of a breakthrough experiment for naphthalene, using a diffusion tube (900 s at 387 mℓ.min^{-1}).

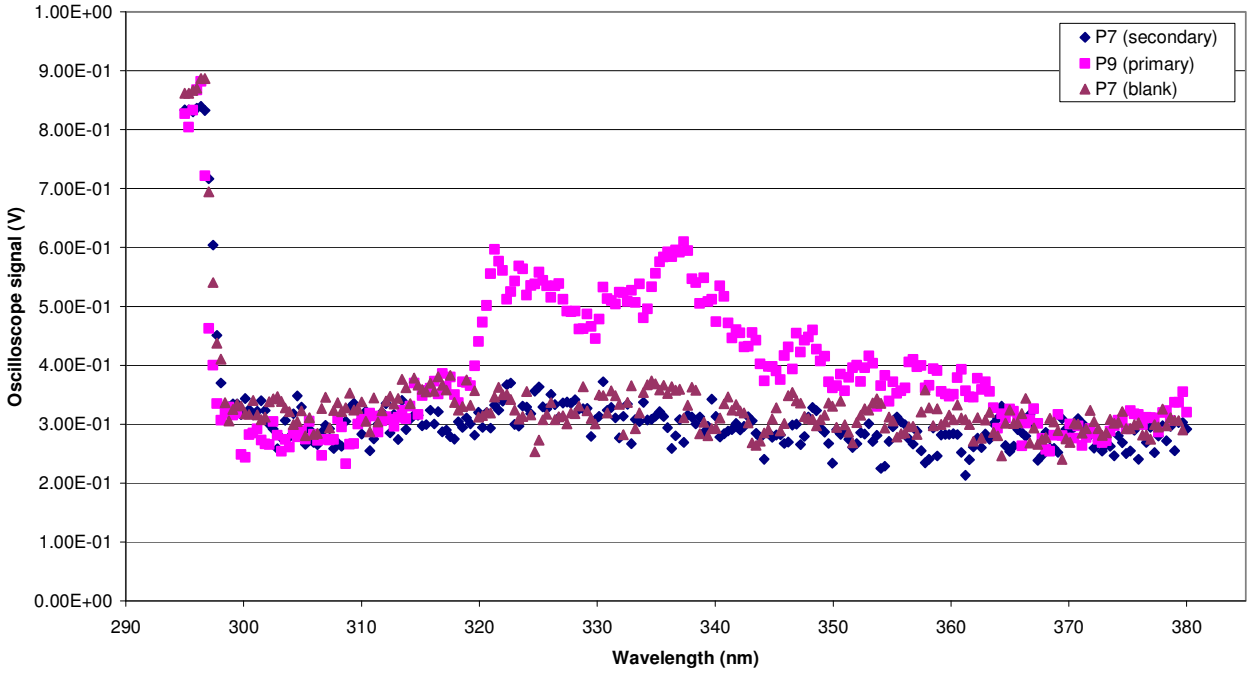

Figure 3.16: Primary, secondary and blank trap spectra obtained after a breakthrough loading experiment using a naphthalene diffusion tube and 292 nm excitation (900 s loading at 387 mℓ.min^{-1}).

Subsequent TD-GC-MS analysis of the two traps indicated that the primary trap contained >300 ng of naphthalene, whilst the secondary trap contained ~200 ng (using a calibration curve of y = 6.262 x 10^3x with r^2 = 0.995). These results are semi-quantitative, as the samples were over the calibration range.

As the silicone rubber portion of the trap was 55 mm long, and the irradiated area was 5 mm in length, the trap may be considered as containing 11 sections or plates. For the primary trap, this would relate to ~27 ng of naphthalene per plate, which is above the LOD of ~20 ng, whilst the secondary trap would contain ~18 ng per plate, which is below the LOD, thus there was no detectable increase in LIF signal.

The trap contained ~300 ng naphthalene when equilibrium conditions had been established at a diffusion tube loading rate of 1.88 ng.s^{-1} (ie, breakthrough sampling conditions

had been established). Equilibrium conditions were reached in the first plate after loading of ~27 ng of naphthalene. This would occur after ~14.5 s at a diffusion rate of 1.88 $ng.s^{-1}$, which compares well to that determined during the LIF limit of detection experiment reported under portion (a) of this section (equilibrium after ~16 s).

Similar results were obtained for the hour long loading experiment, in that no increase in fluorescence intensity at 323 nm at the top of the second trap was evident, although a significant decrease in incident energy occurred during the course of the experiment (the energy decreased from 180 μJ at the start of the experiment to 25 μJ at the end).

A low concentration of naphthalene was found on the secondary trap by TD-GC-MS analysis (75 ng) post LIF, which would relate to < 7 ng of naphthalene on the top spot of the trap (using a calibration curve of $y = 1.852 \times 10^{3}x$ with $r^2 = 0.986$, a 10:1 CIS split was used in the case of the secondary trap, whilst a 100:1 split was used for the standards and primary trap). This accounts for the lack of detection by the LIF method. The primary trap was found to contain 6 794 ng of naphthalene by TD-GC-MS and its distribution through the trap is shown in Figure 3.17. A slight decrease in naphthalene concentration is evident through the trap upon comparison of the oscilloscope signals at 323 nm. The total mass of naphthalene found on both traps by TD-GC-MS would relate to a diffusion rate of 1.9 $ng.s^{-1}$, which agrees with the experimentally derived diffusion rate (refer to Chapter 2).

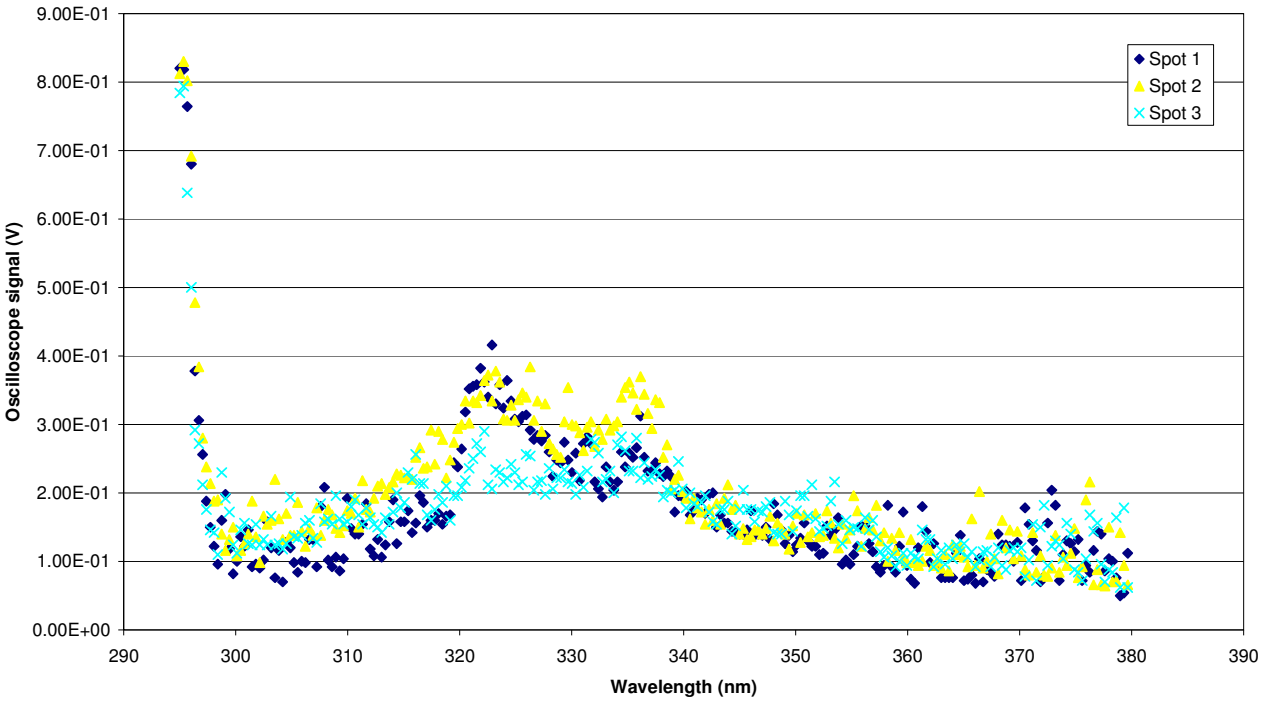

Figure 3.17: LIF scans of the primary trap after 1 h naphthalene diffusion tube loading at 480 mℓ.min^{-1}, where spot 1 is at the top of the trap and spots 2 and 3 are below this.

The naphthalene TD-GC-MS results for the 2 h loading experiment were 9 507 ng for the primary trap and 9 245 ng for the secondary trap, which indicates that the secondary trap had also nearly reached equilibrium conditions (using a naphthalene m/z 127 calibration curve of y = 5.02 x 10^2x with r^2 = 0.998, as the naphthalene m/z 128 results were over range). The LIF scans of the primary and secondary traps post loading also indicated similar naphthalene concentrations (emission at 323 nm, refer to Figure 3.18). A total of 14 400 ng of naphthalene was expected on the traps, using a diffusion rate of 2 ng.s^{-1}, which is lower than the total concentration obtained by TD-GC-MS (18 752 ng, which would relate to a diffusion rate of 2.6 ng.s^{-1}). This may have been due to a higher diffusion rate, variations in the pump flow rate, or as a result of the utilization of liquid standards for TD-GC-MS calibration purposes.

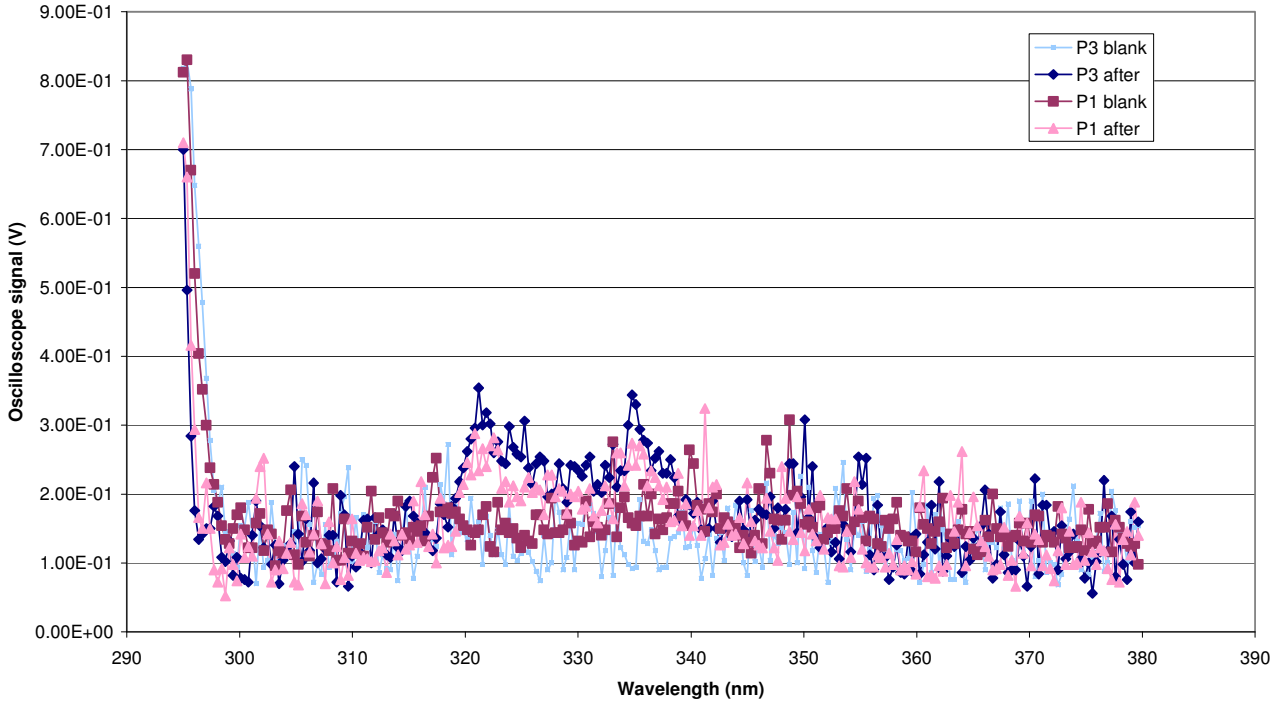

Figure 3.18: LIF scans, showing similar concentrations of naphthalene in the primary (P1) and secondary (P3) traps after 2 hours of diffusion tube loading at 495 mℓ.min^{-1}.

The fluorescence emission at 323 nm of a spot at the top of the secondary trap obtained during diffusion tube loading over 2 hours is shown in Figure 3.19. 59 ℓ of air was drawn through the system of traps during this experiment. The incident energy decreased from 100 µJ to 30 µJ over the 2 hour period, and the excimer laser tripped after ~30 minutes and had to be re-started.

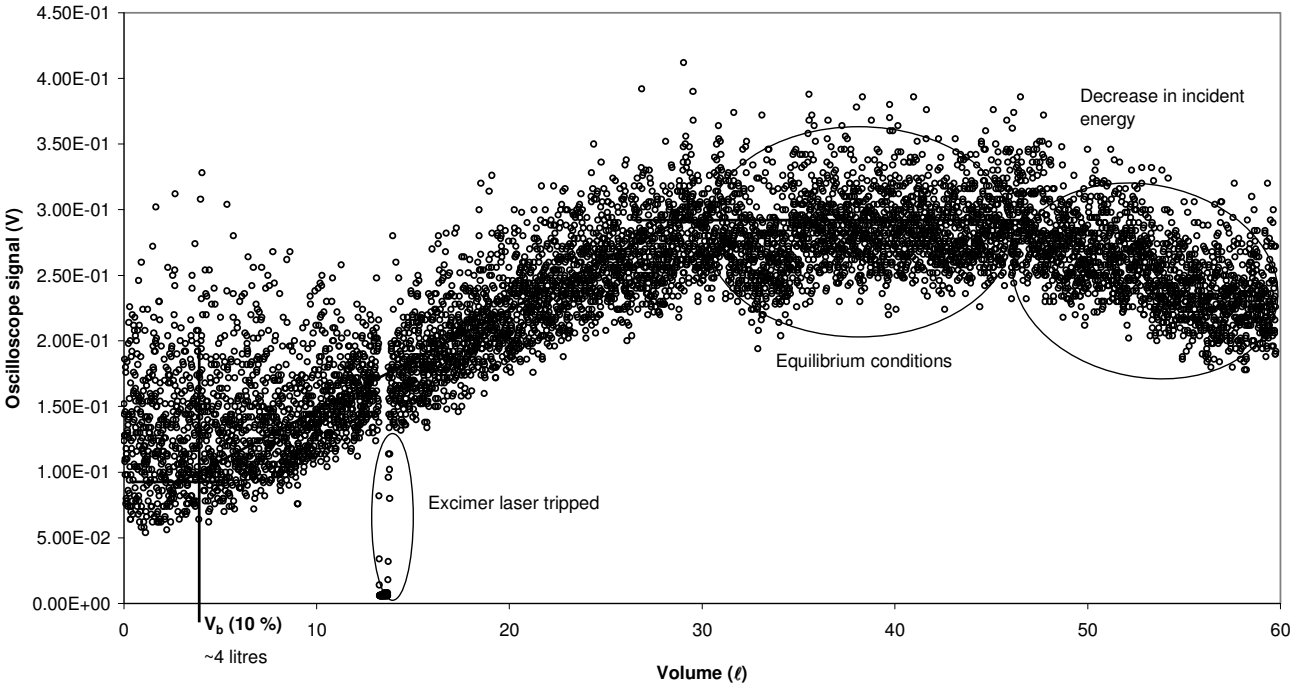

Figure 3.19: Fluorescence at 323 nm of the top portion of the secondary trap during 2 hour naphthalene diffusion tube loading at 495 mℓ.min^{-1}.

A breakthrough volume of ~4 ℓ was estimated for 10 % breakthrough of naphthalene, which relates to a sampling interval of ~8 min at 500 mℓ.min^{-1}. The GC-MS can detect 1 pg with a signal to noise ratio of 400:1 in total ion current (TIC) chromatogram mode, according to the instrument specifications, which would equate to a detection limit of ~0.3 ng.m^{-3} for this breakthrough volume. The breakthrough volume for naphthalene determined in our experiments is significantly higher than that reported previously (0.5 ℓ, Ortner, 1994), which is feasible as the traps used in our study contained twenty two, 55 mm long channels, whilst those used previously contained eight, 105 mm long channels and the PDMS was obtained from different suppliers. The flow rates used also differed, in that Ortner utilized a much lower flow rate of 14 mℓ.min^{-1}.

The loading profile at the top of the secondary trap obtained at a flow rate of 1276 mℓ.min^{-1} is shown in Figure 3.20. It is evident that the excimer laser did not perform well during this experiment, as it tripped twice and the energy dropped from 470 to 348 μJ over the 53 min experiment. In addition there was significant noise in the measurements. A breakthrough volume of ~500 mℓ was roughly estimated from the profile, based on the volume at which the initial fluorescence signal (~0.076 V) had increased by 10 % of the difference between the maximum fluorescence signal (~0.140 V) and the initial fluorescence signal. The diffusion rate may not have been constant over the course of the experiment, as turbulent conditions are expected in the naphthalene diffusion tube at this elevated flow rate. This was tested by varying the flow rate through the diffusion tube holder from ~500 mℓ.min^{-1} to ~700 mℓ.min^{-1} in a separate series of experiments, and it was found upon TD-GC-MS analysis of each of the traps thus loaded for 5 min, that the naphthalene diffusion rate had increased for flow rates > 500 mℓ.min^{-1}.

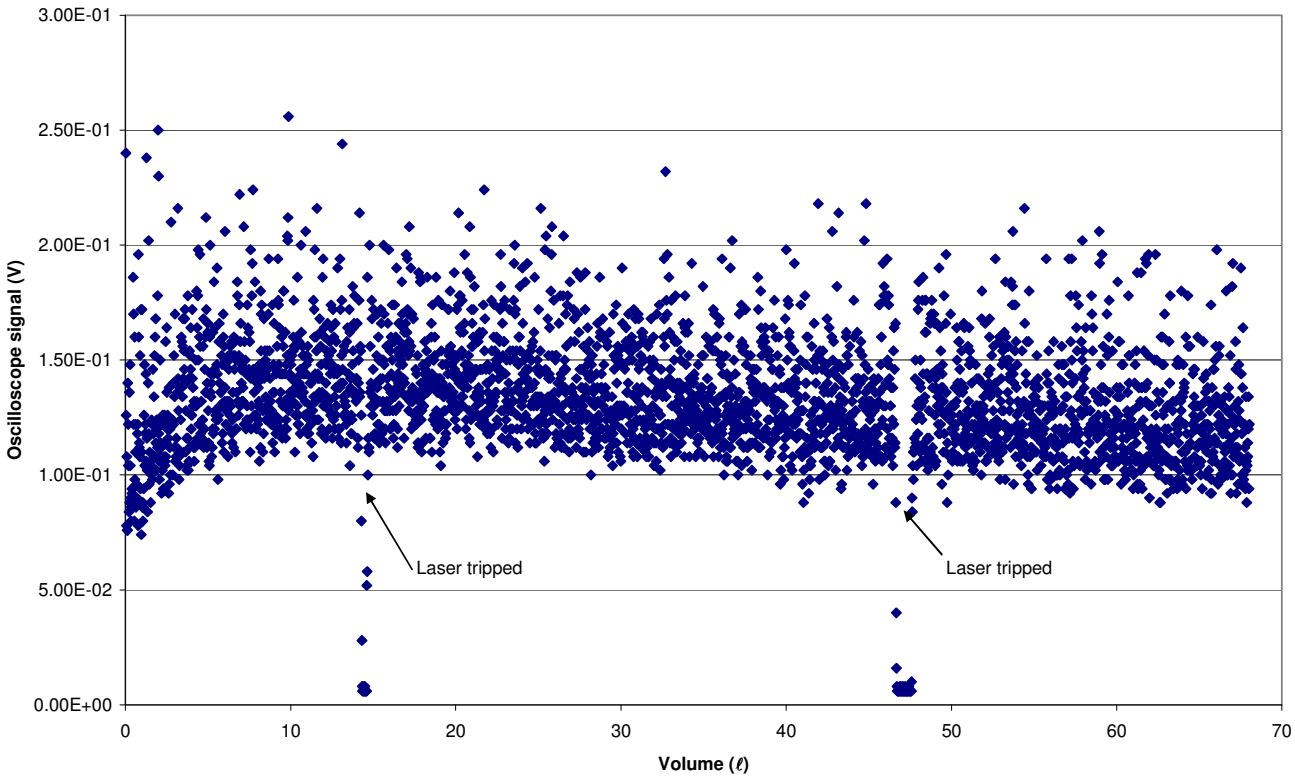

Figure 3:20: Loading profile at the top of the secondary trap with diffusion tube loading at 1276 mℓ.min^{-1} for 53 min (fluorescence at 323 nm).

The experiment at 200 mℓ.min^{-1} was unsuccessful, as the laser energy dropped significantly (to ~100 μJ), therefore an increase in fluorescence signal at the top of the secondary trap was not evident over the 1.5 h duration of the experiment. It was not possible to repeat this low flow rate experiment, as the laser was too unstable over the long time interval required.

ii) TD-GC-MS experiments

The results of the experiment involving variations in diffusion tube loading times are presented in Table 3.11 and Figure 3.21 (TD-GC-MS results are based on a calibration curve of $y = 3.17 \times 10^3 x$ with $r^2 = 0.981$). They should be regarded as semi-quantitative, as many of the results were over the range of the calibration). The diffusion rate was ~3 ng.s^{-1} during these experiments, due to higher room temperatures during the summer months.

Table 3.11: TD-GC-MS results of diffusion tube loading of naphthalene onto two traps for different time intervals.

Parameter	5 min	10 min	20 min	30 min	40 min	60 min
Sampling flow rate (mℓ.min^{-1})	492	473	473	473	478	478
Sample volume (mℓ)	2460	4730	9460	14190	19120	28680
CIS split ratio	30:1	60:1/30:1	100:1	100:1	200:1	200:1
Trap P1 (ng)	826.3	2946	4100	-	5120	-
Trap P4 (ng)	835.1	4608	3720	8470	-	7120
TD-GC-MS average (ng)	851.9	3777	3910	8470	5120	7120
Calculated loading (diffusion rate of 3 ng.s^{-1})	900	1800	3600	5400	7200	10800
Difference (calculated less TD-GC-MS average)	48	(1977)	(310)	(3070)	2080	3680

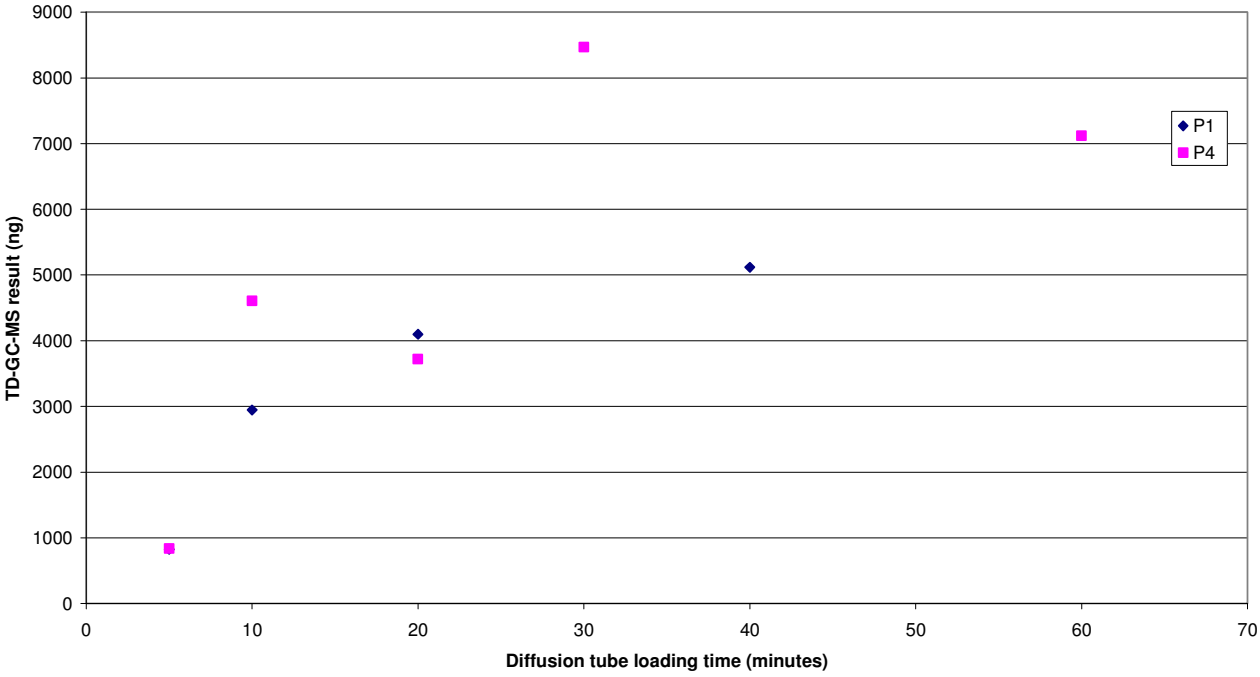

Figure 3.21: TD-GC-MS results for traps loaded with naphthalene from a diffusion tube for different time periods.

From these results, it is evident that the trap continued to accumulate naphthalene throughout the sampling interval (up to 60 min), at which stage the increasing trend appeared to be flattening. From the loading trends in Figure 3.21, it may be estimated that breakthrough occurred at sample volumes > 4730 mℓ (ie: after ~10 min of sampling), although this is not clear from the difference between the amount of analyte which should have loaded from the diffusion tube based on the diffusion rate, and the concentration determined by TD-GC-MS, however it must be borne in mind that the TD-GC-MS results should be regarded as semi-quantitative, as previously mentioned.

The results of the second series of experiments are shown in Figure 3.22, from which a breakthrough volume of ~4 ℓ is also evident.

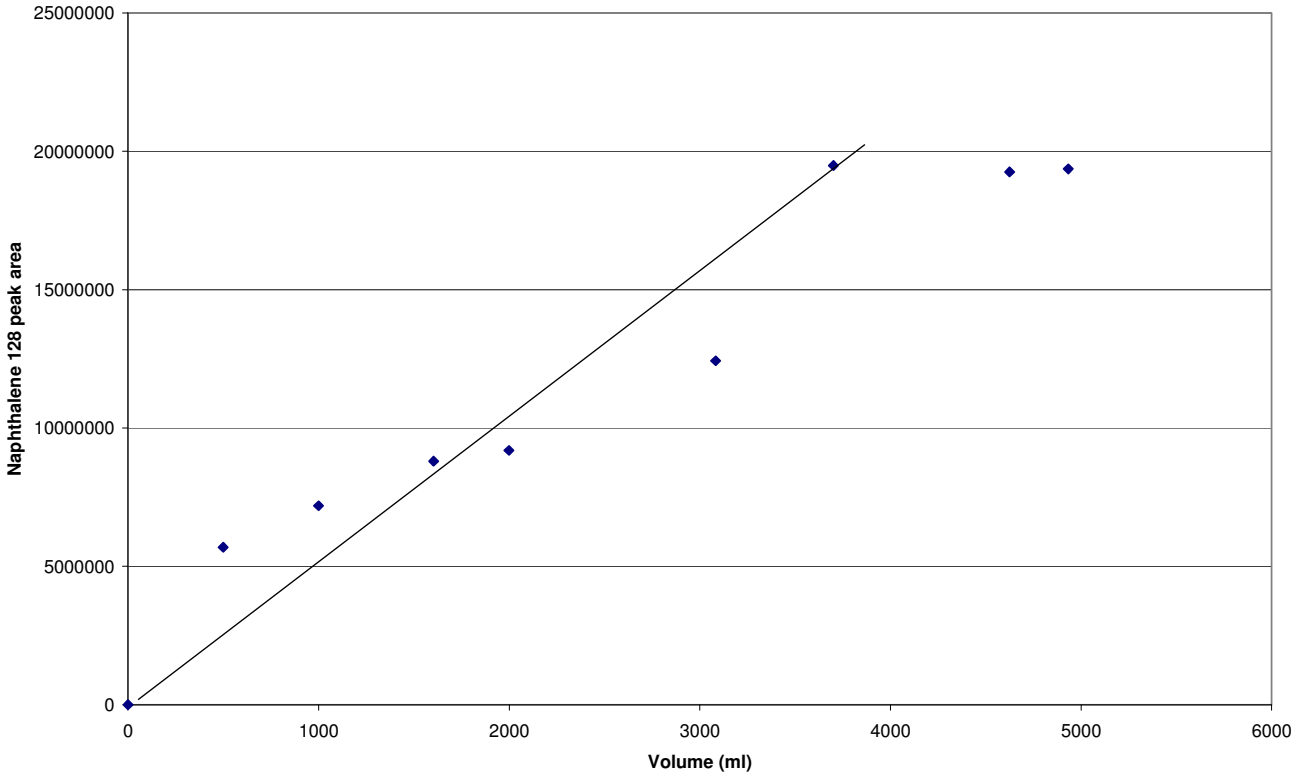

Figure 3.22: TD-GC-MS peak areas for traps loaded with naphthalene from a diffusion tube for different time periods at 370 mℓ.min^{-1}.

The results of the different diffusion tube loading rate experiments are presented in Table 3.12. In these flow rate studies, the impact of faster flow rates on the establishment of equilibrium conditions between the gas and PDMS phases in the sampling trap could be probed. They also allowed for an evaluation of the impact of a faster sampling rate (turbulent conditions) on the rate of diffusion from the diffusion tube.

From the results in Table 3.12, it is evident that there was an over-recovery of naphthalene in all cases, except in the case of ~500 mℓ.min^{-1}. This can be attributed to turbulent conditions in the diffusion tube holder as a result of the higher flow rates, which caused higher rates of loss of naphthalene from the diffusion tube.

Table 3.12: Experimental results obtained for different diffusion tube loading flow rates.

Parameter	Test A	Test B	Test C	Test D
Sampling flow rate (mℓ.min^{-1})	492	641	704	775
Sample volume (mℓ)	2460	3205	3520	3875
CIS split ratio	30:1	30:1	30:1	30:1
Trap P1 (ng)	826	1296	1971	-
Trap P4 (ng)	835	1329	-	1182
TD-GC-MS average (ng)	831	1313	1971	1182
Calculated loading (diffusion rate of 3 ng.s^{-1})	900	900	900	900
Difference (calculated less TD-GC-MS average)	69	(413)	(1071)	(282)

The variation in injection volume for trap calibration purposes was also not ideal, however, due to variations in detector response with changes in solvent volumes during TD-GC-MS analyses, as previously mentioned, which would have contributed to the difference between calculated naphthalene loading and that found by TD-GC-MS analysis.

c) Excitation of other PAHs of interest utilizing 292 nm excitation

i) Pyrene

None of the fluorescence spectra shown in Figure 3.23 contained the characteristic pyrene fluorescence emission peaks (refer to Table 3.4), although slightly elevated oscilloscope signals were obtained at 370 – 390 nm for the 200 ng pyrene sample. The TD-GC-MS results obtained after LIF analysis are summarized in Table 3.13 (using a calibration curve of $y = 4.112 \times 10^{3}x$ with $r^2 = 1.0$). It is evident that conservative loading recoveries were used in determining loading correction factors, thus actual concentrations were ~25 % higher than expected. This variation was consistent between the different concentrations loaded (Table 3.13).

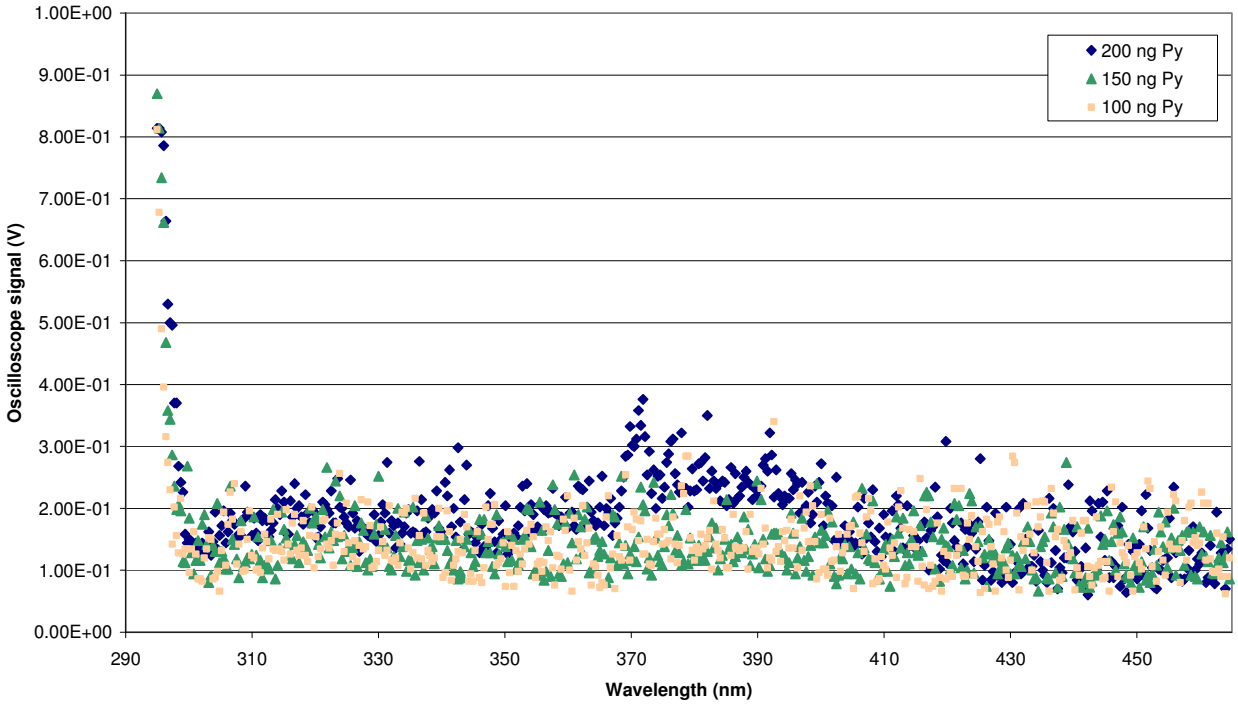

Figure 3.23: Fluorescence spectra of multi-channel silicone rubber traps containing pyrene loaded via gas chromatographic fraction collection, with 292 nm incident radiation (100 µJ in each case).

Table 3.13: Comparison of expected versus actual pyrene concentrations on multi-channel silicone rubber traps loaded via gas chromatographic fraction collection.

Expected pyrene concentration (ng)	**TD-GC-MS pyrene concentration post LIF analysis (ng)**	**% variation**
200	246	23
150	186	24
100	126	26

From the results it is evident that 292 nm is not a suitable excitation wavelength for pyrene, and a longer wavelength would be desirable for this analyte (refer to Table 3.4), although a higher incident energy may also have improved the response obtained.

ii) Phenanthrene

A well resolved fluorescence emission spectrum was obtained when a trap containing 200 ng of phenanthrene was excited with 292 nm radiation, which was characteristic of this PAH (Figure 3.24). The response was much poorer for 150 and 100 ng. The incident energy was lower for the 150 ng trap and it is also possible that channeling occurred through a small number of silicone tubes during gas chromatographic loading of the 150 ng trap, which resulted in the poor response (the laser could have been focused on other silicone tubes to those through which the analyte had preferentially passed). The total amount of phenanthrene loaded onto the trap via gas chromatographic fraction collection would of course be distributed throughout the length of the trap, and not just on the LIF sampling spot, which would contain ~20 ng if 200 ng of analyte is evenly distributed throughout the length of the trap. The profile of phenanthrene through the ~200 ng loaded trap was confirmed qualitatively upon moving the trap slowly upwards in the laser beam, and observing the gradual decrease in oscilloscope signal (and therefore fluorescence emission). A repeat loading and analysis of 100 ng of phenanthrene gave improved results, although the signal to noise ratio of the peaks was still poor, which would impact on detection limits.

There appeared to be some naphthalene contamination of the 150 ng trap, as can be seen by the elevated emission at 323 nm, which was most likely due to carryover during gas chromatographic loading of the trap. Baking out of the gas chromatographic system between trap loading runs may therefore be advisable. TD-GC-MS results of traps post-LIF analysis are presented in Table 3.14 (using a calibration curve of $y = 3.593 \times 10^3 x$ with $r^2 = 1.0$). The amount of phenanthrene loaded onto the traps was higher in the case of the 150 ng loaded trap, and lower for the 100 ng loaded trap, both by 20 %.

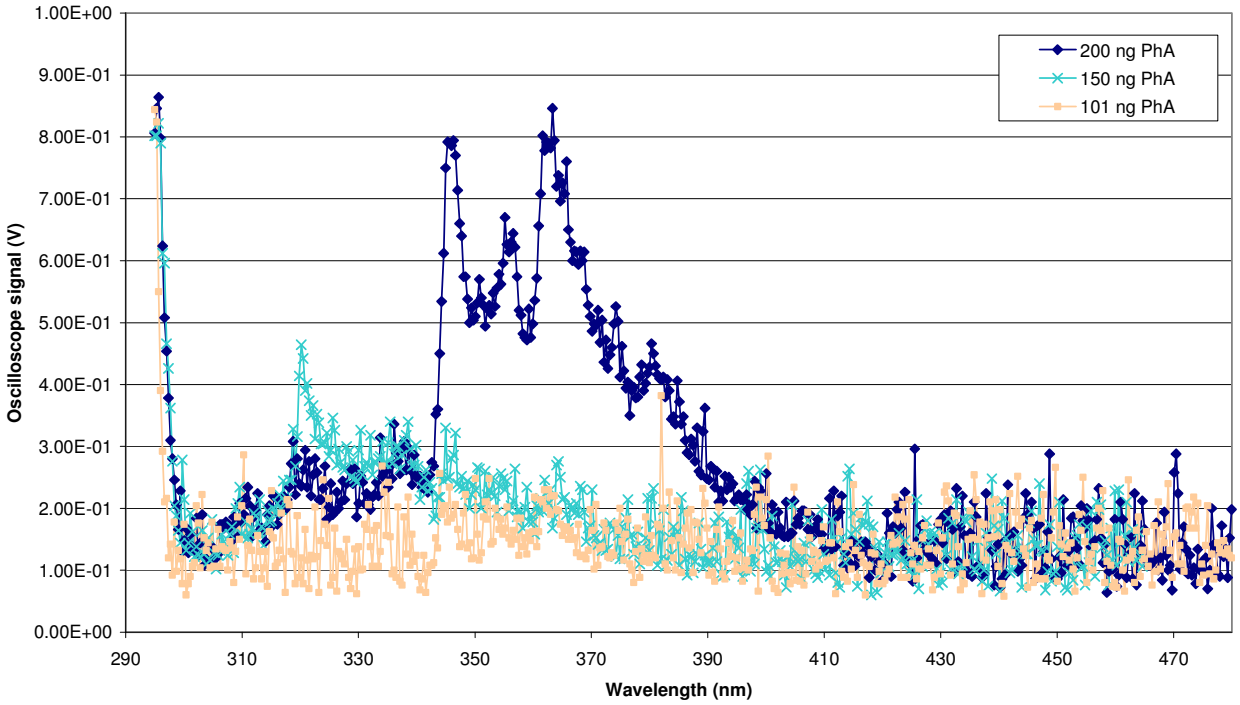

Figure 3.24: Fluorescence spectra of multi-channel silicone rubber traps containing phenanthrene loaded using the gas chromatographic fraction collection method, with 292 nm incident radiation (140 µJ for 200 and 100 ng PhA, 100 µJ for 150 ng PhA).

Table 3.14: Comparison of expected versus actual phenanthrene concentrations on multi-channel silicone rubber traps loaded via gas chromatographic fraction collection (na = not available, as this trap was used for a photodegradation study).

Expected phenanthrene concentration (ng)	**TD-GC-MS phenanthrene concentration post LIF analysis (ng)**	**% variation**
200	na	na
150	180	20
100	80	(20)

3.2.3.4 Conclusion

The LIF method LOD was found to be ~20 ng for a signal to noise ratio of 3:1, and the breakthrough volume (10 %) of the traps was estimated to be in the order of 4 ℓ for

naphthalene based on both LIF and TD-GC-MS experiments. This relates to a sampling interval of ~8 min at 500 mℓ.min^{-1}, and as the GC-MS can detect 1 pg with a signal to noise ratio of 400:1 in total ion current (TIC) chromatogram mode, a detection limit of ~0.3 ng.m^{-3} can be calculated for this breakthrough volume.

Turbulent conditions were established in the diffusion tube holder when sampling flow rates higher than ~500 mℓ.min^{-1} were employed. As flow rates below 500 mℓ.min^{-1} were utilized for all experiments in which the diffusion tubes were used, this was not a cause for concern.

The 292 nm excitation radiation did not prove successful in the case of pyrene fluorescence, which would require longer wavelength excitation radiation. Phenanthrene was successfully detected at this wavelength, however, after ~200 ng was loaded onto a trap via gas chromatographic fraction collection (which would distribute the analyte along the length of the trap). The incident energy will contribute to the sensitivities observed, thus optimization of the LIF system to increase incident energies may improve the results obtained.

Excitation radiation of 292 nm may therefore also be useful for the analysis of phenanthrene in addition to naphthalene, whilst selectivity can be provided by the monochromator for samples containing mixtures of PAHs.

3.2.4 PAH photodegradation

3.2.4.1 Background

PAHs are known to photodegrade under environmental conditions (Kamens et al., 1990), although the rate of this photodegradation is dependent on many factors. Naphthalene, for example, is been reported to photodegrade in the air within a day under moist conditions (ATSDR, 2005). On the other hand, photodegradation of PAHs bound to diesel particulates has been found to be slow under average light intensities, after deposition to ground (Matsuzawa et al., 2001). Photodegradation rates were also found to be minimal for a number of PAHs, including phenanthrene and fluoranthene, adsorbed onto coal fly ash particles

(Korfmacher et al., 1980a and b). It was noted that the photosensitivity of PAHs is strongly dependent upon the nature of the surface onto which they are adsorbed (Korfmacher et al., 1980b).

In terms of photodegradation, PAHs become excited after absorption of photons (ie, by direct photolysis, whilst indirect photolysis occurs when energy is transferred to the target analyte from another excited species). The molecules return to the ground state upon dissipation of the excess energy by means of chemical reactions or by energy transfer processes. The latter may lead to the formation of singlet state oxygen upon energy transfer to oxygen. This product may then attack molecular PAHs via addition reactions (Wang et al., 2005). Singlet oxygen attack and hydrogen abstraction-initiated radical reactions have been proposed as possible mechanisms for the decomposition of PAHs present in atmospheric particulate matter, yielding highly oxygenated compounds (such as dicarboxylic acids; phthalic acid has been observed from naphthalene adsorbed on silica surfaces), polymeric products or hydro-substituted PAHs (Jang and McDow, 1997).

A good correlation was found between the half-life of individual PAHs adsorbed onto particles and their Dewar reactivity number, which is the energy required to remove a π electron at a specific carbon centre from the remaining π system (Behymer and Hites, 1985). Enhanced photodegradation was noted for substrates which had larger surface areas, due to greater PAH dispersion and darker substrates, such as carbon black, were also found to absorb more of the incident light, which reduced the rate of PAH photodegradation (Yokley et al., 1986).

Studies on the influence of UV-B radiation (280 to 320 nm) and temperature on the photodegradation of PAHs dissolved in tetradecane, have indicated that the half-life is dependent on the molecular mass of the PAH concerned, with faster degradation evident for lower molar mass PAHs (Nadal et al., 2006) and similar results were obtained for particle bound PAHs (Ohura et al., 2004b). The degradation rates of PAHs in tetradecane were of the order: naphthalene > pyrene > fluoranthene, although fluoranthene was degraded more slowly than pyrene at low UV-B doses, but faster than pyrene at high temperatures and high UV-B doses (Nadal et al., 2006). The rate of photodegradation of PAHs adsorbed onto wood smoke

particles, which were exposed to midday sun, was strongly influenced by temperature (Kamens et al., 1986). This would result in higher concentrations of PAHs in winter than in summer.

Photolysis of PAHs sorbed onto pine needles showed first order kinetics when exposed to sunlight, with photolysis half-lives ($t_{1/2}$) ranging from 12.9 hours for naphthalene to 51.0 hours for phenanthrene (Wang et al., 2005), as presented in Table 3.15 along with other published PAH $t_{1/2}$ values. The cuticular waxes of the pine needles stabilized the PAHs with respect to photolysis, and it was concluded that the photochemical behaviour of PAHs is dependent on the physical-chemical properties of the substrate onto which they are adsorbed, in addition to the molecular structure of the PAHs (Wang et al., 2005).

Real-time visualization and quantification of PAH photodegradation on and within plant leaves by means of two-photon excitation microscopy revealed that degradation was greater for PAHs at the surface of the leaf as compared to that within epidermal cells of maize leaves (*Zea mays*) (Wild et al., 2005).

Studies investigating the effect of UV-B radiation on the degradation of PAHs sorbed onto the surface of 1-year old spruce needles also yielded first order kinetics (Niu et al., 2003) (refer to Table 3.15 for the $t_{1/2}$ values), with direct photolysis being the most important means of photodegradation (Niu et al., 2004). Similarly, first order rate constants were found in the case of PAHs collected onto filters from residential wood smoke and internal gasoline combustion emissions, where half lives of the order of 1 hour were found under moderate temperature and humidity conditions, with higher decay under higher humidity conditions (Kamens et al., 1988).

Faster photodegradation rates were observed in aqueous solutions ($t_{1/2}$ of the order of 12 min for pyrene), which followed first order reaction kinetics (Lehto et al., 2000). Low et al. (1987) also reported first order reaction kinetics for photodegradation of PAHs in various organic solvents, where benzo(*a*)anthracene, for example, had a $t_{1/2}$ of less than 2 minutes in a number of solvents including acetone and dichloromethane. It was noted that faster degradation occured in more polar solvents, most likely due to the formation of radical cation intermediates (except for phenanthrene which did not show detectable decomposition). The photodegradation products indicated that solvent-induced photodegradation had occurred, and

the rate of photodegradation was found to be higher when irradiation was at wavelengths below 300 nm.

It was concluded that polar solvents should not be used in the extraction of PAHs for analysis, unless light can be excluded. This is another reason why analytical methods for PAHs which do not require solvent extraction steps are preferable.

In the case of the silicone rubber traps, the substrate (i.e. the PDMS) absorbed a very small portion of the incident laser light, thus "filtering" of incident light by the substrate would not occur to any significant extent. This, accompanied by the high intensity of the laser light and the fact that this light is at the maximum PAH absorption wavelength, should result in shorter $t_{1/2}$ values when compared to those of other studies. The fact that PDMS is non-polar may mitigate these effects to some extent.

The products of photodegradation of PAHs have been identified in a number of studies. Naphthalene, for example, was studied when adsorbed onto titanium dioxide, ferric oxide, muscovite (a natural silicoaluminate) and fly ash (Guillard et al., 1993). Naphthalene was chosen for this study, as it is one of the PAHs with the highest atmospheric concentrations. Direct photolysis was prevented by using incident light of $\lambda > 340$ nm. Photocatalysed degradation products were thus noted, particularly with respect to TiO_2 surfaces, in the presence of oxygen, whilst water vapour increased the degradation rate. Products such as 1,4-naphthoquinone (the main intermediate product); 2-naphthol; phthalide; phthaldialdehyde; phthalic acid; acetophenone; benzaldehyde; and benzoic acid were identified. Depending on the volatility of these compounds, some were transferred to the gas phase, whilst others were adsorbed onto the solid surface and underwent further reactions.

Table 3.15: Photolytic half-lives (in hours) of the PAHs of interest, including the light intensity.
Naphthalene was excluded from these studies, as it volatilizes too quickly to be effectively retained on the surface of the spruce needles (Niu et al., 2003).

PAH	Spruce needles (Niu et al., 2004) UV-A 11-16 W.m^{-2}	Tetradecane (Nadal, et al. 2006), UV-B (280 – 320 nm) 20 °C & 22.5 KJ.m^{-2}.day^{-1} (0.26 W.m^{-2})	Spruce needles (Niu et al., 2003) Sunlight 620±50 W.m^{-2}	Maize leaves (Wild et al., 2005) 355-375 nm, 25°C & < 24 W.m^{-2}	Particles (Behymer and Hites, 1985) 300 – 410 nm, 18 W.m^{-2}				Pine needles (Wang et al., 2005) Sunlight, 450 W.m^{-2}	Diesel particulate matter (Matsuzawa et al., 2001) Simulated sunlight, 925 W.m^{-2}	Spruce needles (Niu et al., 2004) UV-A + UV-B 11.43-16.53 W.m^{-2}
					Silica gel	Alumina	Fly ash	Carbon black			
Naph	#	12 – 17	#						12.9		#
PhA	231		75	0.46 (surface)	150	45	49	>1000	51.0	60.63±1.33	158
FlA	182	136 – 201	26	0.09 (surface) 0.24 (cellular)	74	23	44	>1000	25.6	22.16±0.77	151
Py	120	155 – 250	37		21	31	46	>1000	26.1	737.55±124.49	105

The aim of this series of experiments was therefore to determine whether the excitation light provided by the laser system resulted in photodegradation of the PAHs dissolved in the silicone rubber traps. The extent of such photodegradation over a defined time interval was also to be determined, should such degradation be evident, and degradation products were to be identified. These experiments are important in terms of quantitation of PAHs. In addition, it is necessary to determine the photodegradation products so that these are not mistakenly ascribed to the original gas sample. Naphthalene served as a worst case scenario, due to its high volatility and reportedly fast rate of photodegradation (Nadal et al., 2006).

3.2.4.2 Experimental method

a) Photodegradation of naphthalene as determined by LIF

Naphthalene was introduced in the gas phase onto a silicone rubber trap by means of a diffusion tube, after a blank trap fluorescence spectrum had been recorded. The sampling pump was switched off after equilibrium conditions (constant [PAH]) had been established on the sample spot at the top of the trap, as evidenced by a stable oscilloscope signal, which was obtained with the monochromator set to 323 nm (the trap was not end-capped). The laser continued to provide excitation radiation, and the consequent change in oscilloscope signal (and thus [PAH]) was recorded for a period of at least 10 minutes. The laser light intensity was approximately 204 $W.m^{-2}$ (assuming operation at 8 Hz, 500 μJ and a 5 mm spot diameter). Sunlight, by comparison, varies significantly, but was in the order of 450 $W.m^{-2}$ in the pine needle study (Wang et al., 2005). Wild et al. (2005) noted that environmental UV-A intensities average a few $W.m^{-2}$ in temperate latitudes and may reach >10 $W.m^{-2}$ under the most intense tropical conditions.

The experiment was conducted on different days, with different silicone rubber traps and slightly different incident laser pulse energies.

b) Photodegradation of phenanthrene as determined by LIF

Approximately 200 ng of phenanthrene was introduced in the vapour phase onto a silicone rubber trap by means of gas chromatographic fraction collection loading. A LIF scan was recorded of the loaded trap from 295 to 480 nm with 292 nm excitation, after the laser energy had been determined with an energy meter. The laser continued to provide excitation radiation, and the consequent change in oscilloscope signal at 364 nm (and thus [PAH]) was recorded over 30 minutes. The laser light intensity was approximately 41 $W.m^{-2}$ (assuming operation at 8 Hz, 100 μJ and a 5 mm spot diameter).

A LIF scan was recorded again after the 30 minute interval after the laser energy had been determined with a Gentec energy meter.

c) Identification of photodegradation products

Traps were end-capped after the LIF experiments, wrapped in aluminium foil, and were stored in the dark under cool conditions (< 5 ^{o}C) prior to analysis by TD-GC-MS in order to tentatively identify photodegradation products by means of National Institute of Standards and Technology (NIST) library searches. No comparison to standards or quantitation was performed. Six traps which contained naphthalene, three traps loaded with phenanthrene, three traps which contained pyrene, and one trap loaded with both phenanthrene and pyrene were analysed by TD-GC-MS after LIF exposure for various time periods and at different incident energies. TD-GC-MS conditions as described under section 3.2.2.2 were employed. The CIS split ratio was varied between 10:1 and 100:1, depending on the concentration of analytes loaded onto the trap. The mass spectra of ions which were extracted from the total ion chromatogram were compared to those contained in the NIST library. GC peaks which were significantly above the background signal, and target ions from literature were examined.

3.2.4.3 Results and discussion

a) Photodegradation of naphthalene as determined by LIF

Equilibrium conditions were reached in the sample spot at the top of the traps after a loading period of 2 minutes, on average, which related to a total of approximately 240 ng of naphthalene over the trap (based on a diffusion rate of 2 ng.s^{-1}).

A decrease in oscilloscope signal upon continued irradiation, and thus [PAH] was evident from the various repeat experiments conducted, as shown in Figures 3.25, 3.26 and 3.27, with a decrease in oscilloscope signal (and thus [PAH]) of around 12 % over 10 minutes (refer to Table 3.16). The timescale of typical PAH scanning analyses, as detailed under section 3.2.1 was under 5 minutes, which would relate to a decrease in signal of approximately 9 % over this time interval.

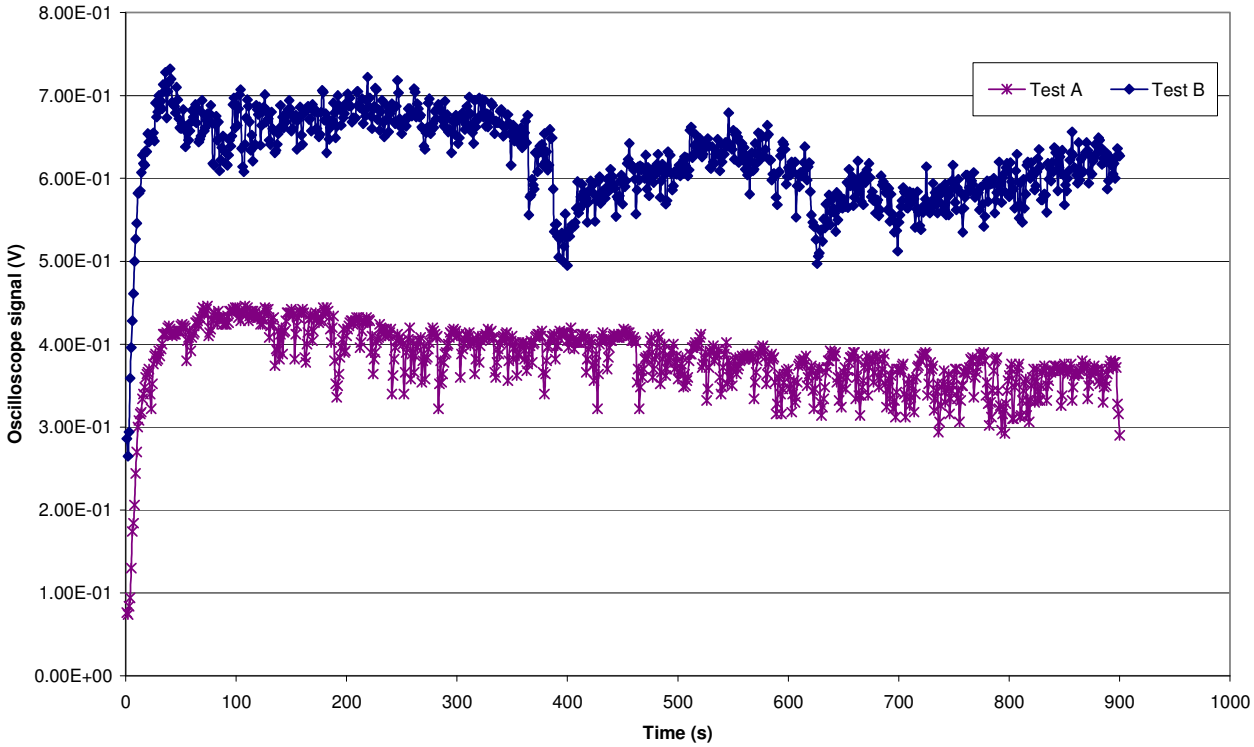

Figure 3.25: Naphthalene 323 nm fluorescence signal upon continued laser irradiation (Test A and B).

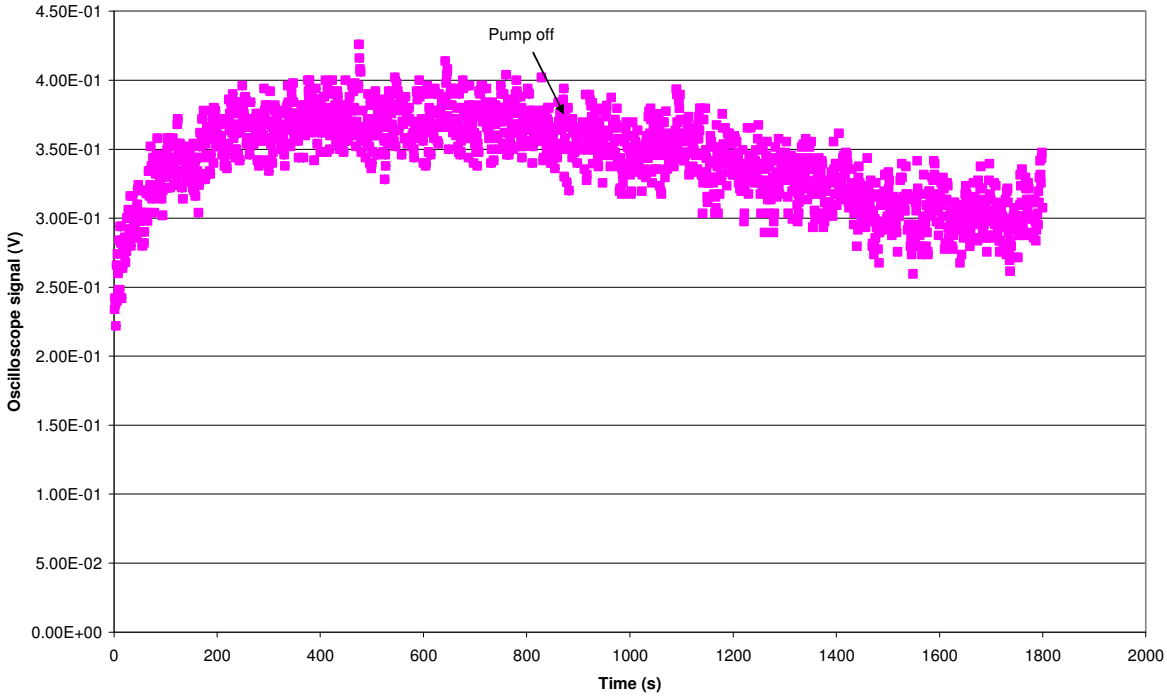

Figure 3.26: Naphthalene 323 nm fluorescence signal upon continued laser irradiation (Test C).

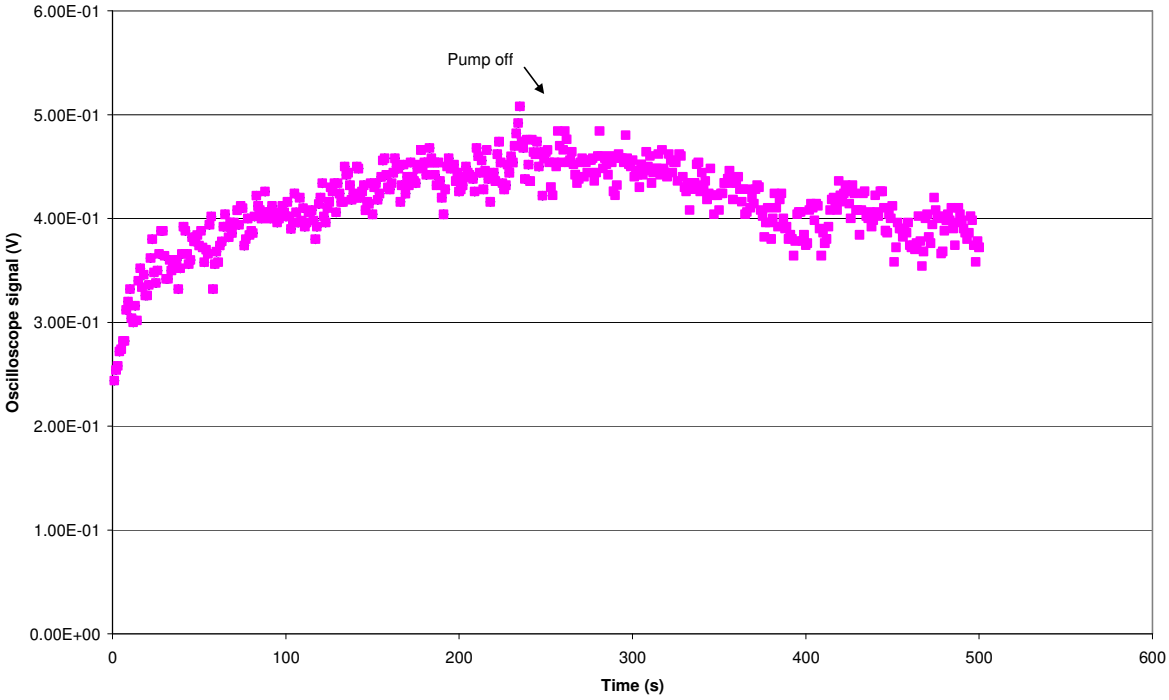

Figure 3.27: Naphthalene 323 nm fluorescence signal upon continued laser irradiation (Test D).

Table 3.16: Naphthalene LIF photodegradation data with estimated fluorescence signal decreases post equilibration.

Test	Energy (µJ)	Loading time (s)	Total irradiation time (s)	Equilibrium oscilloscope signal (V)	% decrease after 5 min	% decrease after 10 min
A	150	110	900	0.444	7 (0.412 V)	14 (0.382 V)
B	386	110	900	0.695	7 (0.648 V)	10 (0.584 V)
C	120	900	1800	0.362	7 (0.338 V)	12 (0.318 V)
D	520	250	500	0.466	14 (0.402 V)	Not available

Similar photodegradation rates were noted in each experiment, although a higher degradation rate was noted in Test D, which could have been due to the relatively high energy of the incident radiation (520 µJ); increased volatilization losses during this experiment; or even due to increased degradation of naphthalene due to the presence of active sites, moisture, or particles in the trap used for this experiment. The cyclic effect in oscilloscope signal observed in Test B was likely to have been caused by laser effects (variations in laser energy).

The time interval over which the experiment was conducted was insufficient to determine the reaction order accurately, as these experiments were conducted over a maximum of 15 minutes, whilst studies in the literature extended over more than 250 hours (Wang et al., 2005; Niu et al., 2003). Upon assuming a first order reaction, as reported in the literature, k can be determined from the equation:

$$\ln \frac{[A]}{[A]_0} = -kt \qquad \text{Equation 3.2}$$

In this case, $[A] \propto V$, where V is the oscilloscope signal. Thus k may be determined from the slope of $ln\ (V_t / V_0)$ versus t. In this manner, $k = 0.0004$ was determined for Test A, although the fit was very poor ($r^2 = 0.4$). The half-life for naphthalene was then calculated to be 29 minutes from the following equation (based on first order kinetics):

$$t_{1/2} = \frac{0.693}{k} \qquad \text{Equation 3.3}$$

The results from each of the datasets are included in Table 3.17. The $t_{1/2}$ for Test D was found to be shorter than the others, possibly due to the reasons previously described, whilst the longest $t_{1/2}$ was determined for Test C, where the incident laser energy was the lowest. An overall average $t_{1/2}$ for naphthalene of approximately 35 minutes was thus calculated. It should be noted that this refers to an overall or total half-life, which incorporates both photodegradation and any volatilization losses.

Table 3.17: Half-life of naphthalene calculated from the LIF experimental data and first order reaction kinetics.

Test	**ln (V_t/V_0) vs t**		
	r^2	**k**	**$t_{1/2}$ (min)**
A	0.4	0.0004	29
B	0.3	0.0003	39
C	0.6	0.0002	58
D	0.7	0.0008	14

b) Photodegradation of phenanthrene as determined by LIF

A decrease in the fluorescence signal of phenanthrene was evident during the 30 min irradiation period, as shown in Figure 3.28. A decrease in phenanthrene fluorescence was also noted upon comparison of the LIF scans obtained before and after the 30 minute irradiation period (Figure 3.29). First order reaction kinetics were assumed, and a photodegradation rate was determined as shown in Figure 3.30.

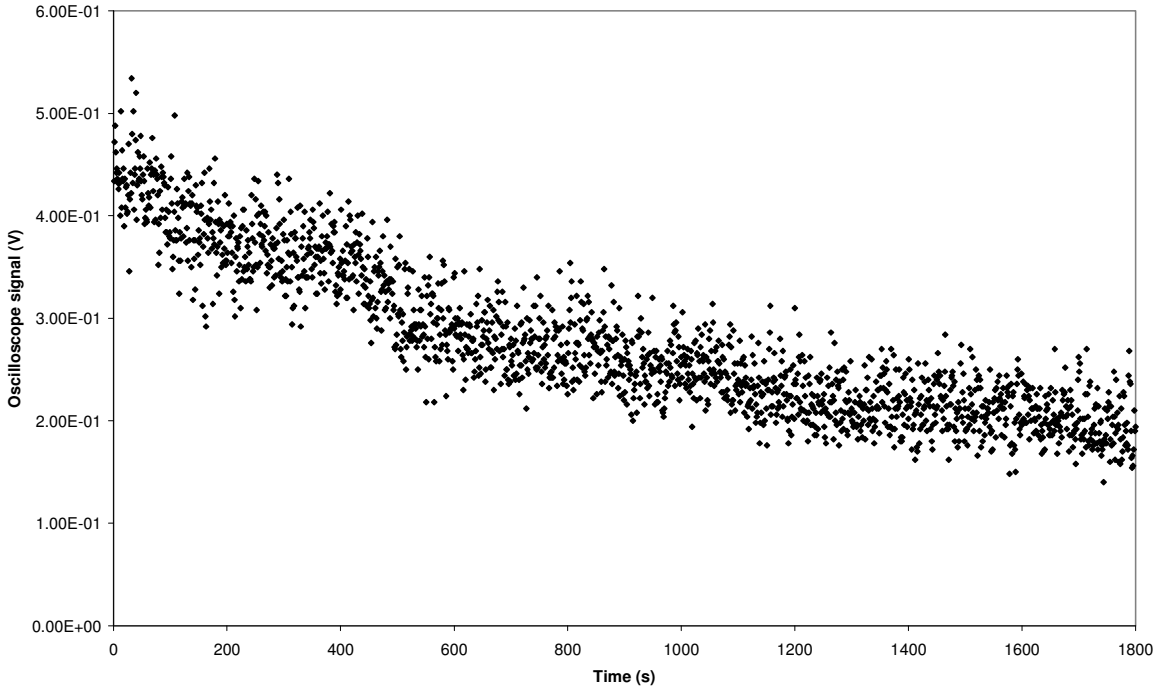

Figure 3.28: Phenanthrene 364 nm fluorescence signal upon continued laser irradiation (200 ng loaded using the gas chromatographic fraction collection method).

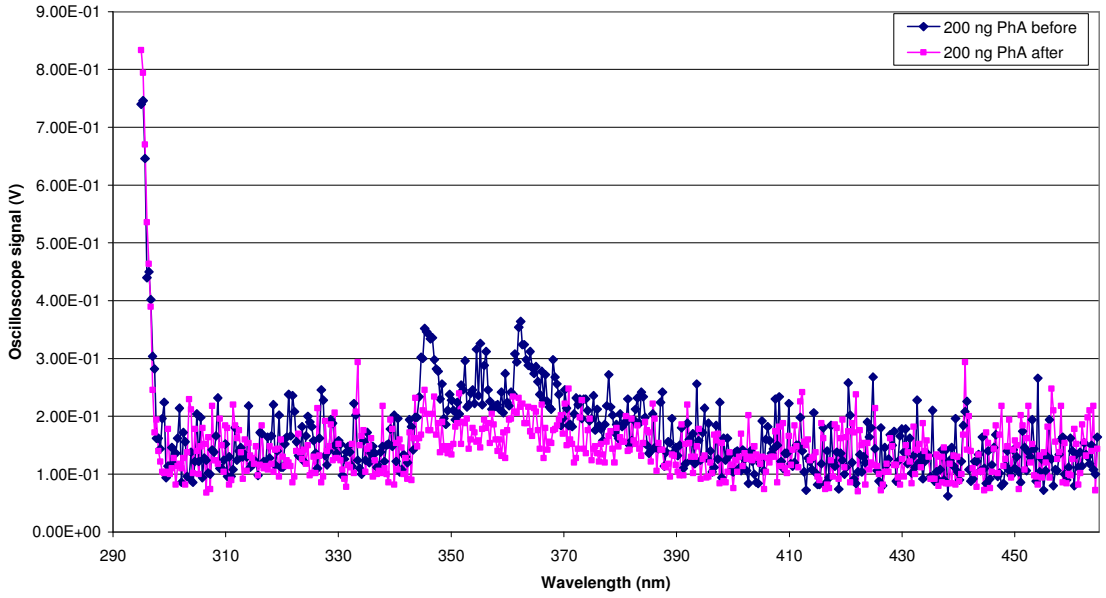

Figure 3.29: LIF scans of phenanthrene before and after 30 minutes of irradiation at 292 nm (200 ng loaded using the gas chromatographic fraction collection method).

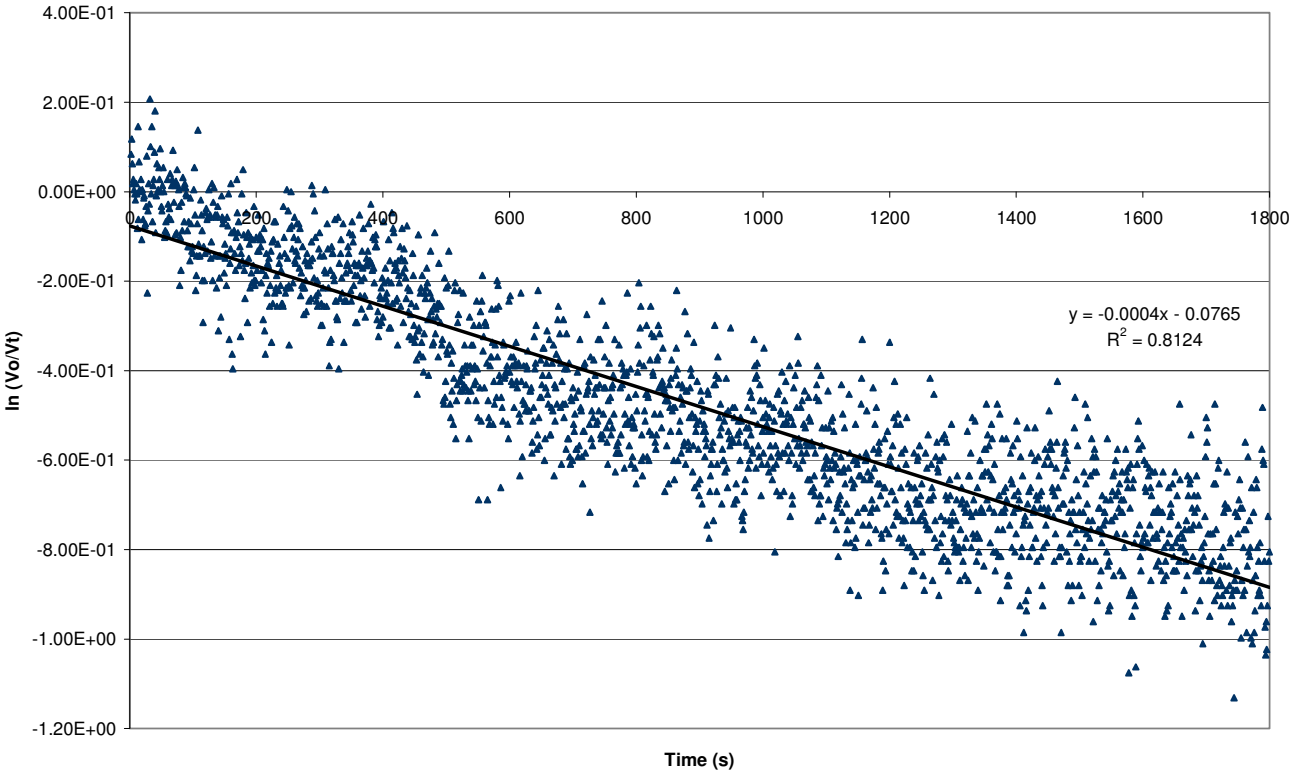

Figure 3.30: First order photodegradation kinetics of 200 ng phenanthrene (loaded using the gas chromatographic fraction collection method) with 292 nm excitation.

The laser energy at the sample position was found to be 100 μJ both before and after the photodegradation experiment was conducted. 117 ng of phenanthrene was found to be present on the trap after the photodegradation experiment by TD-GC-MS analysis. This relates roughly to a 42 % loss after 30 minutes of irradiation, assuming that there was indeed 200 ng of phenanthrene loaded on the trap at the start of the experiment. The oscilloscope signal at 364 nm obtained from the LIF scans also decreased by 44 % after the 30 min irradiation period (refer to Figure 3.28).

A 17 % decrease in oscilloscope signal for a 5 minute LIF scan and a 23 % loss over a 10 minute scan may be estimated from Figure 3.28. A half life of 29 min is obtained from the slope of the kinetics graph (k = 0.0004), which compares favourably to the decrease in oscilloscope signal measured after the 30 minute irradiation period (which is basically equivalent to the half life) and to the TD-GC-MS results.

c) Identification of photodegradation products

The qualitative results of the NIST library searches are presented in Table 3.18, including the laser incident energies and exposure periods for each sample. The photodegradation products were generally present at very low levels, thus the library matches were not very good in some cases, however, they do provide an indication of possible breakdown products.

Five of the six traps which had been loaded with naphthalene were found to contain phenol, whilst four contained both benzyl alcohol and phthalic anhydride. Benzaldehyde, benzoic acid, and benzyl formate were each found on one trap. No breakdown products were found in the naphthalene trap which had only been irradiated for 5 minutes, even though it contained a high concentration of naphthalene, and the laser energy was comparable to that of other LIF analyses where degradation products were detected.

Benzyl alcohol and phthalic anhydride were present on two of the three phenanthrene containing traps, whilst benzyl formate and phenol were present on one of the traps.

Fewer degradation products were generally found in the traps loaded with pyrene, although exposure times were all relatively short (10 minutes). Benzyl alcohol was present on two of the traps, whilst acetophenone, benzyl formate, and phthalic anhydride were each found on one trap.

Phenol, benzaldehyde, and benzyl alcohol were identified on the trap which had been loaded with both phenanthrene and pyrene.

Generally better matches were obtained for traps which had been irradiated for longer or contained more analyte, which would have generated higher concentrations of the breakdown products. The naphthalene trap which was irradiated for the shortest time (5 min) did not contain any detectable concentrations of the breakdown products, therefore such products should not interfere with TD-GC-MS analyses of traps post LIF analysis, as LIF scans are completed in < 5 min. No effect of the variation in laser incident energy on the production of photodegradation products was evident for the range of energies included in this study (12 – 200 μJ). The effect of the photodegradation products (particularly the organic

acids) was also visible in subsequent TD-GC-MS analysis, in that column bleed was evident in the chromatograms (Figure 3.31), due to breakdown of the stationary phase by these acidic compounds.

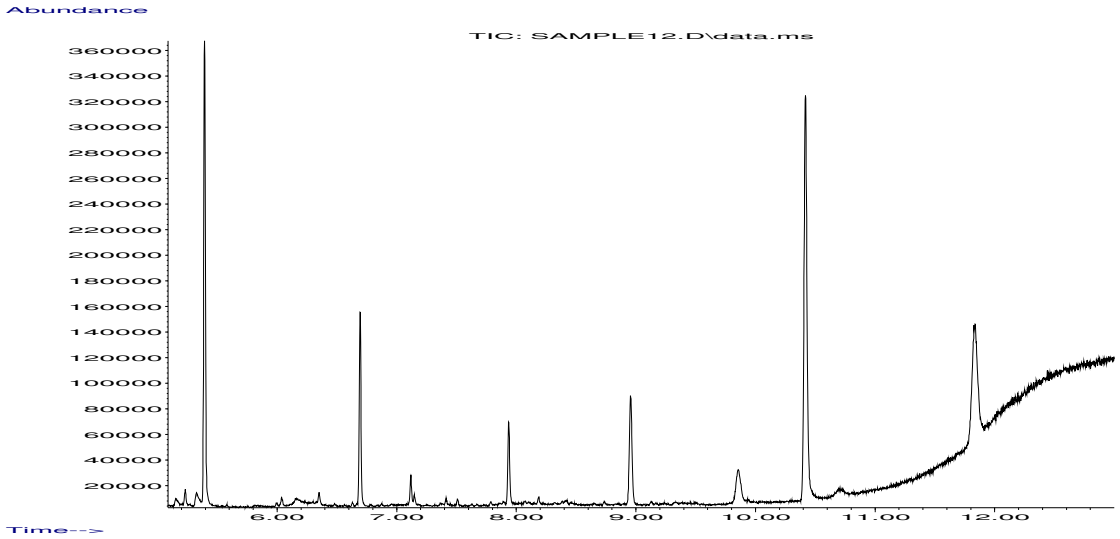

Figure 3.31: Increase in the chromatogram baseline upon the analysis of a sample containing photodegradation products (a mixture of 138 ng of phenanthrene and 100 ng of pyrene irradiated for 10 min at 70 μJ).

Table 3.18: Photodegradation products of naphthalene, phenanthrene and pyrene, as determined by NIST library comparisons.

NOTE: Numbers in brackets reflect the quality of the match between the mass spectrum of the sample to that of the library. Analyte concentrations were determined by TD-GC-MS after LIF analysis. *Naphthalene contamination evident.

Compound	**m/z**	**R_t (min)**	**Trap 1: Naph**	**Trap 2: Naph**	**Trap 3: Naph**	**Trap 4: Naph**	**Trap 5: Naph**	**Trap 6: Naph**	**Trap 1: PhA**	**Trap 2: PhA**	**Trap 3: PhA**	**Trap 1: Py**	**Trap 2: Py**	**Trap 3: Py**	**Trap 1: PhA + Py**
Laser energy at 292 nm (µJ)			160	200	12	25	100	100	140	100	100	100	100	100	70
Approximate irradiation time (min)			15	55	15	80	120	5	10	30	10	10	10	10	10
Analyte concentration post irradiation (ng)			968	31.5	75	6794	9245	9507	80	117	180*	126	246	186	138 (PhA) 100 (Py)
Benzaldehyde	106	5.2	√ (Q7)												√ (Q87)
Phenol	94	5.3	√ (Q5)	√ (Q38)	√ (Q49)	√ (Q49)	√ (Q42)				√ (Q38)				√ (Q80)
Benzyl alcohol	108	5.8	√ (Q86)	√ (Q64)		√ (Q46)	√ (Q52)		√ (Q68)	√ (Q35)			√ (Q64)	√ (Q42)	√ (Q64)
Acetophenone	120	6.1												√ (Q38)	
Benzyl formate	136	6.2	√ (Q91)							√ (Q90)				√ (Q60)	
Benzoic acid	122	6.8				√ (Q43)									
Phthalic anhydride	148	8.0		√ (Q49)	√ (Q49)	√ (Q72)	√ (Q53)			√ (Q83)	√ (Q74)	√ (Q27)			

3.2.4.4 Conclusion

Due to the fact that the silicone rubber traps sample gaseous analytes, and that they effectively serve as denuders, with particles (and thus particle bound analytes) passing through them as discussed in Chapter 4; the presence of solids arising from the sample, which could catalyse the photodegradation reactions, should not be a major consideration.

It was evident that the oscilloscope signal decreased upon laser irradiation of naphthalene and phenanthrene samples, which indicated that the incident laser light was causing photodegradation of these analytes. The overall combined photodegradation and volatilisation rate determined here for naphthalene was of the order of 10 % over the time interval of a scanning LIF analysis (5 min), and would be significantly less for single fluorescence wavelength analyses, which are obtained within the order of seconds. This effect should not have a significantly negative impact on subsequent quantitation by TD-GC-MS, due to the sensitivity of this technique. A half life for naphthalene of ~35 min was determined from first order reaction kinetics. The photodegradation of phenanthrene was slightly more rapid than for naphthalene with 292 nm excitation (17 % decrease in oscilloscope signal over 5 min and $t_{1/2}$ of ~30 min). The LIF photodegradation rates were higher than that reported in most other studies, such as that of PAHs adsorbed onto pine needles, where photolytic half-lives were > 12 h with 450 $W.m^{-2}$ irradiation by sunlight (Wang et al., 2005). This is to be expected as LIF involves single wavelength irradiation at or close to the absorption maximum of the analyte. Shorter half-lives (for example, 28 min for phenanthrene) have been reported for PAHs adsorbed onto maize leaves at < 24 $W.m^{-2}$ with 355 – 375 nm irradiation (Wild et al., 2005).

Once the LIF photodegradation rate has been determined for the target PAH(s) at the experimental wavelength concerned, it is possible to correct for the resulting decrease in analyte concentration upon subsequent quantitative analysis of samples by TD-GC-MS.

Similar oxidative photodegradation products were found in traps loaded with naphthalene and phenanthrene after extended LIF irradiation, primarily phenol, benzyl alcohol, and phthalic anhydride. These compounds were not detected on a naphthalene trap, however, which was irradiated for 5 min, which is the time typically required for a LIF scan.

3.2.5 Energy experiments

3.2.5.1 Background

The laser system utilized in these experiments displayed temporal variability in the pulse energy at the target. This was noted from energy meter measurements at the target site at intervals during experimental runs. Such fluctuations may arise for a number of reasons, including degradation of the laser dye, degradation of the excimer gas, and loss of alignment of optics due to heating effects during experimental runs.

In terms of the degradation of the Rhodamine 6G laser dye, suppliers have published photochemical stability specifications of 316 W.h at 590 nm (the centre of the emission spectrum) when the dye is pumped with an excimer laser (Brackmann, 1986).

$$Eft = P_t \qquad \text{Equation 3.4}$$

Where E is the energy of the excimer laser output in J; f is the repetition rate in Hz; t is the operation time in hours and P_t is 316 W.h.

Thus at 8 Hz and 300 mJ per pulse, the energy of the dye laser output would decrease to 50 % of its initial value after 132 hours of operation (which relates to 3.8 x 10^6 pulses, as $n = 3600.f.t$). This effect should therefore be minimal over the time interval of the experiments, but needs consideration in the long term operation of the laser system.

A series of experiments were therefore conducted in order to quantify the instability of the laser energy in the experimental system, so that the potential impact of this effect could be understood. The relationship between the energy of the excitation radiation and the fluorescence intensity of the analyte (as measured by the oscilloscope signal) was also investigated by means of energy attenuation experiments, in order to determine the relationship between the analyte concentration (oscilloscope voltage) and the incident energy.

3.2.5.2 Experimental method

a) *Laser stability*

Two experiments were conducted with the aid of a Gentec PRJ-M Energy and Power Monitor with the laser system operating at 292 nm and 8 Hz. In the first experiment, the energy at the target was measured, whilst the second experiment focused on the energy of the light exiting the dye laser before it passed through any optics. In this manner, the contribution of the optical path to the energy instability could be determined.

Each experiment was conducted over the period of an hour. The maximum, minimum, and mean energies, as well as the standard deviation were recorded over 100 pulses in each minute (thus sampling over a 12.5 s interval at 8 Hz).

Based on the results of these experiments, further investigations were conducted in order to determine whether the decrease in energy of the dye laser output was due to a decrease in energy of the excimer laser output, which was used to pump the dye laser system. For these experiments, a Molectron Energy Meter (2.13 $V.J^{-1}$; 50 mm diameter) linked to a Tektronix TDS 520A oscilloscope (set at 100 mV and 2 ms per division respectively; and on peak-to-peak averaging over 100 pulses) was used at the exit of the excimer laser, which was operating at 8 Hz and a high voltage setting of 28. The average energy at 248 nm was recorded from the oscilloscope every minute over a period of an hour. The shutter of the laser was closed between readings, in order to minimize thermal effects on the energy meter. The excimer laser had been equipped with fresh chlorine gas and was conditioned a few hours prior to the experiment, and the system was connected to a chiller unit during the course of these experiments.

Two days later, this experiment was repeated at the exit of the dye laser, with an RJ 7610 Energy Radiometer (Laser Precision Corporation) equipped with a Laser Probe Option RQ, which was linked to the same oscilloscope. A high voltage setting of 29 was set on the excimer laser, and measurements were taken over a period of an hour. Immediately following this experiment, measurements were taken over a 15 minute period at the exit of the excimer laser, using the previous method (Molectron Energy Meter).

The RJ 7610 Energy Radiometer was also used to determine the energy stability at the dye laser outlet after the laser system had been further optimized (new gas for the excimer laser and methanol was added to the oscillator of the dye laser to replace that which had evaporated over time).

b) *Relationship between excitation energy and fluorescence emission*

Possible means of attenuating the incident beam were investigated, such as the use of a Brewster crystal; and cover slips of various materials (such as quartz, silica glass, etc). No attenuation of the beam was found when the Brewster crystal was positioned for attenuation of both a vertically or horizontally polarized beam, which indicated that the beam was circularly polarized. Brewster crystals were therefore not effective in attenuating the beam. Glass cover slips (Corning) were also not suitable, as the beam was fully attenuated when two cover slips were placed in the path of the incident light.

Borosilicate glass plates (20 mm x 20 mm x 3.30 mm thick, Glassblowing Industries) were found to be suitable for attenuation of the 292 nm incident beam. A glass plate was thus held in the path of the incident light to a trap which was loaded with naphthalene and the decrease in voltage (fluorescence emission) was recorded. This was repeated with two and three plates in the path of the beam.

The analyte was loaded from a naphthalene diffusion tube at 489 $m\ell.min^{-1}$ for 820 s to ensure equilibrium had been reached in the sample spot at the top of the trap prior to oscilloscope measurements. Loading continued throughout the course of this experiment, in order to prevent variations due to loss of analyte by volatilization or photodegradation.

The trap was then removed from the LIF system and the energy at the trap location was determined by means of an energy meter. The decrease in energy was also recorded when borosilicate glass plates were sequentially placed in the path of the incident beam.

3.2.5.3 Results and discussion

a) *Laser stability*

The results of the first two experimental runs are presented in Figure 3.32, where a decrease in pulse energy over time is evident in both cases.

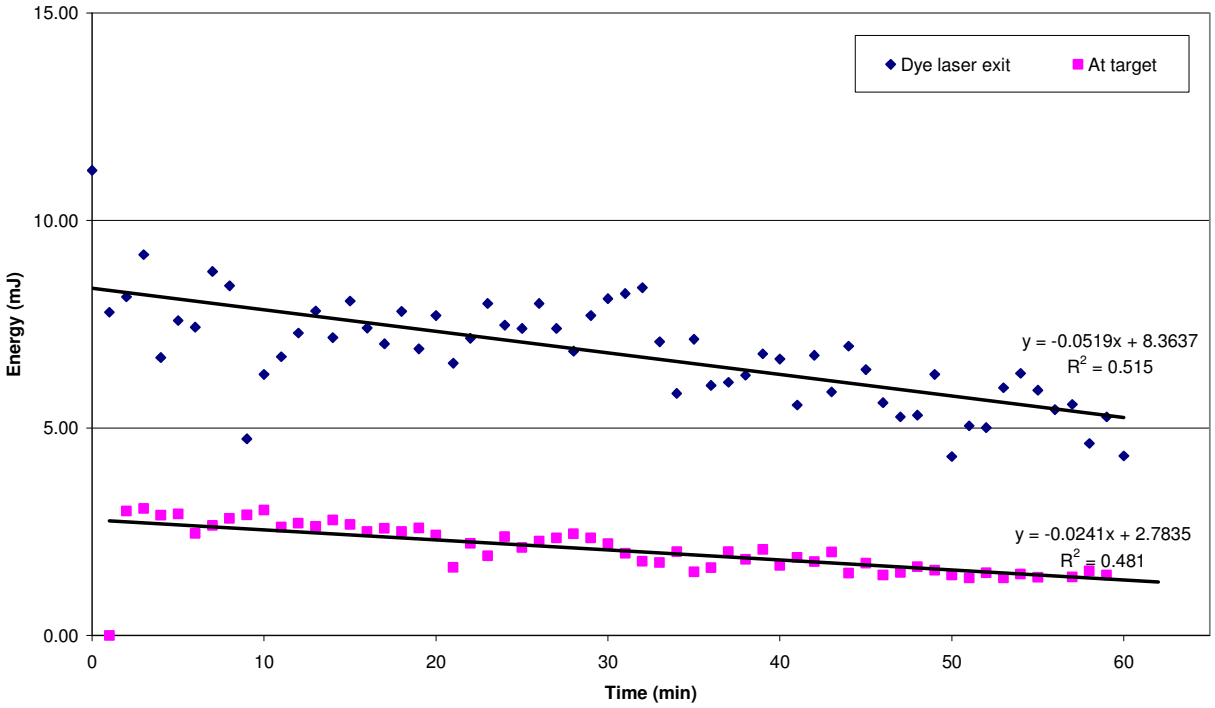

Figure 3.32: Variation in laser energy over time and at various points throughout the system.

The energy exiting the dye laser decreased by approximately 40 % over the period of an hour, whilst the decrease at the target was approximately 50 % over the same time interval. The additional loss in the later case can be attributed to the optics and the effect of heating thereon.

As the timescale of typical PAH LIF scan runs is 5 minutes, the corresponding decreases in energy over this time interval are 3 % and 5 %, respectively.

The results of the second series of experiments are presented in Figure 3.33.

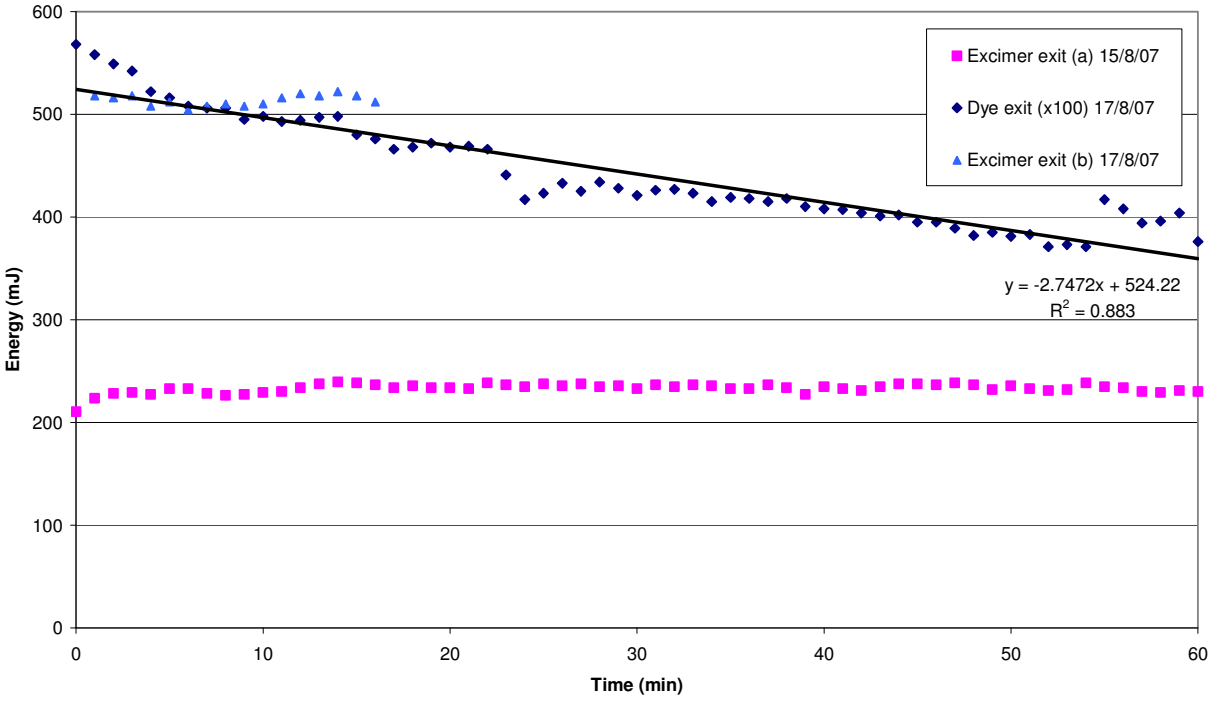

Figure 3.33: Repeat experiment: variation in laser energy over time and at various points throughout the system.

It is evident from these results that the energy of the excimer output was stable over the period of an hour (the higher energy obtained for the second experiment at the excimer exit can be attributed to the increased high voltage, and a longer time for conditioning of the excimer gas). The energy at the dye output decreased by approximately 30 % over an hour (2 % over a 5 min LIF run). There was some improvement in stability over the previous series of experiments (where the decrease was 40 % over an hour), although the energy was slightly lower. It was therefore concluded that the energy fluctuations in the system were mainly due to the dye laser, which thus required optimization.

After optimization, the same energy trend was observed, as shown in Figure 3.34 below. Once again, the energy at the dye output decreased by approximately 30 % over an hour and 2 % over a 5 min LIF run. These losses thus appear to be reproducible.

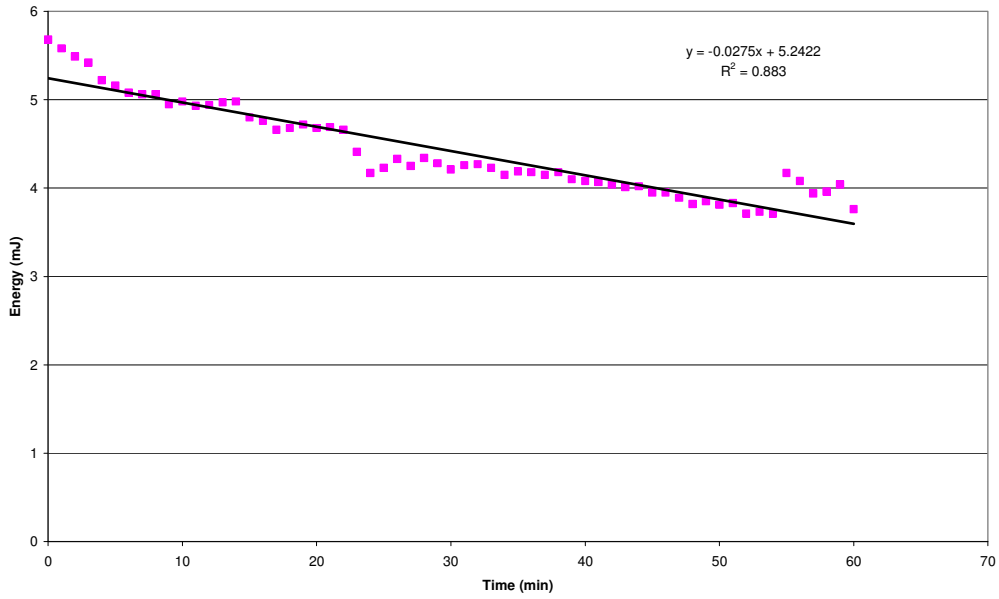

Figure 3.34: Energy at the exit of the dye laser after optimization.

b) *Relationship between excitation energy and fluorescence emission*

The loading of the trap from the naphthalene diffusion tube is shown in Figure 3.35.

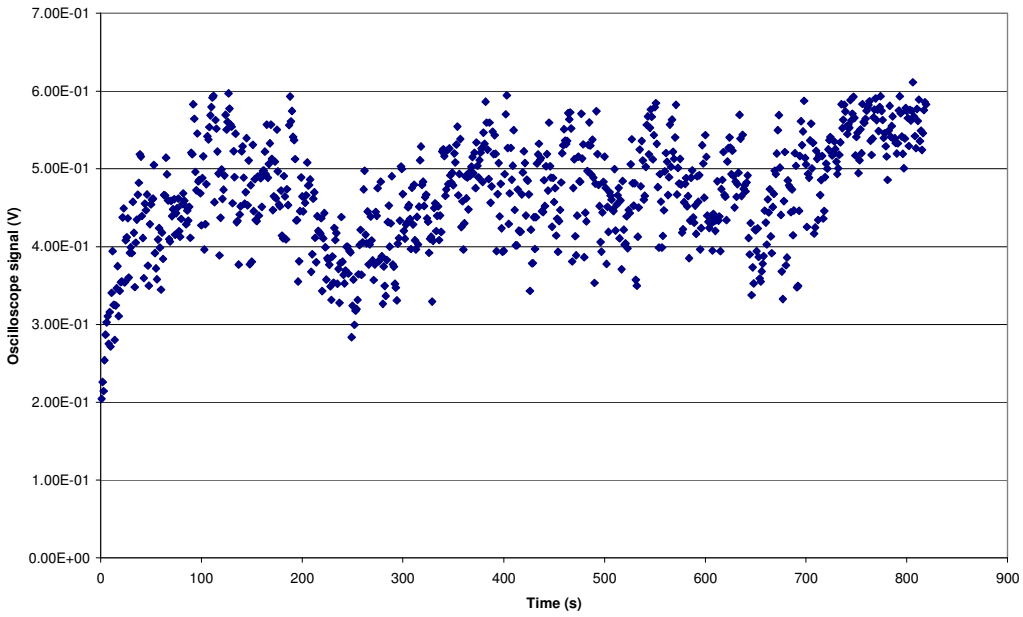

Figure 3.35: Loading of naphthalene onto a silicone rubber trap, prior to energy attenuation experiments.

The decrease in oscilloscope signal with the sequential introduction of borosilicate glass plates in the incident beam is shown in Figure 3.36 and Table 3.19. The measurements taken in between each energy attenuation step indicate that there was no detected change in concentration of naphthalene loaded on the trap during the experiment.

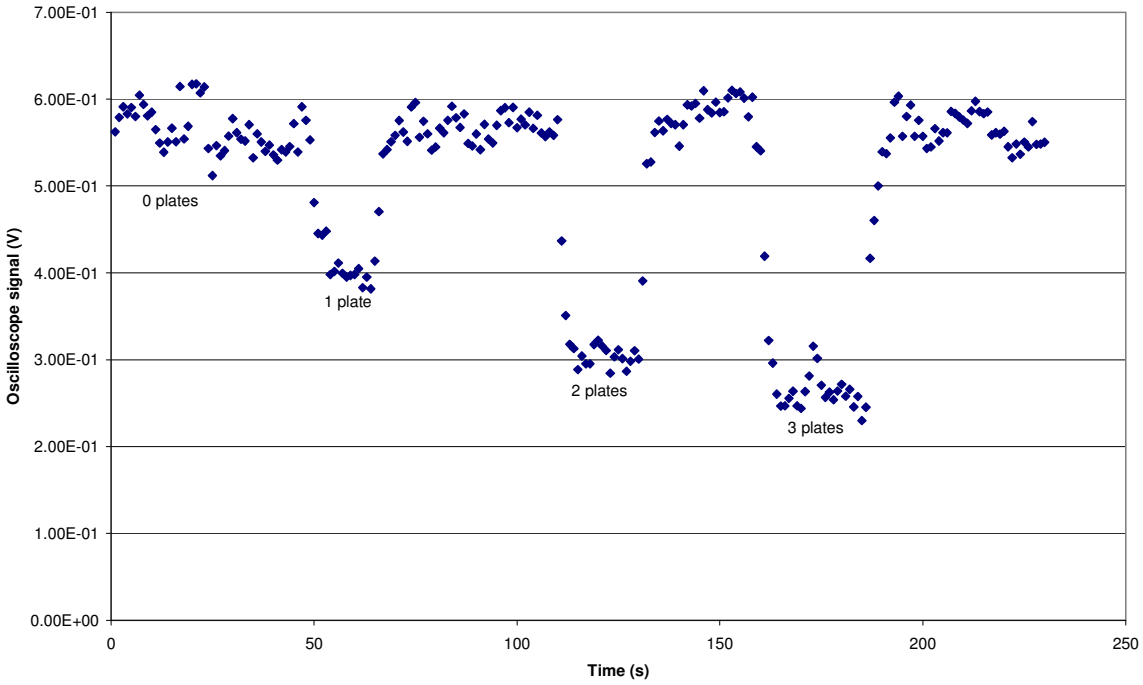

Figure 3.36: Energy attenuation for naphthalene, with n = 0 – 3 (where n represents the number of borosilicate glass plates in the path of the incident beam).

Table 3.19: Energy attenuation by borosilicate glass plates.

Number of borosilicate glass plates in the path of the beam	Average energy at the sample trap location (µJ)	Decrease in energy per plate (%)	Fluorescence signal (V)
0	630	-	0.531586
1	303	52	0.407766
2	182	40	0.306771
3	87	52	0.265053

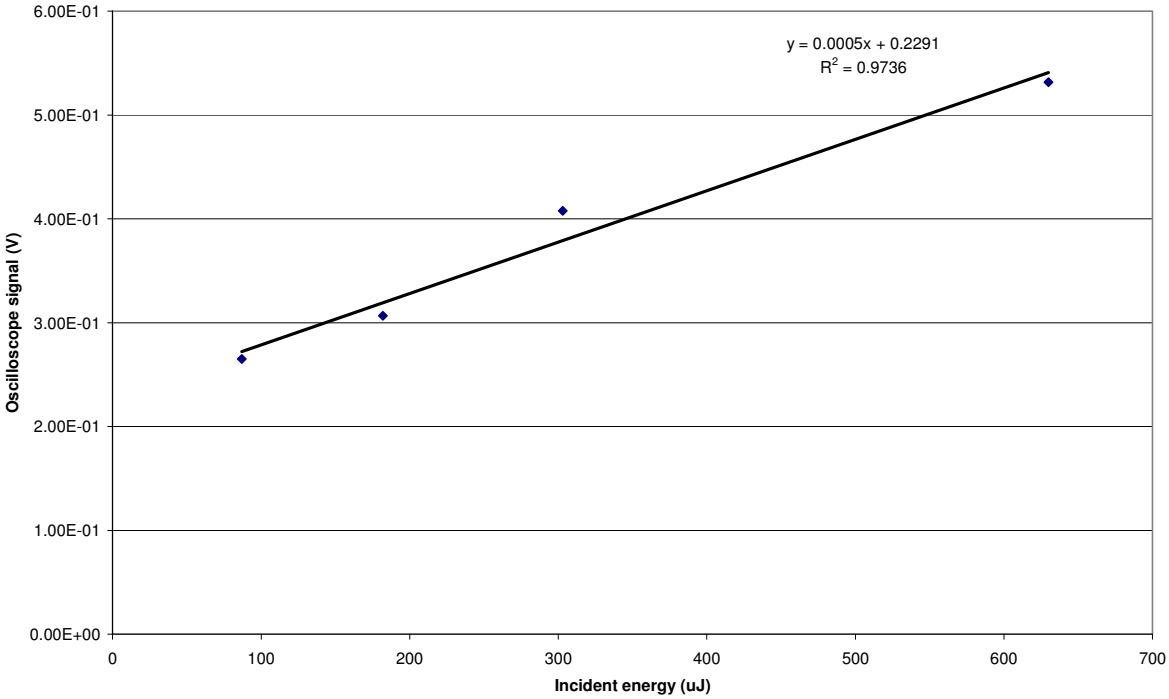

Figure 3.37: Variation in fluorescence signal with changing incident energy.

Some variation in energy attenuation is evident from the decrease in energy signals shown in Table 3.19, and from Figure 3.37. This is probably due to optical imperfections in the plates used.

Due to variations in the system from day to day including the incident energy, slight variations in positioning of the traps, detector response, optical alignment, and so on, the relationship between incident energy, fluorescence signal and concentration would not be constant. This can best be overcome by frequent incident energy measurements throughout analytical runs, as well as by calibration of the system with standard samples of known concentration each day (or more frequently if the measured incident energy fluctuates significantly) and the analysis of quality control samples (of known concentration) in amongst unknowns, as is good laboratory practice.

3.2.5.4 Conclusion

The decrease in energy at the target is largely due to the decrease in pulse energy exiting the dye laser, and there is a smaller contribution due to the optics employed. This decrease will have an impact on the sensitivity of the analytical method, thus the laser system should be carefully optimized to reduce these effects. The contribution of the decrease in energy over time to the results obtained in the photodegradation experiments discussed under section 3.2.4 is also of relevance, as the decreases in oscilloscope signals may not have been only due to photodegradation effects.

The relationship between incident energy, fluorescence signal and concentration is not a simple one, and moreover would not be constant due to concomitant fluctuations in other analytical (system) parameters. This is best overcome by frequent incident energy measurements, and the use of standards to calibrate the system at regular intervals throughout sample analytical runs.

3.2.6 Substrate optimization

3.2.6.1 Background

It is important for the background fluorescence signal obtained from unloaded (blank) traps to be as low as possible, in order to enhance the sensitivity (i.e. to reduce the detection limit) of the experimental method. Silicone rubber is manufactured from liquid silicones by cross-linking induced by an organic peroxide. Background fluorescence experiments were conducted on various silicone rubber substrates, which had been prepared differently; for example by using various monomeric reagents, different cross linking agents, and by employing different post-polymerization product rinsing methods. A number of commercial silicone products, for example that which is sold for household bathroom applications, were also tested.

It is important to note that a concurrent aim of the experiments involving preparation of silicone rubbers, was that the product be useable for air sampling in silicone rubber traps. The

silicone rubber product therefore needed to be non-sticky, easily removed from the preparation plate, as well as non-brittle and elastic, to allow the product to be rolled up for insertion into a quartz tube.

Various stoichiometries were tested in order to determine the effects of increased peroxide content on the properties of the final product.

3.2.6.2 Experimental method and results

a) Preparation of silicones

Stock solutions of various silicone monomers were made by dissolving ~2 g of the silicones (obtained from Alltech Associates (SE-52 and SE-54) and Chromatography Research Supplies Inc. (SE-30)) in 100 mℓ methylene chloride (Merck) (dissolution was assisted by means of ultrasonification).

A measured volume of a stock solution was then mixed with a weighed amount of benzoyl peroxide (The British Drug Houses Inc.) (Figure 3.38) or bis(α,α-dimethylbenzylperoxide) (Merck, 97 % purity), spread on a glass, stainless steel or Teflon plate, and then cured in an oven.

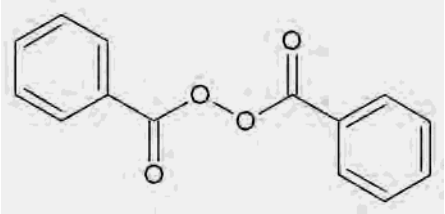

Figure 3.38: Molecular structure of benzoyl peroxide.

The properties of the silicone rubber sheets thus produced were evaluated qualitatively after the silicone rubber had cooled down.

Details of the individual experiments are summarized in Table 3.20.

Table 3.20: Variations in silicone rubber manufacture, where silicone A refers to SE-30, silicone B refers to SE-52 and silicone C refers to SE-54.

Experiment No.	Silicone	Peroxide	Curing conditions	Comments
1	6 mℓ silicone A	10 mg benzoyl peroxide	200 °C for 1 hour on stainless steel	Sticky and broke up into clumps upon removal from the plate.
2	6.5 mℓ silicone A	5.15 mg benzoyl peroxide	200 °C for 1 hour on glass	Stuck to the glass.
3	6 mℓ silicone A	5.40 mg benzoyl peroxide	100 °C for 1 hour then 200 °C for ½ hour, on Teflon	Light brown colour, slightly sticky and was removed from the plate as a sheet.
4	6 mℓ silicone A	11 mg benzoyl peroxide	200 °C for 1 hour on Teflon	Light brown discoloration, brittle, non-sticky product.
5	6 mℓ silicone A	10 mg bis(α,α-dimethylbenzylperoxide)	200 °C for 1 hour on Teflon	Slightly sticky, elastic product.
6	6 mℓ silicone A	19 mg bis(α,α-dimethylbenzylperoxide)	200 °C for 1 hour on Teflon	Sticky, clear product.
7	6 mℓ silicone A	15 mg bis(α,α-dimethylbenzylperoxide)	200 °C for 1 hour on Teflon	Sticky product.
8	25 mℓ silicone A	40 mg bis(α,α-dimethylbenzylperoxide)	200 °C for 1 hour on a larger scale Teflon plate	Clear, thin sheet which was sticky, and gel-like. Was difficult to remove from the plate.
9	6 mℓ silicone B	63 mg bis(α,α-dimethylbenzylperoxide)	200 °C for 1 hour on Teflon	Yellow-brown discoloration, non-sticky.
10	6 mℓ silicone B	40 mg bis(α,α-dimethylbenzylperoxide)	200 °C for 1 hour on Teflon	Slight yellow discoloration, non-sticky.
11	6 mℓ silicone B	35 mg bis(α,α-dimethylbenzylperoxide)	200 °C for 1 hour on Teflon	Clear, non-sticky, slightly elastic. Did not peel off from the plate entirely.
12	6 mℓ silicone B	30 mg bis(α,α-dimethylbenzylperoxide)	200 °C for 1 hour on Teflon	Clear, non-sticky, slightly elastic. Easier to peel off the plate.
13	6 mℓ silicone C	30 mg bis(α,α-dimethylbenzylperoxide)	200 °C for 1 hour on Teflon	Uneven brown discoloration. Easy to remove from the plate. Non-sticky.
14	6 mℓ silicone B	25 mg bis(α,α-dimethylbenzylperoxide)	200 °C for 1 hour on Teflon	Clear, non-sticky. Easy to remove from the plate as a sheet.
15	69 mℓ silicone B	287 mg bis(α,α-dimethylbenzylperoxide)	200 °C for 1 hour on a larger scale Teflon plate	Clear, thin, sticky. Easy to remove from the plate but broke readily. Gel-like.

Different product rinsing solvents were also tested on the SE-30 based silicone rubber, as this step is important in removing any remaining peroxide (in this case bis(α,α-dimethylbenzylperoxide)) or uncross-linked silicone from the final product. It is important that the solvents used do not cause extensive swelling of the PDMS, as this may render the polymer fragile and difficult to handle (Rusina et al., 2007). The experimental conditions and observations pertaining thereto are summarized in Table 3.21 below.

Table 3.21: Effects of solvent rinsing on silicone rubber product, where DCM denotes dichloromethane).

Experiment No.	Solvents	Observations
1	Hexane & acetone, 1:1	Transparent whilst submerged, cloudy upon removal.
2	Hexane	Transparent whilst submerged, sticky and gel-like upon removal and reduced in size.
3	DCM	Translucent whilst submerged, sticky upon removal and became cloudy.
4	Acetone	Appeared to shrink in the solvent and became cloudy.
5	Hexane & DCM, 1:1	Swelled after submersion and was slippery after removal from the solvent.
6	Hexane & DCM, 2:1	Appeared to have shrunk and was slightly cloudy.
7	Hexane & DCM, 1:2	Neither sticky nor cloudy.

b) LIF evaluation

The various silicone rubbers (and silicone monomers) were placed inside a quartz tube (the same dimensions as that used for the multi-channel silicone rubber traps), in the form of a plug, or a rolled sheet, as appropriate. The trap was then placed at the sample target position of the LIF system, as described under section 3.2.1. Various incident wavelengths were used and the resulting fluorescence spectra were recorded over a fairly wide emission wavelength range, in order to cover the range of fluorescence maxima of different PAHs.

The results obtained with 302 nm excitation (suitable for benzo(*a*)pyrene) are presented in Figure 3.39, whilst those with 292 nm excitation (suitable for naphthalene) are given in Figure 3.40.

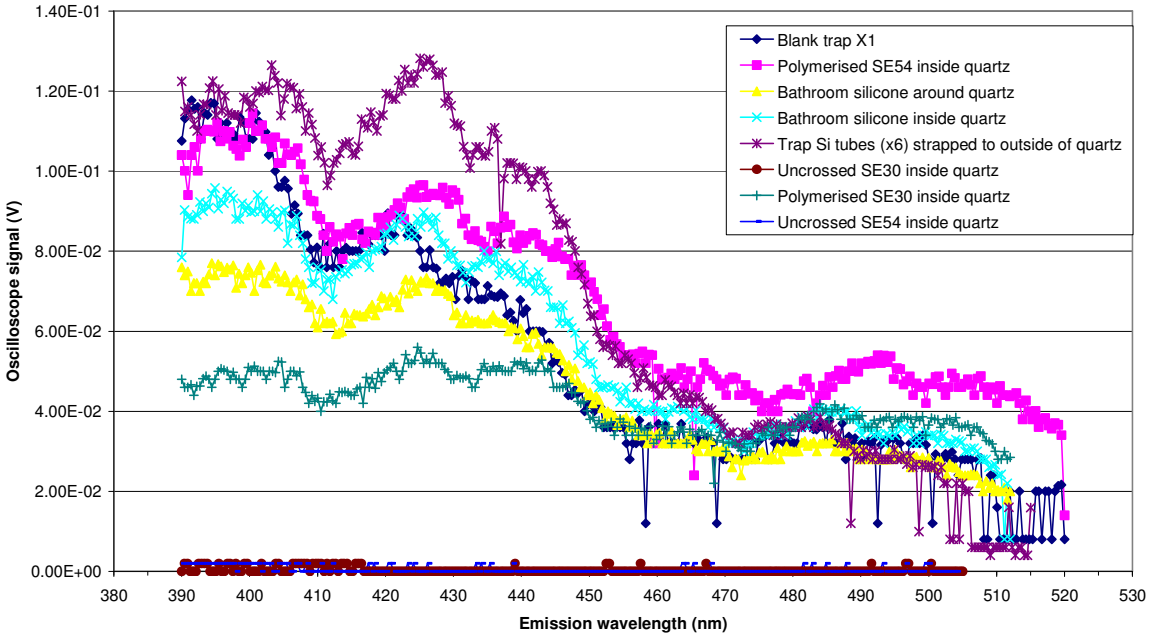

Figure 3.39: Fluorescence spectra of various blank quartz traps, with 302 nm excitation provided by the dye laser system. Blank trap X1 refers to the standard quartz multi-channel silicone rubber traps used in the other experiments.

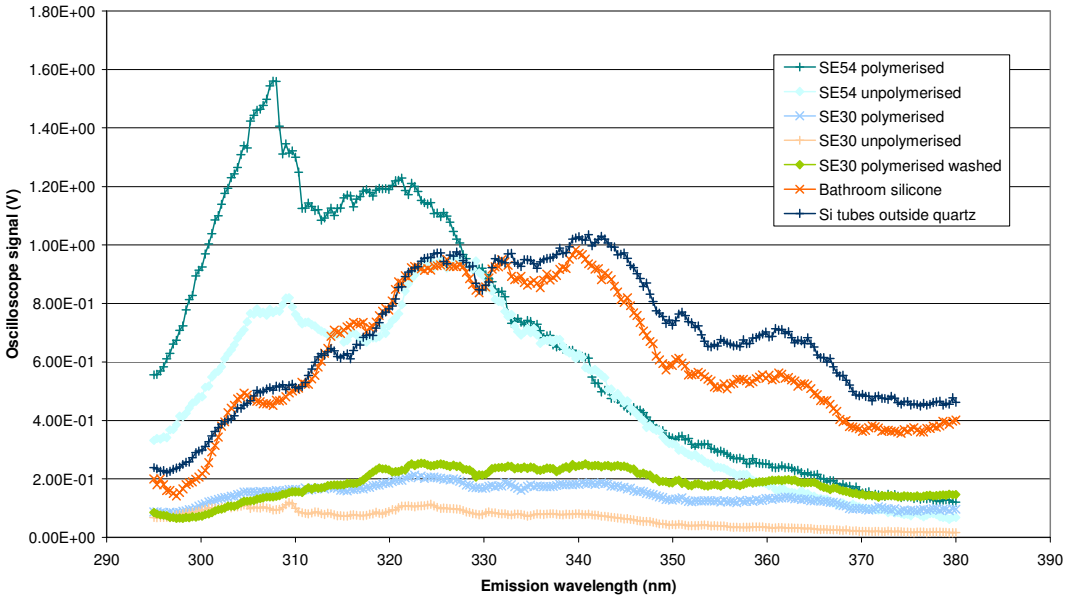

Figure 3.40: Fluorescence spectra of various blank quartz traps, with 292 nm excitation provided by the dye laser system.

3.2.6.3 Discussion and conclusion

In terms of the production of silicone rubber sheets, the results of the various preparation experiments conducted showed that silicone SE-52 (95 % methyl, 5 % phenyl) with (~ 25 % mass/mass) bis(α,α-dimethylbenzylperoxide) yielded a less sticky, more elastic product, which was clear, thus experiment 12 in Table 3.20 yielded the most promising results. The Teflon plate was the most suitable curing surface, as it facilitated the removal of the product.

With respect to solvent rinsing, hexane : DCM :: 1 : 2 yielded the best results (experiment no. 7 in Table 3.21), as this mixture maintained the structure of the silicone rubber product and its clear, translucent property.

The results of the LIF tests are qualitative, as the mass of silicone used in each experiment was not the same. The experiments did, however, successfully show that the lowest background fluorescence signal was obtained for the silicone which had the least aromatic moieties in the final product, as would be expected due to their chromophoric properties.

Similar trends in the background fluorescence signals were found at both excitation wavelengths. A high signal was obtained for the silicone tubes (used to prepare the standard multi-channel silicone rubber traps) strapped to the outside of a quartz tube. This experiment was performed to determine the background signal of the silicone tubes alone, without the influence of the quartz. Presumably more incident light reached the silicone tubes in this case, as compared to when they are housed in quartz, which therefore produced a higher background fluorescence signal. This trend was reversed for the commercial bathroom silicone, however, where it appears that the quartz tube assisted with focusing the incident beam onto the silicone (the 292 nm bathroom silicone measurement also refers to this silicone inside a quartz tube), resulting in a higher fluorescence signal, although this effect was less than that of the silicone tubes, where the difference between oscilloscope signals was larger.

The uncross-linked monomer had a lower background signal, which is most likely due to the lack of influence of the aromatic moieties of the cross-linking agent (peroxide). Although washing of polymerized product would remove remaining excess reagents, the

washing of polymerized SE-30, in the case of 292 nm excitation, increased the fluorescence signal slightly, possibly due to the presence of impurities in the solvents used. The cross-linked SE-54 (methyl silicone, 5 % phenyl, 1 % vinyl silicone) resulted in a higher background signal as compared to SE-30 (methyl silicone), which gave the lowest background fluorescence of all the cross-linked products tested, as would be expected due to the lower aromatic moieties present in this product.

The SE-30 based silicone is therefore a potential alternative to the commercial silicone tubes, although the production methodology requires further development, in order to produce a silicone sheet of reproducible thickness and consistency, which can be rolled up and inserted into a quartz tube in a manner which allows for reproducible sampling flow rates and minimal pressure drop across the trap.

3.3 OVERALL CONCLUSION

The method described has the potential to serve as a screening tool to avoid the comprehensive analysis of samples which do not contain appreciable levels of PAHs. The LIF experimental procedure is simple and rapid, with acceptably low limits of detection, even with the initial, unoptimized optical arrangement and without extensive time-averaging. LIF also provides selectivity without the need for sample clean-up and separation processes, which may entail the use of organic solvents and cryogenic equipment.

The method is basically non-destructive and the sample traps may be subsequently analysed directly by TD-GC-MS. The method developed here may therefore find application in the analysis of combustion products arising from processes of relevance to developing countries including incineration; veld fires; sugar cane burning; and diesel fuel combustion, as described in Chapter 5.

The multi-channel silicone rubber traps allow for the pre-concentration of analytes and in addition they may provide a useful means of simultaneously physically separating mixtures of analytes in air samples in the trap, as a consequence of chromatographic frontal separation processes occurring through the trap during sampling. The first part of the trap may therefore

remove the less volatile PAHs from naphthalene, for example, which will move further down the trap. This physical resolution can then be utilized by focusing the laser on a spot lower down the trap to detect naphthalene, and may also allow for the deconvolution of more complex fluorescence spectra. Such a profiling example was evident in the LIF analysis of traps which had been used to sample emissions from a sugar cane burn, as discussed in Chapter 5.

Further development and optimization of the method is needed in order to ensure its robustness and to provide sufficiently accurate and reproducible results. Specifically the variation in incident energy provided by the laser system should be minimized, which was a challenge in this study due to the age of the laser system employed. In addition, signal averaging and the collection and detection of the fluorescence emission should be optimized, and the capability of the system to resolve the PAH emission spectra in mixtures should be further investigated. The use of time-gated fluorescence spectroscopy may also reduce background effects arising from fluorescence of the PDMS, which would reduce method detection limits. Such an approach has been demonstrated in aqueous systems, where pyrene was detected by LIF (Kuo et al., 2007), for example.

3.4 REFERENCES

Allain, L.R., Stratis, D.N., Cullum, B.M., Mobley, J., Hajaligol, M.R. and Vo-Dinh, T., *Journal of Analytical Applied Pyrolysis,* **2003**, *66*, 145-154.

Agency for Toxic Substances and Disease Registry (ATSDR), USA Department of Health and Human Services, August **1995**, Agency for Toxic Substances and Disease Registry, Public Health Statement: Naphthalene, 1-methylnaphthalene, and 2-methylnaphthalene, accessed on 14 September 2007 at http://www.atsdr.cdc.gov/toxpro2

Agency for Toxic Substances and Disease Registry (ATSDR), USA Department of Health and Human Services, August **2005**, Agency for Toxic Substances and Disease Registry, Public Health Statement: Polycyclic Aromatic Hydrocarbons, accessed on 14 September 2007 at http://www.atsdr.cdc.gov/toxpro2

Balthussen, E., David, F., Sandra, P., Janssen, H.-G. and Cramers, C.A., *Journal of High Resolution Chromatography*, **1998**, *21*, 332-340.

Baltussen, E., Janssen, H.-G., Sandra, P. and Cramers, C.A., *Journal of High Resolution Chromatography*, **1997**, *20*, 385-393.

Behymer, T.D. and Hites, R.A., *Environmental Science and Technology,* **1985**, *19*, 1004-1006.

Boström, C.-E., Gerde, P., Hanberg, A., Jernström, B., Johansson, C., Kyrklund, T., Rannug, A., Törnqvist, M., Victorin, K. and Westerholm, R., *Environmental Health Perspectives*, **2002**, *110* (Suppl. 3), 451-488.

Brackmann, U., **1986**, Lambdachrome Laser Dyes, Lambda Physik.

Chang, K.-F., Fang, G.-C., Chen, J.-C. and Wu, Y.-S., *Environmental Pollution*, **2006**, *142*, 388-396.

Chi, Z., Cullum, B.M., Stokes, D.L., Mobley, J., Miller, G.H., Hajaligol, M.R. and Vo-Dinh, T., *Spectrochimica Acta Part A*, **2001**, *57*, 1377-1384.

Chiang, P.-C., You, J.-H., Chang, S.-C. and Wei, Y.-H., *Journal of Hazardous Materials*, **1992**, *31*, 29-37.

De Coensel, N., Desmet, K., Sandra, P. and Górecki, T., *Chemosphere*, **2008**, *71*, 711-716.

Dos Santos, C.Y.M., de Almeida Azevedo, D. and de Aquino Neto, F. R., *Atmospheric Environment*, **2002**, *36*, 3009-3019.

Fang, M., Zheng, M., Wang, F., To, K.L., Jaafar, A.B. and Tong, S.L., *Atmospheric Environment*, **1999**, *33*, 783-795.

Gevao, B., Al-Omair, A., Sweetman, A., Al-Ali, L., Al-Bahloul, M., Helaleh, M. and Zafar, J., *Environmental Toxicology and Chemistry*, **2006**, *25* (6), 1496-1502.

Gridin, V.V., Inoue, T., Ogawa, T. and Schechter, I., *Instrumentation Science and Technology*, **2000**, *28* (2), 131-141.

Grundl, T.J., Aldstadt, J.H., Harb, J.G., St Germain, R.W. and Schweitzer, R.C., *Environmental Science and Technology*, **2003**, *37* (6), 1189-1197.

Guillard, C., Delprat, H., Hoang-Van, C. and Pichat, P., *Journal of Atmospheric Chemistry*, **1993**, *16*, 47-59.

Gundel, L.A., Lee, V.C., Mahanama, K.R.R., Stevens, R.K. and Daisey, J.M., *Atmospheric Environment*, **1995**, *29* (14), 1719-1733.

Handa, T., Kato, Y., Yamamura, T., Tshii, T. and Matsushita, H., *Journal of Environmental Science and Health*, **1980**, *A15* (6), 573-599.

Harrison, R.M., Smith, D.J.T. and Luhana, L., *Environmental Science and Technology*, **1996**, *30*, 825-832.

Hart, K.M., McDow, S.R., Giger, W., Steiner, D. and Burtscher, H., *Water, Air, and Soil Pollution*, **1993**, *68*, 75-90.

Hawthorne, S.B., St. Germain, R.W. and Azzolina, N.A., *Environmental Science and Technology*, **2008**, *42* (21), 8021-8026.

Hays, M.D., Smith, N.D., Kinsey, J., Dong, Y. and Kariher, P. *Aerosol Science*, **2003**, *34*, 1061-1084.

Jang, M. and McDow, S.R., *Environmental Science and Technology,* **1997**, *31*, 1046-1053.

Jaward, F.M., Farrar, N.J., Harner, T., Sweetman, A.J. and Jones, K.C. *Environmental Toxicology and Chemistry,* **2004**, *23* (6), 1355-1364.

Johnsen, A.R., Wick, L.Y. and Harms, H., *Environmental Pollution*, **2005**, *133*, 71-84.

Kamens, R.M., Guo, J., Guo, Z. and McDow, S.R., *Atmospheric Environment*, **1990**, *24(A)* (5), 1161-1173.

Kamens, R.M., Zhishi, G., Fulcher, J.N. and Bell, D.A., *Environmental Science and Technology*, **1988**, *22*, 103-108.

Kamens, R.M.., Fulcher, J.N. and Zhishi, G., *Atmospheric Environment*, **1986**, *20* (8), 1579-1587.

Kirsh, B.A. and Winefordner, J.D., *Analytical Chemistry*, **1987**, *59* (14), 1874-1879.

Knorr, F.J. and Harris, J.M., *Analytical Chemistry*, **1981**, *53*, 272-276.

Korfmacher, W.A., Natusch, D.F.S., Taylor, D.R., Mamantov, G. and Wehry, E.L., *Science*, **1980a**, *207*, 763-765.

Korfmacher, W.A., Wehry, E.L., Mamantov, G. and Natusch, D.F.S., *Environmental Science and Technology*, **1980b**, *14* (9), 1094-1099.

Kotzick, R. and Niessner, R., *Fresenius Journal of Analytical Chemistry*, **1996**, *354*, 72-76.

Koziel, J.A., Odziemkowski, M. and Pawliszyn, J., *Analytical Chemistry,* **2001**, *73*, 47-54.

Kumke, M.U., Löhmannsröben, H.-G. and Roch, Th., *Journal of Fluorescence*, **1995**, *5* (2), 139-153.

Kuo, D.T.F., Adams, R.G., Rudnick, S.M., Chen, R.F. and Gschwend, P.M., *Environmental Science and Technology*, **2007**, *41* (22), 7752-7758.

Lehto, K.-M., Vuorimaa, E. and Lemmetyinen, H., *Journal of Photochemistry and Photobiology A: Chemistry*, **2000**, *136*, 53-60.

Liu, L.-B., Liu, Y., Lin, J.-M., Ning, T., Hayakawa K. and Maeda, T., *Journal of Environmental Sciences.* **2007**, *19*, 1-11.

Lohmann, R., Northcott, G.L. and Jones, K.C., *Environmental Science and Technology,* **2000**, *34*, 2892-2899.

Low, G., Batley, G. and Brockbank, C.I., *Journal of Chromatography*, **1987**, *392*, 199-210.

Lu, R., Wu, J., Turco, R.P., Winer, A.M., Atkinson, R., Arey, J., Paulson, S.E., Lurmann, F.W., Miguel, A.H. and Eiguren-Fernandez, A., *Atmospheric Environment*, **2005**, *39*, 489-507.

Manahan, S.E., **2000**, Environmental Chemistry, 7th edition, Lewis Publishers, USA, 313.

Marr, L.C., Grogan, L.A., Wöhrnschimmel, H., Molina, L., Molina, M.J., Smith, T.J. and Garshick, E., *Environmental Science and Technology,* **2004**, *38* (9), 2584-2592.

Marr, L.C., Kirchstetter, T.W., Harley, R.A., Miguel, A.H., Hering, S.V. and Hammond, S.K., *Environmental Science and Technology,* **1999**, *33*, 3091-3099.

Martinez, M., Harder, H., Ren, X., Lesher, R.L. and Brune, W.H., *Atmospheric Chemistry and Physics*, **2004**, *4*, 563-569.

Matsuzawa, S., Nasser-Ali, L. and Garrigues, P., *Environmental Science and Technology,* **2001**, *35*, 3139-3143.

Mayer, P., Vaes, W. H. J. and Hermens, J.L.M., *Analytical Chemistry,* **2000**, *72*, 459-464.

Menichini, E., Monfredini, F. and Merli, F., *Atmospheric Environment,* **1999**, *33*, 3739-3750.

Nadal, M., Wargent, J.J., Jones, K.C., Paul, N.D., Schuhmacher, M. and Domingo, J.L., *Journal of Atmospheric Chemistry*. **2006**, *55*, 241-252.

Niessner, R., Robers, W. and Krupp, A., *Fresenius Journal of Analytical Chemistry*, **1991**, *341*, 207-213.

Nikolaou, K., Masclet, P. and Mouvier, G., *Science of the Total Environment*, **1984**, *32*, 103-132.

NIOSH Manual of Analytical Methods, 15 January **1998**, 4th edition, Method 5800: Polycyclic aromatic hydrocarbons (total), Issue 1.

NIOSH Manual of Analytical Methods, 15 January **1998**, 4th edition, Method 5506: Polynuclear aromatic hydrocarbons by HPLC, Issue 3.

Nisbet, I.C.T. and LaGoy, P.K., *Regulatory Toxicology and Pharmacology,* **1992**, *16*, 290-300.

Niu, J., Chen, J., Martens, D., Henkelmann, B., Quan, X., Yang, F., Seidlitz, H.K. and Schramm, K.-W., *Science of the Total Environment*, **2004**, *322*, 231-241.

Niu, J., Chen, J., Martens, D., Quan, X., Yang, F., Kettrup, A. and Schramm, K.-W., *Environmental Pollution*, **2003**, *123*, 39-45.

Odabasi, M., Vadar, N., Sofuoglu, A., Tasdemir, Y. and Holsen, T.M., *The Science of the Total Environment*, **1999**, *227*, 57-67.

Odziemkowski, M., Koziel, J.A., Irish, D.E. and Pawliszyn, J., *Analytical Chemistry,* **2001**, *73*, 3131-3139.

Ohura, T., Amagai, T., Sugiyama, T., Fusaya, M. and Matsushita, H., *Environmental Science and Technology,* **2004a**, *38*, 2045-2054.

Ohura, T., Amagai, T., Sugiyama, T., Fusaya, M. and Matsushita, H., *Atmospheric Environment*, **2004b**, *38*, 2045-2054.

Ono-Ogasawara, M. and Smith, T.J., *Industrial Health*, **2004**, *42*, 389-399.

Ortner, E.K. and Rohwer, E.R., *Journal of High Resolution Chromatography,* **1996**, *19*, 339-344.

Ortner, E.K., August, **1994**, Alternative concentration techniques for the trace analysis of semi-volatile organic air pollutants by capillary gas chromatography, MSc Thesis, University of Pretoria.

Panne, U., Knöller, A., Kotzick, R. and Niessner, R., *Fresenius Journal of Analytical Chemistry*, **2000**, *366*, 408-414.

Park, S.S., Kim, Y.J. and Kang, C.H., *Atmospheric Environment*, **2002**, *36*, 2917-2924.

Prevedouros, K., Brorström-Lundén, E., Halsall, C.J., Jones, K.C., Lee, R.G.M. and Sweetman, A.J., *Environmental Pollution*, **2004**, *128*, 17-27.

Primbs, T., Piekarz, A., Wilson, G., Schmedding, D., Higginbotham, C., Field, J. and Simonich, S.M., *Environmental Science and Technology*, **2008**, *42*, 6385-6391.

Ravindra, K., Wauters, E. and Van Grieken, R., *Science of the Total Environment*, **2008**, *396*, 100-110.

Roper, J.C., Brown, D.M., Sullivan, M.A., Schoonhoven, R., Swenberg, J.A. and Pfaender, F.K., *Environmental Toxicology and Chemistry*, **2006**, *25* (12), 3093-3100.

Rosenberg, C., Winiwarter, W., Gregori, M., Pech, G., Casensky, V. and Puxbaum, H., *Fresenius Journal of Analytical Chemistry*, **1988**, *331*, 1-7.

Rusina, T.P., Smedes, F., Klanova, J., Booij, K. and Holoubek, I., *Chemosphere*, **2007**, *68*, 1344-1351.

Sawicki, E., Elbert, W., Stanley, T.W., Hauser, T.R. and Fox, F.T., *Analytical Chemistry*, **1960**, *32* (7), 811-815.

Schwarzenbach, R.P., Gschwend, P.M. and Imboden, D.M., **2003**, Environmental Organic Chemistry, 2nd edition, Wiley Interscience, USA.

Shekiro, J.M., Skogerboe, R.K. and Taylor, H.E. *Environmental Science and Technology*, **1988**, *22,* 338-344.

Šišović, A., Bešlić, I., Šega, K. and Vadjić, V., *Environment International*, **2008**, *34* (5), 580-584.

Song, J.M., Jagannathan, R., Stokes, D.L., Vo-Dinh, T. and Hajaligol, M.R., *Polycyclic Aromatic Compounds*, **2003**, *23*, 429-439.

Subramanyam, V., Valsaraj, K.T., Thibodeaux, L.J. and Reible, D.D., *Atmospheric Environment*, **1994**, *28* (19), 3083-3091.

Tang, S., Johnson, R., Lanni, T., Webster, W., Tagliaferro, T., Munn, J., Barnes, C., Barnes, D., Newkirk, K., Rivenburgh, D. and Guerrieri, D., **2001**, Monitoring of PM-bound polycyclic aromatic hydrocarbons from diesel vehicles by photoelectric aerosol sensor (PAS); Automotive Emissions Laboratory: New York, accessed at www.ecochem.biz/library/nydec.pdf

Temime-Roussel, B., Monod, A., Massiani, C. and Wortham, H., *Atmospheric Environment*, **2004**, *38*, 1913-1924.

Tsapakis, M. and Stephanou, E.G., *Environmental Pollution*, **2005**, *133*, 147-156.

USA EPA, **2002**, Health Assessment Document for Diesel Engine Exhaust. U.S. Environmental Protection Agency, Office of Research and Development, National Center for Environmental Assessment, Washington Office, Washington, DC, EPA/600/8-90/057F.

Vander Wal, R.L., Jensen, K.A. and Choi, M.Y., *Combustion and Flame*, **1997**, *109*, 399-414.

Wang, D., Chen, J., Xu, Z., Qiao, X. and Huang, L., *Atmospheric Environment*, **2005**, *39*, 4583-4591.

Wauters, E., Van Caeter, P., Desmet, G., David, F., Devos, C. and Sandra, P., *Journal of Chromatography A*, **2008**, *1190*, 286-293.

Westerholm, R.N., Almén, J., Li, H., Rannug, J.U., Egebäck, K.-E. and Grägg, K., *Environmental Science and Technology,* **1991**, *25*, 332-338.

Whitcomb, J.L., Bystol, A. J. and Campiglia, A.D., *Analytica Chimica Acta,* **2002**, *464*, 261-272.

Wild, E., Dent, J., Thomas, G.O. and Jones, K.C., *Environmental Toxicology and Chemistry,* **2007**, *26* (12), 2486-2493.

Wild, E., Dent, J., Thomas, G.O. and Jones, K.C., *Environmental Science and Technology,* **2005**, *39*, 268-273.

Wild, S.R. and Jones, K.C., *Environmental Pollution,* **1995**, *88*, 91-108.

Yang, H.-H., Tsai, C.-H., Chao, M.-R., Su, Y.-L. and Chien, S.-M., *Atmospheric Environment*, **2006**, *40*, 1266-1274.

Yokley, R.A., Garrison, A.A., Wehry, E.L. and Mamantov, G., *Environmental Science and Technology*, **1986**, *20*, 86-90.

Zhang, X., Cheng, S., Zhu, C. and Sun, S., *Pedosphere*, **2006**, *16* (5), 555-565.

Chapter 4

The use of multi-channel silicone rubber traps as denuders

4.1 INTRODUCTION

PAHs may be present in air samples both in the gaseous phase and adsorbed onto the surface of particles, where PAHs of molecular mass > 228 are found mainly in the particle phase (Kamens et al., 1986). It is important to be able to quantify the relative contributions of each of these phases of the analyte, as they may have different environmental impacts. This is of particular importance to human health toxicities, as deposition and uptake of inhaled toxic species depends on their phase distribution (Gundel et al., 1995 and Temime-Roussel et al., 2004). The environmental fates of semi-volatile organic compounds are also phase dependant, due to the fact that atmospheric reactions including photodegradation, as well as transport and deposition processes differ for vapour and particle phase species (Bidleman, 1988).

The partitioning of atmospheric semi-volatile organic compounds between the vapour phase and the particle phase is dependent on the vapour pressure of the compound, as well as on the amount of particles available, and can be described by a partition coefficient K_{vp} which varies with particle loading and has the dimensions of [particle]$^{-1}$ (Krieger and Hites, 1994);

$$K_{vp} = \frac{(F/TSP)}{A}, \qquad \text{Equation 4.1}$$

where F is the particulate phase concentration of the compound in the atmosphere (in ng.m^{-3}); TSP is the total suspended particulate loading in the atmosphere (in µg.m^{-3}); and A is the vapour phase concentration of the compound in the atmosphere (in ng.m^{-3}).

The partition coefficient is a function of atmospheric temperature, T (Krieger and Hites, 1994);

$$\frac{d(\ln K_{vp})}{d(1/T)} = \frac{H_d}{R}, \qquad \text{Equation 4.2}$$

where H_d is the energy required to desorb and vapourise the compound from the particle (in kJ.mol^{-1}), and is of similar magnitude to the compound's heat of vapourisation, and R is the gas constant.

Effective sampling of the two phases is needed to ensure that the analytes adsorbed onto particles which are volatilized upon re-equilibration (after collection onto filters, for example), are not lost from the sampling process (Eatough et al., 1993). Likewise, contact between particles and gas phase analytes should be minimized during sampling in order to prevent adsorption. Volatilization of organic analytes from collected particles may be minimized by ensuring a low pressure drop across the filter and by maintaining constant temperature conditions during sampling (Ligocki and Pankow, 1989).

Partitioning measurements based on high volume samplers containing a glass fibre filter which removes particles from the sample flow prior to adsorption of the gas phase analytes onto an adsorbent such as Tenax, or polyurethane foam (PUF), for example, may introduce analytical artifacts. These may arise from sorption of gas phase analytes onto the filter or particles; from desorption of analytes from the particles collected on the filter; or from reaction of the analyte with reactive species in the air, such as OH• or O_3.

Prevention of analyte loss via reaction of PAHs with atmospheric oxidants has been accomplished by the use of "oxidant denuder systems", which are coated with water/glycerol KNO_2 solution in order to retain O_3 and oxidants (Tsapakis and Stephanou, 2005). Coutant et al. (1988) investigated the potential for PAH artifact formation due to volatilization and reaction with ozone. Losses from the filter (particulate phase) were evident during sampling

episodes in both the summer and winter months, but no evidence was found for the reaction of ozone with particles during the field sampling experiments.

The adsorption of gas phase analytes onto the filter medium can be significant and may be estimated from a second particle free backup filter. Ideally no gas phase analytes should adsorb onto either filter. The levels of PAHs of interest found on the secondary filter as a percentage of the primary filter concentrations which were obtained from such a study conducted in an urban residential area of the USA, are presented in Table 4.1.

Table 4.1: Levels of PAHs sorbed onto a glass fibre filter medium, as a percentage of that found on the primary filter (Ligocki and Pankow, 1989).

PAH	% of primary filter (mean ± 1σ)
PhA	5.5 ± 13
FlA	19 ± 27
Py	12 ± 18

The results of an urban air monitoring study based on a filter/PUF sampling system are shown in Table 4.2 for both winter and summer months, where a significantly lower total PAH concentration is evident for summer (Harrison et al., 1996). Although TSP concentrations were measured in the study, they were not reported.

Table 4.2: Winter and summer gas phase and particulate PAH concentrations, derived from filter and PUF sampling (Harrison et al., 1996).

PAH	Winter filter conc ($ng.m^{-3}$)	Winter PUF conc ($ng.m^{-3}$)	Total winter conc ($ng.m^{-3}$)	Ratio PUF/ filter for winter	Summer filter conc ($ng.m^{-3}$)	Summer PUF conc ($ng.m^{-3}$)	Total summer conc ($ng.m^{-3}$)	Ratio PUF/ filter for summer
Naph	0.69	12.55	13.24	18.19	0.14	1.73	1.87	12.36
PhA	1.08	23.03	24.11	21.32	0.25	3.59	3.84	14.36
FlA	1.17	11.19	12.36	9.56	0.35	1.76	2.11	5.03
Py	2.36	35.68	38.04	15.12	0.55	2.78	3.33	5.05

Park et al. (2002) noted that the contribution of the vapour phase component to the total PAH concentration exceeded that of the particulate phase by a factor of 2.3 in an urban air monitoring study conducted in Seoul. The particulate and vapour phase concentrations for the PAHs of interest are shown in Table 4.3. The total particulate loading was not given. The vapour to particulate PAH ratios are similar to those reported in Table 4.2, except for naphthalene where higher vapour concentrations were found in the study of Park.

The partitioning results of a similar study conducted in an urban residential area of the USA are shown in Table 4.4. It is evident that a higher proportion of the PAHs shown were present in the gas phase as compared to the study of Park et al. (2002), although the total [PAH] for each analyte was of a similar order of magnitude in the two studies.

Table 4.3: Gas phase and particulate PAH concentrations, derived from filter and PUF sampling (Park et al., 2002).

PAH	Particulate [PAH] ($ng.m^{-3}$)	Vapour [PAH] ($ng.m^{-3}$)	Total [PAH] ($ng.m^{-3}$)	Ratio of vapour [PAH]/particulate [PAH]
Naph	0.14	11.09	11.23	79.2
PhA	1.46	15.03	16.49	10.3
FlA	2.27	5.83	8.10	2.6
Py	2.25	10.31	12.56	4.6

Table 4.4: Gas phase and particulate phase PAH concentrations, derived from filter and PUF (primary and backup plug) sampling (Ligocki and Pankow, 1989).

PAH	Particulate [PAH] ($ng.m^{-3}$)	Vapour [PAH] ($ng.m^{-3}$)	Total [PAH] ($ng.m^{-3}$)	Ratio of vapour [PAH]/particulate [PAH]
PhA	0.28 ± 0.25	26 ± 10	26.28 ± 10.25	93
FlA	0.53 ± 0.31	7.9 ± 3.1	8.43 ± 3.41	15
Py	0.62 ± 0.37	6.7 ± 2.7	7.32 ± 3.07	11

Air samples in an urban and industrialized area of Prato (Italy) during 2002, gave an average total PAH concentration of 59.4 ± 26.5 $ng.m^{-3}$, where a quartz fibre filter preceded two PUF plugs (Cincinelli et al., 2007). The total gas phase concentration was much higher

(45.5 ± 23.9 ng.m^{-3}) than the total particle phase concentration (14.0 ± 5.58 ng.m^{-3}), due to the dominance of more volatile PAHs, particularly phenanthrene.

In a roadway tunnel study utilizing Teflon (or in some cases glass fibre) filters and PUF plugs, 88 % of the phenanthrene was in the vapour phase (184 ng.m^{-3}), as was 45 % of fluoranthene (25.6 ng.m^{-3}), and 49 % of pyrene (28.3 ng.m^{-3}) (Benner, 1989). It should be noted that the PAH concentrations were significantly higher in this impacted environment than those previously discussed in this section.

Denuders are sampling devices which have been effectively employed in partitioning applications. Their principle of operation involves the movement of molecules and particles as a result of two mechanisms (Kloskowski et al., 2002):

a) movement in the direction of the gas stream, as a result of the gas flow
b) movement perpendicular to the longitudinal gas flow, due to radial diffusion.

It is interesting to note that denuders were initially used to denude air particulate samples of gaseous components (Ali et al., 1989). In 1979, however, Ferm used an oxalic acid coated denuder as a gas sampling device to sample atmospheric ammonia, whilst interfering particle-borne ammonium ions passed through.

Separation in denuders is achieved as a result of gas phase analytes having high diffusion coefficients, thus they can be retained by a sorptive surface perpendicular to the gas flow (typically on the walls of a denuder). Particles, however, pass through the denuder, and can be collected on a downstream filter. A sorbent cartridge may be employed downstream of the filter, to trap analytes desorbed from the filter, and any gaseous analytes not removed by the denuder (under breakthrough conditions). Gravitational settling of particles is avoided by vertical placement of the denuder, and possible desorption of analyte from particles during transport through the denuder section should be minimized by short transit times (sufficiently high flow rates). The possible contribution of this desorption to the measurement uncertainty would also be small for the more volatile PAHs, for which the particle phase contribution to the total concentration is low (Gundel and Lane, 1998). Cyclones or impactors may be used to remove large particles from the sample gas stream before it enters the denuder system (Ali et

al., 1989 and Koutrakis et al., 1990), although the resulting high pressure drops across the sampling device may enhance evaporative losses from particles (Zhang and McMurry, 1991).

For denudation to be effective, it is important that the gas flow through the device is stable and laminar; and that the temperature distribution is uniform within the sampled gas stream. Steady state conditions of temperature and pressure are also necessary, and longitudinal diffusion of gaseous analytes should be negligible as compared to the linear gas flow velocity (Kloskowski et al., 2002). The sorption material employed should effectively sorb the analytes (they should provide infinitely large, perfect sinks for the analyte), and no chemical reactions and transformations of sorbed analytes should occur (both during the sampling and desorption stages).

In order to ensure laminar flow conditions as well as to allow for sufficient residence time in the denuder, to allow for molecules to diffuse to the denuder walls, low flow conditions are required (< 20 $\ell.min^{-1}$, as compared to high volume samplers which operate at around 1000 $\ell.min^{-1}$) (Krieger and Hites, 1994).

A number of denuder geometries have been developed, with cylindrical and annular denuders being the most widely reported (Figures 4.1 and 4.2). Cylindrical denuders consist of a tube with the inner walls providing a sorptive surface, whilst annular denuders contain an additional internal cylindrical rod which provides a larger sorptive surface (Possanzini et al., 1983). This additional surface allows for annular denuders to be almost an order of magnitude shorter than cylindrical denuders (~0.20 m versus ~2 m). Coiled cylindrical denuders have also been tested, which improves mass transfer to the sorptive surface coated wall, and thus allows for a reduction in length of the denuder (Pui et al., 1990).

Conventional commercial denuders are usually coated with a sorptive medium which requires replacement after a period of time. They are typically solvent extracted prior to analysis.

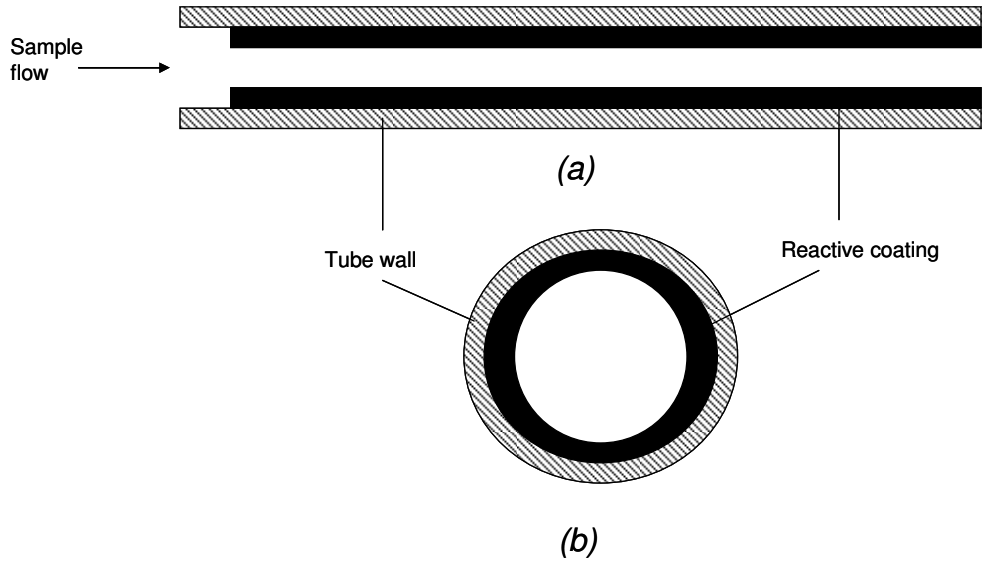

Figure 4.1: Schematic diagram of a cylindrical denuder from a longitudinal (a) view and in cross-section (b) (adapted from Ali et al., 1989)

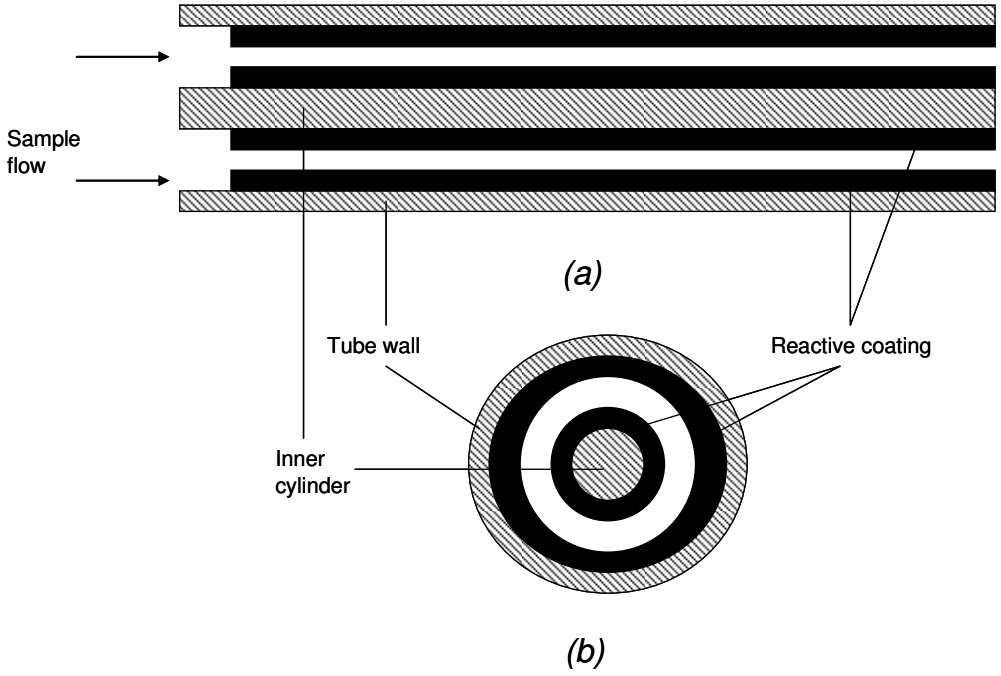

Figure 4.2: Schematic diagram of an annular denuder from a longitudinal (a) view and in cross-section (b) (adapted from Ali et al., 1989)

A high-volume compound annular denuder (consisting of a series of 12 nested denuders, 0.20 m long with an overall outer diameter of 80 mm) was developed for the collection of PAH vapour, which utilized high-vacuum silicone grease as a sorptive medium (coating thickness of 4-100 μm) (Coutant et al., 1989). SE-30 and silicone pump oil had also been tested by these authors, but the SE-30 was found to gradually oxidize upon exposure to air, hindering collection efficiency; and the silicone oil coating was too thin, which decreased the capacity of the device. The compound annular design is rather large and cumbersome, and contamination from impurities in the silicone grease employed in the final design could be of concern.

Compound annular denuders are now available commercially, and these devices have been evaluated for PAH sampling (Temime et al., 2002 and Temime-Roussel et al., 2004). In both these studies and those of Coutant et al. (1989), naphthalene was used as a reference compound in evaluating denuder performance, due to its high volatility, and thus lower collection efficiency than PAHs of lower volatility (Gundel et al., 1995). Any overestimation of the denuder collection efficiency is therefore avoided, and results may be considered as minimum trapping efficiencies for PAHs in general (Temime et al., 2002).

In later studies by Coutant et al. (1992), the silicone grease coated annular denuder was tested for additional PAHs, including phenanthrene and pyrene. A filter placed upstream of the denuder was spiked with perdeuterated PAH standard solutions (200 ng from each 5 ng.μℓ^{-1} PAH standard), which were transferred onto the denuder and XAD trap by means of high purity air flow at 7 ℓ.min^{-1} for 4 hours. The filter, denuder and XAD were then analysed and good repeatability in collection efficiencies (which were between 81 and 94 %, all with RSD < 5 %) were found for four PAHs.

In the study of Temime-Roussel et al. (2004), the denuder tube was coated with crushed and solvent cleaned Amberlite XAD-4 styrene-divinylbenzene polymer resin, which followed on from previous work by Gundel et al. (1995). The cleaning step is crucial, due to the impurities known to be present in this resin, including naphthalene and its derivatives, thus multiple cleaning steps are required before clean blanks are obtained (Gundel et al., 1995). The resin was applied to the denuder as a slurry in hexane, which could also introduce impurities into the sampling system. After sampling, solvent extraction (30 min), filtration

and pre-concentration sample preparation steps were needed prior to HPLC analysis with fluorescence detection. Collection efficiencies of above 90 % were obtained under a range of environmental and sampling conditions (temperature; relative humidity; gas phase concentration; sampling flow rates; and sampling duration) (Temime-Roussel et al., 2004). It is evident that the main problems of this method are the contamination issues and time consuming denuder preparation and sample extraction processes.

A composite cylindrical denuder, composed of a collection of capillary gas chromatography columns as the sampling tubes, was tested for use in atmospheric PAH (and polychlorinated biphenyls (PCBs)) sampling, as compared to that using a PUF sampler (Krieger and Hites, 1992 and 1994). The denuders were between 15 and 0.5 m long, and the capillary column used was 530 µm i.d. with 8 µm thick methylsilicone stationary phase. Initial experiments utilized 5 µm thick DB-1 fused silica capillary column segments, bonded together with epoxy resin. This yielded a sampling device of 2.4 mℓ internal volume (operated at 1.5 $\ell.min^{-1}$) (Krieger and Hites, 1992), which is a factor of 10 larger than that of the silicone rubber trap used in our study (0.23 mℓ). The results obtained from the denuder were not statistically different to those of the PUF sampler, however, a liquid extraction and sample cleanup procedure had to be employed, as the denuder (epoxy resin) was not resilient to thermal desorption conditions (Krieger and Hites, 1994).

The silicone rubber trap used in our study effectively retains gaseous organic analytes whilst transmitting particulates, due to its open geometry allowing laminar air flow. Thus the addition of a downstream particle filter and second denuder (to capture desorbed analytes from the particulates on the filter) would allow for both gaseous and particle phases of PAHs to be separately sampled.

The suitability of these traps as denuders was therefore investigated from a theoretical perspective, as detailed in this Chapter, and then in a number of applications, which are discussed in Chapter 5.

4.2 THEORETICAL CONSIDERATIONS

In order to determine whether the multi-channel silicone rubber trap had potential to perform as a denuder, a number of theoretical calculations were performed to ensure that the requirements for denudation could be met in this sampling device. The silicone rubber trap would be classified as a composite cylindrical type denuder, with each of the 22 silicone tubes effectively performing as a cylindrical denuder (Kloskowski et al., 2002). The non-circular inter-tube channels were ignored in the first calculations to estimate flow conditions inside the composite denuder.

4.2.1 Verification of laminar flow

As discussed under section 4.1, laminar flow is a prerequisite for denudation. The Reynolds number (R_e) relating to the gas flow conditions in the silicone rubber tubes of the traps was therefore calculated as follows.

$$R_e = \frac{VD}{\upsilon}, \qquad \text{Equation 4.3}$$

where V is the linear velocity; D is the internal diameter of the silicone tubes; and υ is the kinematic viscosity.

Further, υ can be determined from

$$\upsilon = \frac{\mu}{\rho}, \qquad \text{Equation 4.4}$$

where μ is the dynamic viscosity; and ρ is the gas density.

Using typical values of μ = 1.87 X 10^{-5} kg.m^{-1}.s^{-1} and ρ = 1.168 kg.m^{-3} for air at 25 ^{o}C and 1 atm, a kinematic viscosity of 1.60 x 10^{-5} m^2.s^{-1} is obtained.

For a sampling flow rate of 500 mℓ.min^{-1} through a 22 channel trap, with the internal diameter (i.d.) of the silicone tubes being 0.3 mm; the linear velocity per silicone tube is 5360 mm.s^{-1}. This is a worst case, "high velocity" scenario, where it is assumed that the entire sample flow passes at the same flow rate through each of the silicone tubes only, and not

through any spaces between tubes. This is based on the assumption that each tube is equivalent and that no perturbations in the tube geometries, such as kinks or twists, occurred during trap manufacture.

A Reynolds number of 101 is thus obtained from equation 4.3. As mentioned, this is a worst case scenario, where the linear velocity does not account for a decreased flow rate through the inside of the silicone tubes as a consequence of a portion of the gas flowing through the spaces between the tubes. If the total open cross sectional area of 4.1 mm^2 for a quartz tube of 3.5 mm i.d. containing 22 silicone tubes of 0.64 mm outer diameter is used, a linear velocity inside the silicone rubber tubes of 2030 $mm.s^{-1}$ would be obtained, which would yield an even lower R_e of 38.

In both cases, R_e satisfies the condition for laminar flow that $R_e << 2300$, thus it can be concluded that the gas flow is laminar in the silicone rubber trap. The low R_e would minimize impaction of large particles on the walls of the denuder.

It should be noted that laminar flow conditions would be achieved a short distance l, from the trap inlet. For a tube of diameter d (Ali et al., 1989):

$$l = 0.07 d R_e \qquad \text{Equation 4.5}$$

In the case of the silicone tubes, d = 0.3 mm and R_e = 101. This yields a length of 2.1 mm from the inlet of the silicone rubber tubes, after which laminar conditions would be established. The non-laminar portion accounts for < 5 % of the total length of the silicone tubes (55 mm).

4.2.2 Verification of negligible linear velocity arising from longitudinal diffusion

In order to verify that the contribution of longitudinal diffusion to linear velocity is negligible compared to the linear velocity arising from the pumping of sample gas through the denuder, the Peclet number (P_e) was determined, which needed to meet the following requirement (Kloskowski et al., 2002):

$$P_e = \frac{2R\upsilon}{D_A} > 10, \qquad \text{Equation 4.6}$$

where R is the internal radius of the denuder (silicone rubber tube) (cm) ie 0.015 cm; υ is the actual linear velocity of air flow (cm.s^{-1}) at a given distance from the centre; and D_A is the diffusion coefficient of analyte A in the sample gas (cm^2.s^{-1}) ie: D_{Naph} = 0.069 cm^2.s^{-1}; D_{PhA} = 0.058 cm^2.s^{-1}; and D_{FlA} = D_{Py} = 0.055 cm^2.s^{-1}, where A is the PAH of interest (Danish Environmental Protection Agency, 2006).

Further, for laminar flow the linear flow profile in an open tube is shown in Figure 4.3 and can be given by:

$$\upsilon = 2\upsilon_{av}\left(1-\frac{r^2}{R^2}\right), \qquad \text{Equation 4.7}$$

where υ_{av} is the linear velocity of the sample gas flow (cm.s^{-1}); and r is the distance from the longitudinal axis of the silicone tube (cm).

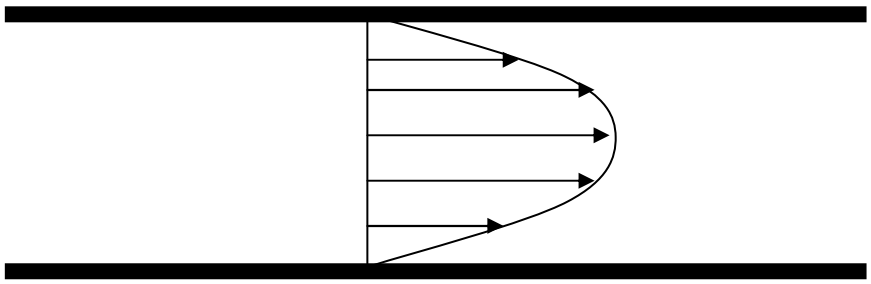

Figure 4.3: Laminar flow conditions inside an open tube.

If the average linear velocity of 203 cm.s^{-1} - calculated under section 4.2.1 for a 22 silicone rubber tube trap sampling at a flow rate of 500 mℓ.min^{-1} - is used as the actual linear velocity, a Peclet number of 88 is obtained for Naph, 105 for PhA; and 111 for FlA and Py. These results meet the requirement that the Peclet number be greater than 10, thus the contribution to the linear velocity from longitudinal diffusion is indeed negligible. Very close to the silicone walls, however, the linear flow rate would be less than the average value, thus longitudinal diffusion may become important.

4.2.3 Calculation of the efficiency of removal of gaseous components by the denuder

In order to determine the efficiency of analyte removal by the denuder, as well as the parameters which affect this removal efficiency, the rate of change of gaseous concentration of analyte, *A*, is usually determined from the general mass balance equation for *A* in a cylindrical, sorption based denuder (where analyte removal is permanent) (Katsanos and Roubani-Kalantzopoulou, 1995):

$$\frac{\partial c_A}{\partial t} = -\upsilon \frac{\partial c_A}{\partial z} + D_A \frac{\partial^2 c_A}{\partial z^2} + D_A \left(\frac{\partial^2 c_A}{\partial r^2} + \frac{1}{r} \frac{\partial c_A}{\partial r} \right) - r_A , \qquad \text{Equation 4.8}$$

where $c_A = c_A(t, z, r)$ in the gas phase in mol.cm^{-3}, as a function of t (time) in s; length along the denuder, z, in cm; and distance from the cylinder axis, r, in cm; and r_A is the rate of a gaseous chemical reaction of A in mol.cm^{-3}.s^{-1}.

The first term on the right hand side of equation 4.8 describes convective movement along the denuder, whilst the second term is due to longitudinal diffusion along the cylinder axis. The third term arises from radial diffusion and the fourth term relates to homogeneous chemical reactions in the denuder.

A number of assumptions can be made in order to simplify equation 4.8 and allow for a solution to be found.

The first of these is to assume steady state conditions, where the composition of the air does not change during its flow along the denuder, ie:

$$\frac{\partial c_A}{\partial t} = 0$$

Further, the second term relating to longitudinal diffusion may be ignored if it is assumed that the linear velocity of analyte *A* resulting from longitudinal diffusion is negligible compared with the linear velocity resulting from pumped sample air flow, ie:

$$v\frac{\partial c_A}{\partial z} >> D_A\frac{\partial^2 c_A}{\partial z^2}$$

This was confirmed for the silicone rubber trap in section 4.2.2.

It is also assumed that no homogeneous reactions occur in the denuder, thus equation 4.8 may be simplified to:

$$v\frac{\partial c_A}{\partial z} = D_A\left(\frac{\partial^2 c_A}{\partial r^2} + \frac{1}{r}\frac{\partial c_A}{\partial r}\right), \qquad \text{Equation 4.9}$$

which leads to the Gormley-Kennedy solution of this equation (Gormley and Kennedy, 1949):

$$\frac{c_{av}}{c_0} = 0.8191\exp(-7.314z^*) + 0.0975\exp(-44.61z^*) + 0.0325\exp(-113.9z^*) + \ldots,$$

Equation 4.10

where c_0 is the gas concentration entering the denuder; c_{av} is the average gas concentration leaving the tube; and z^* is a dimensionless factor given by:

$$z^* = \frac{\pi}{2}\frac{D_A L}{V}, \qquad \text{Equation 4.11}$$

where L is the length of the denuder; and V is the volumetric flow rate.

The assumptions made in this solution are that: analyte A is a trace gas; laminar flow is developed with constant viscosity; the temperature is constant; and the amount of analyte collected on the tube wall is small compared with the available capacity of the denuder (Katsanos and Roubani-Kalantzopoulou, 1995).

For L = 5.5 cm (length of silicone rubber tubes); V = 8.33 $cm^3.s^{-1}$; and D_{Naph} = 0.069 $cm^2.s^{-1}$; D_{PhA} = 0.058 $cm^2.s^{-1}$; and D_{FlA} = D_{Py} = 0.055 $cm^2.s^{-1}$: $z_{Naph} = 0.072$; $z_{PhA} = 0.060$ and $z_{FlA} = z_{Py} = 0.057$.

This gives: $\left(\frac{c_{av}}{c_0}\right)_{Naph} = 0.49$; $\left(\frac{c_{av}}{c_0}\right)_{PhA} = 0.53$ and $\left(\frac{c_{av}}{c_0}\right)_{FlA} = \left(\frac{c_{av}}{c_0}\right)_{Py} = 0.55$.

The fraction of analyte retained on the denuder (collection efficiency) can be determined from:

$$\left(1 - \frac{c_{av}}{c_0}\right)$$

Thus for Naph the fraction of analyte retained on the denuder is 0.51 or 51%; whilst that pertaining to PhA is 0.47 or 47 %; and the fraction for FlA and Py is 0.45 or 45 %.

The collection efficiency may be increased by increasing L, and by decreasing the sampling flow rate (V). Collection efficiencies will also be higher for analytes with higher diffusion coefficients, which can be seen from the higher calculated collection efficiency for naphthalene.

A number of alterations to the Gormley-Kennedy solution have been suggested. One of these takes into account an *effective length* of the denuder, which decreases with time as a consequence of the depletion of the active surfaces of the denuder with increasing sample volume, which would decrease the collection efficiency (Ali et al., 1989). This alteration is significant only when the depletion rate is high as a result of high analyte concentrations, high moisture levels, or low surface capacities, and therefore would be of minor significance in trace gas analysis, but would be of relevance under breakthrough conditions. This does not apply in the case of silicone rubber tubes which absorb analytes by dissolution and do not adsorb analytes onto an active surface, which may be easily saturated.

Another alteration is based on the collection surface not performing as a perfect sink and a reaction probability is incorporated into the solution, which requires knowledge of the reaction probability factor and the diffusional behaviour of the analyte (Ali et al., 1989).

In the case of the multi-channel silicone rubber traps, the Gormley-Kennedy approximation is valid for analytes of lower volatility (with higher retention volumes), such as pyrene and phenanthrene; but would not be valid for more volatile analytes (with lower retention volumes) such as naphthalene. Here a chromatographic model is more appropriate due to continuous partitioning behaviour, where the PDMS-air partition coefficients are expected to be proportional to the octanol-air partition coefficients (De Coensel et al., 2007) and experimentally derived breakthrough volumes for each analyte give an indication of the efficiency of removal of gaseous components.

4.2.4 Calculation of the efficiency of particle transmission by the denuder

Loss of particles in denuders, which are configured vertically to prevent gravitational settling and operate under laminar flow conditions, may arise from electrostatic or diffusion effects. These were studied by Ye et al. (1991) by means of particle concentration determinations. It was found that losses in the 0.1 – 1 µm diameter range were only a few percent, which is of relevance as it has been noted that PAHs are found on particles in the size range of < 5 µm (Nikolaou et al., 1984).

Other studies have indicated that 95 % of particulate PAH is found on particles < 3.3 µm in diameter (Harrison et al., 1996); > 80 % are associated with the $PM_{2.5}$ fraction (particulate matter of size ≤ 2.5 micron) (Ohura et al., 2004); or that the particle size is bimodal: < 1 µm particles containing the relatively nonvolatile PAHs formed by adsorption which remain airborne for extended time periods and are thus transported long distances; and > 1 µm particles containing the condensed volatile PAHs (Harrison et al., 1996). Another study found that almost half of the particle bound PAHs are associated with the particle size range 0.075 – 0.12 µm (Miguel and Friedlander, 1978).

Particle size is an important consideration in terms of dust retention in the human respiratory tract, and it has been found that more PAHs are associated with the respirable fraction in winter (Van Vaeck et al., 1979). Larger particles have also been observed in

suburban ambient air, as compared to urban air (Horvath et al., 1996), which may be ascribed to particle growth processes during ageing of the urban aerosol.

Higher particle transmission losses are experienced in denuders for smaller particles, due to their higher diffusion coefficients. Losses of charged particles may occur due to localized electrostatic fields on the denuder wall, which may arise due to low humidity or as a result of handling. Experiments to determine electrostatic losses are difficult to repeat (Ye et al., 1991), as they depend on these environmental and localized conditions, thus only losses of neutral particles due to diffusion were considered in this study. In some applications, such as the use of the silicone rubber traps in the denuder configuration for the monitoring of PAHs arising from sugar cane burning in KwaZulu-Natal (Chapter 5), electrostatic effects would have been minimal due to the high humidity at this coastal location. It would also be possible to supplement sample air with moist air, if necessary, and then correct for dilution effects.

Experimental results relating to the diffusional losses of neutral particles in an annular denuder compared favourably to theoretical calculations based on equations developed for a channel of rectangular cross section (Ye et al., 1991). The annular denuder channel was considered in an "unrolled and flattened" state as a parallel plate configuration in order to relate the channel geometry to a rectangle.

For the silicone rubber traps, however, diffusive loss theories for particles traversing tubes of circular cross section were appropriate, as applied in Hermann et al. (2001) and Ferm (1979). The transport efficiency, E_{diff}, is given by:

$$E_{diff} = 1 - 2.564\mu^{2/3} + 1.2\mu + 0.1767\mu^{4/3}, \qquad \text{Equation 4.12}$$

for $\mu \leq 0.02$, and

$$E_{diff} = 0.819\exp(-3.657\mu) + 0.0975\exp(-22.305\mu) + 0.0325\exp(-56.961\mu) + 0.0154\exp(-107.62\mu) \qquad \text{Equation 4.13}$$

for $\mu > 0.02$, where

$$\mu = \frac{\pi D_p L}{Q}, \qquad \text{Equation 4.14}$$

and where D_p is the diffusion coefficient of a particle of a specific diameter, in $m^2.s^{-1}$; L is the length of the denuder in m; and Q is the volumetric flow rate in $m^3.s^{-1}$.

The particle diffusion coefficients were calculated from

$$D_p = \frac{C_c kT}{3\pi d_p \mu_{abs}}, \qquad \text{Equation 4.15}$$

where C_c is the Cunningham slip correction factor (obtained from USA EPA, 2007); k is the Boltzmann constant (1.3806503 x 10^{-23} $m^2.kg.s^{-2}.K^{-1}$); T is the temperature in K; d_p is the diameter of the particle in m; and μ_{abs} is the absolute (or dynamic) gas viscosity in $kg.m^{-1}.s^{-1}$.

The particle diffusion coefficients, μ values, and corresponding transport efficiencies, E_{diff}, were calculated for a number of particle sizes, ranging from 0.001 to 10 µm at 25 °C, for a silicone rubber trap denuder of length 0.055 m operating at 500 $m\ell.min^{-1}$. The results are presented in Table 4.5 and Figure 4.4.

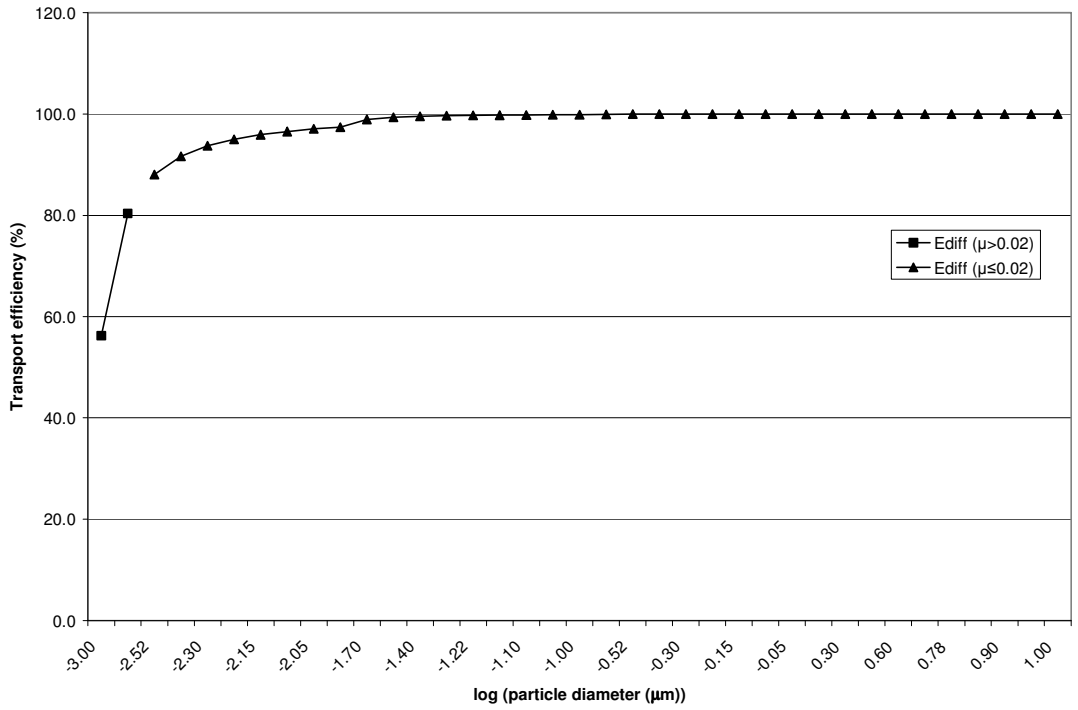

Figure 4.4: Particle transport efficiency through a silicone rubber trap with respect to diffusive losses.

Table 4.5: Neutral particle transport efficiencies for different particle sizes.

d_p (µm)	C_c	D_p ($m^2.s^{-1}$)	µ	Transport efficiency (%)
0.001	222	5.18E-06	1.07E-01	56.2
0.002	111	1.30E-06	2.69E-02	80.4
0.003	74.3	5.78E-07	1.20E-02	88.1
0.004	55.8	3.26E-07	6.76E-03	91.7
0.005	44.8	2.09E-07	4.34E-03	93.7
0.006	37.4	1.46E-07	3.02E-03	95.0
0.007	32.2	1.07E-07	2.23E-03	95.9
0.008	28.2	8.23E-08	1.71E-03	96.5
0.009	25.1	6.52E-08	1.35E-03	97.0
0.01	22.7	5.30E-08	1.10E-03	97.4
0.02	11.7	1.36E-08	2.82E-04	98.9
0.03	7.98	6.21E-09	1.29E-04	99.4
0.04	6.15	3.59E-09	7.45E-05	99.6
0.05	5.06	2.36E-09	4.90E-05	99.7
0.06	4.34	1.69E-09	3.50E-05	99.7
0.07	3.82	1.28E-09	2.65E-05	99.8
0.08	3.44	1.01E-09	2.08E-05	99.8
0.09	3.15	8.16E-10	1.69E-05	99.8
0.1	2.91	6.80E-10	1.41E-05	99.9
0.2	1.89	2.21E-10	4.58E-06	99.9
0.3	1.57	1.23E-10	2.54E-06	100.0
0.4	1.42	8.32E-11	1.73E-06	100.0
0.5	1.34	6.25E-11	1.30E-06	100.0
0.6	1.28	4.98E-11	1.03E-06	100.0
0.7	1.24	4.14E-11	8.58E-07	100.0
0.8	1.21	3.53E-11	7.33E-07	100.0
0.9	1.19	3.08E-11	6.38E-07	100.0
1	1.17	2.73E-11	5.66E-07	100.0
2	1.08	1.27E-11	2.63E-07	100.0
3	1.06	8.22E-12	1.71E-07	100.0
4	1.04	6.08E-12	1.26E-07	100.0
5	1.03	4.83E-12	1.00E-07	100.0
6	1.03	4.00E-12	8.30E-08	100.0
7	1.02	3.42E-12	7.09E-08	100.0
8	1.02	2.98E-12	6.18E-08	100.0
9	1.02	2.64E-12	5.49E-08	100.0
10	1.02	2.38E-12	4.93E-08	100.0

It is evident that the theoretical transport efficiencies of particles larger than 0.05 µm are essentially 100 %. Transmission losses of > 5 % are only evident for the particle size

fraction < 0.006 µm. It is of note that the calculated transport efficiency at molecular dimensions (1 nm or 0.001 µm) was 56.2 %, which would correspond to a collection efficiency of 43.8 %. This correlates well with the gaseous PAH collection efficiencies calculated in section 4.2.3 using the Gormley-Kennedy equation, which ranged from 45 to 51 %. The low Reynolds numbers for the flow rate utilized in this study should also minimize loss of particles due to impaction (as calculated in section 4.2.1).

The particle size fractions of most significance in the monitoring applications investigated in this study are discussed in Chapter 5.

It is also important that the transit time of particles through the denuder is sufficiently fast to prevent re-equilibration of particle bound analyte to the gas phase during transit, as this would produce a positive bias in terms of the gas phase concentration. For semi-volatile organic compounds, a transit time of ≤ 0.3 s is recommended (Kamens and Coe, 1997 and Gundel and Lane, 1998). In the case of the silicone rubber traps used in our study, a transit time of ~0.03 s would occur at a 500 $m\ell.min^{-1}$ sampling flow rate, which is far below this cut-off. Re-equilibration during transit was therefore not deemed to be significant, particularly as the target PAHs of interest are found predominantly in the gas phase under the sampling conditions.

4.3 DISCUSSION AND CONCLUSION

Denuders allow for the separation of gas and particulate phases, without the generation of artifacts which may occur with filter-based methods (filtration prior to gas sampling). The method also allows for pre-concentration of the gaseous analyte.

Conventional cylindrical denuders have a number of disadvantages, as their use is labour intensive due to coating and extraction procedures. The silicone rubber traps used in our study do not require coating or solvent extraction therefore the possibility for solvent introduced artifact formation is minimized and the elimination of sample handling steps also reduces the chance of sample contamination and degradation.

A number of denuders have been reported which are analysed by thermal desorption methods. Denuders based on parallel sections of capillary chromatographic columns (typically ~120 parallel 0.25 m long sections), for example, have been used in the sampling of VOCs and SVOCs, followed by thermal desorption using specially designed systems (Krieger and Hites, 1992; Dudek et al., 2000; Dudek et al., 2002 and Tobias et al., 2007). The traps used in our study are unique and are compatible with commercially available thermal desorption systems.

Another problem which may be associated with cylindrical denuders is the need for long sampling times due to the limited flow rates inherent to their design, which may lead to artifact formation, although higher flow rates are possible with annular denuders (Ali et al., 1989). In the case of our denuder, total transfer onto the GC column is possible (as compared to solvent extraction based methods), which enhances sensitivity and allows for shorter sampling times and lower flow rates.

It is evident from the results of the theoretical considerations presented in this Chapter that the multi-channel silicone rubber traps have the potential to serve as efficient denuders. The application of these traps in the denuder configuration was therefore tested experimentally in a number of applications of relevance to South Africa, as described in Chapter 5.

4.4 REFERENCES

Ali, Z., Thomas, C.L.P. and Alder, J.F., *Analyst*, **1989**, *114*, 759-769.

Benner, B.A., Gordon, G.E. and Wise, S,A., *Environmental Science and Technology,* **1989**, *23*, 1269-1278.

Bidleman, T.F., *Environmental Science and Technology*, **1988**, *22* (4), 361-367.

Cincinelli, A., Del Bubba, M., Martellini, T., Gambaro, A. and Lepri, L., *Chemosphere*, **2007**, *68*, 472-478.

Coutant, R.W., Callahan, P.J. and Chuang, J.C., *Atmospheric Environment*, **1992**, *26 (A)* (15), 2831-2834.

Coutant, R.W., Callahan, P.J., Kuhlman, M.R. and Lewis, R.G., *Atmospheric Environment*, **1989**, *23* (10), 2205-2211.

Coutant, R.W., Brown, L., Chuang, J.C., Riggin, R.M. and Lewis, R.G., *Atmospheric Environment*, **1988**, *22* (2), 403-409.

Danish Environmental Protection Agency, Guidelines on remediation of contaminated sites, Appendix 5.5 Physical and chemical data, **2006**, accessed on 17 February 2006 at http://www.mst.dk/udgiv/publications

De Coensel, N., Desmet, K., Górecki, T. and Sandra, P., *Journal of Chromatography A*, **2007**, *1150*, 183-189.

Dudek, M., Kloskowski, A., Wolska, L., Pilarczyk, M. and Namieśnik, J., *Journal of Chromatography A*, **2002**, *977*, 115-123.

Dudek, M., Wolska, L., Pilarczyk, M., Zygmunt, B. and Namieśnik, J., *Journal of High Resolution Chromatography*, **2000**, *23* (6), 449-454.

Eatough, D.J., Wadsworth, A., Eatough, D.A., Crawford, J.W., Hansen, L.D. and Lewis, E.A., *Atmospheric Environment*, **1993**, *27(A)*, 8, 1213-1219.

Ferm, M., *Atmospheric Environment*, **1979**, *13*, 1385-1393.

Gormley, P.G. and Kennedy, M., *Proceedings of the Royal Irish Academy*, **1949**, *52*, 163-169.

Gundel, L.A., Lee, V.C., Mahanama, K.R.R., Stevens, R.K. and Daisey, J.M., *Atmospheric Environment*, **1995**, *29* (14), 1719-1733.

Gundel, L.A. and Lane, D.A., Sorbent-coated diffusion denuders for direct measurement of gas/particle partitioning by semi-volatile organic compounds, January **1998**, Ernest Orlando Lawrence Berkeley National Laboratory, Report LBNL-41278.

Harrison, R.M., Smith, D.J.T. and Luhana, L., *Environmental Science and Technology*, **1996**, *30*, 825-832.

Hermann, M., Stratmann, F., Wilck, M. and Wiedensohler, A., *Journal of Atmospheric and Oceanic Technology*, **2001**, *18*, 7-19.

Horvath, H., Kasahara, M. and Pesava, P., *Journal of Aerosol Science*, **1996**, *27*(3), 417-435.

Kamens, R.M. and Coe, D.L., *Environmental Science and Technology*, **1997**, *31*(6), 1830-1833.

Kamens, R.M., Fulcher, J.N. and Zhishi, G., *Atmospheric Environment*, **1986**, *20* (8), 1579-1587.

Katsanos, N.A. and Roubani-Kalantzopoulou, F., *Journal of Chromatography A*, **1995**, *710*, 191-228.

Kloskowski, A., Pilarczyk, M. and Namieśnik, J., *Critical Review in Analytical Chemistry*, **2002**, *32* (4), 301-335.

Koutrakis, P., Wolfson, J.M., Brauer, M. and Spengler, J.D., *Aerosol Science and Technology*, **1990**, *12*, 607-612.

Krieger, M.S. and Hites, R.A., *Environmental Science and Technology,* **1994**, *28*, 1129-1133.

Krieger, M.S. and Hites, R.A., *Environmental Science and Technology,* **1992**, *26*, 1551-1555.

Ligocki, M.P. and Pankow, J.F., *Environmental Science and Technology,* **1989**, *23*, 75-83.

Miguel, A.H. and Friedlander, S.K., *Atmospheric Environment*, **1978**, *12*, 2407-2413.

Nikolaou, K. Masclet, P., and Mouvier, G., *Science of the Total Environment*, **1984**, *32*, 103-132.

Ohura, T., Amagai, T., Sugiyama, T., Fusaya, M. and Matsushita, H., *Atmospheric Environment*, **2004**, *38*, 2045-2054.

Park, S.S., Kim, Y.J. and Kang, C.H., *Atmospheric Environment*, **2002**, *36*, 2917-2924.

Possanzini, M., Febo, A. and Liberti, A., *Atmospheric Environment*, **1983**, *17* (12), 2605-2610.

Pui, D.Y.H., Lewis, C.W., Tsai, C.-J. and Liu, B.Y.H., *Environmental Science and Technology*, **1990**, *24* (3), 307-312.

Temime, B., Francois, S., Monod, A. and Wortham, H., *Environmental Pollution*, **2002**, *120*, 609-616.

Temime-Roussel, B., Monod, A., Massiani, C. and Wortham, H., *Atmospheric Environment*, **2004**, *38*, 1913-1924.

Tobias, D.E., Perlinger, J.A., Morrow, P.S., Doskey, P.V. and Perram, D.L., *Journal of Chromatography A*, **2007**, *1140*, 1-12.

Tsapakis, M. and Stephanou, E.G., *Environmental Pollution*, **2005**, *133*, 147-156.

USA EPA, Basic Concepts in Environmental Sciences, Module 3: Characteristics of Particles, Collection Mechanisms and Appendix B, **2007**, accessed on 6 July 2007 at www.epa.gov/eogaptil/module3/collect/collect.htm

Van Vaeck, L., Broddin, G. and Van Cauwenberghe, K., *Environmental Science and Technology,* **1979**, *13* (12), 1494-1502.

Ye, Y., Tsai, C.-J., Pui, D.Y.H. and Lewis, C.W., *Aerosol Science and Technology*, **1991**, *14*, 102-111.

Zhang, X. and McMurry, P.H., *Environmental Science and Technology*, **1991**, *25*, 456-459.

Chapter 5

Applications

5.1 INTRODUCTION

There are numerous anthropogenic sources of PAHs, therefore the LIF screening method and the denuder technology developed in this study have many potential applications. A number of these are explored in this chapter, namely the monitoring of emissions from domestic cooking fires, biomass burning, vehicular diesel combustion and industrial processes.

5.2 DOMESTIC FUEL BURNING

5.2.1 Background

In developing countries, fuel is often combusted within homes in order to provide space heating, light, and heat for cooking purposes. It has been estimated that approximately half of the world's population uses solid fuels for cooking and heating (Gustafson et al., 2008). These fuels include wood, paper, charcoal, agricultural wastes (such as maize husks) and animal dung. Combustion conditions are often not optimal, leading to emissions of pollutants including smoke and PAHs. The World Health Organisation has therefore identified indoor air pollution from solid fuel as one of the world's ten major causes of mortality and morbidity (Gustafson et al., 2008). Soot derived from the combustion of biomass fuels (including wood, crop residues, grass, bushes and rice straw) in residential stoves in China was found to have steroid modulating effects, and results showed that PAHs and their derivatives were a major contributor to endocrine disruption (Wu et al., 2002).

The twenty-four hour indoor air levels of a number of PAHs in homes utilizing wood for space heating were significantly higher (3 to 5 times) than in homes without wood-burning appliances (Gustafson et al., 2008). The outdoor air levels of PAHs adjacent to homes combusting this fuel were generally higher than the indoor air levels, and phenanthrene was the PAH at the highest concentration in both indoor and outdoor air (14 $ng.m^{-3}$ and 8.1 $ng.m^{-3}$, respectively). Fluoranthene and pyrene were also detected in both the indoor and outdoor air samples at concentrations of ~2 $ng.m^{-3}$, and the gaseous phase accounted for over 90 % of the 3-ring PAHs. Fluoranthene, which has been suggested as a supplementary indicator of carcinogenicity to benzo(*a*)pyrene (Boström et al., 2002), contributed the most of the 3- and 4-ring PAHs to cancer potency, and the sum of the phenanthrene, anthracene, fluoranthene and pyrene concentrations accounted for ~80 % of the total PAH concentration.

A maximum total PAH concentration of 2.6 $\mu g.m^{-3}$ was obtained in Kenyan kitchen air samples collected onto glass microfibre filters and XAD-2 resin, where charcoal burning stoves were used (Gachanja and Worsfold, 1993). PAH exposures of women cooking on biomass burning stoves were determined in India by means of personal air samplers containing glass fibre filters (Smith et al., 1983). Here only benzo(*a*)pyrene was determined, as this sampling method is not suitable for the more volatile species. PAH monitoring in traditional houses in Burundi revealed that naphthalene was by far the main PAH contaminant, with a mean concentration of ~29 $\mu g.m^{-3}$ (Viau et al., 2000). It was also found that the total PAH concentration correlated with the CO concentration and that the mean concentrations of naphthalene, fluorene, phenanthrene and acenaphthalene exceeded 1 $\mu g.m^{-3}$.

Domestic fuel burning is also a potential source of PAHs in South Africa, therefore the denuder technology developed in this study was tested in this application in order to assess PAH levels and gas/particle partitioning, which is important for human health impact studies.

5.2.2 Experimental method

a) Sampling

Air samples were collected adjacent to an informal trader in Atteridgeville, Pretoria, whilst chicken was cooked over a coal and wood-fired brazier outdoors, adjacent to a busy roadway in the early evening (19h00).

A quartz fibre filter was punched to the correct size (6 mm o.d.), washed with methanol followed by dichloromethane, and then oven dried at 100 ^{o}C for 30 min. The filter was used in conjunction with multi-channel silicone rubber traps in the trap-filter-trap denuder configuration with Teflon connections (see Figure 5.5, section 5.4.3). Sampling was conducted using a portable Gilair sampling pump operating at 517 mℓ.min^{-1} for 5 min, at ~1 m above ground level (hand height) and ~5 m from the brazier. After sampling, the filter was transferred to a sealed 2 mℓ amber vial and the traps were end-capped and wrapped in aluminium foil. Samples were then refrigerated prior to analysis.

b) Analysis

The traps and filter were analysed by thermal desorption-gas chromatography-mass spectrometry (TD-GC-MS) (Gerstel TDS 3 with CIS and Agilent GC 7890A with Hewlett Packard 5975 inert XL MSD). Desorption was from 0 °C (0.2 min) to 270 °C (1.5 min) at 120 °C.min^{-1} in the solvent vent mode (100 mℓ.min^{-1} until 0.2 min). Cryo-focusing of the PAHs was achieved using liquid nitrogen at -40 °C followed by rapid heating at 12 °C.s^{-1} to 300 °C (10 min). The GC (CIS) inlet was in the split mode (10:1) with helium (Ultra High Purity, Afrox) as the inlet gas. An Agilent HP5 (30 m x 250 µm x 0.25 µm) GC column was used with 68.8 kPa column head pressure. The flow rate through the column was 1.3 mℓ.min^{-1} at 40 °C. The GC oven was temperature programmed from 40 °C (10.5 min) at 20 °C.min^{-1} to 150 °C (0 min) and at 30 °C.min^{-1} to 300 °C (1 min). The GC-MS transfer line was at 300 °C, the mass scan range was 80-250 atomic mass units (amu), the solvent delay 6.8 min, and the electron multiplier voltage was ~1070 V.

Calibrations were performed by the analysis of 1 µℓ injections of mixed PAH standard in toluene (1, 2, 10, 20 and 300 ng for naphthalene and 1, 2, 10, 20 and 40 ng for phenanthrene, anthracene, fluorene and pyrene) onto blank traps or clean filters. NIST library searches were also conducted on the GC-MS data.

5.2.3 Results and discussion

The primary trap obtained from the open fire experiment contained ~16 ng of naphthalene (6.5 µg.m^{-3}), whilst negligible amounts (< 1.5 ng) were present on the filter and secondary trap, which indicates that no appreciable breakthrough of this analyte occurred with the 2.6 ℓ sampling volume. No particle associated naphthalene was detected in the freshly formed smoke sampled.

For this low sample volume, no significant amounts of the other target PAHs were detected in the samples including the filter, although ~1.5 ng (0.6 µg.m^{-3}) of phenanthrene was detected on the primary trap and ~2 ng (0.8 µg.m^{-3}) of pyrene was found on both the primary and secondary trap. The portion of pyrene present in the secondary trap would have arisen from blow off of particle-associated pyrene from the filter. Our results thus show that in the fresh, particle laden smoke plume, phenanthrene (3 aromatic rings) was present only in the gas phase, whilst the pyrene (4 aromatic rings) was distributed approximately equally between the gas and particle phases. Pyrene, fluorene, anthracene and phenanthrene are regarded as PAH markers for coal and wood combustion (Harrison et al., 1996).

The NIST library searches indicated the presence of both saturated and unsaturated hydrocarbons and their aldehyde and carboxylic derivatives on the primary trap (Q > 80), and a smaller number of these compounds were indicated on the secondary trap and filter, as shown in Table 5.1.

Table 5.1: Non-PAH products of domestic fuel burning found in the trap and filter samples, as determined by NIST library comparisons of the TD-GC-MS data.

Compound	R_t (min)	Primary trap	Secondary trap	Filter
Dodecane	15.864	√ (Q91)		
Decanal	15.930	√ (Q96)	√ (Q95)	
1-Pentadecene	16.584	√ (Q87)		
2,4-Decadienal	16.785	√ (Q90)		
Phthalic anhydride	16.826	√ (Q90)		
2-Dodecenal	17.092			√ (Q80)
3-Tetradecene	17.222	√ (Q90)		
Tetradecane	17.265	√ (Q87)		
Dodecanal	17.340			√ (Q90)
Pentadecane	17.797	√ (Q94)		
Tetradecanal	17.867		√ (Q86)	
Cis-7-tetradecen-1-yl acetate	18.161	√ (Q87)		
Tetradecanoic acid	18.963			√ (Q95)
n-Decanoic acid	20.369			√ (Q89)
14-Pentadecenoic acid	20.243	√ (Q91)		

NOTE: Numbers in brackets reflect the quality of the match between the mass spectrum of the sample to that of the library.

This experiment could not be used to assess the efficiency of the denuder system in terms of gas/particle separation, as no target PAHs were present on the filter and the TD-GC-MS analytical method did not lend itself to the detection of even higher boiling PAHs, but it was useful in testing the naphthalene breakthrough volume under practical conditions. The denuder system performed well in that gas phase naphthalene was successfully retained in the primary trap, thus no breakthrough occurred for this PAH, which is not particle associated at room temperature. Should any other PAHs be found in the secondary trap in other experiments performed under similar conditions, it can be inferred that they originated from blow off of PAHs from the particle phase collected on the filter, due to the fact that naphthalene is the PAH with by far the lowest breakthrough volume.

The results also demonstrated the importance of naphthalene as an indicator for PAHs, as it was present at the highest levels, which is in agreement with the literature (Viau et al., 2000). Although the burning was being conducted outdoors in our experiment, indoor fuel burning is also common in South Africa and is even more of concern in terms of potential human health effects.

5.3 DIESEL EXHAUST EMISSIONS

5.3.1 Background

The importance of emissions from road traffic as a source of PAHs has been noted in numerous studies (Wild and Jones, 1995), since the isolation and identification of various carcinogenic compounds in gasoline engine exhaust gas (Hoffmann and Wynder, 1963; Blumer et al., 1977). Road traffic emission studies based in the developing world have been reviewed by Han and Naeher (2006) and the only country on the African continent which has a study included in this review is Egypt, where an average total particulate bound PAH concentration of 32 $ng.m^{-3}$ was reported. Very low levels were found in Croatia (annual average of 1.87 $ng.m^{-3}$), and very high values were found in Mexico City (median ranged from 60-910 $ng.m^{-3}$) in comparison.

In the UK, annual atmospheric emissions of 60 tons of PAHs arise from leaded and unleaded petrol car emissions, with higher emissions from unleaded fuel, due to its higher aromatic fraction (Wild and Jones, 1995). Peak atmospheric PAH concentrations of 1600 $ng.m^{-3}$ have been measured in winter in Los Angeles, during morning rush-hour traffic conditions (Lu et al., 2005).

The composition of diesel emissions is dependent on many factors, including the type of engine, operating conditions, lubricating oil, fuel additives and composition, and emission control systems. Some of the PAHs emitted from diesel engines originate from the fuel itself, as these molecules are relatively refractory and thus a portion survives combustion. Studies by Rhead and Hardy (2003), which utilized a radiotracer technique with the addition of ^{14}C labeled PAHs to the fuel, indicated < 1.25 % of PAHs arising from the fuel are not combusted

and are emitted. Mean concentrations of the PAHs of interest in diesel fuel are given in Table 5.2, where very high concentrations of naphthalene are evident. Another study also found naphthalene to be the predominant PAH present in both diesel (up to 1600 ppm) and gasoline (up to 2600 ppm) (Marr et al, 1999).

Table 5.2: Mean PAH concentrations in class A2 diesel fuel (Rhead and Hardy, 2003).

PAH	Mean concentration (ppm)
Naphthalene	1292
Fluorene	571
Phenanthrene	945
Anthracene	19
Fluoranthene	36
Pyrene	83
Chrysene	41
Benzo(*a*)pyrene	0.4

Pyrosynthesis of PAHs during the high temperature combustion conditions also contributes to emission levels, although most of the combustion products are oxidized prior to emission (USA EPA, 2002). Pyrosynthesis has been found to be most prominent under high speed and load conditions (Rhead and Hardy, 2003). The concentrations of selected PAHs associated with diesel particles from light duty diesel engine exhausts, are summarized in Table 5.3.

Table 5.3: PAHs extracted from diesel particles from light duty diesel engine exhausts (USA EPA, 2002).

PAH	Concentration ($ng.mg^{-1}$ extract)
PhA	2186 – 4883
FlA	3399 – 7321
Py	3532 - 8002

Other factors which have been found to influence PAH emissions from automobiles include the engine power (with increased emissions at higher engine powers) and the aromatic

content of the fuel, particularly the C_9 and C_{10} aromatics. Higher PAH emissions were found from low sulphur fuel combustion, and very rich and very lean air:fuel ratios lead to high emissions of particulates and PAHs. A close relationship between PAH emissions and the age of the car has also been recorded, where the PAH emissions increased with increase in car speed of high mileage cars (Nikolaou et al., 1984). In another study, PAH emissions were found to increase with increased mileage but no correlation was found between PAH exhaust emissions and the amount of PAHs in the lubricating oil (Stenberg, 1985).

When a cold engine is started, the emission rates of PAHs are similar for both diesel and petrol engines, and are ~six times higher than with warm starts. With warm engine starts, however, the emissions from diesel engines were higher than that of petrol engines, although this conclusion is complicated by the difference in volume of exhaust gas emitted from each of these engine types, as the higher volume of diesel emissions has a diluting effect on the PAH concentrations (Nikolaou et al., 1984). The elevated emissions under cold start conditions were found not to be related to the combustion chamber wall temperature, but were rather the result of the low air:fuel ratio and higher engine load which both result in increased emissions of PAHs (Pedersen et al., 1980). It should be noted that a cold start is generally defined as the starting of a vehicle which has been standing for at least 12 hours at room temperature (Stenberg, 1985).

In terms of particle size, approximately 50 – 90 % of the number of particles in diesel exhaust are in the ultrafine size range (0.005 – 0.05 μm, with the mode at 0.02 μm), although in terms of mass, ultrafine diesel particulate matter accounts for only 1 – 20 % of the total mass. Approximately 80 – 95 % of the diesel particulate mass is in the range 0.05 – 1.0 μm, with the mean particle diameter of ~0.2 μm (USA EPA, 2002). The distribution of PAHs is shifted to smaller particle sizes for lower vehicle loads (Zielinska et al., 2004). Particle losses in the silicone rubber trap denuder developed in this study would be minimal for these particle size ranges (< 5 % loss for particles > 0.006 μm and 0 % for particles > 0.05 μm), as discussed in Chapter 4.

Krieger and Hites (1992) utilized a denuder based on capillary columns to sample diesel exhaust 0.2 m from the exhaust pipe of an idling diesel bus (at approximately 35 ^{o}C), yielding a 40 ℓ sample volume. Lower vapour pressure PAHs were not present in the denuder

itself, indicating that impaction of particles was not significant and that transmission of particles was effective. It was noted that the sample was fresh, thus there was not sufficient time for equilibrium partitioning between the vapour and particle associated phases. Phenanthrene, for example, was found in equal concentrations in the two phases. *n*-alkanes in the diesel exhaust were used to assess breakthrough, particularly of analytes which had a retention index of < 1300, which were distributed between the denuder and the post-filter PUF plug. Compounds with retention indices of between 1300 and 1600 were only present on the denuder, and thus were present in the vapour phase only. Analytes with retention indexes higher than this were associated with particles, and were completely associated with particles at retention indices > 2200 (Krieger and Hites, 1992).

Sampling the entire effluent is an alternative to the use of a dilution tunnel, and eliminates the complexities associated with isokinetic sampling (Boubel and Ripperton, 1963). However, the USA EPA requires dilution sampling for testing of diesel engines (Lipsky and Robinson, 2005) therefore various large and complex dilution sampling systems have been developed by car manufacturers, which operate at ~1000 ℓ.min^{-1} with mixing tunnels > 1 m long. More portable systems have also been designed, which have dilution tunnels < 1 m long and operate at flow rates of ~175 ℓ.min^{-1} (Lipsky and Robinson, 2005). Dilution samplers should simulate atmospheric dilution, minimize contamination and sampling losses, as well as provide adequate residence time for aerosol processes to occur. Measurements of CO_2 in the undiluted and diluted exhausts may be employed to determine the dilution ratio (Lipsky and Robinson, 2005). Dilution may, however, effect the particle size distribution and partitioning of semi-volatile organic compounds arising from diesel combustion (Lipsky and Robinson, 2006). To overcome these problems, Benner et al. (1989) sampled in a roadway tunnel, where concentrations of 18; 20; and 27 ng.m^{-3} were found for phenanthrene; fluoranthene and pyrene, respectively.

The distribution of PAHs between the gas and particle phases determined from samples taken in a dilution tunnel at ~30 ^{o}C for both gasoline and diesel exhausts is shown in Table 5.4. It is evident that a higher fraction of PAHs are associated with particles in the case of diesel exhausts (which tend to emit more particles), as compared to gasoline (Stenberg, 1985).

Table 5.4: Percentage distribution of PAHs between the gas and particle phases in gasoline and diesel exhausts (Stenberg, 1985).

PAH	Gasoline		Diesel	
	% gas phase	% particles	% gas phase	% particles
PhA	95	5	53	47
FlA	36	64	9	91
Py	25	75	6	94

Zielinska et al. (2004) found that 80-90 % of the four-ring PAHs (including fluoranthene and pyrene) were present in the 8-channel, polystyrene-divinylbenzene (XAD-4) coated denuder portion of a sampling train used to monitor vehicular emissions, and were therefore in the gas phase under engine idling conditions. Under high loads, a much larger portion of these compounds were partitioned to the particle phase. It should be noted that an extensive XAD-4 cleaning procedure was needed prior to use, and organic solvent sample extraction was required prior to analysis. A sampling flow rate of 90 ℓ.min^{-1} was used and the exhaust gases were diluted prior to sampling. Naphthalene breakthrough under these conditions was found to be ~20 %, which was considered acceptable as the flow rate was optimized for phenanthrene to minimize particle loss to the walls of the denuder, as well as evaporative losses of more volatile PAHs from particles during their residence time in the denuder.

Continuous, real-time instruments, based on a photoelectric aerosol sensor have been used to determine total particulate PAH concentrations in diesel emissions, impacted ambient, and occupational exposure sites, including a bus terminal and a distribution centre (Marr et al., 2004). Median total particulate concentrations along Mexico City's roadways ranged from 60 to 910 ng.m^{-3}, with a detection limit of 1 ng.m^{-3}. It was noted that the instrument is slightly more sensitive to larger PAHs, due to their lower photoionisation energies.

Kozielet al. (2001) compared needle trap devices to PDMS SPME fibres in sampling diesel vehicle exhaust emissions and found that the reproducibility for SPME was slightly better, averaging at 25 % for targeted PAHs. Uncertainties were ascribed to sampling errors

including short sampling times (2 min), small sampling volumes (20 mℓ), and turbulence in the sampling train used.

It is clear from this discussion that there are many factors which contribute to the emissions of PAHs from diesel vehicles, which makes comparison of results from different studies difficult. Due to the potential contribution of vehicular emissions to atmospheric PAH levels in South Africa, the use of our PDMS-based denuder technology was investigated in this application.

5.3.2 Experimental method

Quartz fibre filters were punched to the correct size (6 mm o.d.), washed with methanol followed by dichloromethane, and then oven dried at 100 ^{o}C for 30 min. These were used in conjunction with multi-channel silicone rubber traps in the following three sampling configurations and sampling flow rates:

i) Trap-filter-trap (433 mℓ.min^{-1})
ii) Tube-filter-trap (443 mℓ.min^{-1})
iii) Trap-trap (366 mℓ.min^{-1}).

Teflon tubing connections were used in each case. Sampling of the exhaust of an idling diesel vehicle (2006 Citroen C3, 1.4) was performed under cold start conditions for 11 min, by means of battery-operated portable Gilair sampling pumps, as shown in Figure 5.1. The weather conditions during sampling were clear and sunny, with a moderate gusty wind. The ambient temperature was 28 ^{o}C. After sampling, the filters were transferred to sealed 2 mℓ amber vials and the traps were end-capped and wrapped in aluminium foil. Samples were then refrigerated prior to analysis by TD-GC-MS according to the details given in section 5.2.2 (b).

Figure 5.1: Sampling of diesel vehicle emissions with multi-channel silicone rubber traps and quartz fibre filters. Sampling configurations from left to right were: tube-filter-trap; trap-filter-trap and trap-trap.

5.3.3 Results and discussion

The results of the diesel vehicle emission monitoring experiments are summarized in Table 5.5. The primary trap of the trap-filter-trap sampling configuration contained significantly more naphthalene than any of the other traps. This was due to the positioning of this sampling system, which placed the trap closer to the emission source than the other two sampling configurations (refer to Figure 5.1). This impacted on the results due to the gusty wind conditions experienced during sampling. The same amount of naphthalene was collected in the primary trap of the trap-trap configuration and in the trap of the tube-filter-trap configuration, which confirmed that no gas phase naphthalene was adsorbed onto the filters during sampling. Although the filter was blackened due to particle loading, no particle-associated naphthalene was found at the sampling temperature (28 ^{o}C), as was expected due to its volatility. Visual inspection of the filters and traps showed that particles had been successfully collected on the filters and had not been lost in the primary trap. No breakthrough of naphthalene was evident in the secondary traps at the low sample volumes employed (4.0 to 4.9 ℓ), and no fluorene, anthracene, phenanthrene or pyrene were detected in any of the samples. As a result of the low sample volumes and the TD-GC-MS analytical method

employed, which did not allow for the detection of heavier boiling PAHs as mentioned under section 5.2.3, the sampling system could not be effectively tested as a denuder for the heavier PAHs in this experiment.

Table 5.5: Naphthalene concentrations ($\mu g.m^{-3}$) in diesel vehicle emissions sampled onto multi-channel silicone rubber traps and quartz fibre filters with TD-GC-MS analysis.

SAMPLING CONFIGURATION	PRIMARY TRAP	FILTER	SECONDARY TRAP
i) Trap-filter-trap	4.3	nd	nd
ii) Tube-filter-trap	na	nd	1.8
iii) Trap-trap	1.8	na	nd

na = not applicable; nd = not detected (<1 ng).

The NIST library search indicated that hydrocarbons and their oxidized derivatives may have been present in the samples, including aldehydes, carboxylic acids and esters (Q > 80) as shown in Table 5.6.

Table 5.6: Non-PAH products of diesel vehicle emission trap and filter samples, as determined by NIST library comparisons of the TD-GC-MS data.

Compound	R_t (min)	Filter (trap/filter /trap)	Secondary trap (trap/filter /trap)	Filter (tube/filter /trap)	Trap (tube/filter /trap)	Primary (trap/ trap)	Secondary (trap/ trap)
Decanal	15.930	√ (Q90)	√ (Q96)				√ (Q94)
n-Decanoic acid	17.065						√ (Q94)
Tetradecane	17.265				√ (Q81)		
6,10-Dimethyl-5,9-undecadien-2-one	17.582	√ (Q81)	√ (Q80)				
Dodecanoic acid	18.089						√ (Q99)
Hexadecane	18.265				√ (Q96)		
Tetradecanoic acid	18.922	√ (Q92)	√ (Q90)	√ (Q94)	√ (Q93)		√ (Q97)
Isopropyl myristate	19.173			√ (Q87)			
14-Pentadecenoic acid	19.301		√ (Q90)				
1-Nonadecanol	19.396						√ (Q91)
Hexahydro-1-oxa-cyclopropa(*d*)inden-2-one	19.591	√ (Q80)					
Pentadecanoic acid	19.652					√ (Q86)	
Oxybenzone	20.026	√ (Q91)		√ (Q96)	√ (Q90)		√ (Q97)
1-Hexadecanol	20.089						√ (Q91)
Oxacyclotridecan-2-one	20.241		√ (Q90)				
2-Propenoic acid	20.374	√ (Q91)		√ (Q91)		√ (Q83)	√ (Q91)
Thianaphthene-2-carboxylic acid	20.833	√ (Q83)			√ (Q83)		

NOTE: Numbers in brackets reflect the quality of the match between the mass spectrum of the sample to that of the library.

5.4 SUGAR CANE BURNING

5.4.1 Background

Sugar cane (*Saccharum officinarum*) is a tall perennial grass (as shown in Figure 5.2), which is cultivated in approximately 200 countries for sucrose production. In South Africa, approximately 430 000 hectares of sugar cane is currently under cultivation, and this is mainly distributed along the coastal region of KwaZulu-Natal, with a number of inland areas in both KwaZulu-Natal and Mpumalanga (South African Sugar Association, 2006).

Figure 5.2: Sugar cane (*Saccharum officinarum*) growing in KwaZulu-Natal, South Africa.

In general, agricultural open burning is used as a rapid means of disposing of crop residues, releasing nutrients for the next growth cycle and clearing land. In the case of sugar cane, burning removes dry leaves and eradicates any pests (such as snakes and cane rats) which may be present in the plantation prior to manual harvesting, which is the primary harvesting method in use in South Africa. Burning makes manual harvesting of the moisture-

rich stalks using knives or machetes easier, which has financial benefits. It also reduces the unused leaf mass that must be transported to the sugar mills, and may increase the sugar content by weight, due to evaporation of water. The roots (or canes) which remain post harvest send up new stalks called ratoons, which grow and develop into the new harvest.

Although the pre-harvest sugar cane burns have time saving and thus financial benefits, they are also potential sources of large amounts of air pollutants (Figure 5.3), thus monitoring of these events is important especially as sugar cane is cultivated close to residential areas, particularly in KwaZulu-Natal. Numerous PAH congeners have been identified in fly soot extracts derived from sugar cane burns (Zamperlini et al., 1997), with phenanthrene, fluoranthene and pyrene being major contributors (Godoi et al., 2004a), and particulate matter from sugar cane burning has been found to be at least as toxic as that produced by traffic (Mazzoli-Rocha et al., 2008). Analysis of particulate matter arising from the combustion of sugar cane leaves and bagasse in controlled experiments gave concentrations of up to 242 $ng.m^{-3}$ of phenanthrene, 369 $ng.m^{-3}$ of anthracene, 341 $ng.m^{-3}$ of fluoranthene and 182 $ng.m^{-3}$ of pyrene (dos Santos et al., 2002).

Figure 5.3: Particle laden plume arising from a sugar cane burn in KwaZulu-Natal.

Emissions from open burning, on a mass of pollutant per mass of fuel basis, are greater than those from well-controlled combustion sources, although biomass open burning sources typically emit less PAHs than combustion of anthropogenic materials (Lemieux et al., 2004). Open burning raises human health concerns because the emissions are released at ground level and not through tall stacks which may aid dispersion. They are also episodic in time or season and enforcement of bans or regulatory controls is difficult. The fuel source is often heterogeneous which complicates emission estimates (Lemieux et al., 2004). The moisture content of the fuel (i.e. the sugar cane vegetation), the meteorological conditions, and the topographical features of the burn site all contribute to modify the burning conditions as the fire spreads, thus different degrees of combustion efficiency are attained during a burn. The dry vegetation is usually combusted first, releasing energy which dries green, live material, which is subsequently burnt.

Open combustion sources produce particles of a wide size range, which depends in part on the rate of energy release of the fire. In high-intensity fires, a bimodal particle volume distribution has been noted, with peaks around 0.3 μm and > 10 μm. The larger size fraction may be composed of ash and partially burnt plant material, and is entrained in the smoke plume due to the turbulence arising from the high-intensity fire (USA EPA, 1996). As discussed in Chapter 4, particles of these sizes should be fully transmitted by the multi-channel silicone rubber trap denuder system. The fine, respirable particle fraction has been found to dominate in sugar cane burn samples and may therefore impact on human health (Godoi et al., 2004b). The PAH particle-phase concentrations and PAH particle fraction are strongly influenced by burning conditions (Jenkins et al., 1996).

Total particulate PAH concentrations of up to 342 $ng.m^{-3}$ were measured in winter in Brazil during seasonal sugar cane burning events (de Almeida Azevedo et al., 2002), where phenanthrene was the most abundant PAH (2.15 – 21.5 $ng.m^{-3}$). Higher concentrations of the more unstable PAHs, (which contain five-membered rings, such as fluoranthene), than that of the more stable isomers containing only six-membered rings (such as pyrene), may indicate a combustion or anthropogenic source (dos Santos et al., 2002). PAHs have been investigated as potential tracers for biomass combustion products, where phenanthrene, fluoranthene and pyrene were found in aerosols from sugar cane burns (Ballentine et al., 1996).

Due to the rate of occurrence of sugar cane burning events in South Africa and the proximity of residents to the sugar cane growing areas, it was deemed important to consider this potential source of PAH emissions. The PDMS denuder system was tested in this application, and the sample traps were analysed by both the LIF screening method and by TD-GC-MS.

5.4.2 Experimental method

Two multi-channel silicone rubber traps were employed in series, separated by a quartz fibre filter, which was held in place with a Teflon connector, in order to sample emissions from a sugar cane burn at Umhlali on the KwaZulu-Natal North Coast on 14 August 2006. A Gilair portable sampling pump equipped with a low flow module was used to sample air in the emission plume for 10 minutes at 500 mℓ.min^{-1}, as shown in Figure 5.4. Sampling was then repeated with a second set of traps and a quartz fibre filter (Figure 5.5a). After sampling, the traps were end-capped, wrapped in aluminium foil and refrigerated prior to analysis.

Figure 5.4: Sampling train with pump, located approximately 20 m from the burn front.

One set of silicone rubber traps and quartz fibre filter was thermally desorbed using a thermal desorber system (TDS) and the desorbed PAHs were cryogenically focused via a

cooled injection system (CIS) (Gerstel) on 4 September 2006. The traps and filter were desorbed from 30 °C (3 min) to 280 °C (10 min) at 60 °C.min^{-1} in the splitless flow mode. Cryo-focusing of the PAHs was achieved using liquid nitrogen at -20 °C at 12 °C.s^{-1} to 300 °C (10 min). The GC-MS system was an Agilent GC 6890A coupled to a Hewlett Packard 5973 mass selective detector (MSD). The GC inlet was in the solvent vent mode with helium (Ultra High Purity, Afrox) as the inlet gas. The vent flow was 60 mℓ.min^{-1}, the vent pressure 65 kPa until 0 min, and the purge flow to split vent was 60 mℓ.min^{-1} at 1 min. The GC column was from Restek RTX1-MS (30 m x 250 µm x 25 µm) and the column head pressure was 65 kPa in the constant pressure mode using helium as the carrier gas. The velocity of the gas was 39 cm.s^{-1} (1.1 mℓ.min^{-1}) at 60 °C. The GC oven was temperature programmed from 60 °C (5 min) at 20 °C.min $^{-1}$ to 280 °C (5 min). A post run was performed at 300 °C (2 min) at 100 kPa. The GC-MS transfer line was at 300 °C, the mass scan range was 45-450 atomic mass units (amu) and the electron multiplier voltage 1700 V.

The second set of traps and filter were analysed by LIF on 7 September 2006, using the method described in Chapter 3 and an excitation wavelength of 292 nm. These traps (which had been analysed by LIF), were then re-capped and stored in a refrigerator at 5 ^{o}C and the filter was stored at room temperature in a sealed 2 mℓ amber vial until 26 February 2009 when the samples were analysed by TD-GC-MS, according to the procedure detailed in section 5.2.2 (b). A mixed PAH standard was used for calibration purposes (0.1; 1 and 10 ng).

5.4.3 Results and discussion

It is acknowledged that the sampling system should have been placed vertically to ensure efficient denudation (as discussed in Chapter 4), however, the horizontal positioning used did not appear to have significantly impacted on the results. Visual inspection of the traps after sampling clearly showed that the fine particles had passed through the first silicone trap, and were present on the filter, as shown in Figure 5.5b). The system served as a denuder in that gas phase analytes were trapped by the first silicone rubber trap, whilst particle-bound analytes were trapped by a quartz fibre filter. Any analytes which entered the gas phase after impacting on the filter were trapped by the second silicone rubber trap, as were any gas phase analytes which broke through the first trap.

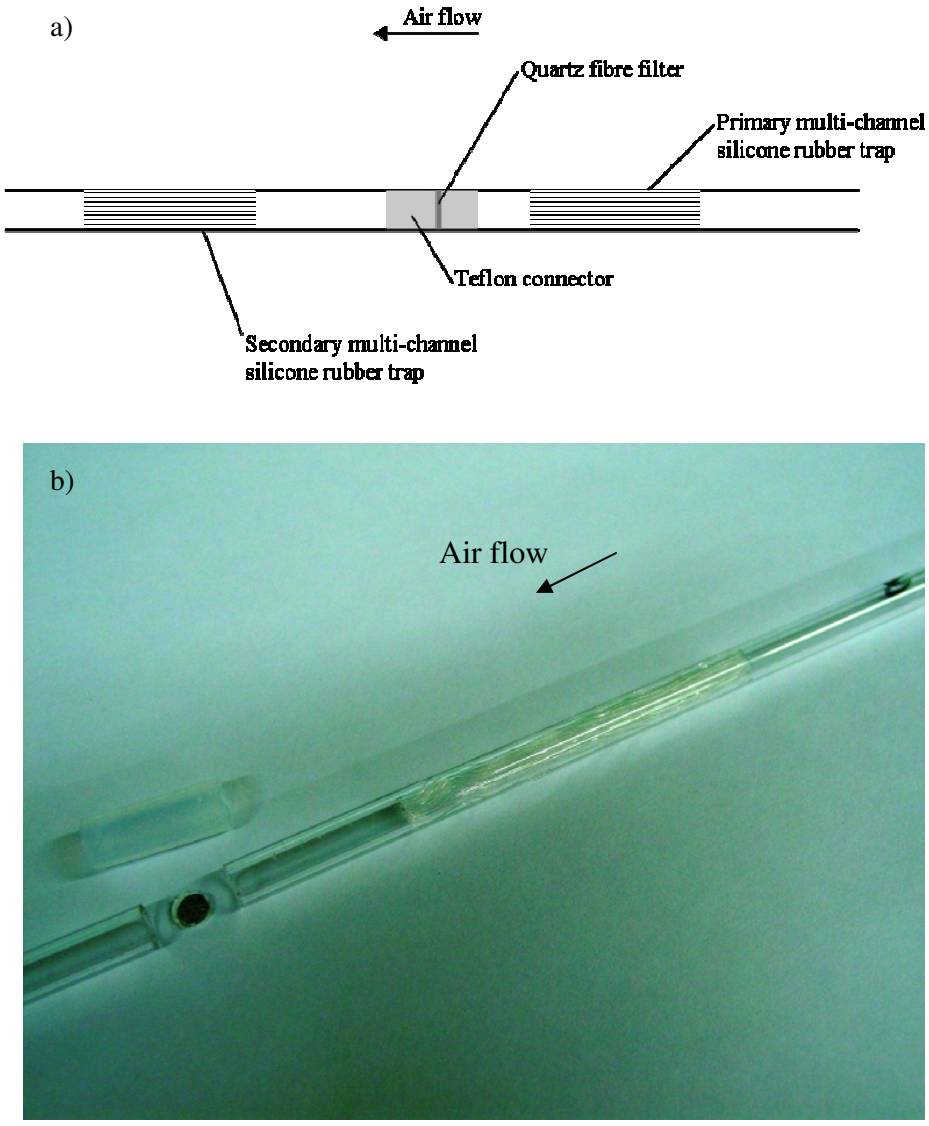

Figure 5.5: a) Multi-channel silicone rubber traps and a quartz fibre filter employed in the denuder configuration. b) Dismantled silicone trap system after sugar cane burn sampling, with no particles evident on the trap, whilst the filter which was downstream of the trap is heavily loaded with particles.

LIF results of the traps focused on naphthalene, which showed a concentration profile through the sampling system (refer to Figure 5.6), with possible overlap of heavier PAH emission spectra at the inlet side of the first trap. The samples therefore screened positive for naphthalene via the LIF method, indicating the need for quantitative GC-MS analysis. This experiment proved the concept of our LIF method as a screening tool. The profile in Figure 5.6 also indicates the possibility of spectral deconvolution by the sequential subtraction

of spectra obtained consecutively down a trap in order to enhance resolution. This is possible as separation of different analytes occurs as the air sample moves through the PDMS trap in the same manner as in chromatographic frontal analysis. Subtraction of fluorescence spectra has been shown to be a useful means of enhancing resolution in the analysis of complex mixtures of aromatic compounds by liquid chromatography with a fluorometric photodiode array detection system (Gluckman et al., 1985), for example.

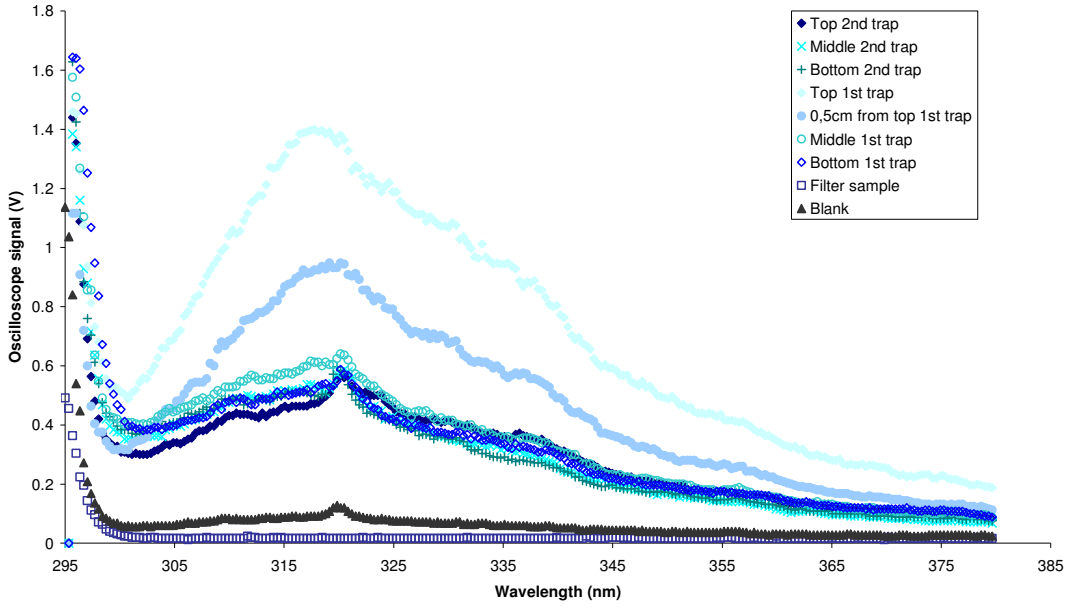

Figure 5.6: Naphthalene fluorescence spectra of the first and second traps at different positions along their lengths (where the top indicates the sample inlet side), and the filter, with excitation at 292 nm.

The TD-GC-MS results obtained on 4 September 2006 are summarized in Table 5.7. There was significant co-elution with respect to the naphthalene peak using this GC method, thus results are semi-quantitative. The first trap contained ~1 ng (0.2 $\mu g.m^{-3}$) of naphthalene (comparison with peak area of a 0.1 ng standard analysis), whilst very small amounts were present on the filter, as expected for this volatile compound. Better results were obtained for phenanthrene; fluoranthene and pyrene. Due to their lower volatility, higher concentrations of these analytes were present in the particle phase. Other studies have similarly shown that the

naphthalene content of sugar cane soot was a factor of ~7 times lower than that of phenanthrene, fluoranthene and pyrene (Godoi et al., 2004a), with concentrations ranging from 0.42 ng.m^{-3} for naphthalene to 3.3 ng.m^{-3} for fluoranthene.

Table 5.7: Sugar cane burn PAH TD-GC-MS results (analysis on 4 September 2006), indicating concentrations (for naphthalene) or relative % contributions (for the other PAHs).

Parameter	Naphthalene	Phenanthrene	Fluoranthene	Pyrene
R_t (min)	9.7	14.2	15.8	16.1
1st trap (gas phase)	~ 1 ng	81 %	71 %	65 %
Filter (particle bound)	< 0.1 ng	2 %	9 %	12%
Second trap	Co-elution	17 %	20 %	23 %

The percentage of phenanthrene, fluoranthene and pyrene present in the gas and particle phases compare favourably with those reported for ambient air samples in the literature (refer to Table 4.3 in Chapter 4), although a lower portion of the total pyrene was found in the gas phase in this study, possibly due to the high particulate loading in the smoke plume. Most sugar cane PAH monitoring has focused on particulates, therefore data on gas/particle partitioning for this source is rather limited.

The TD-GC-MS results obtained on 26 February 2009 proved the stability of trapped samples, as naphthalene (the most volatile PAH) was still present on the traps after refrigerated storage for over two years. The primary trap was found to contain 13 ng of naphthalene (2.6 µg.m^{-3}) and 3.3 ng of phenanthrene (0.7 µg.m^{-3}), whilst the secondary trap contained 1.8 ng of naphthalene (0.4 µg.m^{-3}), which indicates that some breakthrough had occurred at the 5 ℓ sampling volume. Breakthrough was also evident from the LIF results (Figure 5.6)

Better resolution was obtained with this GC-MS method, thus more confidence could be placed on the resulting naphthalene concentrations than in those determined previously, which would seem to have been underestimated. The two sample sets were also taken sequentially, which would also contribute to the inter-sample variation.

The filter samples had been stored in 2 mℓ amber vials at room temperature, therefore volatilization losses were expected. No target PAHs were found on the filter, and the NIST

library search on the GC-MS data indicated that esters and carboxylic acids of hydrocarbons, as well as aromatic aldehydes and esters may have been adsorbed onto the particulate matter (Q > 80). The possible presence of both phenol derivatives and oxidized hydrocarbon and aromatic derivatives were evident from the library search results of the primary trap data. In addition, biphenyl (Q = 87), *o*-hydroxybiphenyl (Q = 97), and 2-methyl naphthalene (Q = 90) may also have been present on the primary trap. The secondary trap may have contained *o*-hydroxybiphenyl (Q = 96), and 2,6-diisopropylnaphthalene (Q = 94).

The multi-channel silicone rubber trap denuder system and the LIF screening method were therefore successfully tested in this application, where PAH partitioning between the gas and particle phase was evident.

5.5 INDUSTRIAL EMISSIONS

5.5.1 Background

Industrial atmospheric emissions may contain PAHs when processes involve organic compounds and elevated temperatures, such as those of incinerators, diesel-fired boilers and oil refineries. A sampling campaign was therefore performed in the Vaal region of South Africa, which has been declared a priority area in terms of air quality under the National Environmental Management: Air Quality Act (Act No. 39 of 2004) (Department of Environmental Affairs and Tourism, 2006). A relatively low atmospheric particulate load was expected therefore the denuder sampling configuration was not employed. Breakthrough conditions were, however, tested by sampling onto two traps in series.

5.5.2 Experimental method

Prior to sampling, blank multi-channel polydimethylsiloxane rubber sample traps were analysed by LIF and TD-GC-MS. Gas phase air samples were collected actively onto two traps in series, using portable Gilair personal sampling pumps. Sampling was performed in triplicate at roughly the breathing zone height at three locations in the vicinity of an oil refinery:

- Site 1: At the fence-line down wind of the oil refinery
- Site 2: Adjacent to a power station and surrounded by various industries in the area, but upwind of all these sources
- Site 3: Similar location to site 1, but slightly further east.

In order to evaluate breakthrough volumes and optimal sampling flow rates, three different sampling flow rates were employed at each site as well as different sampling intervals (10 or 25 min), such that sample volumes ranged from 3.7 to 31.9 ℓ, as shown in Table 5.8.

Table 5.8: Sampling conditions for the monitoring of PAHs in industrial atmospheric emissions.

Pump	Flow rate (mℓ.min^{-1})	Sampling interval (min)	Total sample volume (ℓ)
A	184	25	4.6
B	370	10	3.7
C	1276	25	31.9

The samples (including a field blank) were analysed by LIF using 292 nm excitation radiation according to the method developed in Chapter 3, and the emission spectra were recorded from 295 to 465 nm. A positive or negative screening result was determined by comparing the fluorescence signal at 323 nm of the trap blank with that obtained after sampling. The traps were then analysed directly by TD-GC-MS, using the method described in section 5.2.2 (b), and six target PAHs (naphthalene, phenanthrene, pyrene, fluoranthene, fluorene and anthracene) were quantified using a mixed PAH standard for calibration purposes (0.1; 1; 10 and 100 ng).

5.5.3 Results and discussion

No PAHs were detected on the blank traps prior to sampling by LIF and TD-GC-MS. During sampling, it was noted that the wind speed was moderate and that weather conditions were sunny. A strong chemical (cresol-like) smell was noted at the first (where the smell came in wafts) and third sampling sites, whilst no particular odours were evident at the second site.

The various sampling flow rates and sample volumes allowed for the successful confirmation of laboratory derived breakthrough volumes for the analytes of interest, as it was evident that breakthrough only occurred at the highest sampling flow rate, where the corresponding sample volume was 31.9 ℓ (Table 5.9).

The TD-GC-MS results at the first sampling site indicated a naphthalene concentration of between ~10 $\mu g.m^{-3}$ (for the 25 minute samples), and ~25 $\mu g.m^{-3}$ (for the 10 minute sample). This difference is likely due to variations in concentration of PAHs in the air over the sampling interval, as noted from the wafting chemical smell during sampling. No other target PAHs were detected.

The target PAH concentrations were all below the limit of detection of the GC-MS for the samples from the second site (< 0.1 ng on trap). This was to be expected, as sampling was conducted upwind of the industrial sources.

The industrial odour evident at sampling site 1 was less evident during sampling at site 3 (taken 1 hr & 20 min later). This was reflected in the results, as the naphthalene concentration was ~3 $\mu g.m^{-3}$. Excellent reproducibility was found between traps in this case, indicating a more constant concentration over the sampling interval. No other target PAHs were detected.

An example of a fluorescence spectrum of a primary trap which screened positive is shown in Figure 5.7.

Table 5.9: Industrial monitoring LIF screening and TD-GC-MS naphthalene results for the three sampling sites and different sampling volumes.

Analytical method	4.6 ℓ sampling volume 25 min at 184 mℓ.min^{-1}		3.7 ℓ sampling volume 10 min at 370 mℓ.min^{-1}		31.9 ℓ sampling volume 25 min at 1276 mℓ.min^{-1}	
	Primary trap	**Secondary trap**	**Primary trap**	**Secondary trap**	**Primary trap**	**Secondary trap**
			Sampling site 1			
LIF	Positive	Positive	Positive	Negative	Positive	Positive
TD-GC-MS	44 ng 9.6 µg.m^{-3}	ND	95 ng 26 µg.m^{-3}	ND	214 ng 6.7 µg.m^{-3}	102 ng 3.2 µg.m^{-3}
			Sampling site 2			
LIF	Negative	Negative	Negative	Negative	Negative	Negative
TD-GC-MS	ND	ND	ND	ND	ND	ND
			Sampling site 3			
LIF	Positive	Positive	Negative	Positive	Positive	Positive
TD-GC-MS	12 ng 2.6 µg.m^{-3}	ND	11 ng 3.0 µg.m^{-3}	ND	82 ng 2.6 µg.m^{-3}	16 ng 0.5 µg.m^{-3}

ND = not detected

Three false positives were recorded with the LIF screening. All of these were for secondary traps sampled at contaminated sites, therefore it is possible that non-target molecules of fairly high volatility, which contained fluorophores, were present in these traps. The field blank, however, also gave a false positive, although no naphthalene was detected by TD-GC-MS, as expected.

One false negative was recorded (primary trap for site 3 at 370 mℓ.min^{-1} sampling flow rate), which related to a naphthalene content of only 11 ng over the entire trap, thus the amount of naphthalene in the top 5 mm spot of the trap, as analysed by LIF, was below the detection limit.

Elevated fluorescence signals at $\lambda > 323$ nm were noted for the site 2 secondary trap obtained at a 184 mℓ.min^{-1} sampling flow rate, which also indicates the possibility of the

presence of other fluorophores. A correct LIF negative screening result was still obtained for this trap, as the fluorescence signal at 323 nm was not above blank levels.

Thus overall, LIF proved to be a useful screening tool in this application, and it should be noted that false positives are more acceptable than false negatives in such an environmental screening application, where a worst case scenario should be provided.

Upon further analysis of the TD-GC-MS data using the NIST library for tentative analyte identification, 1- and 2-methylnaphthalene were noted in some of the primary traps (qualifier matches of > 85) from sampling sites 1 and 3. In addition, volatile organic compounds (VOCs), specifically benzene adducts such as phenols and indene, were found in most of the traps from sites 1 and 3.

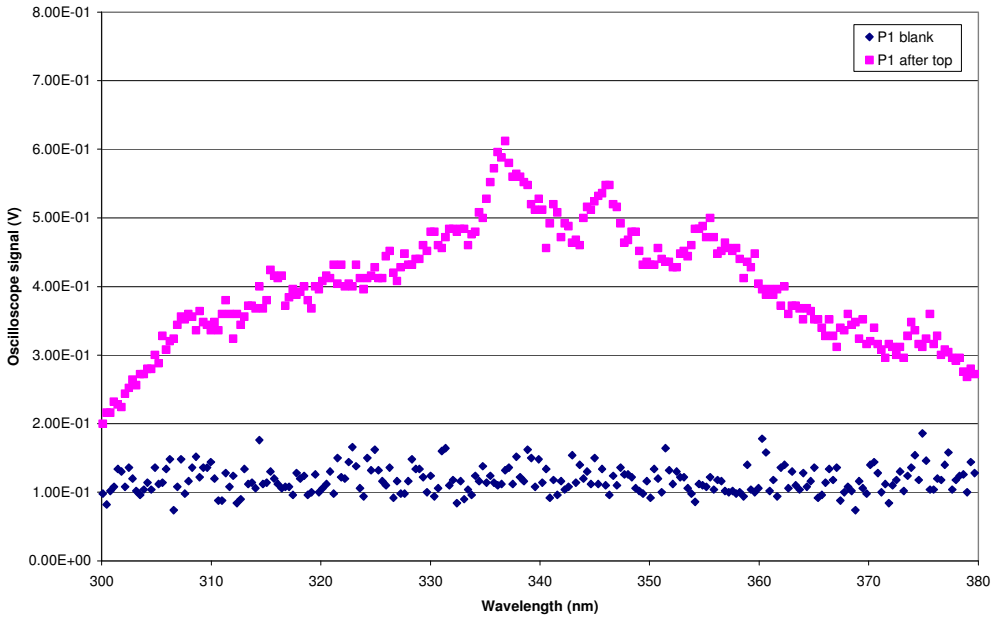

Figure 5.7: Laser induced fluorescence spectra of a primary trap before and after sampling at site 3 (31.9 ℓ of air was sampled over 25 min, LIF excitation at 292 nm).

5.6 CONCLUSION

The LIF PAH screening method and multi-channel silicone rubber trap denuder technology were tested in various applications, which demonstrated the practical use of the method at relevant environmental concentrations. The detected naphthalene concentration in

the primary traps ranged from 1.8 $\mu g.m^{-3}$ (diesel vehicular emissions) to 26 $\mu g.m^{-3}$ (industrial emissions).

The domestic cooking fire emission monitoring results revealed that naphthalene was the most abundant PAH generated and that breakthrough of this analyte was unlikely with a 2.6 ℓ sampling volume. Naphthalene was not particle associated in the freshly formed smoke sample, and no less volatile PAHs were detected. Although the fuel burning was being conducted outdoors in our experiment, indoor fuel burning is also common in South Africa and may incur health effects.

The diesel vehicle exhaust monitoring experiments indicated that there was no adsorption of gas phase naphthalene onto filters during sampling, as the same amount of naphthalene was collected in the primary trap of the trap-trap configuration and in the trap of the tube-filter-trap configuration. Visual inspection of the filters and traps showed that particles had been successfully collected on the filters and had not been lost in the primary trap. No breakthrough of naphthalene was evident in the secondary traps at the sample volumes employed ($\leq$ 4.9 ℓ), which were larger than that used in the household fire emission experiment. Again naphthalene was not particle associated and no less volatile PAHs were detected at these low sampling volumes, although gas phase naphthalene was successfully collected.

The multi-channel silicone rubber trap denuder system and the LIF screening method were successfully tested in the sugar cane burn application, where PAH partitioning between the gas and particle phase was evident. These experiments also demonstrated that the system can be exposed to highly particle-laden atmospheres with minimal interference from the particle content.

The LIF results of the traps showed a naphthalene concentration profile through the sampling system, with possible overlap of heavier PAH emission spectra at the inlet side of the first trap. The samples therefore screened positive for naphthalene via the LIF method, indicating the need for quantitative GC-MS analysis. This experiment proved the concept of our LIF method as a screening tool and showed that enhanced resolution by spectral deconvolution by the sequential subtraction of spectra may be possible and should be further

investigated. Breakthrough occurred with respect to naphthalene at the 5 ℓ sampling volume, which was evident from both the LIF and TD-GC-MS results. The long term stability testing of stored samples containing naphthalene was also successful.

The various sampling flow rates and sample volumes used in the industrial monitoring experiments again allowed for the successful confirmation of the laboratory derived naphthalene breakthrough volume, as it was evident that breakthrough only occurred at the highest sampling volume and flow rate (31.9 ℓ sample volume).

The LIF screening method allowed for the differentiation between impacted and non-impacted industrial sampling sites, as is required of such a method. Three false positives were recorded with the LIF screening, which may have been due to the presence of non-target fluorescent compounds. One false negative was recorded where the naphthalene concentration was below the LIF detection limit. It should be noted that false positives are more acceptable than false negatives in such an environmental screening application, where a worst case scenario should be provided.

The multi-channel silicone rubber trap denuder technology and LIF screening method were therefore tested in various applications where sources were of relevance in the South African context. It is clear that breakthrough of naphthalene occurred at sampling volumes > 5 ℓ, although larger sampling volumes than this are required for sufficient pre-concentration of the lower concentration, less volatile PAHs in order to ensure that they are above the TD-GC-MS detection limit. It may therefore be necessary to sample in duplicate (one low sample volume and one higher sample volume) in order to allow for accurate quantitation by a suitable TD-GC-MS method across the range of PAH concentrations and volatilities.

Total transfer and detection of collected analyte is possible with our TD-GC-MS method, which enhances detection limits and allows for shorter sampling times and flow rates and the denuder sampling system provides particle and gas phase concentrations. It has been demonstrated that our method performs well in real practical applications and PAH concentrations.

The experiments also verified the importance of naphthalene as an indicator for atmospheric PAHs, as the TD-GC-MS results showed that naphthalene was the most abundant

PAH in the various applications which were investigated. This validates our focus on utilising the LIF method to screen for naphthalene.

5.7 REFERENCES

Ballentine, D.C., Macko, S.A., Turekian, V.C., Gilhooly, W.P. and Martincigh, B., *Organic Geochemistry,* **1996**, *25* (1), 97-104.

Benner, B.A., Gordon, G.E. and Wise, S.A., *Environmental Science and Technology,* **1989**, *23*, 1269-1278.

Blumer, M., Blumer, W. and Reich, T., *Environmental Science and Technology,* **1977,** *11* (12), 1082-1084.

Boubel, R.W. and Ripperton, L.A., *Journal of the Air Pollution Control Association*, **1963**, *13* (11), 553-557.

Boström, C.-E., Gerde, P., Hanberg, A., Jernström, B., Johansson, C., Kyrklund, T., Rannug, A., Törnqvist, M., Victorin, K. and Westerholm, R., *Environmental Health Perspectives*, **2002**, *110* (Suppl. 3), 451-488.

De Almeida Azevedo, D., dos Santos, C.Y.M. and de Aquino Neto, F.R., *Atmospheric Environment*, **2002**, *36*, 2383-2395.

Department of Environmental Affairs and Tourism, 21 April **2006**, Government Gazette No. 28732, Notice No. 365.

dos Santos, C.Y.M., de Almeida Azevedo, D. and de Aquino Neto, F.R., *Atmospheric Environment*, **2002**, *36*, 3009-3019.

Gachanja, A.N. and Worsfold, P.J., *The Science of the Total Environment*, **1993**, *138*, 77-89.

Gluckman, J.C., Shelly, D.C. and Novotny, M.V., *Analytical Chemistry*, **1985**, *57*, 1546-1552.

Godoi, A.F.L., Ravindra, K., Godoi, R.H.M., Andrade, S.J., Santiago-Silva, M., Van Vaeck, L. and Van Grieken, R., *Journal of Chromatography A*, **2004a**, *1027*, 49-53.

Godoi, R.H.M., Godoi, A.F.L., Worobiec, A., Andrade, S.J., de Hoog, J., Santiago-Silva, M.R. and Van Grieken, R., *Microchimica Acta*, **2004b**, *145*, 53-56.

Gustafson, P., Östman, C. and Sällsten, G., *Environmental Science and Technology,* **2008**, *42* (14), 5074-5080.

Han, X. and Naeher, L.P., *Environment International*, **2006**, *32*, 106-120.

Harrison, R.M., Smith, D.J.T. and Luhana, L., *Environmental Science and Technology*, **1996**, *30*, 825-832.

Hoffmann, D. and Wynder, E.L., *Journal of the Air Pollution Control Association*, **1963**, *13* (7), 322-327.

Jenkins, B.M., Jones, A.D., Turn, S.Q., and Williams, R.B., *Atmospheric Environment*, **1996**, *30* (22), 3825-3835.

Koziel, J.A., Odziemkowski, M. and Pawliszyn, J., *Analytical Chemistry,* **2001**, *73*, 47-54.

Krieger, M.S. and Hites, R.A., *Environmental Science and Technology,* **1992**, *26*, 1551-1555.

Lemieux, P.M., Lutes, C.C. and Santoianni, D.A., *Progress in Energy and Combustion Science*, **2004**, *30*, 1-32.

Lipsky, E.M. and Robinson, A.L., *Environmental Science and Technology*, **2006**, *40*, 155-162.

Lipsky, E.M. and Robinson, A.L., *Aerosol Science and Technology*, **2005**, *39*, 542-553.

Lu, R., Wu, J., Turco, R.P., Winer, A.M., Atkinson, R., Arey, J., Paulson, S.E., Lurmann, F.W., Miguel, A.H. and Eiguren-Fernandez, A., *Atmospheric Environment*, **2005**, *39*, 489-507.

Marr, L.C., Grogan, L.A., Wöhrnschimmel, H., Molina, L., Molina, M.J., Smith, T.J. and Garshick, E., *Environmental Science and Technology,* **2004**, *38* (9), 2584-2592.

Marr, L.C., Kirchstetter, T.W., Harley, R.A., Miguel, A.H., Hering, S.V. and Hammond, S.K., *Environmental Science and Technology,* **1999**, *33*, 3091-3099.

Mazzoli-Rocha, F., Magalhães, C.B., Malm, O., Saldiva, P.H.N., Zin, W.A. and Faffe, D.S., *Environmental Research,* **2008**, *108*(1), 35-41.

Nikolaou, K., Masclet, P. and Mouvier, G., *Science of the Total Environment*, **1984**, *32*, 103-132.

Pedersen, P.S., Ingwersen, J., Nielsen, T. and Larsen, E., *Environmental Science and Technology*, **1980**, *4* (1), 71-79.

Rhead, M.M. and Hardy, S.A., *Fuel*, **2003***, 82*, 385-393.

Smith, K.R., Aggarwal, A.L. and Dave, R.M., *Atmospheric Environment*, **1983**, *17* (11), 2343-2362.

South African Sugar Association, **2006**, Sugar Industry Directory for 2005/2006, accessed on 10 August 2007 at www.sasa.org.za

Stenberg, U.R., Chapter 4: PAH emissions from automobiles in *Handbook of Polycyclic Aromatic Hydrocarbons*, Ed. Bjorseth, A., **1985**, *2*, 87-111.

USA EPA, **2002**, Health Assessment Document for Diesel Engine Exhaust. U.S. Environmental Protection Agency, Office of Research and Development, National Center for Environmental Assessment, Washington Office, Washington, DC, EPA/600/8-90/057F.

USA EPA, **1996** (October), AP 42, 5th edition, Volume 1, Chapter 13: Miscellaneous sources, Supplement B, accessed on 8 September 2007 at www.epa.gov/ttn/chief/ap42/ch13

Viau, C., Hakizimana, G. and Bouchard, M., *International Archives of Occupational and Environmental Health*, **2000**, *73*, 331-338.

Wild, S.R. and Jones, K.C., *Environmental Pollution,* **1995**, *88*, 91-108.

Wu, W.Z., Wang, J.X., Zhao, G.F. and You, L., *Journal of Environmental Science and Health*, **2002**, *A37* (4), 579-600.

Zamperlini, G.C.M., Silva, M.R.S. and Vilegas, W., *Chromatographia,* **1997**, *46* (11/12), 655-663.

Zielinska, B., Sagebiel, J., Arnott, W.P., Rogers, C.F., Kelly, K.E., Wagner, D.A., Lighty, J.S., Sarofim, A.F. and Palmer, G., *Environmental Science and Technology*, **2004**, *38*, 86-90.

Chapter 6

Conclusion

Combustion of fuels, particularly fossil fuels, is a major source of air pollutants in developing countries in addition to industrial emissions. Traffic densities in urban areas are also increasing which mainly involves an aged vehicle fleet without catalytic converters. Poor indoor air quality is often of concern, due to the use of open fires for cooking and heating purposes in the developing world.

Inorganic air pollutants were found to be far more routinely monitored than organic air pollutants in southern Africa, which is of concern due to the potential for release of organic species from the sources present, as well as due to the potential human toxicity of such molecules including polychlorinated dibenzodioxins and polyaromatic hydrocarbons.

The lack of organic atmospheric pollutant monitoring in southern Africa may be due to a number of reasons including socio-political priorities and lack of equipment, funding and skilled human resources. The use of alternative cost-effective analytical methods for air pollutants to the standard comprehensive techniques may therefore provide for more widespread monitoring campaigns in the region. Such alternatives may include the use of passive samplers, the monitoring of indicator compounds, or screening methods.

This study was initiated in order to develop such alternative methods for organic air pollutant monitoring, which are more applicable to developing countries. The techniques were required to be rapid, and have acceptably low limits of detection for the envisaged applications thereof. In addition, sufficient selectivity and minimal sample clean-up and separation

processes prior to analysis were needed, and the possibility for interfacing with more comprehensive techniques for further quantitative analysis post screening was preferable.

Multi-channel silicone rubber traps were applied as pre-concentrators of the target organic air pollutants in this study and they provided the advantage of allowing for direct thermal desorption - gas chromatographic analysis of samples, thereby negating the need for solvent extraction and pre-concentration, which can lead to sample loss or contamination. The multi-channel silicone rubber traps, which contained twenty two parallel, 55 mm long 0.3 mm i.d. PDMS tubes housed in a 178 mm long, 6 mm o.d. quartz tube, were inexpensive to manufacture and could be re-used.

It was shown theoretically that these traps can serve as denuders in PAH sampling, where the gas phase analyte is collected on a primary trap, whilst particle associated analyte is collected on a downstream quartz fibre filter. Any gas phase PAHs which break through the primary trap, as well as any analyte which re-volatilises from the particle associated phase, is collected on a secondary trap placed after the filter. The traps can then be analysed directly by LIF and/or TD-GC-MS (which also allows for direct TD analysis of the filters). TD allows for the total transfer of the sampled analytes onto the GC column, which enhances sensitivity as compared to solvent extraction based methods, and thereby facilitates shorter sampling times and lower sampling flow rates. The use of denuders in PAH monitoring is important due to the different potential health and environmental impacts of these analytes in different phases, therefore denudation was tested in various applications of relevance to southern Africa.

Trace organic air pollutant analysis requires reliable gas standards. For the LIF method developed in this study it was also necessary for the analyte to be evenly spread over the 22 PDMS tubes contained in the sample trap. Permeation tubes were found to be suitable for the generation of gas standards of the more volatile trace organic air pollutants such as chlorobenzene and the dichlorobenzenes, with permeation rates in the range of a few to ~40 $ng.min^{-1}$, whilst cost effective, custom made diffusion tubes were found to provide reliable quantities of naphthalene at ~ 2 $ng.s^{-1}$. A portable sampling pump was used to load known amounts of analytes from these tubes onto sample traps.

A gas chromatographic fraction collection method utilizing a GC equipped with a modified FID was optimized for the loading of traps with pre-determined quantities of other trace organic air pollutants which were less volatile than naphthalene, including phenanthrene and pyrene. This collection technique was possible due to the open geometry of the trap, which did not impact on the GC column flow rate. Even though collection efficiencies were not optimal (50 – 60 %), reasonably reproducible recoveries allowed for the correction of analyte losses during loading. Comparison of LIF and GC-MS analyses of the less volatile PAHs was possible with this standard collection method, which would be cost effective for laboratories equipped to analyse the analytes of interest, where GC equipment and solid standards are available. The fraction collection technique offers the additional advantage of loading analytes after capillary chromatographic purification in cases where high purity standards are not readily available, and it may find application in other spectroscopic studies.

The novel LIF method which was developed in this study utilizes the inherent fluorescent properties of PAHs, where a tunable dye laser with a frequency doubling crystal provides excitation radiation of a specific wavelength for the target PAH which has been sampled onto a quartz multi-channel silicone rubber trap. Additional selectivity is provided by the use of a monochromator to detect the fluorescence emission. It was found that a 292 nm excitation wavelength, which was optimal for naphthalene, was also potentially suitable for phenanthrene determinations, but not for pyrene.

The LIF technique was found to be basically non-destructive, with low photodegradation losses over the time interval of a screening analysis, as the photolytic half life of naphthalene was ~35 min. The traps could therefore be subsequently quantitatively analysed by TD-GC-MS without the need for any sample extraction or additional pre-concentration. The LIF method LOD was found to be ~20 ng for a signal to noise ratio of 3:1, and the breakthrough volume (10 %) of the traps was estimated to be in the order of 4 ℓ for naphthalene based on both LIF and TD-GC-MS experiments. This relates to a sampling interval of ~8 min at 500 mℓ.min^{-1}, and as the GC-MS can detect 1 pg with a signal to noise ratio of 400:1 in total ion current (TIC) chromatogram mode, a detection limit of ~0.3 ng.m^{-3} can be calculated for this breakthrough volume.

The variation in incident laser energy proved to be the greatest source of variability in results of LIF repeatability experiments, although the ≤15 % RSD in oscilloscope response was deemed acceptable for a screening method.

The methods developed were successfully tested in a number of applications which are of relevance to southern Africa, as emissions from sugar cane burning, household fires, diesel vehicles and industries were sampled onto the quartz multi-channel silicone rubber traps, which were in the denuder configuration in some cases. The samples were successfully screened by LIF and were subsequently analysed by TD-GC-MS. The LIF method allowed for the differentiation between impacted and non-impacted industrial sampling sites, and the importance of naphthalene as an indicator for atmospheric PAHs was verified in that this PAH was the most abundant in the various applications which were investigated. Our focus on utilizing the LIF method to screen for naphthalene was therefore validated.

The LIF method developed in this study has the potential to serve as a screening tool to avoid the comprehensive analysis of samples which do not contain appreciable levels of PAHs. The experimental procedure is simple and rapid, with acceptably low limits of detection, even with the initial, unoptimized optical arrangement and without extensive time-averaging. LIF also provides selectivity without the need for sample clean-up and separation processes, which may entail the use of organic solvents and cryogenic equipment.

The multi-channel silicone rubber traps allow for the pre-concentration of analytes and in addition they may provide a useful means of simultaneously physically separating mixtures of analytes in air samples in the trap, as a consequence of chromatographic frontal separation processes occurring through the trap during sampling, allowing for the deconvolution of more complex fluorescence spectra.

The LIF method could be further optimised by improving the laser energy stability, as well as by the investigation of possible time resolution techniques, for example. It is possible that the LIF method could be utilized in real-time applications, with continuous air sampling through a multi-channel silicone rubber trap. This could provide an indication of changing PAH levels with good time resolution even at low concentrations, due to the sensitivity of the method.

As equipment cost considerations were important, it is possible that the LIF screening method could find application in a centralized environmental laboratory for the southern African region. Alternatively, a portable atmospheric PAH screening tool based on the principles developed here could be developed. This would facilitate the widespread monitoring of atmospheric PAHs in a cost effective manner.

Appendices

Appendix A

Published papers based on thesis work

A1. P.B.C. Forbes and E.R. Rohwer, Monitoring of trace organic air pollutants – a developing country perspective, *WIT Transactions on Ecology and the Environment*, **2008**, *116*, 345-355.

A2. Patricia B.C. Forbes and Egmont R. Rohwer, Investigations into a novel method for atmospheric polycyclic aromatic hydrocarbon monitoring, *Environmental Pollution*, **2009**, *157*, 2529-2535.

A3. Patricia Belinda Crosby Forbes, Andreas Trüe and Egmont R. Rohwer, Laser induced fluorescence of polycyclic aromatic hydrocarbons: An approach to gas standards, *Environmental Chemistry Letters*, DOI 10.1007/s10311-009-0238-6.

A4. Additional outputs based on thesis work.

Appendix A4

Additional outputs based on thesis work

Invited lecture

Patricia B.C. Forbes and Egmont R. Rohwer, "Laser induced fluorescence as a screening method for atmospheric polycyclic aromatic hydrocarbons", *Optics and Laser Applications in Medicine and Environmental Monitoring for Sustainable Development Conference*, 19-24 November **2007**, Cape Coast, Ghana.

Oral presentations

Patricia B.C. Forbes and Egmont R. Rohwer, "A novel screening method for atmospheric polycyclic aromatic hydrocarbons", *National Association for Clean Air Conference*, 10-12 October **2007**, Drakensberg.

P.B.C. Forbes and E.R. Rohwer, "Monitoring of trace organic air pollutants – a developing country perspective", *Air Pollution 2008*, 22-24 September **2008**, Skiathos, Greece.

Poster presentations

P.B.C. Forbes, E. Harden, Y. Naudé and E.R. Rohwer, "A novel technique for the analysis of atmospheric polycyclic aromatic hydrocarbons", *Analitika 2006*, 10-13 September **2006**, Pilansberg.

P.B.C. Forbes, B. Dryden-Schofield, Y. Naudé and E.R. Rohwer, "A novel screening method for atmospheric PAHs arising from biomass burning", *Atmospheric Chemistry at the Interfaces 2006*, 17-22 September **2006**, Cape Town. Also presented at *ChromSAAMS 2008*, 12-15 October **2008**, Bela Bela.

P.B.C. Forbes, A. Trüe and E.R. Rohwer, "A novel denuder for trace organic air pollutant monitoring", *ChromSAAMS 2008*, 12-15 October **2008**, Bela Bela.

Provisional patents

A method of detecting an analyte, SA provisional patent application ZA 2006/07539; E.R. Rohwer, P.B.C. Forbes and Y. Naudé; filed on 8 September **2006**.

A method of analysing a gas sample, SA provisional patent application ZA 2006/07760; E.R. Rohwer, B. Dryden-Schofield, P.B.C. Forbes and Y. Naudé; filed on 15 September **2006**.